



<https://theses.gla.ac.uk/>

Theses Digitisation:

<https://www.gla.ac.uk/myglasgow/research/enlighten/theses/digitisation/>

This is a digitised version of the original print thesis.

Copyright and moral rights for this work are retained by the author

A copy can be downloaded for personal non-commercial research or study,
without prior permission or charge

This work cannot be reproduced or quoted extensively from without first
obtaining permission in writing from the author

The content must not be changed in any way or sold commercially in any
format or medium without the formal permission of the author

When referring to this work, full bibliographic details including the author,
title, awarding institution and date of the thesis must be given

Enlighten: Theses

<https://theses.gla.ac.uk/>
research-enlighten@glasgow.ac.uk

A POWER SYSTEM SIMULATOR FOR
ON-LINE TESTS OF GENERATING PLANT

A thesis submitted to the Faculty of Engineering of the
University of Glasgow for the degree of

Doctor of Philosophy

by

David Kenneth Stewart Fraser B.Sc.

ProQuest Number: 10997960

All rights reserved

INFORMATION TO ALL USERS

The quality of this reproduction is dependent upon the quality of the copy submitted.

In the unlikely event that the author did not send a complete manuscript and there are missing pages, these will be noted. Also, if material had to be removed, a note will indicate the deletion.



ProQuest 10997960

Published by ProQuest LLC (2018). Copyright of the Dissertation is held by the Author.

All rights reserved.

This work is protected against unauthorized copying under Title 17, United States Code
Microform Edition © ProQuest LLC.

ProQuest LLC.
789 East Eisenhower Parkway
P.O. Box 1346
Ann Arbor, MI 48106 – 1346

To my father

ACKNOWLEDGEMENTS

I would like to thank Professor J. Lamb for the provision of laboratory facilities in the Department of Electronics and Electrical Engineering.

The work described in this thesis was funded by the SERC and their support in the form of a CASE award is acknowledged.

I am indebted to Dr H. Davie and Dr M. Macauley for their careful supervision. I would also like to thank other members of staff, especially Dr D. Winning, Dr D. Muir and Dr T. Foord for many constructive suggestions and considerable practical assistance.

I would like to thank the NSHEB for financial support and for the provision of site test facilities at Loch Sloy and Stornoway Power Stations where the assistance and interest of station staff has been greatly appreciated. Thanks are due to Mr P. Johnson and Mr I. Morgan for all their help.

Throughout this work, considerable assistance was received from within the NSHEB and also from the SSEB, the CEGB and GEC: I would particularly like to thank the staff of Peterhead, Longannet, Rugeley 'B', Hams Hall 'C' and Dinorwig Power Stations and the NSHEB, SSEB and CEGB Midlands Region grid control centres; Mr P. Simmons of the CEGB National Technical Training Centre, Mr P. Murphy and Dr C. Aris of Dinorwig Power Station, Mr R. Ward of CEGB System Technical Branch and Dr A. Doubt of GEC.

Fellow research students Dr J. Clink, Mr D. Loomes, Mr. W.C. Michie and Mr. M. Fletcher are thanked for much useful discussion.

Finally, I would like thank to my mother and my friends for their encouragement and also Lynda for her support and her patience.

CONTENTS

ACKNOWLEDGEMENTS	i
CONTENTS	ii
SUMMARY	vi
CHAPTER 1 INTRODUCTION	1
1.1 The Interconnected Power System and its Control	2
1.2 Contributions to System Response	4
1.3 Hydro-turbine Characteristics	6
1.4 Governor Characteristics for Large Turbines	8
1.5 Analysis of Hydro-turbine Governor Behaviour	10
1.6 On-line Testing of Hydro-turbine Governors	11
1.7 The Concept of the Power System Simulator	12
1.8 Outline of Thesis	15
CHAPTER 2 THE POWER SYSTEM SIMULATOR	18
2.1 The Simulator Hardware	18
2.2 The Power Station Interface	19
2.3 Correction for Grid Frequency Deviations During a Test	21
2.4 The Operator Interface	22
2.5 The Test Procedure	23
2.6 Data Acquisition	24
2.7 Software for Real-time Simulation	25
2.8 Software Development Facilities	27
2.9 Methods of Numerical Integration	28
2.9.1 Review of the Methods Available	29
2.9.2 Multiple Rate Integration Schemes	31
2.9.3 Implementation of the Euler Method	33
2.10 Laboratory Testing Facility for the Simulator	33
2.11 Off-line Simulation	34
CHAPTER 3 MODELS FOR POWER SYSTEM RESPONSE SIMULATION	36
3.1 Power System Simulation	36
3.2 A Comparison of National Systems	38
3.3 Proportions of Plant on the UK System	39
3.4 Power Station and Grid Control Centre Operation in Practice	40
3.5 Nuclear Plant	40
3.6 Thermal Plant	40
3.6.1 Thermal Plant Operation	41
3.6.2 An Example of Plant Operation - Load Changes on a 600MW Unit	42
3.6.3 Some General Observations on Thermal Plant Modelling	44
3.6.3.1 Boiler Auxiliaries	44
3.6.3.2 Turbine Bypass Circuits	45
3.6.3.3 Interceptor Valves	45
3.6.3.4 Range of Validity	46
3.6.4 Boiler Models	46

3.6.5	A Thermal Plant Model for Preliminary Tests of the Simulator	46
3.6.6	A More Flexible Thermal Plant Model	48
3.6.6.1	Master Pressure Control	48
3.6.6.2	Fuel Feed System	49
3.6.6.3	Boiler Drum	50
3.6.6.4	Representation of Oil-fired Plant	50
3.6.6.5	Steam Turbine Governor	50
3.6.6.6	Governor Valves	52
3.6.6.7	Steam Turbine	54
3.6.7	The Effect of Low System Frequency on Auxiliary Plant	56
3.6.8	Co-ordinated Boiler-turbine Control Schemes	57
3.7	The Variation of Consumer Demand with Frequency	59
3.8	The Equivalent Machine Model of the Interconnected Generators	61
3.8.1	System Inertia Values	64
3.9	Implementation of the Power System Model	65
CHAPTER 4 PRELIMINARY TESTS OF THE TECHNIQUE		66
4.1	Tests Using an Electronic Governor	66
4.1.1	Tests of Isolated Load Operation	67
4.1.2	Preliminary Tests of a Mixed Hydro-thermal System	69
4.1.3	Some Experiments with the Simulator	70
4.2	Tests Using a Mechanical-hydraulic Governor	72
4.2.1	Tests of Isolated Operation Using Speeder Motor Injection	73
4.3	Conclusion	74
CHAPTER 5 A MULTIPROCESSOR SIMULATOR		75
5.1	Multiprocessor Systems	76
5.2	Some Applications of Multiprocessor Systems	77
5.3	Parallel Processing in the Multibus Environment	78
5.4	Bus Access Arbitration	79
5.5	A Programming Language for the Multiprocessor	80
5.6	An Operating System for the Multiprocessor	81
5.7	Mutual Exclusion	82
5.8	Initial Synchronisation of the Processors	84
5.9	Deadlock Avoidance	85
5.10	Decomposition of the Power System Model	85
5.11	Scheduling of Tasks	86
5.12	Implementation of a Power System Model on the Multiprocessor	86
5.13	Semi-automatic Decomposition	88
5.14	Alternative Configurations	89
5.15	Degradation in Performance due to Bus Contention	90
CHAPTER 6 DETAILED TESTS OF A MIXED HYDRO-THERMAL SYSTEM		91
6.1	Electronic Governor in a Mixed System with One Thermal Unit	93
6.1.1	Operation with Non-reheat Plant	94
6.1.2	Variation of Plant Proportions	95
6.1.3	Variation in Hydro-turbine Operating Point	96

6.1.4	Increased Base Load Capacity	98
6.1.5	Larger Reserve on Thermal Plant	98
6.2	Electronic Governor in a Mixed System with Two Thermal Units	99
6.2.1	Different Thermal Plant Operating Points	99
6.2.2	Operation with Non-reheat Plant	100
6.2.3	Increased Base Load Capacity	100
6.3	Operation of the Grid Frequency Correction Mechanism	101
6.4	Hydraulic Governor in a Mixed System with Two Thermal Units	101
6.5	A Comparison of the Two Governor Types	102
6.6	Conclusion	103

CHAPTER 7 APPLICATION OF THE TECHNIQUE TO DIESEL ENGINES IN AN ISOLATED POWER SYSTEM 104

7.1	The Benefit of On-line Tests of Diesel Engine Response	105
7.2	The Western Isles Power System	107
7.3	Simple Diesel Engine Models for Preliminary Studies	108
7.4	Test Signal Injection Possibilities	109
7.5	Operation of the Grid Frequency Correction Mechanism	111
7.6	Simulation of Isolated Operation with the Electronic Governor	112
7.7	Tests of a Mixed Diesel-thermal System	113
7.8	Simulation of Isolated Operation with the Hydraulic Governor	114
7.9	The Integration of Wind Energy Conversion Systems	115
7.10	Simulation Studies of Wind-diesel Systems	116
7.11	Features of Wind Turbine Dynamics	117
7.12	A Simulation Model of the 3MW Wind Turbine	118
7.12.1	Torque Transmission System	119
7.12.2	Turbine Blade Characteristics	122
7.12.3	Tip-blade Pitch Control	123
7.13	On-line Tests with the Wind Turbine Model	123
7.13.1	Response to a Step Change in Wind Speed	124
7.13.2	Response to a Wind Gust	127
7.13.3	Response to a System Load Increase	128
7.14	Parameters for the Diesel Engine and Governor Model	130
7.15	Conclusion	130

CHAPTER 8 A DEVICE TO ENHANCE THE PERFORMANCE OF EXISTING HYDRO-TURBINE GOVERNORS 132

8.1	Possible Adjustments to Hydraulic Governors	133
8.2	A Hydro-turbine Load Controller	133
8.3	A Governor Enhancement Device Using the Load Controller	135
8.4	A Low Frequency Relay Device	136
8.5	A Continuous Frequency Device	138
8.6	Comparison with the Basic Governor Types	140
8.7	Conclusion	141

CHAPTER 9 CONCLUSIONS AND RECOMMENDATIONS FOR FURTHER WORK 142

9.1	Further Work	143
-----	--------------	-----

REFERENCES	144
APPENDIX 1 A NON-LINEAR HYDRO-TURBINE AND PIPELINE MODEL	161
APPENDIX 2 EQUATIONS AND DATA FOR THE OIL-FIRED PLANT MODEL	162
APPENDIX 3 EQUATIONS AND DATA FOR THE COAL-FIRED PLANT MODEL	164
APPENDIX 4 EQUATIONS AND DATA FOR THE WIND TURBINE MODEL	166

SUMMARY

This thesis describes the development of a simulator for use in the real-time study of a mixed hydro-thermal power system. This equipment can be used to incorporate real plant in system response studies in order to eliminate modelling uncertainties. It can also be used to exercise speed governors on real plant through a wide range of operating conditions obtained artificially. This is particularly valuable for large conventional or pumped-storage hydro-turbines.

To couple the real plant to the simulator, a measurement of generator power is required and a means of injecting a simulated system frequency into the governor of the test machine must be provided. Two methods of test signal injection are described: One for electronic equipment and the other for mechanical-hydraulic governors.

The power system models used in the development and subsequent use of the simulator are discussed with particular reference to the representation of thermal plant behaviour.

Interfacing techniques and secure operating procedures were established during preliminary tests with the simulator at Loch Sloy Power Station. The results of these tests indicate the potential of the technique in a wide range of investigations and on a variety of equipment.

A multiprocessor version of the power system simulator was developed to alleviate the constraints on model complexity imposed by the finite computation speed of a single processor.

On-line tests with a coal-fired plant model demonstrate some of the features of the behaviour of hydro-thermal power systems. The use of the simulator to establish the merits of a particular governor configuration is also illustrated.

Tests on a diesel engine in the isolated system of the Western Isles demonstrate the application of the technique to generating plant that forms a significant proportion of the real power system. In this situation, which would be encountered if the technique were to be used on large hydro-electric or steam turbines, the simulator must prevent effects of the test on the real system from influencing the test result.

Finally, the power system simulator is used to investigate the potential of a device to enhance the performance of existing governors, and to compare the response obtained with that of the standard equipment. In this way, the use of the technique to study novel governor designs is demonstrated.

CHAPTER 1

INTRODUCTION

A power system simulator has been developed to investigate the response of generating plant to load changes on the national grid. The value of this equipment is twofold: Firstly, it may be used to incorporate real plant in studies of system response in order to eliminate modelling uncertainties and, secondly, speed governors on real plant can be exercised throughout a wide range of operating conditions obtained artificially.

The project was carried out in collaboration with the North Of Scotland Hydro-Electric Board (NSHEB), and so attention was particularly directed to governors for hydro-turbines, although the power system simulator can, in principle, be applied to most types of generating plant supplying power to the national grid. The focus of attention is worthwhile because conventional and pumped-storage hydro-electric plant has an important role to play in the operation of the grid system and because hydro-turbines exhibit rather unusual transient behaviour requiring governors with specialised control characteristics. The power system simulator was also used to study the performance of diesel engines supplying power to isolated systems in conjunction with wind-turbine generators.

The techniques used to control a power system and the contribution made by hydro-electric generators will be described in this chapter. The principal hydro-turbine governor types will also be outlined before the concept of the power system simulator is introduced.

1.1 THE INTERCONNECTED POWER SYSTEM AND ITS CONTROL

Since 1935, the generation, transmission and distribution of electricity in the United Kingdom has employed the national grid system,¹ providing for the nation a cheaper and more secure supply of electrical power. Economies of scale have been made with the construction of very large power station complexes and the size of individual generating units has increased with 660MW machines now the norm.

The centralisation of power generation resources has led to a general reduction in operational flexibility accelerated by the shift to nuclear fuels and so the onus for system control has fallen on a smaller proportion of the generating plant. The expected daily demand curve, usually predicted with an accuracy of about 1%, can be met approximately by manual ordering of the available machines. However, the system's initial response to random variations, abrupt changes in demand and sudden disconnection of generation or load must be provided by automatically controlled generators. Plant waiting in a partly-loaded 'spinning' or 'immediate reserve' state must be available to cope with generation deficits and the prime movers must also respond to load reduction by decreasing their output. Rapid load changes as large as 2GW can occur in connection with television programmes or in the event of a trip of the cross-channel d.c. link or a loss of night-time pumping load at pumped-storage power stations.^{2,3}

Under normal operating conditions, the system's generators run synchronously and supply together the power that is being drawn by the consumer loads and the transmission losses. If a balance does not exist between the electric energy production and consumption rates then the difference adds to or depletes the

kinetic energy stored in the rotating machinery synchronised to the grid. As the kinetic energy stored depends upon generator speed, a power imbalance will translate into a speed (and frequency) deviation⁴ and so the precise matching of generation to load is achieved by regulating prime mover speed and hence electrical frequency. While the supply frequency is subject to statutory limits of 49.5 to 50.5Hz, it is normally kept between 49.8 and 50.2Hz.

Although manual intervention is important in the longer term, short-term control is provided automatically by speed governing equipment fitted to the generating plant. When the system frequency deviates from its nominal value, the governors sense a speed error and adjust the mechanical power supplied to the electrical generators. The fractional power change per fractional frequency deviation is the effective gain of a governor, and its inverse is referred to as the droop. In the UK system, governor droops of around 1 to 4% are typical, corresponding to governor gains in the range 100 to 25. Following a disturbance and subsequent governor action, system operators request loading changes to move the system frequency back to 50Hz.

Regulation of the transmission system voltage is dependent on the import and export of reactive power and is essential for the correct transfer of power between areas with the minimum loss⁴. Control of a generator's terminal voltage is performed by an automatic voltage regulator (AVR), whose dynamics are usually faster than those of the speed governor on the set. The resilience of the power system to short circuits or less severe disturbances in the electrical network is dependent on generator dynamics and AVR operation⁴. The system and generator voltage control functions may occasionally affect governor operation but apart from where

the electrical system impinges on governor tests, it will not be discussed further here.

1.2 CONTRIBUTIONS TO SYSTEM RESPONSE

In the event of a sudden generation deficit, thermal plant, fuelled by coal, oil or gas, normally contains the initial system frequency swing by providing power from the kinetic energy stored in the rotating masses and from thermal energy reserves in the boiler and pipework. The frequency is restored to a post-transient steady-state value determined by the overall droop of the system and the extent by which the load changes with frequency. However, the steam plant is unable to maintain this situation because the boiler pressures fall before firing rates can be increased. By this time, hydro-electric plant, will have increased its output in response to the fall in frequency. It may be able to provide sufficient power to maintain a constant frequency until the boiler-turbine units are once again able to increase their output, or manual intervention recovers the situation by starting gas turbines and increasing output from the generating plant already on the system.

The operational flexibility of nuclear generation is limited and it normally plays no part in this sequence of events. In the UK, nuclear power stations are not normally required to follow system load changes because rapid reductions in output cause a 'poisoning' of the reactor with xenon. This effect inhibits subsequent increases in output for a period of some hours,⁵ although, in countries with a high proportion of nuclear plant such as France, Belgium and Sweden, this drawback has to be accepted and the individual units take their turn on load-following duty in rotation, allowing time for reactor recovery.⁶

As indicated above, conventional and pumped-storage hydro-

electric turbine-generators have an important contribution to make to system response and indeed Dinorwig Power Station in Wales was built for precisely this purpose. Two of the station's six 300MW machines are sufficient to provide most of the immediate reserve requirement of the Central Electricity Generating Board (CEGB).⁷ These turbines can be maintained in an unwatered spinning (synchronised) condition waiting to load rapidly in response to low-frequency relays set at 49.85Hz, say, or at the request of the grid control centre. The turbines are capable of reaching full-load output from the initial 'spinning generate' mode in 11 seconds. Rapid changes in pumping load are also used to control the system. Once loaded, the Dinorwig turbines are highly responsive to changes in grid frequency. The governors have a droop setting of 1% giving a change in generator output of about 60MW for a 0.1Hz change in frequency.⁸ The other pumped-storage stations, Ffestiniog (4x90MW)⁸, Cruachan (4x100MW)⁹ and Foyers (2x150MW)¹⁰ are also extensively used to accommodate short-term system load fluctuations. It is advantageous to use hydro-electric power to control the system because fossil-fired thermal sources suffer efficiency loss if their operating point is manipulated.

The control applied to each turbine must be appropriate to the overall dynamics of the mixed nuclear-hydro-thermal system. The behaviour of the system frequency with changing loads depends very much on the system size and composition. Especially severe situations occur following the separation of sections of the network, a real possibility in parts of the Scottish system. 'Islanding' of the Scottish system as a whole has also occurred,¹¹ although this is now less likely than in the past.

Turbines of Francis design are used in all the larger conventional hydro-electric installations in the UK and, by virtue

of their reversibility, are ideal for pumped-storage schemes. The following description of hydro-turbine control will, therefore, relate to the governing of turbines of this design rather than variable-pitch propeller 'Kaplan' turbines where control of the impeller or 'runner' blades must also be considered.¹²

1.3 HYDRO-TURBINE CHARACTERISTICS

Hydro-turbines accommodate large load changes much more readily than steam plant. The only restrictions imposed are limits on the rate of movement of the governor valve guide vanes. A maximum loading rate is imposed to prevent the surge shaft emptying completely causing the entrainment of air in the pipeline and possible damage to the turbine runner. In the form of a minimum guide vane opening time, this has a value of about 20s for Sloy (4x32.5MW)¹³ and 7s for Dinorwig¹⁴ turbines. A maximum closing rate is also imposed to prevent over-pressure in the pipeline after sudden load reductions, although turbine bypass 'relief' valves help to alleviate this problem on schemes with surface pipelines where it is more dangerous. Minimum closing times for Sloy and Dinorwig are 4 and 7s respectively.

The water in the tunnel between the dam and the surge shaft is prone to mass oscillation and large load rejections followed by reconnection of load after a few minutes can cause problems.¹⁵ At Sloy, this oscillation occurs at a frequency of around 0.004Hz.¹⁶

The constraints imposed on hydro-turbines are quite modest in comparison with the restrictions on thermal generation. However, the dynamics of the plant are rather unusual and it is difficult to harness fully the hydro-turbine's natural ability to contribute to system response.

The most prominent factor which makes a hydro-turbine unco-operative is the inertia of the water column in the pipeline.¹⁷

Although the turbine valve opening may be changed rapidly, the water column inertia prevents the flow from increasing as rapidly. As a result, after a rapid increase in gate opening and before the flow rate has had time to change appreciably, the water head at the turbine runner drops as a function of the increase in area of valve opening. So the turbine power, which is proportional to the product of head and flow, drops before it increases. For small deviations around an operating point, this behaviour can be described by the following transfer function:¹⁸

$$\frac{\Delta W}{\Delta A} = \frac{1-sT_w}{1+0.5sT_w} \quad 1.1$$

where ΔW is the normalised change of power of the turbine, ΔA is the normalised change of control valve area and T_w is the water inertia time. T_w varies with pipeline geometry and valve position and is calculated from:¹³

$$T_w = \frac{1}{gH} \sum \frac{QL}{A} \quad 1.2$$

where H is the total head and Q is the volumetric flow in sections of pipeline of length, L and cross-sectional area, A . g is the acceleration due to gravity. Full load values of T_w for Sloy and Dinorwig turbines are $1.1s$ ¹³ and $1.6s$ ¹⁴ respectively. In schemes with more than one turbine, T_w increases above the value for one set as other turbines come on load and change Q in the common sections of pipeline.

The water column inertia makes a hydro-turbine difficult to control and, if a purely proportional governor is used, as on most other prime movers, stability is lost when the generator becomes isolated from thermal plant with its high inertia. The governor must, therefore, have additional components to provide isolated load stability. Unfortunately, these components also reduce the rate of response to frequency deviations when the hydro-turbine is

connected to the grid. It is difficult to combine stability under all operating conditions with a rapid response to disturbances in a large system.

Most hydraulically-controlled hydro-electric schemes, including those of the NSHEB, utilise 'temporary droop' speed governors (Figure 1.1), which use proportional action with a dashpot providing a temporary increase in feedback (i.e. a decrease in gain) during speed transients.

1.4 GOVERNOR CHARACTERISTICS FOR LARGE TURBINES

Paynter¹⁹ indicated that the optimum temporary droop governor response was obtained with a temporary droop of

$$b_t = 2.5 \frac{T_w}{T_a} \quad 1.3$$

and a temporary droop time constant of

$$T_d = 5.9 T_w \quad 1.4$$

Where T_a is the alternator inertia time constant. When substituted in the governor transfer function, these settings give a dominant governor time constant of

$$T_g = \frac{14.7 T_w^2}{b_p T_a} \quad 1.5$$

where b_p is the permanent droop setting. Without greater capital expenditure to increase the cross-sectional area of the pipeline, T_w is generally larger for big hydro-turbines and in order to avoid slow response during grid-connected operation, alternative forms of governor must be considered. For Sloy turbines with a 3% droop ($b_p=0.03$), $T_w=1.1s$ and $T_a=7.0s$, the dominant governor time constant, T_g is 85s. Dinorwig figures of $T_w=1.6s$ and $T_a=8.6s$ give 145s for a 3% droop and, in fact, the situation is even worse because a 1% characteristic is required.

A reduction in response time to about one fourth that of the temporary droop design can be obtained with the double derivative governor shown in Figure 1.2.^{20,21} The first derivative term

accomplishes the same function as the temporary droop feedback in the more conventional governor. Both produce a single phase lead term in the numerator of the transfer function which compensates for the water column inertia. The second derivative provides an additional lead term to overcome the lag inherent in the valve servomotor.

The same performance can be obtained with a three-term 'PID' controller²² (Figure 1.3) with proportional, integral and derivative components. Long-term droop is provided by the feedback of valve position or a measurement of generator power output to the proportional and integral terms of the controller after comparison with a power setpoint. However, the double-derivative scheme offers a number of practical advantages such as a more convenient insertion of the load control signal.^{20,21,23} The double derivative governor uses the pilot servomotor to perform the function of integration whereas the PID governor requires a rapid closed-loop response from the pilot servomotor and is, therefore, harder to implement. Various modifications are appropriate depending on the type of electro-hydraulic actuation employed. In both configurations, the compensating terms may be complex giving a faster rise time. The performance is, therefore, superior to that of a cascade compensator of the same order.²⁰ These governors are intended to increase the hydro-turbine's contribution to system response whilst maintaining stability under all conditions. They do not attempt to improve isolated load performance.

Hydraulic implementation of these governor characteristics is generally not practicable and so they were not used on earlier installations. However, the availability of electronic equipment has led to the adoption of both double derivative and PID

governors for recently constructed plant.^{20,24,25}

A microprocessor-based governor with a double-derivative algorithm was developed and installed on a 32.5MW hydro-turbine at Loch Sloy Power Station in the course of previous work at Glasgow University.^{13,26,27,28} This governor provided a considerably faster response than the existing temporary droop type, but further improvements were possible if the control parameters were adapted according to the operating point of the turbine. It was then possible to compensate for the load-varying water time constant and other non-linearities.²⁶ The microprocessor approach permitted this adaption to take place in a straightforward manner.

1.5 ANALYSIS OF HYDRO-TURBINE GOVERNOR BEHAVIOUR

A range of analytical techniques have been used in the search for optimum governor settings. Paynter¹⁹ defined a stability region for a hydro-turbine with a temporary droop governor on isolated load by direct experimentation on an electronic analog simulation. Hovey²⁹ put this work on a theoretical footing using the Routh-Hurwitz technique and applied it to fixed-blade propeller turbines in a practical power system. The effects of the permanent droop feedback and the load self-regulation had been omitted but these were added by Chaudry.³⁰

Thorne and Hill developed a more detailed model of a 100MW Kaplan turbine with an electronic PID governor for simulation studies³¹ and used eigenvalue analysis to investigate stability³²; the Routh-Hurwitz technique being impractical for a model of this complexity. The effects of the derivative gain and other factors were considered subsequently.³³ Other authors considered the effects of the derivative term with a simple turbine model using eigenvalue analysis³⁴ and the Routh-Hurwitz and root-locus techniques.³⁵

All of these studies used linearised models and took no account of governor deadband which can have a significant effect on stability.^{36,37} Stein³⁶ and Fasol³⁷ studied the effect of governor deadband using harmonic response tests and describing function methods. The effects of governor valve rate and position limits and the non-linear relationship between gate position and turbine torque were assessed by Undrill and Woodward³⁸ using digital computer simulation. Other studies of hydro-turbine behaviour have been reported by various authors.

In using the techniques which position poles in the complex frequency plane, it must be borne in mind that adding damping to reduce the power output overshoot may not be desirable. Given that a particular hydro-turbine is stable on isolated load, increasing the governor damping beyond a certain point will increase the frequency overshoot following a change in load.³⁶ Acceptability of the time domain response should also be considered.

1.6 ON-LINE TESTING OF HYDRO-TURBINE GOVERNORS

Actual tests of isolated operation have been carried out on some hydro-turbines,¹³ but the progressive interconnection of systems and the increasing size of the machines has made such tests increasingly difficult to perform.³⁹

After studying the optimisation of temporary droop governors using analog simulation,¹⁷ Schleif and Angell³⁹ devised a technique for examining the performance of the actual turbine and governing system at any load setting as though it were actually serving an isolated load. By simulating isolation of the hydro-turbine unit under test, Schleif dispensed with the need to measure all the turbine and governor parameters because all the unknowns are represented in the plant itself. In particular, all the non-linearities are automatically included and tedious

calculations of water inertia times at various load levels are avoided. This technique has been used in previous work at Glasgow University²⁶ and elsewhere.^{40,41} Use of this technique has consistently shown the need for more stabilisation than the analytical studies suggest.^{39,40}

To simulate isolated operation, a measurement of generator power is connected to a simulation of the alternator inertia and the load characteristics. The output of the simulator is a simulated system frequency which is, in principle, substituted for the machine speed signal normally fed to the governor. The governor is tricked into thinking that the hydro-turbine is isolated from the grid. In the original work, the simulated frequency signal was injected mechanically. In more recent tests on electronic governors, the signal was injected either as a d.c. voltage at the summing junction of an operational amplifier²⁶ or using a voltage controlled oscillator to drive the normal governor input in place of the machine speed transducer.⁴¹

Other simulators have been built to check out the performance of power plant controls,^{42,43} but these are different in concept in that they replace the plant itself rather than the surrounding system.

1.7 THE CONCEPT OF THE POWER SYSTEM SIMULATOR

With the increasing use of hydro-turbine plant to control large power systems and the availability of governors able to select alternative parameters on load, it is important to investigate the performance of the mixed hydro-thermal system as a whole. A governor must provide isolated load stability before a hydro-turbine is synchronised, but afterwards it can switch to parameters which provide a greater contribution to system response. The governed turbine is then no longer stable under all

operating conditions and the stability limit occurs for some islanded system where the hydro-turbine is a larger than anticipated proportion of the generating plant. For example, it is recommended that the Dinorwig turbines are not operated with the high governor gains intended for system operation if the grid size falls below 5GW.²⁵

Off-line simulation has been used to study the effect of particular governor settings on overall system behaviour⁴⁴. Such studies require the simulation of a number of coupled generation blocks of differing characteristics (Figure 1.4). The outputs of these generation units are weighted according to their relative predominance in the power system to be modelled and the total output is then compared with the consumer demand which may vary with frequency. The model is completed by an equivalent machine representation of generator inertia. This single flywheel model of the individual alternators uses a lumped acceleration constant appropriate to the particular mix of plant on the system. This is an average system frequency model⁴⁵ where voltage effects and inter-machine oscillations are ignored. It is assumed that the deviations in frequency from the system average, which are associated with inter-machine oscillations, have no appreciable effect on the machine governors and mechanical power. Load flow calculations are not included because the changes in transmission loss following a disturbance have a only a secondary effect on the system response.

While valuable results may be obtained from off-line studies, there is considerable incentive to test the response of the real hydro-turbine plant under a comprehensive range of conceivable operating conditions. The benefit of such on-line testing lies in the elimination of modelling uncertainties, particularly those

associated with plant non-linearities such as governor linkage backlash. It is also useful to demonstrate that an installed governor can perform its control function effectively and to check the tuning of its parameters.

It is impracticable to perform extensive testing on the real power network because the disruption necessary to establish a particular grid sub-system would be unacceptable. However, as an extension of Schleif's method for simulating isolated operation, the power system dynamics seen by a particular item of generating plant may be altered through the use of a real-time power system simulator connected into the speed governor control loop. A wide range of tests may then be carried out without unduly disturbing the normal operation of the grid. The generation and load dynamics in the power system of interest are represented in the simulator.

The arrangement employed for the on-line studies remains as outlined in Figure 1.4. However, the nuclear, coal and oil fired plant are all simulated in real time, while the hydro-electric generation is represented by the actual plant. The simulated mechanical output torques from the thermal plant are summed along with a measure of the real mechanical output torque from the hydro-turbine. This composite torque is fed into a real-time simulation of the system inertia and load, and the resultant simulated frequency signal is fed back to the governors of all of the generation units, both simulated and real. In this manner the dynamic behaviour of the hydro-generator is coupled into the simulator, although the machine continues to supply the grid. This scheme is an enhancement of the technique for simulating isolated operation.

The relative amounts of each generation type and the characteristics of the inertia and load may be altered with ease

and generation excess or deficit incidents can be simulated. The disturbance of interest often involves a generation deficiency caused by a loss of generation. However, it is conceptually easier to view this as an increase in load. With an appropriate choice of parameters, the one (real) hydro-turbine can be used to represent a much larger machine or a group of similarly-governed machines whose total output is of significance to the grid.

If a large pumped storage scheme were to be built in Scotland with governors settings appropriate to system operation, a real possibility of instability would exist in the event of islanding. Although predictions could be made using off-line simulation, no on-line confirmation could be obtained without the use of a power system simulator.

Novel governor designs, perhaps intended for smaller plant in remote parts of the system, can also be thoroughly investigated with this equipment.

1.8 OUTLINE OF THESIS

Chapter 2 will describe practical aspects of the power system simulator and its use in more detail, covering the digital computer hardware and software implementation, numerical integration methods for the simulation models, interfacing requirements and the on-site test procedure.

The models used in the simulator will be discussed in Chapter 3 with particular emphasis on the dynamics of the thermal plant providing the bulk of the electricity production in the UK. Particular reference will be made to the models used by the CEGB in system response studies.

Preliminary tests of the power system simulator technique at Loch Sloy Power Station will be reported in Chapter 4 with the results of both isolated and mixed hydro-thermal system tests. The

test signal was coupled into the real plant in two ways: one by direct injection into an electronic governor and the other by using the speeder motor on a mechanical-hydraulic governor.

As the complexity of the system response test increases, the computational resources of the basic computer hardware configuration is no longer adequate to complete numerical solution of the model equations in real time. Chapter 5 describes the development of a multiprocessor simulator to alleviate this problem. The multiple computer configuration was also used to provide additional input/output facilities.

The results of tests at Sloy using a more elaborate power system model are presented in Chapter 6. The behaviour of both double derivative and temporary droop governors was investigated in a number of power system configurations with thermal plant of various types.

Chapter 7 describes the application of the technique to diesel engine generators in an isolated power system. Particular problems arose, because the engine under test constituted a significant part of the real system. Some of these difficulties were overcome and the power system simulator was used to investigate the behaviour of wind-diesel power systems.

The power system simulator was also used to examine the potential of electronic devices that could be connected easily to existing hydro-turbine governors and provide an improvement in their response to system disturbances. Chapter 8 looks at the performance of these devices in comparison with the double derivative and temporary droop governors.

The overall conclusions that can be drawn from the work will be presented in Chapter 9 together with recommendations for further work.

Aspects of the work reported in this thesis have been published in References 46, 47 and 48.

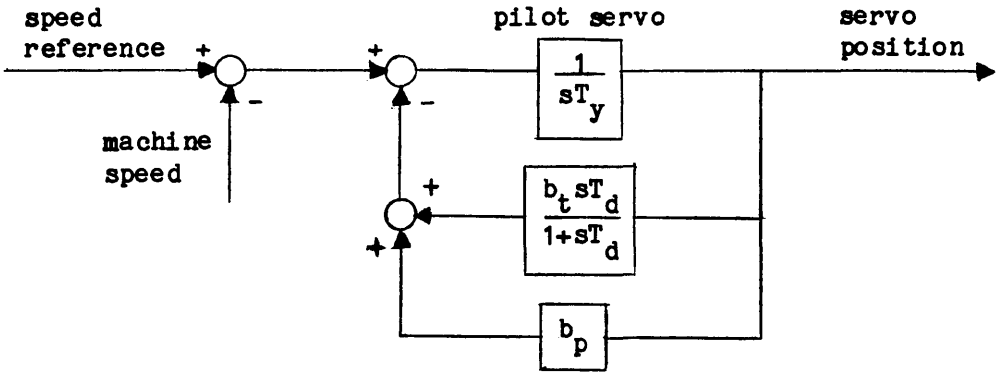


Figure 1.1 Temporary droop governor

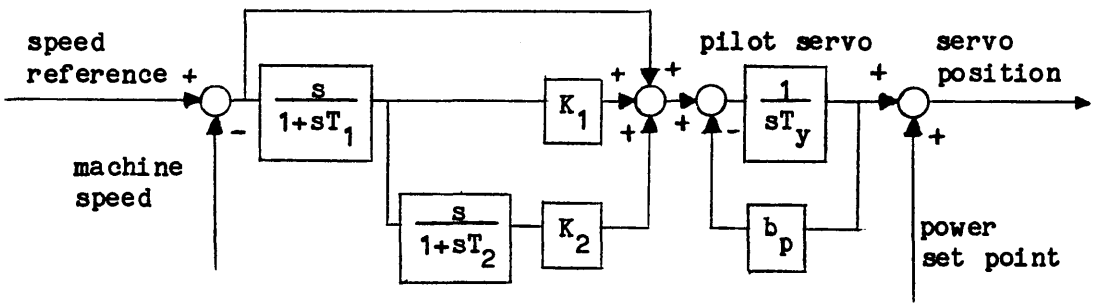


Figure 1.2 Double derivative governor

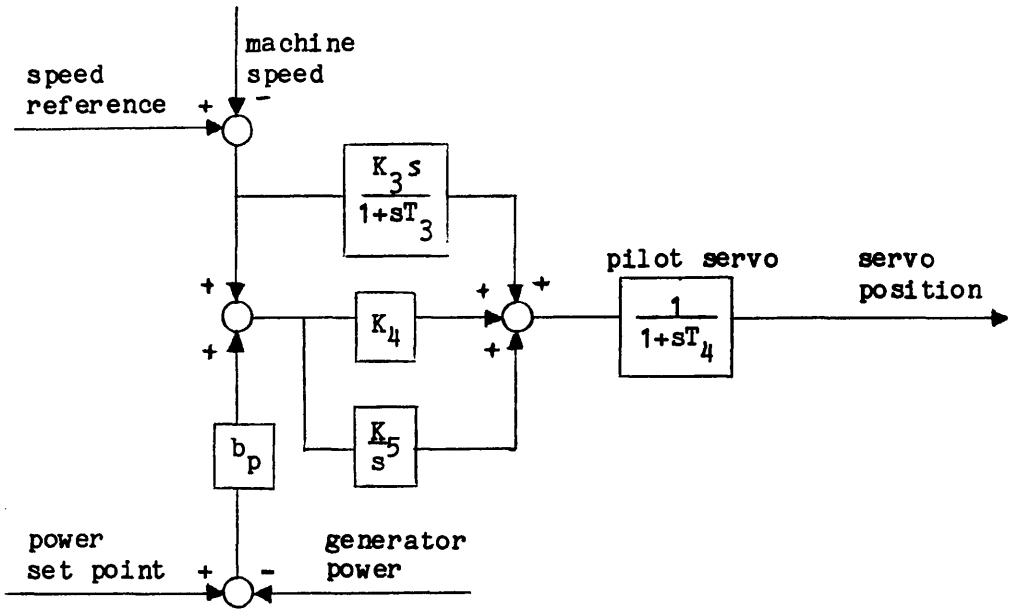


Figure 1.3 PID governor

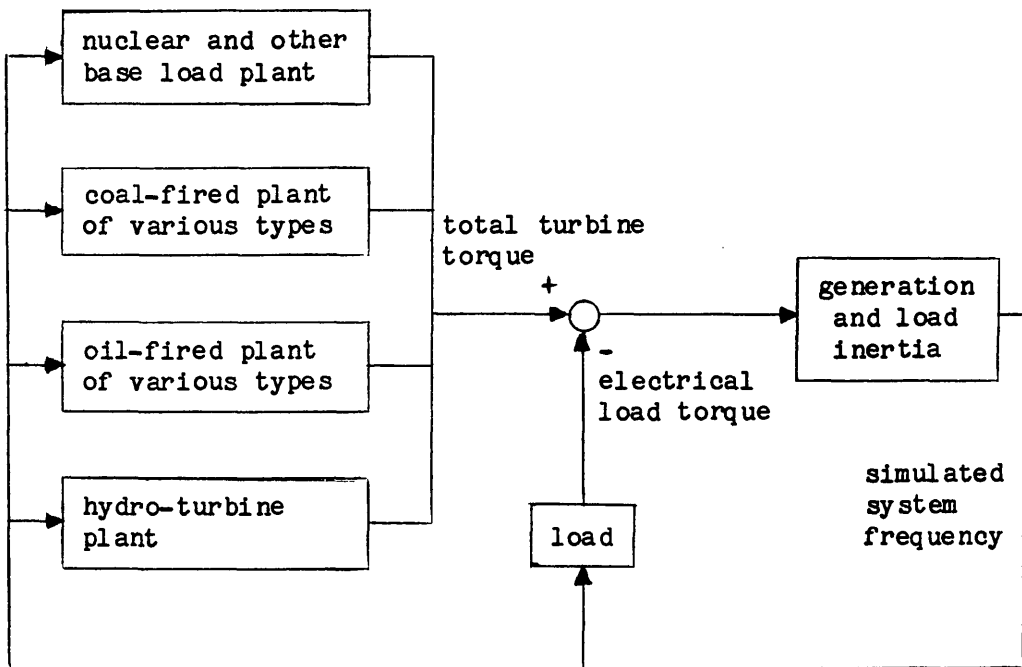


Figure 1.4 System response simulation

CHAPTER 2

THE POWER SYSTEM SIMULATOR

This chapter describes the implementation of the real-time power system simulator with particular attention to the arrangements for on-line tests and the design and development of the software. The choice of numerical integration method used to solve the power system model in real-time is also discussed. Development of the simulator continued throughout the study and evolution of its hardware structure and software organisation took place between site visits and so the test results were obtained with several different configurations. In the following description, reference will generally be made to the equipment in its later stages of development.

The real-time simulation is carried out digitally in a microcomputer system. Despite its digital nature, the simulator can be made to appear very much like a box of traditional linear electronics. However, the use of a digital simulation technique allows the direct modelling of process non-linearities required for large-signal tests.⁴⁹ It also provides flexible implementation of plant and operator interfaces which can then be adapted quickly to meet changing requirements. Of course, because continuous signals are approximated by discrete time series in the digital implementation, the input/output data rate must be fast enough to avoid compromising the accuracy of the simulation.

2.1 THE SIMULATOR HARDWARE

The real-time power system simulator was constructed using Intel Multibus products. The first implementations of the simulator used an Intel SBC 86/14 single board computer, which is

based on the 8086 16-bit microprocessor. In addition to its processor and memory, this board contains programmable digital input/output ports and additional modules expand this capability to include analog-to-digital (A/D) and digital-to-analog (D/A) channels. The board fits into a rack-mountable chassis with a Multibus backplane which permits additional single board computers, memory, and input/output cards to be included as required. This approach provides flexibility for future expansion.

A computer intended for real-time simulation work must be able to perform numerical calculations at high speed. In the past, the complexity of the mathematical model used in a simulator has usually been limited by finite computational speed rather than small memory size or inadequate interfacing facilities. The capability of this microcomputer system was enhanced by fitting a module containing an Intel 8087 numeric co-processor. This chip removes the burden of mathematical computation from the main processor by performing floating-point operations in hardware with consequent substantial speed improvements.

2.2 THE POWER STATION INTERFACE

Figure 2.1 shows in detail the arrangement of the simulator for on-line tests. As with many control experiments on real plant, the means adopted for test signal injection dictates the scope of investigation possible. In this case, the ideal injection point for simulated frequency deviation is the summing junction where the hydro-turbine governor compares the machine frequency with the frequency reference. An additional electrical analog input can usually be provided at this point in an electronic governor.

In the older mechanical-hydraulic governors, injection at the summing junction is impractical because speed sensing is performed

by flyball movement which is compared mechanically with a speed reference and used to operate a hydraulic piston. In these cases, however, it is possible to perform limited testing using the raise/lower controls of the speeder motor which positions the frequency reference (a mechanical component). By moving the frequency reference in the opposite sense to the simulated frequency transient, the governor can be perturbed just as if the test signal had been applied directly to the summing junction. The raise/lower controls normally drive a d.c shunt motor and so the rate of movement should be independent of the torque load on the motor. The speeder motor can, therefore, be expected to integrate the raise and lower pulses quite accurately. Various experiments show that, in practice, this is the case. This injection technique is established by controlling the raise/lower interposing relays from an additional relay box connected to a digital I/O port on the simulator. The injection signal can be disabled quite simply by unplugging the 240V a.c. supply to this box. In Figure 2.1, the availability of two injection techniques is notionally indicated with a switch.

Providing the measurement of turbine mechanical torque required by the simulator generally presents less of a problem. The alternator attached to the hydro turbine is normally grid-connected and hence running at near constant speed. A measure of its electrical output power, therefore, provides a good representation of the mechanical torque supplied by the turbine. When the electrical output power is measured, it is important to minimise the lag associated with power transducer filtering so the 'two-wattmeter' method of three-phase power measurement with its inherently fast response is desirable. Suitable digital filtering

is applied to the power measurement in the simulator to guard against the effects of electrical noise. At the start of a simulator run, a reading of the generator power output meter is supplied by the operator. This is used by the simulator to calibrate the generator power output signal.

2.3 CORRECTION FOR GRID FREQUENCY DEVIATIONS DURING A TEST

In both of the signal injection techniques, the real machine speed signal remains connected to the governor. This is necessary to ensure that proper control of the turbine can be maintained. The plant under test can be immediately returned to its normal operational mode simply by removing the simulated frequency from the governor. However, this arrangement also means that the turbine and governor under test will respond to genuine grid frequency variations because the generator is synchronised to the grid. However, the effects can be nullified by measuring the real grid frequency and then offsetting the simulated frequency deviation in the appropriate direction. In order to retain control of turbine speed if abnormal conditions arise, this correction is only applied if the grid frequency stays within the normal operational limits of 49.8 to 50.2Hz.

To obtain a measure of the grid frequency for this correction, a squared-up grid voltage waveform is used to generate interrupts in the simulator, and these cause the program to read a digital counter in the computer running at 1.2288MHz. A number of such readings are averaged in order to reduce the effects of mains waveform distortion and noise resulting from slight variation in the interrupt response time of the microprocessor. The input voltage waveform is taken from any convenient 240V a.c. outlet. It is essential that the square wave signal is applied through a

monostable because multiple cross-overs occur quite frequently due to switching glitches and other electrical noise. The interrupt controller on the single board computer is quite unable to cope with two interrupts in rapid succession on the same channel without suspending operation of the main program. The monostable ensures that only one triggering transition per cycle is applied to the interrupt input.

2.4 THE OPERATOR INTERFACE

The main processor board in the simulator was interfaced via two 8-bit parallel input/output channels to a BBC Microcomputer. This computer with its screen and keyboard is employed as an intelligent terminal to permit the selection of model parameters and configurations before executing a simulation. This approach was found to contribute significantly to security of operation. In contrast to an arrangement based on potentiometers and switches, the operator is forced by terminal prompts to consider test options and controls in a sequential manner and the risk of oversight is considerably reduced. The selected parameters are automatically stored on floppy disk for subsequent retrieval and printing to make a permanent record of the values used in all of the tests.

Once the simulation is running, the BBC microcomputer is used to monitor and display graphically the analog signal connections between the simulator and the real plant. The computer's screen shows the selected signal as a slow-speed trace rather akin to that of an ultra-violet recorder. A chosen signal can be displayed in real-time as a test progresses and this was found to be very useful. The time scale of the display can be altered and once the trace reaches the right hand side of the screen, it can be

restarted at the left hand side. A permanent record of tests is made separately as described in Section 2.6. This display system is also a powerful tool in the development and set-up stages because it can be used to examine any signal that can be applied to its A/D converter.

2.5 THE TEST PROCEDURE

It is important to achieve a 'bump-less' transition of the turbine from normal to simulator-connected running. This is straightforward with computer-based test equipment. Operating points for the internally represented generation blocks are selected during the simulator initialisation dialogue and the hydro-electric generator is set at a suitable loading from the control room desk. The simulator can be made active at any time thereafter by pressing a particular key on the operator terminal. The software automatically sets the initial consumer demand equal to the weighted sum of the simulated and real generator outputs. In this way, the simulator initial conditions are matched to the operating point of the real plant.

Once the simulator has been started, it is usual to allow time for the closed loop system comprising the real and simulated plant to settle, since it is rare for the hydro-turbine to be exactly in a steady state when simulator operation is initiated. The complete system can then be perturbed using demand trajectories of a preselected form and magnitude. These computer-generated perturbations are triggered by operating a simple digital switch connected to the simulator.

It is useful to interpose a potentiometer between the simulator output and the governor test input. This can be used to remove a standing test signal returning the turbine to its initial

operating point in a gradual fashion. In the event of a failure of the simulator system, this device can be very useful.

If speeder motor injection is employed to carry out tests on a mechanical-hydraulic governor, the maximum rate of governor reference movement is generally too slow to reproduce the frequency swing caused by an instantaneous demand step. However, by applying the perturbation at a finite rate, it is possible to obtain accurate test responses. Initially, a linear increase from initial to final demand was used for this purpose. This trajectory was not entirely satisfactory because it contains two discontinuities and the response to the second is superimposed on that of the first which results in a confused picture. A simpler form of finite rate transient can be obtained by passing a step through a first order lag. This type of perturbation produces more easily characterised responses and is probably more representative of actual loading disturbances.

2.6 DATA ACQUISITION

During test runs, signals of interest are presented as analog voltages to a computer-based data acquisition system based on a general-purpose microcomputer fitted with 12-bit analog-to digital conversion hardware, where they are recorded in a digital form. In the early stages of the project, a Vector Graphic MZ was used but this was later replaced by an IBM PC, allowing faster sampling rates, longer logging times and some filtering of the input signals. The provision of data acquisition facilities was maintained by Dr H. Davie and Dr M. Macaulay.

The logged data are stored on floppy disks and subsequently plotted using the computer. The use of a computer-based logging system offered various advantages in that the plotted data can be

scaled readily in both voltage and time axes allowing sections of the recorded signal to be expanded for detailed examination. Duplicate copies of the logged data can also be made easily.

The use of a data logger with analog inputs is not entirely satisfactory because some of the signals recorded are already available as digital quantities within the simulator which measures them for its own purposes, taking the average of a number of samples. In order that these quantities can be recorded by the logger, they are once again converted to analog voltages and subjected to a noisy environment. A more satisfactory arrangement would incorporate a direct digital connection between the logger and the simulator allowing such signals to be recorded without any unnecessary interconversions, saving on execution time and avoiding the ingress of noise. In fact, if sufficiently powerful hardware was available, a fully developed form of the equipment would perform both functions on the same computer.

2.7 SOFTWARE FOR REAL-TIME SIMULATION

It is unfortunate that the adjective 'real-time' is frequently used to describe computer systems that are not in any way synchronised to physical time; rather, these computers are 'interactive', having a response sufficiently fast that they may operate on-line and service their user's request with reasonable speed. The 'real-time' nature of the power system simulator is quite different. The complexity of a general purpose multi-tasking operating system like RMX⁵⁰ is not required and an interrupt subroutine and a few lines of code in the main simulator program are sufficient to achieve synchronisation with real time and control the operation of the equipment. Figure 2.2 outlines the structure of the software for the simulator.

The dynamic model solution computed by the power system simulator must be produced in synchronism with physical time. To achieve this, a hardware counter/timer operating from a 153.6kHz clock is used to generate processor interrupts at a specified rate (600Hz). The subroutine which handles these interrupts maintains a count of the number of times it has been called. In order to provide filtering of the turbine power output measurement, the subroutine also obtains an A/D conversion value from the appropriate channel and adds it to an integer sum of these values. When the specified number of interrupts have occurred (30 for an integration interval of 0.05s), a flag is set by the subroutine and the count of clock intervals is reset to zero. The main program remains in a waiting loop until it finds that this flag has been set. It then calculates an average value of turbine output from the integer sum of the A/D values and performs one step of the simulation procedure. The simulated system frequency signal to be injected and other signals to be recorded are then written to the appropriate D/A channels. Finally, the timing flag is reset and the main program returns to the waiting loop.

A second interrupt handler activated by the a.c. supply cross-over signal obtains values from the 1.2288MHz timer for grid frequency measurement. These values are written to a circulating buffer and are then used by the main program to calculate an averaged grid frequency value. The cross-over interrupt has a higher priority than the real-time synchronisation interrupt to minimise variation in the delay between the cross-over itself and the point at which the timer is actually read.

Interrupts of both types continue to occur throughout the execution of one step of the main program. To avoid corruption,

the processor interrupts must be temporarily disabled when the main program accesses the values that are obtained by the interrupt subroutines. The interrupt handlers are restricted to integer arithmetic so that use of the 8087 numeric coprocessor is avoided. There is then no danger of problems with the 8087 such as overflow of the internal stack in the event of two nested interrupts.

2.8 SOFTWARE DEVELOPMENT FACILITIES

In the early stages of the project, software development was carried out on an Intel Microprocessor Development System (MDS). This process was later transferred to an IBM PC AT which offered considerably reduced compilation times through the use of its hard disk. The programming language used was an Intel implementation of Fortran specifically intended for stand-alone system development. It provides additional procedures to handle peripheral devices such as input/output ports, timers and interrupt controllers. Using this compiler, it is also possible to deal with processor interrupts entirely within the high-level language. This meant that low-level assembly language programming was only used for a few special-purpose routines where precise handling of individual data bits is required or where particular control of the processor itself is important.

The program to be tested can be 'down-line loaded' from the MDS to the target system, in this case the 86/14, via a serial interface and then debugged using the rather primitive facilities of a machine code monitor. Alternatively, an in-circuit emulator (ICE) may be used to provide a considerably more powerful debugging facility. For example, the emulator maintains a trace of the instructions and data that have been processed. It also

provides details of any interrupts received by the microprocessor. The emulation can be stopped at the press of a key and so a program that is operating incorrectly can be caught at the particular time when its execution starts to go wrong. Examination of the trace information coupled with the use of the other ICE facilities will often reveal the nature of the fault.

The final version of the machine code for a particular simulator is normally stored in erasable programmable read only memory (EPROM) chips which are installed in sockets on the single board computer. Operation of the computer reset button is then sufficient to set the program running. This means that the simulator is a stand-alone system with no need for floppy disk storage or keyboard input to load and run its software. This is a considerable advantage when the equipment is used for real plant tests.

Although the simulator software is developed and debugged in the laboratory, experience has shown that limited revisions may be required on-site. The Intel MDS is not readily transportable and so an IBM PC is normally taken on-site to permit such revisions. No ICE facilities are employed with this system so debugging facilities are restricted to the machine code monitor incorporated in the down-line loader.

2.9 METHODS OF NUMERICAL INTEGRATION

Due consideration was given to the selection of the numerical integration method used to solve the power system models in the simulator. A system response simulation is an initial value problem in a system of ordinary differential equations and there is available a wealth of published work on possible numerical integration techniques, see, for example References 51, 52, 53,

54, 55 and 56. However, few authors mention real-time applications where the requirements are rather different. Indeed, many integration methods exist which allow a system to be simulated very accurately and efficiently, but many of these are only suitable for use in non real-time or 'off-line' applications.

A numerical integration technique used in a real-time simulator must be able to cope with discontinuous inputs and model non-linearities and it must provide a model solution which can be made to proceed in synchronism with the outside world. Absolute accuracy is not the prime consideration because of limited measurement accuracy and the finite (12-bit) resolution of the A/D and D/A convertors.

The ease of implementation of the Euler method is an almost over-riding consideration, but, in fact, there are other sound reasons why this algorithm should be used.

2.9.1 Review of the Methods Available

A number of integration techniques achieve high performance in off-line simulation by adapting their integration interval according to the needs of the solution as it progresses. These variable-step methods provide a complete problem solution in the minimum computation time but may be very slow at some stages, particularly in the region of discontinuities where repeated reduction of the step size is necessary. This makes them unsuitable for a simulation which must proceed in synchronism with real time.

Numerical integration methods of fixed (and variable) step length may be divided into those which operate on information available in the current integration interval, the single-step methods, and those which draw on information available in previous

intervals as well. The second group, the multiple-step methods, are efficient in 'smooth' problems where derivative evaluations are computationally expensive⁵⁶, but they have difficulty with discontinuities⁵¹ and are, therefore, not as suitable for use in a real-time simulator where the inputs are not smooth. Predictor-corrector algorithms^{54,55,56} are in this category.

A further classification can be made into methods of explicit form where a calculation stage draws only on numerical values formed in previous stages and implicit methods where this restriction is relaxed. The backward Euler and trapezoidal rule are implicit methods of first and second order respectively. The trapezoidal rule, in particular has been widely used in power system studies.^{57,58,59,60} These methods are unconditionally stable for poles in the left hand half of the complex plane,^{56,61} but they require an iterative solution. To avoid this, the differential equations can be incorporated in the integration algorithm, but, for non-linear systems, this is awkward to carry out and not always successful. State variable limits are also more difficult to apply.⁶¹ These drawbacks preclude the use of implicit methods for the solution of the non-linear equations used in the real-time simulator.

After these eliminations, only single-step explicit 'Runge-Kutta' methods remain.

Use of the simulator involves the coupling of a discrete-time system to continuous-time plant and so simulation accuracy must be evaluated in the continuous-time domain i.e. the simulation error must be evaluated over all time, t , not just at the successive points of the solution, $t=kh$ (where h is the integration step length and k is an integer). A previous study²⁷ has shown that

this consideration tends to favour methods of lower order, in particular the first-order Runge-Kutta 'Euler' method. The Euler method can achieve a higher continuous accuracy with a given processor computation speed than the fourth-order Runge-Kutta method, notwithstanding the higher point accuracy and longer step length possible with the latter. This is particularly true in the region of discontinuities.

There is a further problem with the higher order Runge-Kutta methods because correct implementation requires new A/D conversion values at each intermediate stage of the algorithm. This is inconvenient and erodes the computation time saved through the use of a longer step length.

The Euler method has poor stability for poles close to the imaginary axis but fortunately this is not a problem. The dynamic behaviour involved in the simulation of power system response to loading disturbances is generally well-damped with a predominance of poles on or near the real axis of the complex plane. The complexity of high order methods which achieve stability for poles near the imaginary axis is, therefore, unnecessary.

2.9.2 Multiple Rate Integration Schemes

Generally, power system dynamic models exhibit widely different rates of change of variables or of groups of variables.⁵¹ This 'stiff' system property can result in excessive computation times and round-off errors if the slower parts of the model have to be integrated with step lengths short enough to provide stability for the fast components.⁶¹ Implicit methods and other more specialised solution algorithms^{53,54,56,62,63} are able to avoid this problem but these are unsuitable for implementation in real-time due to their complexity and their use of iterative

calculations and variable step lengths.

In power system studies, subsets of equations of differing response times are easily identified and there are often only a few interface variables between subsets.⁵¹ An intuitive grouping of the equations guided by the physical partitioning of the modelled system is, therefore, effective. The subsets can be solved using different step lengths (and/or methods) consistent with the rates of change of their variables and a large saving in computation time can be obtained in this way. Such schemes have been used for off-line simulation in transient stability studies⁵¹ and for real-time simulation of a fossil-fuelled power plant in an operator training simulator.⁶⁴

Formal model decomposition algorithms have been applied to the long-term simulation of power systems.⁶⁵ Although these methods may achieve a greater computation saving than the ad hoc approach described above, they are not easily applied to large-signal, non-linear models. The ad hoc scheme also has the merit of simplicity and requires less programming effort.

A multiple rate integration scheme was used for the off-line simulation carried out in this study. This allowed simulation runs of complex systems to be obtained rapidly. The power system model can be decomposed simply by separating the equations for the different generation types. For example, the thermal unit models can be integrated adequately at a rate slower than that required for the hydro-turbine models. If a greater computational saving is necessary, the thermal models could be split into boiler and turbine sections. The boiler equations could then be integrated at an even slower rate. This ad-hoc approach to decomposition can be guided by the time-frame of the response of the various

components.⁶⁶

In the work reported here, the real-time simulator did not reach a sufficient complexity to require multiple rates of integration. However, if larger problems were to be studied, it might be advantageous to use a multiple rate scheme to relieve the computational load on the hardware. This could be implemented most easily on a multiprocessor system and so this possibility will be discussed further in Chapter 5.

2.9.3 Implementation of the Euler Method

The Euler method was used in the power system simulator and the plant simulator described below. It was also used in all the off-line simulation studies carried out in the course of this work. This provided the maximum correspondence between on-line and off-line conditions.

The integration algorithm can be described quite simply in words: Calculate the values of the model derivatives i.e. the derivatives of the state variables, multiply these by the integration step length and add the result to the previous value of the state variable, then repeat. Expressions for the initial conditions of the state variables can be obtained in terms of the model operating point by setting the derivatives to zero.

The adequacy of an integration step size for a particular model was checked by the simple expedient of repeating a sample off-line simulation with a smaller step size and checking that no change in the results could be seen.⁵⁶

2.10 LABORATORY TESTING FACILITY FOR THE SIMULATOR

In order that correct operation of the power system simulator can be verified before it is coupled to the real hydro-turbine plant, a general-purpose 'plant' simulator was established using

an IBM PC fitted with analog-to-digital and digital-to-analog conversion hardware. A simulation of a hydro-turbine and its governor was programmed using the Microsoft assembler and Fortran compiler. Real-time synchronisation is achieved using a timer internal to the PC and the plant interfaces are emulated in detail using the same voltage scalings as the Sloy microprocessor governor. A non-linear model of the hydro-turbine and its governor is used so that the simulator represents the behaviour accurately over almost the full operating range. Alternative parameters can be selected easily in the initialisation stage. The Euler integration method is used with a step length of 0.01s and the model equations and data are given in Appendix 1.

This equipment is used in the laboratory during the development of the power system simulator. It is also used, both in the laboratory and on site, for trial runs with particular simulator configurations intended to verify that untoward situations will not occur when the equipment is coupled to the real plant. Several versions were developed to cater for the different plant types encountered. These included Sloy turbines with either electronic or speeder motor injection and, later, Stornoway diesel engines. The plant simulator was used to test various other items of equipment including an implementation of the load controller described in Chapter 8.

2.11 OFF-LINE SIMULATION

An IBM PC AT programmed with Turbo Pascal was used for the majority of the off-line simulation work carried out in connection with this study and a simulation package was established with graphics facilities. In order to obtain results in a reasonably short time, a multiple rate Euler integration algorithm is used as

discussed in Section 2.9.2

Special arrangements must be made when Pascal is used for simulation: The variables in the model procedures must be made global otherwise they will not retain their values from one integration step to the next. This approach is somewhat at odds with conventional Pascal usage but the alternative of long parameter strings in procedure calls is impractical. However, the use of variables that are only declared once is much less error prone than the COMMON block construction of Fortran. The variables for a particular model are contained in a 'record' so that multiple copies of a particular model can be used without changing all the variable names. The model procedures have three sections: A dialogue phase, an initialisation phase and an execution phase. This avoids the need for extensive parameter passing.

Off-line simulation was used in the development and evaluation of the power system models used in the simulator. The generation block and alternator models were implemented as separate procedures which could be included or not depending on the mix of plant to be studied. The models were then implemented in the real-time simulator in a fully developed form. The simulation package was very much more interactive than the real-time simulator equipment and so it was much more convenient for investigating changes of parameters and configurations.

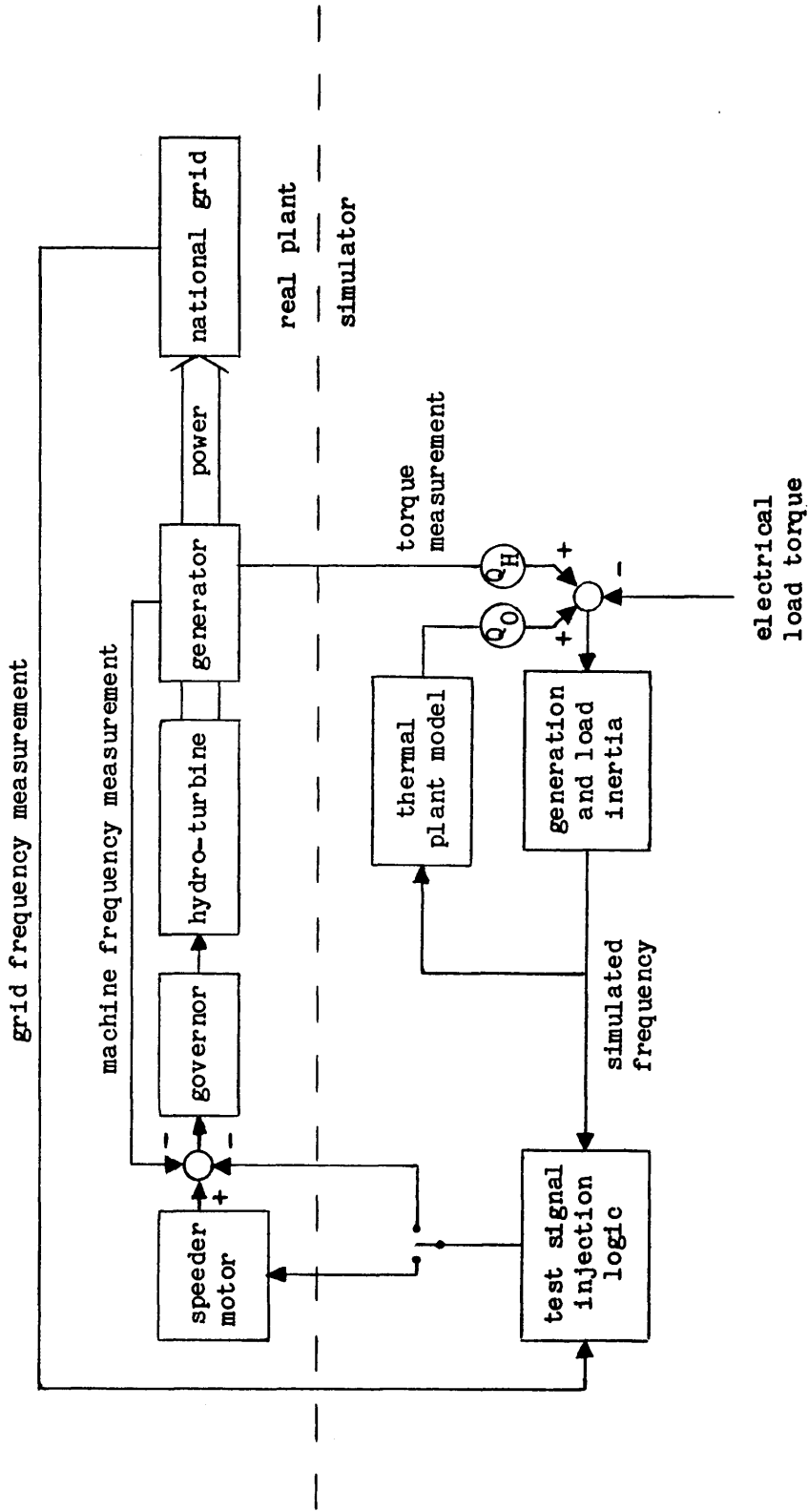


Figure 2.1 Arrangement of the simulator for on-line tests

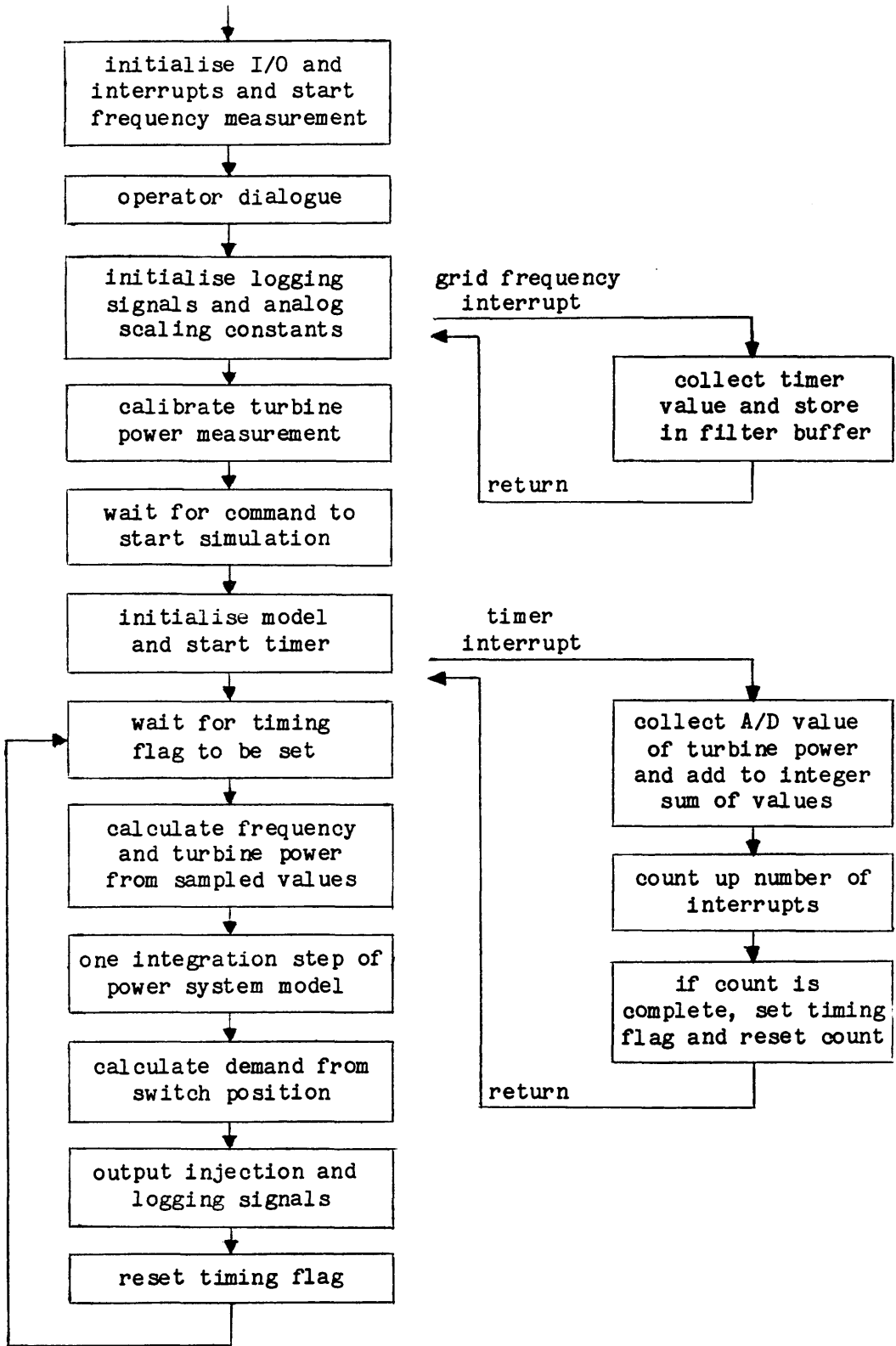


Figure 2.2 Structure of the simulator program

CHAPTER 3

MODELS FOR POWER SYSTEM RESPONSE SIMULATION

Realistic mathematical models of a number of power system components had to be assimilated in a form suitable for real-time simulation before the simulator could be used to study problems of practical interest. Included in the list were boilers burning coal, oil or gas; steam turbines; nuclear plant; generator inertia; and consumer loads. It is the purpose of this chapter to describe the dynamic models used in the hydro-thermal power system study.

The general state of power system simulation will be reviewed in the context of the UK system and compared with power station and grid control centre operation in practice. The features of an oil-fired boiler-turbine model used for preliminary tests will be outlined briefly before a coal-fired plant model is described in full. This second model was used for more detailed studies of a mixed hydro-thermal system reported in Chapter 6. The development of co-ordinated control schemes for boiler-turbine units will also be considered. To complete the power system model, a mathematical description of the variation in consumer demand with system frequency will be presented along with a single alternator model of the generators.

3.1 POWER SYSTEM SIMULATION

A wealth of material has been published on power system simulation applied to a number of problem areas such as transient stability,^{67,68,69,70} system operator training,^{58,71,72,73} boiler-turbine control⁷⁴, long-term system dynamics,^{44,59,75} and, in the USA, automatic generation control.^{57,76,77} Although the time scales are different,⁶⁶ a substantial common ground exists between

these applications.

The response time of a large fossil-fired boiler is of the order of minutes,⁷⁸ so transient stability analyses for steam plant usually include the dynamics of the turbine but assume that the boiler pressure remains constant over the time-span of interest (10s). Conversely, longer-term studies do not need to include detailed models of synchronous machine behaviour.

The models used in studies of governor response should be valid for the first few minutes following a disturbance. Thereafter, measures taken by grid control engineers such as the starting of gas turbine or pumped-storage plant take effect and governor response is no longer the primary concern. It is not necessary to model longer-term effects such as load increases due to voltage regulation at load bulk supply points. These features are more relevant to studies of load-shedding policies.⁷⁵

A system response model has been developed by the CEGB.^{2,44,79} This model has been validated against system tests⁸⁰ and it has been used to study the response of pumped-storage plant and to review load-shedding relay policies.⁴⁴

A simulation methodology for long-term power system dynamics has been developed in the USA under the direction of the Electric Power Research Institute (EPRI).^{60,75,81} It has been used in studies of system behaviour following major disturbances^{82,83} and automatic generation control.⁷⁷ This package is intended to provide a complete simulation of a power system over both short and long time scales and so it includes representation of individual machines and the transmission network. A transient stability program is used for a period of about 10s following an electrical disturbance. Thereafter, the simulation switches to a long-term mode where the inter-machine oscillations are removed by

artificially increasing the damping term in the swing equations of the individual machines.⁸⁴ The trapezoidal integration method is used to provide numerical stability for a step length appropriate to the components of the long-term model. The dissimilar responses of generating units can lead to excessive tie-line loading following large system upsets,⁸⁵ and so a load-flow calculation is included so that protective tripping of transmission lines can be predicted. The software has been written in such a way as to allow the selection of model configurations by appropriate choice of data without any need for recoding.⁸⁶ However, some difficulty has been encountered in recent EPRI work to develop a 'production grade' program for full simulation of power systems for periods of up to 20 minutes.^{59,60} It has been found that the modelling requirements for long-term simulation are incompletely defined and that little data is available for the parameters of the models used in the simulation.

3.2 A COMPARISON OF NATIONAL SYSTEMS

International variation in the relative capacities of different types of generating plant is considerable for economic, historical and political reasons. There is high dependence on nuclear power in France, Belgium, Sweden, Taiwan and Korea⁶ and considerable hydro-electric development in Norway, France, Italy, Canada and the USA.⁸⁷

Much work on power system modelling has been done in the USA, but the grid system in the North American Continent differs markedly from that in Britain in a number of respects. The American system is about six times larger.^{78,87} Some of the load and generation centres are very widely separated and, therefore, tend to be less tightly coupled in the transmission system than the supply and load points in the UK and European systems. 3600rpm

generators are difficult to construct so 1800rpm generators with two pairs of poles are frequently used in the 60Hz American system. This tends to lower the system inertia for reasons discussed further in Section 3.8. In the USA, considerable attention is directed to the automatic generation control equipment (AGC) preserving the scheduled power interchanges between the individual electricity supply utilities, which are mostly in private ownership. The grid frequency is very tightly controlled in order to maintain the power transfers in the system. In the UK, programmed transfers between the CEGB regions, the SSEB and the NSHEB are regulated adequately by manual control at the grid control centres.

3.3 PROPORTIONS OF PLANT IN THE UK SYSTEM

The approximate proportions of plant capabilities in the UK system are as follows:⁸⁷

Coal	61%
Oil	21%
Hydro	2%
Pumped-storage	5%
Nuclear	11%

The corresponding values for the Scottish system are:

Coal	36%
Oil	28%
Hydro	10%
Pumped-storage	6%
Nuclear	20%

Gas turbines are expensive to run for long periods and are, therefore, only used for 'peak-opping' at times of very high demand. However, they can be started quickly and are used in emergencies. The balance between coal and oil plant depends on the relative cost of these fuels which can be quite variable. However, oil-fired boilers are generally more flexible and are, therefore, more suitable when generation is required for short periods. The mix of generating plant and frequency regulation of the system

varies with the daily demand curve and can be affected greatly by industrial action.⁸⁸

3.4 POWER STATION AND GRID CONTROL CENTRE OPERATION IN PRACTICE

In order to evaluate more effectively the wide range of power system response models available, some time was spent observing at first hand the operation of power stations and grid control centres in the UK. Hams Hall 'C' (6x65MW, non-reheat), at that time burning natural gas; Rugeley 'B' (2x500MW, reheat, coal-fired) and Peterhead (2x660MW, reheat, oil or gas-fired) were visited and inspected in some detail as were a number of hydro-electric stations in the NSHEB area. The operation of the coal-fired boiler-turbine units at Longannet (4x600MW) and the pumped-storage units at Dinorwig (6x300MW) was observed during a longer period. The system control function was seen at the NSHEB, SSEB and CEGB Midlands Region grid control centres.

3.5 NUCLEAR PLANT

Dynamic models of nuclear plant are available⁸⁹, but, as indicated in Section 1.2, reactors in the UK play no part in system regulation and so they are represented in the simulator by a power contribution that does not vary with frequency.

3.6 THERMAL PLANT

Realistic dynamic models of coal- or oil-fired boiler-turbine units are essential in a simulation of the UK power system because of the predominance of this type of plant. The system frequency is normally regulated in the medium term using pumped-storage plant. However, large fossil-fired units should control the initial frequency swing and will be required to contribute significantly in the event of a failure of the pumped-storage units or a system split which leaves a section of the system without such plant. This is a possible occurrence because all of the pumped-storage

plant is in relatively remote parts of the grid system.

3.6.1 Thermal Plant Operation

The arrangement of a modern coal-fired boiler-turbine unit based on the reheat cycle is outlined in Figure 3.1 and a much simplified description of its operation follows: Water is circulated in the tubes forming the wall of the furnace and the steam produced separates in the boiler drum at 360°C and 160bar. It then flows through the superheater where its temperature is raised to about 560°C. This improves the thermodynamic efficiency of the overall cycle and ensures that the steam entering the turbine is absolutely dry. The steam flows from the superheater through the governor valves to the high pressure (HP) turbine and is then taken back to the boiler where it passes through the reheater at a pressure of about 32bar to have its temperature restored to 560°C. The steam then flows through the interceptor valves into the intermediate pressure (IP) cylinder and subsequently into two, or possibly, three low pressure (LP) cylinders. Finally the steam, at a pressure of about 0.04bar (absolute) is condensed and returned to the boiler drum by the boiler feed pump which is, in fact, driven by a small steam turbine. Some thermodynamic advantage is obtained by passing the condensate through a series of feed water heaters where its temperature is raised to about 252°C by steam bled from the turbine at various stages. Fans maintain a supply of combustion air to the furnace and a proportion, the 'primary' air, is used to transport pulverised coal from the mills to the burners on the furnace wall. Usually, all the turbine rotors are mounted on a single shaft along with those of the alternator and the exciter.

Traditionally, thermal units have been controlled in a 'boiler-following-turbine' mode of operation where the governor

valve is positioned according to the frequency of the system and the desired loading on the unit. Movements of this valve cause a change in steam flow rate from the boiler drum through the turbine stages. For an increase in flow caused by a fall in system frequency, say, the steam pressure in the boiler drum falls. A 'master pressure controller' senses this fall in pressure and increases the fuel input to the boiler by increasing the speed of the coal feeders or the rate of oil supply to the burners in an oil-fired furnace. If a large change of firing is required on a coal-fired boiler, then it is necessary to change the number of coal mills in service. Changes in firing take some time to work through to an increase in steam production.^{3,90}

3.6.2 An Example of Plant Operation - Load Changes on a 600MW Unit

Some time was spent at Longannet Power Station observing the operation of a 600MW unit. Only scheduled load changes were observed because the unit was operating at a high load level without free governor action. However, observation of the plant behaviour illustrated two things: Firstly, that governors on high merit plant like the Longannet unit are often wound well out of range with the speeder motor so that the steam valves are fully open. This achieves electricity production at maximum efficiency but means that the unit will not contribute to frequency regulation without manual intervention. Secondly, the plant behaviour is to an extent unpredictable and time-dependent with a complex interaction of a number of components.

Figure 3.2 shows the behaviour of the plant during a mill changeover. The same behaviour would, in fact, be observed if the unit was required to decrease its output by 100MW and immediately increase it again by the same amount because a load change of this size is implemented by manually starting or stopping a coal mill.

Six mills out of eight available are required for full load on the unit and so one mill provides fuel for about 100MW. Closer control of firing is obtained by varying the speed at which the coal is fed to the mills in service.

When the process of taking a mill out of service begins, the unit output rises initially as the pulverised coal supply from the mill increases as it empties after the feed is stopped. Once the mill has emptied completely, the unit output falls quite rapidly. When the fuel/air valves are closed, the unit output rises again as the primary air supply to the removed mill becomes available for the other mills.

When the new mill is put into service, the unit output drops initially due to a reduction in the primary air supplied to the other mills when the new mill is warmed through with air before it is supplied with coal. The output then rises, taking about 30 minutes to reach a steady state.

Notice that there is a temporary drop in power output towards the end of the operation due to a fall in superheater temperature as feed water is sprayed into the steam before it enters the superheater in order to arrest the temperature drift. The split in the two-sided drum level measurement is reduced after the mill change because the new burner combination provides a more even flame.

Although it does not show the response of a regulating thermal unit to a system frequency excursion, this example does illustrate the difficulty in modelling thermal plant. The behaviour has unpredictable aspects and only some of the plant is automatically controlled. Detailed modelling of a particular unit's behaviour would be very difficult to accomplish and would not represent the aggregate behaviour of all the boiler-turbine

units on the system. It is only possible to produce a model which behaves in a fashion that is typical of thermal plant. Experience shows that the observed behaviour varies considerably from power station to power station.⁴⁴ The dynamics of all units are different, and differ in themselves with time and with load level.

Elements of the plant dynamics are time-dependent caused by factors such as boiler tube slagging, variability in condenser vacuum, air leakage in the mills and air heaters, mill wear and coal quality and wetness. The inability of existing control loops to cope with these and similar situations leads to many instances where the operator has to revert to manual control.³ Mill control is particularly difficult. Different mills have different responses and their influence depends on the position of the associated burners on the furnace wall.

While many units operate with at least some degree of manual control, it must be assumed that the average effect of manual intervention on a number of units is comparable to the effect of a reasonable automatic control.

Tests are carried out on the national grid to investigate the response of thermal plant to system disturbances. However, their realism is doubtful because the unit operators are forewarned and have their plant in a higher state of readiness than is normal.

3.6.3 Some General Observations on Thermal Plant Modelling

Prior to a discussion of particular boiler and turbine models, it is appropriate to state some general points relating to thermal plant modelling.

3.6.3.1 Boiler Auxiliaries

In a system response simulation, it is not necessary to model all of the components of a boiler-turbine unit. It is generally held that while feed water control on drum boilers is critically

important to plant operation, it does not greatly affect the dynamic behaviour of the unit power output. This is also true for temperature control.^{44,91} In Figure 3.2, the 600MW unit shows a dip in power output that can be associated with a fluctuating superheater temperature. However, this was the result of manual intervention and it is assumed that, when the outputs of several units are averaged, the effects of temperature deviations will cancel out.

3.6.3.2 Turbine Bypass Circuits

In United States and Continental practice, various turbine bypass circuits are employed, particularly with once-through boilers. These are used during unit start-up and shut-down or to accommodate load rejections without tripping the unit. Steam bypass circuits are not normally provided on British fossil-fired plant⁹² and are, therefore, not included here.

3.6.3.3 Interceptor Valves

The interceptor valves and their control were not included in the models used here because their action is normally restricted to limiting overspeed in load rejection situations⁹³ and 'fast valving' to improve transient stability.⁹⁴ (Fast valving is the term applied to the use of special hydraulic components to effect rapid movement of the interceptor and, possibly, governor valves, on the detection of a power system fault, usually by means of an acceleration signal.^{95,96}) Its contribution to system frequency regulation is, therefore, infrequent and rather unpredictable and its inclusion here would not be beneficial. Use of the interceptor valve for normal governing could increase the spinning reserve capability of a unit.⁹⁷ However, this would result in a loss of efficiency and is, therefore, not common practice.

3.6.3.4 Range of Validity

The model used should be valid over a range of at least 50 to 100% of full load. The range of validity of linearised models is not sufficient and a non-linear model must be employed. This is not a problem because non-linear equations often relate clearly to the physical properties of the plant components and can be implemented quite easily on a computer-based simulator.

3.6.4 Boiler Models

A number of very detailed models using 100 equations or more are available to describe the dynamic behaviour of large boilers, see for example Kwan⁹⁸ and Armor⁹⁹. These and other detailed models of parts of the plant such as the coal milling equipment,¹⁰⁰ feed water system¹⁰¹ and draught plant¹⁰² are intended for use in the development of boiler controls and are too complex for power system response simulation.

Boiler simulators have been constructed for the purposes of operator training,^{103,104} but these are unsuitable for this application because the expertise of a fully-trained operator is required to complete a model of boiler response.

Some of the published models describe 'once-through' designs usually intended for supercritical steam conditions. These are not directly applicable in this study because there is only one boiler-turbine unit (300MW) of this type in the UK.⁸⁷

The boiler models used to study the response of the UK⁴⁴ and USA^{59,60} systems are roughly similar and it has been shown that boiler models of apparently quite different structure can be essentially equivalent.¹⁰⁵

3.6.5 A Thermal Plant Model for Preliminary Tests of the Simulator

A simple non-linear boiler model of a 160MW boiler-turbine unit developed by Astrom and Eklund¹⁰⁶ was used in earlier work at

Glasgow University by Thompson.¹⁰⁷ This model is based on physical principles with one differential equation to describe the rate of change of boiler drum pressure:

$$\frac{dp}{dt} = - a_1(u_2 p^{5/8} - a_4) + a_2 u_1 - a_3 u_3 \quad 3.1$$

where p is the drum pressure, u_1 is the fuel input, u_2 is the governor valve position and u_3 is the feedwater flow. a_1 - a_4 are constants derived from experiments on the plant. Thompson added representations of the oil fuel and feed water circuits and their controllers. Both circuits were described by first-order lags and the controllers were of proportional-plus-integral form. The boiler drum level was obtained by integrating the difference between the feed water and steam flow rates.

Two algebraic relationships were used by Astrom to derive the turbine output power and boiler steam flow. Thompson replaced these by a more detailed representation of the turbine similar to that described below in Section 3.6.6.7.

Astrom assumed a linear relationship between governor valve position and steam flow, and so Thompson was able to incorporate a more detailed governor valve description by replacing u_2 in Equation 3.1 with a variable u_4 which was the per unit steam flow. The equation used (3.12) is given in below in Section 3.6.6.6.

This boiler-turbine model was used in early versions of the power system simulator for the purposes of establishing the feasibility of the technique for on-line studies. A simple description of the governor valve was re-instated in order to remove the computational burden associated with the elaborate expression used by Thompson.¹⁰⁷ Although adequate for preliminary tests, this thermal plant model proved unsatisfactory in that its form was not suited to the selection of alternative parameters and adaption to represent other plant. The results of tests using this

model are presented in Chapter 4 and the equations and numerical data used are listed in full in Appendix 2.

3.6.6 A More Flexible Thermal Plant Model

Later versions of the power system simulator used a thermal plant model based on that used by the CEGB in system response studies^{2,44} and in earlier work at Glasgow University by Aitken.¹⁰⁸ Although the turbine section was substantially similar, this model offered a number of advantages over that described in the previous section. The components of the boiler were more readily identified allowing more flexible selection of parameters. The model also proved to have a greater ability to cope with extreme disturbances making the simulator more robust in its operation. Where a specific source of data is not indicated below, the values used were obtained by Aitken¹⁰⁸ from NSHEB staff. In the final equation set, all variables are normalised with respect to full load values.

The boiler model used by the CEGB for system response studies is outlined by the block diagram in Figure 3.3. The components of the fuel feed system model do not directly correspond to particular items of plant but they are chosen to have an overall response characteristic similar to that of the real plant auxiliaries.

3.6.6.1 Master Pressure Control

The drum pressure error, p_e is the difference between the boiler pressure, p_b and a set-point, p_s (1pu):

$$p_e = p_s - p_b \quad 3.2$$

The integral term of the pressure controller is described by

$$\frac{dy}{dt} = k_1 p_e \quad 3.3$$

where y is the output of the integrator. The master firing control signal, M is given by

$$M = y + k_2 p_e \quad 3.4$$

This signal is limited to 0.2 to 1.2pu. Aitken found reasonable values of k_1 and k_2 to be 0.015 and 5.0 respectively. Derivative action is not normally included in a master pressure controller due to unsatisfactory operation in practice because of short plant lags and dead times.¹⁰⁹

3.6.6.2 Fuel Feed System

Modelling the fuel feed system in a general way is difficult because the installed equipment varies considerably from unit to unit. However, typical dynamic behaviour can be obtained with the following model.

Coal transportation to the coal mills is described by a pure time delay of length, T_d :

$$E_m = M e^{-sT_d} \quad 3.5$$

where E_m is the coal feed rate to the mill. E_m is limited to the range 0.001 to 1.05pu. The implementation of fuel feed delay used in the power system simulator differs slightly from that used by the CEGB. It is difficult to determine whether a particular disturbance would require the starting of additional coal mills. In an off-line simulation, a mill start delay can be modelled by limiting E_m to a particular value until a set time has elapsed following an increase in demand. In a simulator for on-line tests this is not possible because disturbance events and power inputs are not predetermined. A T_d value of 60s⁸⁰ was used to approximate the effect of coal feed transport delay and mill starting time combined over several units.

The mill grinding process is represented by a first-order lag:

$$\frac{dF_i}{dt} = (E_m - F_i) / T_c \quad 3.6$$

where F_i is the fuel that is picked up by the primary air. A

suitable value for T_c is 45s.

There is some storage of pulverised fuel in the mills and coal/air pipes and this is described by

$$\frac{dF_d}{dt} = (F_i - Q_i) / T_m \quad 3.7$$

where F_d is the fuel density and Q_i is the input to the boiler. A suitable value of the time constant, T_m is 2s. F_d is also limited to the range 0.001 to 1.05pu.

The delay in the fans providing combustion air is assumed to be negligible⁹¹ and so the heat input to the boiler is the product of control signal and fuel density⁴⁴:

$$Q_i = MF_d \quad 3.8$$

(It is assumed that the feed water enthalpy is constant.)

3.6.6.3 Boiler Drum

The boiler drum pressure variation is described by

$$\frac{dp}{dt} = (Q_i - W_1) / T_b \quad 3.9$$

where W_1 is the steam flow rate and a suitable value for the time constant, T_b is 240s.⁸⁰

3.6.6.4 Representation of Oil-fired Plant

Oil-fired plant may also be represented with this model by reducing the fuel feed delay, T_d and mill time constants, T_c and T_m . The boiler time constant, T_b should also be reduced slightly because oil-fired furnaces are physically smaller than coal-fired furnaces of the same rating.

3.6.6.5 Steam Turbine Governor

The governor is described by the differential equation

$$\frac{da}{dt} = ((f_{ref} - f_s) / b_p - a_x) / T_g \quad 3.10$$

where $T_g = 0.1s$ and the governor output, a_x is limited to the range 0.001 to 1.0pu. f_{ref} is the governor frequency reference, f_s is the system frequency and b_p is the governor droop.

The valve actuator equation is

$$\frac{da_2}{dt} = (a_x - a_2) / T_{gv} \quad 3.11$$

where a_2 is the valve position. Many hydraulically operated valves are opened under oil pressure and closed by the action of a spring and so they can be closed very quickly at the expense of slower opening.¹¹⁰ This asymmetrical governing was included in the model because system test results cannot otherwise be reproduced.^{44,91} For opening, $T_{gv}=0.1s$ and, for closing, $T_{gv}=0.7s$. Additional small lags or a pure time delay could be added to the governor and valve actuation models if required,¹¹⁰ but this was not done here.

The governor droop, b_p is normally found to vary with operating point.⁹¹ Although the overall droop may be 4%, the incremental droop is often lower at low load levels and may be very large near full load with almost no governor response to frequency changes. Analysis of system disturbances shows that overall system regulation (droop) is often much higher than the specified 4% because many units are not operated with free governor action.⁸⁹

The model used here is representative of a mechanical-hydraulic governor. This is appropriate because the majority of steam turbines in the UK have governors of this type.

The characteristics of electro-hydraulic governors are broadly similar to those of mechanical-hydraulic governors, although the flexibility of electronic implementation allows various features to be added. These are intended to improve the reliability and protection of the turbine and to provide the capability to interface to other control equipment. By reducing the minimum times for governor valve opening (0.25s) and closing (0.15s), electro-hydraulic actuation also provides a faster response to load changes and is able to make a contribution to generator transient stability.^{94,111} This is particularly

important on modern sets which have relatively low inertia. With electronic governors, it is possible to employ a non-linear droop characteristic. For example, on high-merit plant, it might be appropriate to have no regulation between the limits of 49.95 and 50.05Hz, and 4% droop outside these limits.

3.6.6.6 Governor Valves

Modern steam turbines normally have four governor valves, each admitting steam to one quadrant of the HP turbine. British practice favours simultaneous operation of these valves giving throttle control, whereas sequential opening 'nozzle' control is sometimes used in the United States and elsewhere.⁹² Some turbines in the UK have a throttle control arrangement but, up to 50% m.c.r. (maximum continuous rating), two out of four valves are opened. Above this level, the first pair of valves are fully open and the turbine is controlled on the other two. This arrangement complicates the characteristic relating grid frequency to unit output.

The flow characteristic of a steam valve gives rise to a non-linear steady-state relationship between the steam valve position and the turbine power output. This can be modelled by the following expression for the steam flow:^{70,112,113}

$$W_i = A p_i \left[\frac{2\gamma}{1-\gamma} \frac{1}{RT} \left[\left(\frac{p_o}{p_i} \right)^{\frac{\gamma+1}{\gamma}} - \left(\frac{p_o}{p_i} \right)^{\frac{2}{\gamma}} \right] \right]^{\frac{1}{2}} \quad 3.12$$

where γ is the index of isentropic expansion, R is the universal gas constant, T is the absolute temperature of the steam, p_i is the inlet pressure and p_o is the outlet pressure. This expression was used by Thompson.¹⁰⁷ Although it describes the relationship between effective valve area, A, and steam flow rate, W_i , the non-linear dependence of valve area on governor output is not included. In practice, the overall relation between steam flow

rate and governor output is linearised approximately (for one value of valve inlet pressure⁷⁰) through the use of variable ratio levers or cams in mechanical actuation and electrical function circuits in electro-hydraulic actuation.⁹⁴ (Feedback of a measurement of first turbine stage pressure is commonly used in the USA.⁹²) In a simulation model, it is reasonable, and certainly convenient, to assume that all non-linearity is fully compensated and to omit these features, although, in fact, the limited rates of valve movement prevent full linearisation during rapid changes in position. With this approximation, the expression for the per-unit steam flow can be greatly simplified to:^{67,70}

$$W_i = a_2 p_i \quad 3.13$$

A lag is used to represent the steam storage between the valve and the first stage of the HP cylinder:⁶⁷

$$\frac{dp}{dt} = (W_i - W_o) / T_L \quad 3.14$$

where W_i and W_o are the steam flows into and out of the storage volume and T_L is in the range 0.1 to 0.4 s.¹¹⁴

Alternatively, neglecting this lag, the governor can be considered to regulate pressure rather than flow. The per-unit HP inlet pressure, p_1 is then the product of the boiler drum pressure, p_b and the per-unit valve position, a_2 .

i.e.
$$p_1 = a_2 p_b \quad 3.15$$

This simple description of the governor valve is widely used^{44,115} and was chosen for the work reported here.

No deadband or backlash was included in the model although deadband caused by wear in mechanical governors can lead to very high effective droop at rated speed.⁹⁴ Limit cycling has been experienced on some plant at around 75% m.c.r.¹¹⁶ caused by a combination of wear and a change in direction of the steam force acting on the governor valves. In a system response study it is

normally assumed that the aggregate thermal plant response shows no evidence of backlash.⁹¹ When several units are operating together, the effects of backlash on the individual machines tend to cancel out when their power outputs are summed.

3.6.6.7 Steam Turbine

Steam transit times for turbine cylinders are of the order of 10ms. This is a negligible period for most turbine control problems and so a cylinder can be considered as a single unit.¹¹⁰ Indeed, the intermediate and low pressure stages of the turbine are normally lumped together for the purposes of simulation with negligible loss of accuracy. Over the range of speed and load level of interest in system response studies, the efficiencies of the turbine stages are approximately constant and can, therefore, be removed from a normalised model.^{70,110}

A linear model of a steam turbine¹¹⁴ has been widely used in a number of power system simulation studies, see, for example, references 57, 58, 68, 75 and 94. In this transfer function model, the turbine and pipework steam storage is represented by a cascade of first order lags and the stage power outputs are taken off at appropriate points. However, this model does not take into account the effect of turbine stages on the stages lying upstream.^{110,117}

Following an increase in governor valve opening, the initial change in the high-pressure turbine output is greater than the steady-state change. This is because the back pressure on this stage increases relatively slowly due to steam storage in the reheater. The inlet pressure, however, increases quickly and so the enthalpy drop across the stage is larger than when steady-state conditions are reached.¹¹¹

The effect of this interstage coupling can be represented by

the following equation:^{67,110}

$$W_1 = K \sqrt{p_1^2 - p_2^2} \quad 3.16$$

where W_1 is the steam flow, K is a constant and p_1 and p_2 are the inlet and outlet pressures. A number of more detailed equations can be used if desired.^{110,112}

The stage power output, P_{m1} is proportional to the product of steam flow and enthalpy drop:^{67,110,113}

$$P_{m1} = K \left[1 - \left(\frac{p_2}{p_1} \right)^{\frac{\gamma-1}{\gamma}} \right] \quad 3.17$$

where γ is 1.3 for superheated steam and K is a constant.

After normalisation, these expressions for steam flow and power output become

$$W_1 = p_1 \frac{\left[1 - R \left(\frac{p_2}{p_1} \right)^2 \right]^{\frac{1}{2}}}{1 - R^2} \quad 3.18$$

$$P_{m1} = K_4 W_1 \frac{1 - R \left(\frac{p_2}{p_1} \right)^{0.231}}{1 - R^{0.231}} \quad 3.19$$

where R is the ratio of full-load reheater pressure to full-load boiler drum pressure. A reasonable average value for this parameter is 0.35. Modern steam units have a rather smaller ratio.

K_4 is the proportion of the turbine capacity constituted by the HP stage and a suitable value is 0.2. In Equation 3.18, precautions are taken to prevent the simulation program failing in an attempt to calculate the square root of a negative number.

The reheater is modelled as a storage element with

$$\frac{dp}{dt} = (W_1 - W_2) / T_r \quad 3.20$$

where W_2 is the steam flow in the IP/LP stage and $T_r = 10.0$ s for modern plant. Setting $T_r = 2.0$ s makes the overall behaviour that of non-reheat plant. (Some lag is retained because the LP cylinder itself constitutes a significant fraction of the total storage volume.) The transport delay associated with the reheater pipework

has been modelled by some authors⁷⁰ but the effect is small and has not been included here.

The intermediate and low pressure turbine stages taken together can be considered as a condensing turbine where the back pressure is so low, at about 0.1% of inlet pressure, that it does not affect the steam flow through the cylinder.^{67,110} The normalised equation for IP/LP steam flow is, therefore, simply:

$$W_2 = P_2 \quad 3.21$$

Calculation of enthalpy drop for the IP/LP stage is complicated because the steam becomes wet in transit through this stage. However, the power output from the stage, P_{m2} is found to be approximately proportional to the steam flow,^{67,110} so, in per-unit terms:

$$P_{m2} = (1 - K_4) W_2 \quad 3.22$$

The impedance of the steam piping has been neglected in this boiler-turbine model because it is small when compared with that of the partially-closed governor valve.⁹¹ The superheater is, therefore, not represented.

It is also assumed that the steam bled from the various turbine stages remains a fixed percentage of the steam flow and can, therefore, be omitted from a normalised model.¹¹²

A number of other authors have used the turbine model described in this section with various minor alterations and additions.⁹⁷

3.6.7 The Effect of Low System Frequency on Auxiliary Plant

Prolonged periods of under-frequency can lead to a reduction in output from thermal generation when the performance of electrically-powered auxiliary plant is impaired.⁸³ However, for frequency excursions limited to perhaps 2%, excess auxiliary capacity is normally sufficient to maintain the required power

output.¹¹⁸ This effect was, therefore, not included in the power plant models used in this study.

3.6.8 Co-ordinated Boiler-turbine Control Schemes

The above model describes a boiler-following-turbine mode of operation with free governor action which in many ways is no longer typical of all thermal plant in the UK. Many units operate under pressure control where the governor valve is held open and the turbine output is controlled by varying the firing to the boiler and allowing the drum pressure to vary with load. This 'turbine-following-boiler' mode is often achieved under entirely manual control although some automatic control schemes have been developed to support this turbine-following-boiler or 'sliding pressure' mode of operation. Feed-forward control of boiler firing directly from frequency disturbance has been suggested but, because of the phase lag associated with the slow mill and boiler dynamics, such control has a de-stabilising effect on the grid system^{74,119} and so widespread implementation is not desirable.

Sliding pressure schemes undoubtedly reduce the immediate response capability of a boiler-turbine unit although they are convenient for the plant operators and increase the efficiency of the unit. Because of the long mill and boiler time constants of coal-fired plant, an immediate response can only be provided by making use of energy stored in the boiler⁷⁸ and this is impossible if the governor valves are already fully open. There is ultimately a conflict between the objectives of electricity production at maximum efficiency and satisfactory control of the power system. Re-appraisal of boiler-turbine control has become necessary particularly as modern boilers store less energy in relation to their size than older plant¹⁰⁹ but the governor is an inherent part of a turbine and modifications would be very expensive.

Recent approaches to this problem have focussed on co-ordinated boiler-turbine control schemes usually implemented on computers.^{78,85,92,109} In some respects these schemes are a compromise between the system operator's desire to obtain the maximum response from the thermal plant and the need to protect the boiler from large drum pressure and level excursions with attendant risk of furnace tube failure and water carry-over to the turbine. The governor remains connected and is available in the event of problems with the co-ordinated control equipment.

One particular scheme for co-ordinated 'unit' control of boiler-turbine plant has been applied successfully to a 120MW coal-fired unit at Rugeley A power station and on a 500MW oil-fired unit at Fawley power station.^{3,109,116,119} A 'pressure-governing' loop maintains the boiler pressure at a set value by operating the speeder motor to open or close the governor valves. The task of the other boiler control loops, notably those regulating the boiler drum level and final steam temperature, is made easier when the drum pressure is tightly controlled.¹¹²

Frequency regulation is obtained in the first few minutes following a disturbance by using energy stored in the boiler which is made available by modifying the set-point of the pressure governor loop. As with traditional operation, the first response comes from the mechanical turbine speed governor, with subsequent control via the pressure set-point controller. In the longer term, regulation is obtained by changing the firing signal to the boiler. When the unit output is increased with no net change in boiler pressure, there is an increase in energy stored in the boiler and the mills.¹⁰⁹ During an increase in load, the fuel input to the boiler must be greater than its final value, so 'over-firing' of the boiler is used to avoid a shortfall in

generated power.

This boiler-turbine control scheme achieves a higher degree of system stability than is common with conventional boiler pressure control which is often not capable of coping with isolated conditions.¹¹⁹ This suggests that although the present operation of the grid system is satisfactory, some frequency disturbances are unnecessarily large.

Co-ordinated control schemes have appeared in some simulation studies,^{60,120} but the status of these schemes in the UK is uncertain and discussion with the CEGB indicated that modelling of such control for system response studies has not yet been carried out. Following the completion of the mixed hydro-thermal system tests, which are reported in Chapter 6 and used the coal-fired plant model described above, a worthwhile next step would be a study of co-ordinated control schemes alongside hydro-turbine plant. Although some preliminary work was done on the implementation of a model of this type of control, it was not possible to use it for on-line tests.

3.7 THE VARIATION OF CONSUMER DEMAND WITH FREQUENCY

Comparatively little is known about the behaviour of power system loads with changing frequency, but a linear one percent increase in real power load for every percent increase in frequency is commonly assumed for large systems in a number of countries^{2,26,41,44,57,119,121} although some sources have suggested a higher figure.^{31,57,122} This is equivalent to 2%/Hz in a 50Hz system. The effect is of significance to system response, particularly in systems with low inertia and marginal stability, because load increases with frequency contribute positive damping beneficial to system stability.

This variation of the load with frequency can be described by

$$\frac{dP}{P} = k_f \frac{df}{f} \quad 3.23$$

where P is the load power, f is frequency and k_f is the load self-regulation factor. Berg^{123,124} presents typical values of k_f for a few types of load often encountered in practice:

Filament lamp	0.0
Fluorescent lamp	-1.0
Heater	0.0
Induction motor, half load	1.5
Induction motor, full load	2.8
Reduction furnace	-0.5
Aluminium plant	-0.3

Individual areas may exhibit values both lower and higher than 2%/Hz depending on the relative predominance of motor and impedance loads in that locality.^{13,123}

Measurements of the overall system load/frequency characteristic are elusive because the effect is difficult to separate from that of the governor droop characteristics relating generated power to frequency.¹²² Large generation loss incidents, the usual basis for estimates, present a picture which is confused by the effects of system inertia and accompanying voltage depressions.¹²⁵ However, available results do support a 2%/Hz variation¹²², which is an intermediate value from a stability point of view.

In line with CEGB system response studies,^{2,44} a load/frequency variation of 2%/Hz i.e. $k_f=1.0$ was used in the simulator. This is a convenient value to use because it equates to a constant electrical load torque for frequencies around 50Hz. That this is so established by the following where P is power, T is torque and f is frequency:

$$P = T\omega = 2\pi Tf \quad 3.24$$

so
$$dP = 2\pi fdT + 2\pi Tdf \quad 3.25$$

and
$$\frac{dP}{P} = \frac{dT}{T} + \frac{df}{f} \quad 3.26$$

but, for $k_f=1.0$,

$$\frac{dP}{P} = \frac{df}{f} \quad 3.27$$

so

$$\frac{dT}{T} = 0 \quad 3.28$$

That is, the fractional change of torque is zero.

If the load demand is P_D at 50Hz and P_L at a frequency, f ,

then

$$P_L = P_D + dP \quad 3.29$$

Normalising

$$\frac{P_L}{P_o} = \frac{P_D}{P_o} + \frac{dP}{P_D} \frac{P_D}{P_o} \quad 3.30$$

$$= \frac{P_D}{P_o} \left(1 + \frac{dP}{P_D} \right) \quad 3.31$$

where P_o is the chosen system MW normalisation base, here equal to the total system capacity.

So

$$P'_L = P'_D \left(1 + \frac{df}{f} \right) \quad 3.32$$

$$= P'_D \frac{f + df}{f} \quad 3.33$$

$$= P'_D f' \quad 3.34$$

where, for clarity, ' denotes a per-unit quantity. So, in per-unit terms, the actual load is numerically equal to the demand at 50Hz multiplied by the actual system frequency.

3.8 THE EQUIVALENT MACHINE MODEL OF THE INTERCONNECTED GENERATORS

Studies of electrical transient stability and generator dynamics require the representation of individual generators and the electrical network⁶⁹, but this is not necessary in a simulation of loading disturbances in a power system that is tightly coupled electrically.² For such systems, there is no need to incorporate load flow calculations because the changes in transmission loss following a disturbance are quite small relative to the generation/load imbalance. Prediction of circuit tripping due to overload is not required in a simulation that is intended for the study of governor response.

The kinetic energy, E_K (J) stored in the rotating components of a turbine-generator set at a speed, ω (rads⁻¹) is

$$E_K = \frac{1}{2} I \omega^2 \quad 3.35$$

where I is the moment of inertia (kgm^2) about the centre-line. The H constant of the set is the ratio of E_K at rated speed, ω_o , to the power rating, P_o (W).

$$H = \frac{1}{2} \frac{I \omega_o^2}{P_o} \quad 3.36$$

Notice that the stored energy and the H constant are proportional to the square of speed. This explains why hydro-turbines and other lower speed machines are much more sensitive to proportionate power imbalances than 3000rpm steam turbines even though their rotational parts may have considerably more mass.

Strictly, H is the ratio of E_K to the MVA rating¹¹⁰ and has units of MWsMVA^{-1} . So for a generator with a particular H constant, neglecting the rated power factor (typically 0.8) results in a 20% underestimate of the stored energy and the inertia time constant. However, uncertainty in the measurement of the inertia of an interconnected power system makes this omission insignificant. This uncertainty is discussed further in the following section.

For a difference in mechanical (generated) power, P_m and electrical (load) power, P_e ,

$$P_m - P_e = \frac{dK}{dt} \quad 3.37$$

$$= \frac{1}{2} I 2\omega \frac{d\omega}{dt} \quad 3.38$$

Manipulating Equations 3.36 and 3.38 and normalising:

$$\frac{d\omega}{dt} = \frac{P'_m - P'_e}{2H\omega'} \quad 3.39$$

$$\text{or} \quad \frac{df'}{dt} = \frac{P'_m - P'_e}{2Hf'} \quad 3.40$$

$$\text{or, in terms of torque} \quad \frac{d\omega'}{dt} = \frac{T'_m - T'_e}{2H} \quad 3.41$$

where $\omega' = \frac{\omega}{\omega_o}$, $f' = \frac{f}{f_o}$, $P' = \frac{P}{P_o}$ and $T' = \frac{T}{T_o}$

In an isolated load simulation, Equation 3.40 or 3.41 represents the alternator. $T_a = 2H$ is often referred to as the alternator or inertia time constant.

For N interconnected generators,

$$E_{Ktot} = \frac{1}{2}I_1\omega_1^2 + \dots + \frac{1}{2}I_N\omega_N^2 \quad 3.42$$

$$\text{So } P_{mtot} - P_{etot} = \frac{1}{2}I_1 2\omega_1 \frac{d\omega_1}{dt} + \dots + \frac{1}{2}I_N 2\omega_N \frac{d\omega_N}{dt} \quad 3.43$$

If the machines are electrically coupled, their normalised speeds must be the same, neglecting intermachine oscillations

$$\text{i. e. } \omega_1' = \frac{\omega_1}{\omega_{o1}} = \dots = \omega_N' = \frac{\omega_N}{\omega_{oN}} = \omega' \quad 3.44$$

$$\text{So } P_{mtot} - P_{etot} = \left(\frac{1}{2}I_1\omega_{o1}^2 + \dots + \frac{1}{2}I_N\omega_{oN}^2 \right) 2\omega' \frac{d\omega'}{dt} \quad 3.45$$

$$\text{and } \frac{d\omega'}{dt} = \frac{P'_{mtot} - P'_{etot}}{\left(\frac{1}{2}I_1\omega_{o1}^2 + \dots + \frac{1}{2}I_N\omega_{oN}^2 \right) \omega' / (P_{o1} + \dots + P_{oN})} \quad 3.46$$

$$\text{and } H_{sys} = \frac{P_{o1}H_1 + \dots + P_{oN}H_N}{P_{o1} + \dots + P_{oN}} \quad 3.47$$

So the overall system H constant is the weighted average of the individual machine H constants, as expected intuitively, assuming that the load has zero inertia.

For a system with a real hydro-turbine and simulated plant consisting of base load (non-regulating) generation and two thermal units, the single alternator equation is

$$\frac{df}{dt} = \left((Q_n P_{on} + Q_{c1} P_{oc1} + Q_{c2} P_{oc2} - P_L) / f_s + Q_h P_{oh} / f_g \right) / T_a \quad 3.48$$

where f_s and f_g are the simulated system and real system frequencies respectively; P_{on} , P_{oc1} and P_{oc2} are the simulated nuclear and thermal plant outputs and P_{oh} is the measured hydro-turbine power output. All these quantities are in per-unit form. Q_n , Q_{c1} , Q_{c2} and Q_h are the chosen proportions of each plant type in the system to be studied. Note that:

$$T_a = 2H_{sys} \quad 3.49$$

$$P_{oc} = P_{m1} + P_{m2} \quad 3.50$$

and $Q_n + Q_{c1} + Q_{c2} + Q_h = 1 \quad 3.51$

3.8.1 System Inertia Values

For a predominantly thermal system, an H_{sys} value of 5s is reasonable. However, the values of H_{sys} obtained from tests on various power systems tend to be between 1.3 and 3.0 times this theoretical estimate.^{80,89,125} The source of this discrepancy is unclear but two explanations have been advanced. It could be that the inertia of the load contributes very significantly to the total inertia but transient stability analysis of the natural oscillations of the power system rules out this possibility.¹²⁵ It has also been suggested that the apparent increase in system inertia is due to a voltage depression following the disturbance, which reduces the load, but again this is not supported by transient stability analysis. Under-estimation of the overall system droop certainly does not account for the discrepancy.¹²⁶

Ashmole¹²⁵ reported that a good fit to system test data was obtained if the system inertia constant was set to 10.4s at the time of the disturbance but decayed exponentially to 5.2s with a time constant of about 4s. Auto-correlation analysis of system response to small loading fluctuations suggests a system inertia value close to the total generation inertia. Only larger disturbances seem to produce an inertia discrepancy. These studies suggest that the apparent increase in inertia is due to some non-linear network effect that does not persist for long and is not represented by transient stability programs.

In system response studies, the CEGB normally use a fixed system inertia constant with a value of $10s^{44}$ (i.e. an alternator time constant of 20s) and this figure was used for the mixed

system studies reported here.

3.9 IMPLEMENTATION OF THE POWER SYSTEM MODEL

A simulation of the coal-fired plant model was established using the Euler integration method as described in Section 2.9.3. A integration step length of 0.05s was found to be suitable. Equations for the single alternator and system load models were added to complete the power system simulation. Off-line studies showed that this model produced responses that were comparable with those obtained from real system tests⁴⁴ and it was concluded that the model provided a reasonably realistic simulation of the UK power system and its response to loading disturbances.

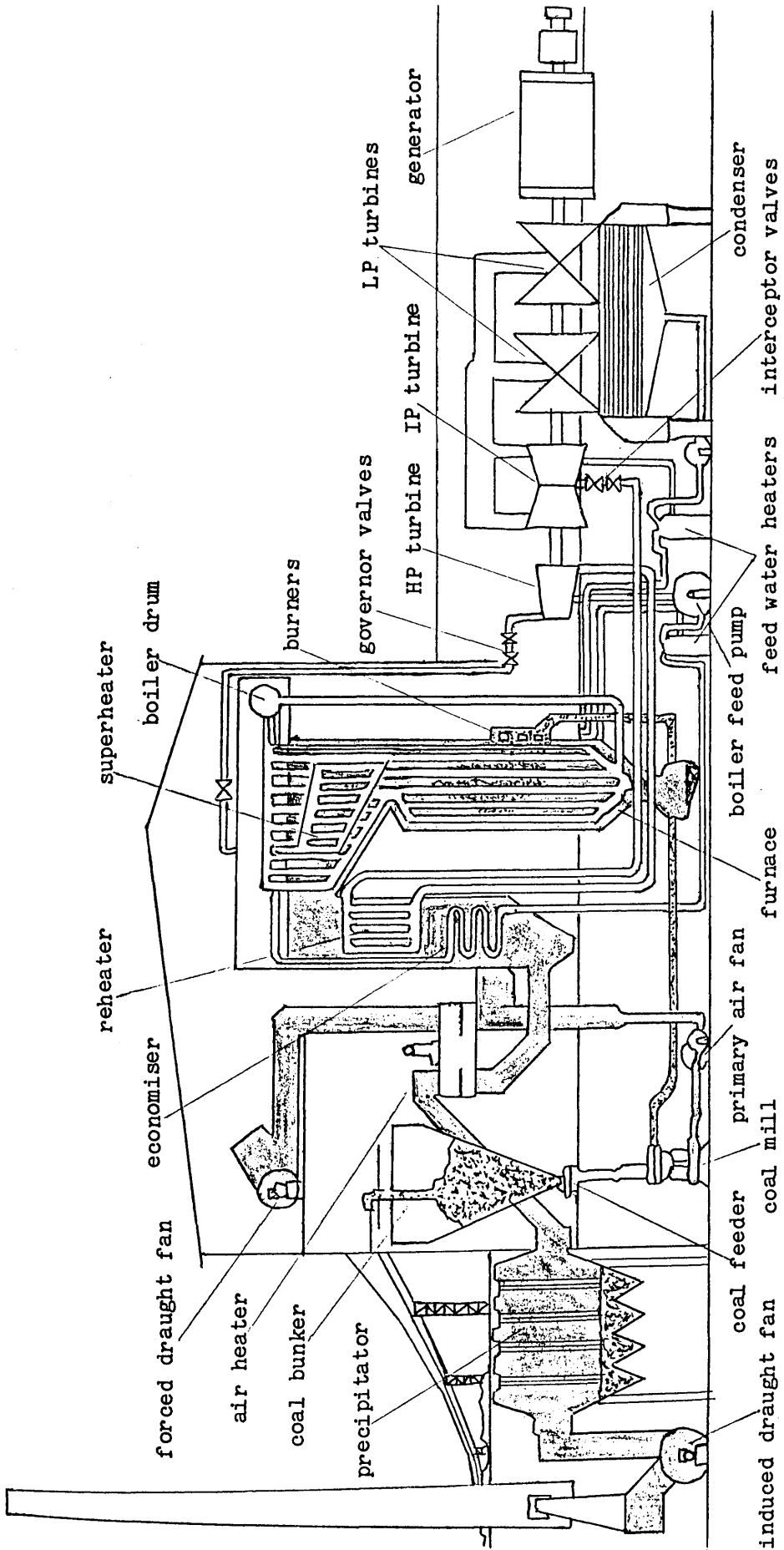


Figure 3.1 Arrangement of a coal-fired boiler turbine unit

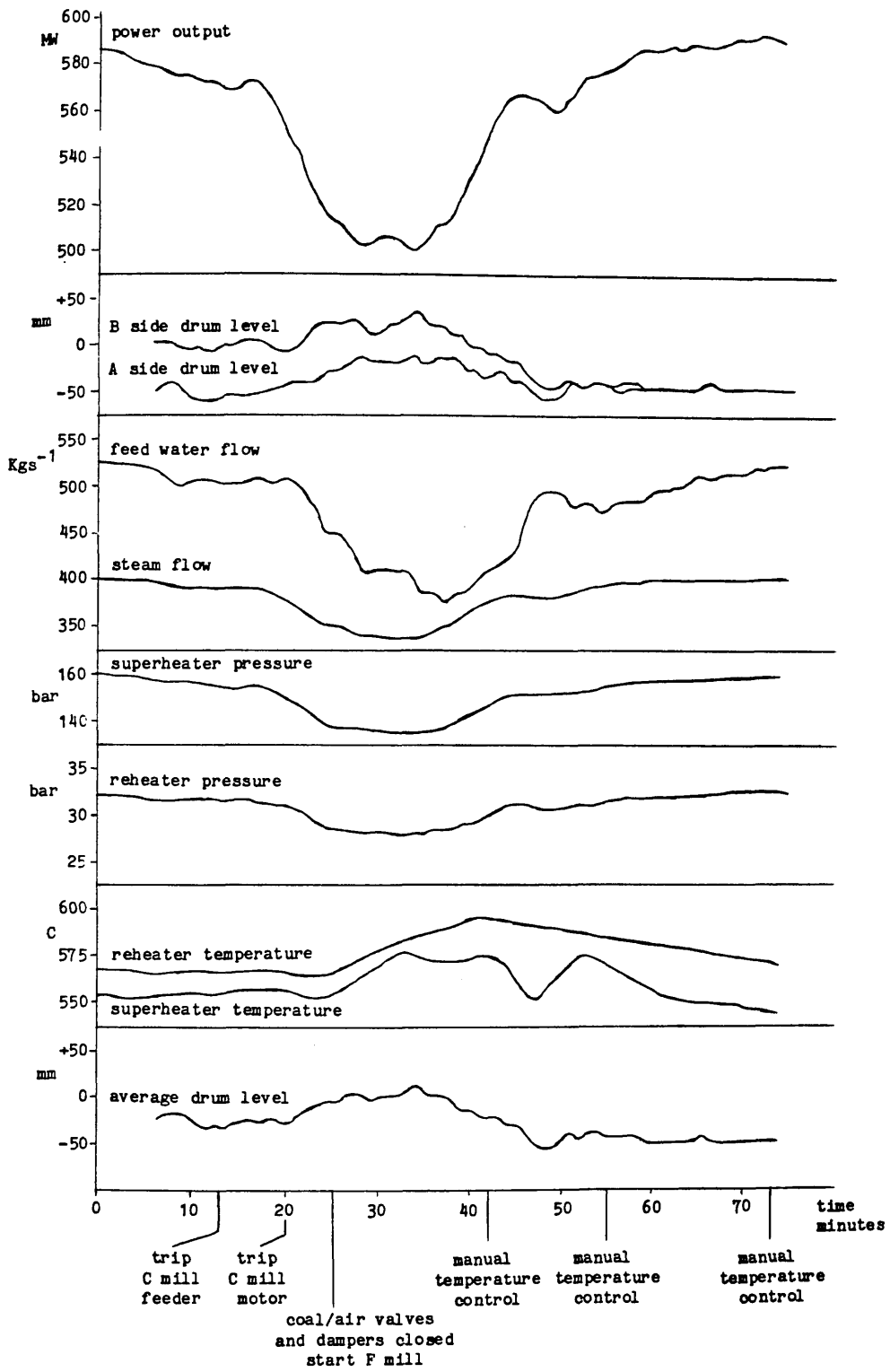


Figure 3.2 Load changes on a 600MW unit

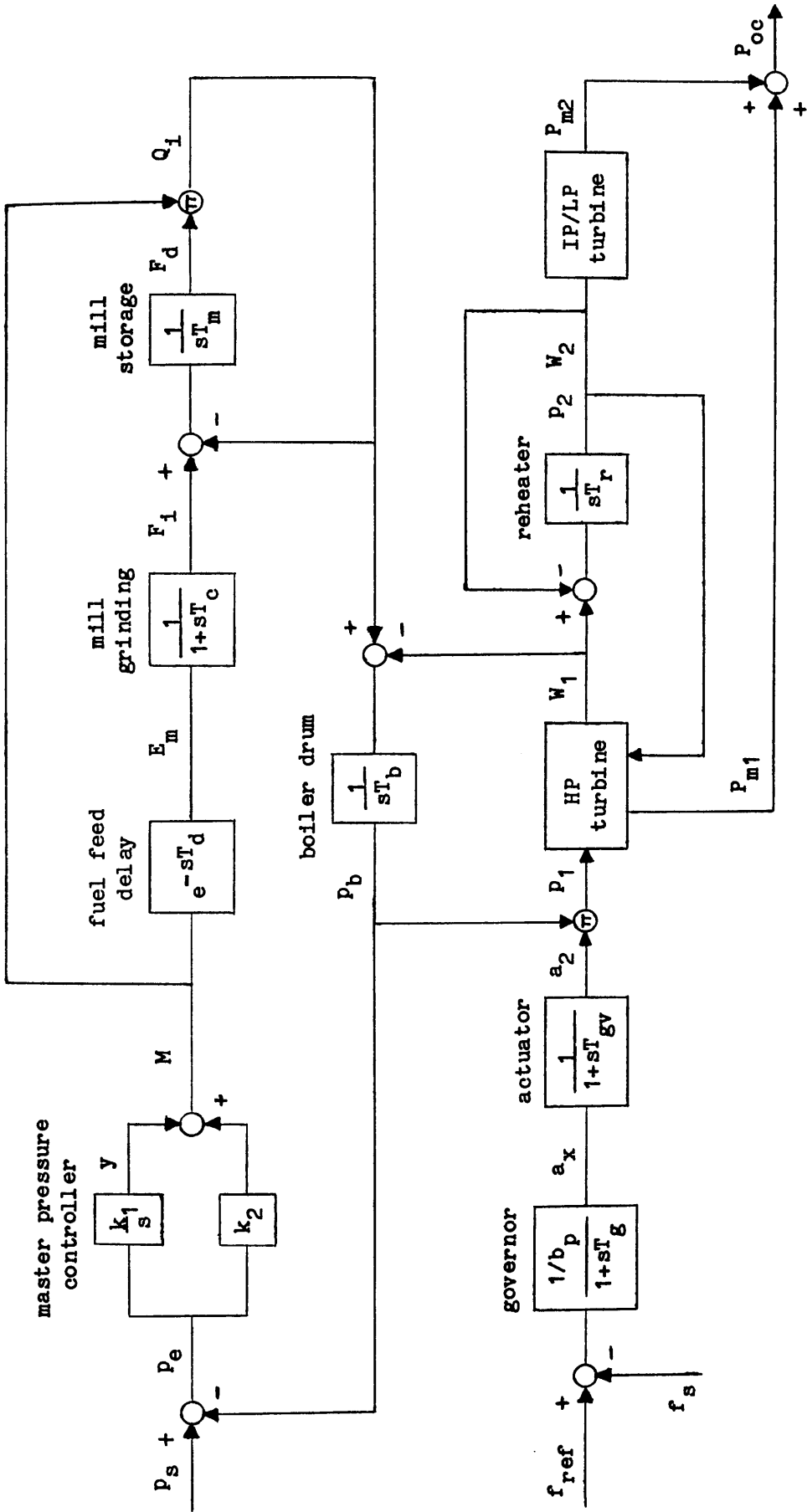


Figure 3.3 Thermal plant model

CHAPTER 4

PRELIMINARY TESTS OF THE TECHNIQUE

Preliminary evaluation of the power system simulator was carried out on the 32.5MW hydro-electric turbine generators at Loch Sloy Power Station. Two types of test were performed: For the first, the electronic double derivative governor available on No.3 machine was used, while the second involved a temporary droop hydraulic governor on No.1 machine. This chapter presents the results of these tests which were intended to prove the viability of the simulator system and to establish secure operating procedures.

4.1 TESTS USING AN ELECTRONIC GOVERNOR

Due to the relative simplicity of the interfacing required, the power system simulator was initially tested on a hydro-turbine with an electronic governor. The microprocessor governor on Sloy No.3 machine is equipped with a range of additional test inputs and signal outputs. An additional frequency term can be injected on the front panel and a two-wattmeter measurement of generator power is available. Both of these signals are in the form of analog voltages.

It was important to verify that the maximum rate of change of prime mover torque that could be initiated by injecting signals into the electronic governor was not sufficiently fast to cause significant oscillation of the generator rotor angle. This was achieved by applying a voltage step to the test frequency input on the electronic governor and observing the effect on the governor output, generator power and machine frequency. The logged transients for a 1.0V step, corresponding to a frequency change of

0.5Hz, are shown in Figure 4.1. The response of the governor and the turbine corresponds to that for a frequency change of 0.5Hz on the national grid. In effect, Figure 4.1 shows the open-loop transient response of the double derivative governor because the generator constitutes a very small part of the power system and has very little effect on its frequency. The slight dip in power output at the start of the response is due to the effect of the water column inertia discussed in Section 1.3.

The machine frequency measurement is derived from current and voltage transformers connected at the generator terminals and any significant rotor angle oscillation will appear as a corresponding 'ringing' on this signal and on the power output. For comparison, Figure 4.2 shows the same signals as Figure 4.1 during synchronisation of the generator to the grid. Quite severe oscillation is evident on the power and frequency (speed) traces with some sign of a response from the governor. There is no evidence of oscillation on any of the signals in Figure 4.1 which is a satisfactory result, because it demonstrates that there is no coupling between the test frequency input and the machine frequency signal seen by the governor. It also means that the turbine torque can be accurately inferred from the measurement of generator power.³⁹

4.1.1 Tests of Isolated Load Operation

As a first step in the development of the power system simulator, the new equipment was used to reproduce the results of earlier studies of isolated load operation.¹³ By configuring the simulator to represent a system with alternator inertia only and no other generation, the turbine was made to appear to the governor as if disconnected from the grid. The model used

consisted of a single alternator with a time constant, T_a of 7.0s which is the appropriate value for Sloy generators, and a load/frequency dependence of 2%/Hz i.e. a load torque independent of frequency.

The plot of injected frequency, governor output and generator power shown in Figure 4.3 shows limit cycle oscillation building up to an approximately steady amplitude. This oscillation occurs when a turbine operates in isolation from the rest of the grid and is caused by backlash in the mechanical linkage between the governor actuator and the turbine guide vanes. Figure 4.3 also shows the effect of a 4% step increase in demand at about 90s and Figure 4.4 a corresponding decrease also at about 90s. In these tests, the hydro-turbine was operating at around 4MW and 10MW respectively. The turbine and governor responses are superimposed on the limit cycles and tend to shorten the period of oscillation. The linkage backlash is quite difficult to model in an off-line simulation and one advantage of real plant test is that such effects are automatically included in the study.

Figure 4.5 shows the response for an 8% increase in demand at about 90s and a decrease in demand of the same size at about 140s. The power output from the turbine was initially about 6.5MW. The effect of limits on the rate of governor servo movement can be seen clearly on the governor output. The maximum rate of closure is full-stroke in 4s whereas that for valve opening is 20s and so the governor is very much more hampered by the rate limit for a step in the loading direction and the result is a significant frequency and power overshoot.

These test runs, where a steady-state oscillation is present, illustrate the need for 'point-of-wave' switching when a step

change in demand is applied if consistent results are to be obtained. It is best to apply a step in the loading direction when the power output reaches its lowest value in the limit cycle oscillation and vice versa. If this is not done, the deadband in the governor linkage tends to absorb a proportion of the governor's response to the disturbance.

During these tests, no attempt was made to prevent the governor responding to genuine grid frequency fluctuations but these are negligible compared with the large signals injected when isolated operation is simulated. The grid frequency in fact remained reasonably constant throughout all of these runs.

When tests are conducted on hydro-turbine plant, it is important to ensure that the disturbances do not excite 'waterhammer' pressure waves in the pipeline. The frequency of oscillation involved in isolated load operation is about 0.05Hz which is much lower than the lowest waterhammer frequency at Sloy which is approximately 0.37Hz.¹³ It is also well above the mass oscillation frequency of the water in the low pressure tunnel between the dam and the surge shaft (0.004Hz). These tests, therefore, do not cause any problems in the pipeline system.

The results of the simulated isolation tests described in this section are quite similar to the results of real isolated operation tests carried out in earlier work on the same machine.¹³ This confirms that the configuration of the simulator and the governor is suitable for on-line tests.

4.1.2 Preliminary Tests of a Mixed Hydro-thermal System

A simple model of an oil-fired boiler-turbine unit was used for the first attempts to couple the electronically-governed hydro-turbine to a thermal plant simulation. This model was

established in earlier work at Glasgow University¹⁰⁷ and was described in Section 3.6.5.

In these preliminary tests, the simulator parameters were chosen such that the hydro and thermal components of the system were of equal rating. The behaviour of the oil-fired plant was represented within the simulator while the dynamics of the hydro-electric component were furnished by the real plant. The simulator was configured to reproduce the response of a power system provided with 32.5MW oil-fired and 32.5MW hydro-electric generation. By changing the values on the plot axes, the representation could be of a system with hydro and thermal units of 660MW rating.

The simulated frequency transient for a step increase in consumer demand of 13MW is shown in Figure 4.6 together with the responses of the simulated oil-fired plant and the real hydro-electric plant. The initial thermal and hydro power outputs were 20MW and 6MW respectively. The plots clearly show the initial, fast pick-up by the thermal plant followed by a reduction in output once the boiler steam reserves have been exhausted while the response from the hydro component is slower but sustained. The frequency trajectory is similar in form to that of genuine grid incidents.

This result was not obtained at the first attempt, but methods for reliable and repeatable testing were established quite quickly using the equipment and techniques described in Chapter 2.

4.1.3 Some Experiments with the Simulator

Once a procedure had been developed for incorporating real plant in system response studies using the power system simulator, the effect of various model parameter changes were investigated.

The existing oil-fired plant model used in the simulator was made into a crude representation of coal-fired plant by increasing the time constant of the first-order lag in the fuel feed section. Instead of the original 10s, a much larger value of 600s was used to correspond to the transport delays in the coal handling and milling equipment. This has only a small effect on the response in the first 120s (Figure 4.7) with a slightly greater fall in output from the steam turbine and a lower frequency of 49.57Hz rather than 49.69Hz at 120s. The drawn-out nature of the response after the initial transient is evident in Figure 4.8 where the test has been plotted over a much longer time scale. The thermal plant response falls off dramatically before the fuel feed to the furnace can be increased. This type of response is typical of coal-fired plant. During this test, the grid frequency varied considerably and the effect on the results is quite apparent. If longer term tests such as this are to be performed, some method of compensation for the effects of grid frequency fluctuation is required.

Another modification to the model involved an increase in the thermal plant governor droop from 4% to 8%, with the fuel feed time constant returned to 10s. By reducing the frequency sensitivity of the steam plant to a level considered to be an appropriate average for thermal plant on the UK system, the onus for system control falls more heavily on the hydro component of the system. The initial frequency swing is increased (Figure 4.9), reaching 48.88 rather than 49.27Hz (Figure 4.6) and the hydro-turbine responds more rapidly and with a larger change in output.

4.2 TESTS USING A MECHANICAL-HYDRAULIC GOVERNOR

The second series of tests was performed on No.1 set which has a mechanical-hydraulic governor. The test signal was, therefore, injected through pulsed closure of the speeder motor interposing relays. A measurement of machine power output was obtained from control desk metering which had a response that was adequate for the purposes of tests of a hydro-thermal system. The simulator was again configured to reproduce the response of a power system provided with 32.5MW oil-fired and 32.5MW hydro-electric generation.

Figure 4.10 shows the response of the hydro-turbine to a raise pulse of 3.54s duration. From this type of test, the length of pulse required for a full load change in output was estimated to be 7.5s. Together with a value of the permanent droop of the governor (3%), this speeder motor calibration figure is used by the simulator to calculate the pulses that have to be injected to approximate a particular frequency transient.

The pulse shown in Figure 4.10, in fact, corresponds to a frequency drop of about 0.7Hz (over 3.54s). In comparison with Figure 4.1, which shows the response of the double derivative governor to a 0.5Hz change in frequency, the slower response of the temporary droop governor is quite evident.

The simulated frequency transient for a 13MW increase in consumer demand at a rate of 2.6MW per second is shown in Figure 4.11 together with the responses of the simulated oil-fired plant and the real hydro-electric plant. The speeder motor pulses applied to represent approximately this frequency transient have also been plotted. In this test, the initial thermal and hydro power outputs were 20MW and 12MW respectively.

Figure 4.12 shows the corresponding test with the electronic double derivative governor. The response is not directly comparable with Figure 4.11 because the electronic governor test used a step rather than a ramp change in demand. However, the effect of the different governor characteristics can be seen in the detailed shape of the plots. With both governors, the initial delay before the hydro-turbine responds is due to the backlash in the guide vane linkage which absorbs some of the initial governor output. With the hydraulic governor, a slight tendency to oscillation can be observed on the frequency and power traces.

The test described in this section shows that useful results can be obtained for hydraulic governors by injecting a signal via the speeder motor. This is important because governors of this type are still in the majority on conventional hydro-turbines.

4.2.1 Tests of Isolated Operation Using Speeder Motor Injection

The above section described tests that were performed on a mechanical-hydraulic governor with a temporary droop characteristic. The success of this approach suggested that it might be possible to simulate isolated load operation using the same method. This is a more difficult proposition because the simulated system frequency that has to be injected is considerably more lively due to the reduction in alternator inertia appropriate for isolated load simulation. The application of step changes in demand is certainly not possible, but it was found that results can be obtained using 10% demand steps applied through a first-order lag with a time constant of 7.5s.

Figure 4.13 shows the response of the turbine to a reduction in demand when its initial power output was 30.5MW. Limit cycle oscillation is evident following the disturbance. The fourth

channel plotted is a signal produced by the simulator which indicates the error involved in using the speeder motor injection technique. This signal is the difference between the simulated system frequency and the signal that is actually injected. During the initial transient, there is some error because even when the lower control is held on continuously, the rate of change of frequency reference is too slow to reproduce the fast swing.

A repeat of this test at 12MW is shown in Figure 4.14. The limit cycle behaviour is quite different and the oscillation is hardly sustained. Variation in the form of limit cycle oscillation was observed throughout all of these tests with particularly large amplitudes occurring at a 20MW operating point.

Although these tests of isolated operation using the speeder motor can show up some of the features of the governor's behaviour, the rate limiting effect of the speeder motor makes development of this technique quite difficult. However, there is no other way to check the isolated load performance of hydraulic governors apart from real tests in an isolated system. Power measurement lag has an effect on this type of test and, ideally, two-wattmeter instrumentation should be used.

4.3 CONCLUSION

This chapter has presented results which demonstrate the feasibility of the power system simulator technique and its potential for real plant tests. Methods of injecting the test signal have been developed which will allow the simulator to be used with the majority of hydro-turbines and other generating plant. The more flexible approach is possible with electronic governors, but useful results can also be obtained for mechanical-hydraulic equipment.

Labels for Figures 4.1 to 4.14

POH - hydro-turbine power output
DSP - hydro-turbine governor output (desired servo position)
NBFREQ - generator frequency
FES - simulated system frequency
POO - oil-fired plant power output
GFREQ - real grid frequency
SPDINP - speeder motor pulses
FDISC - error signal for speeder motor injection

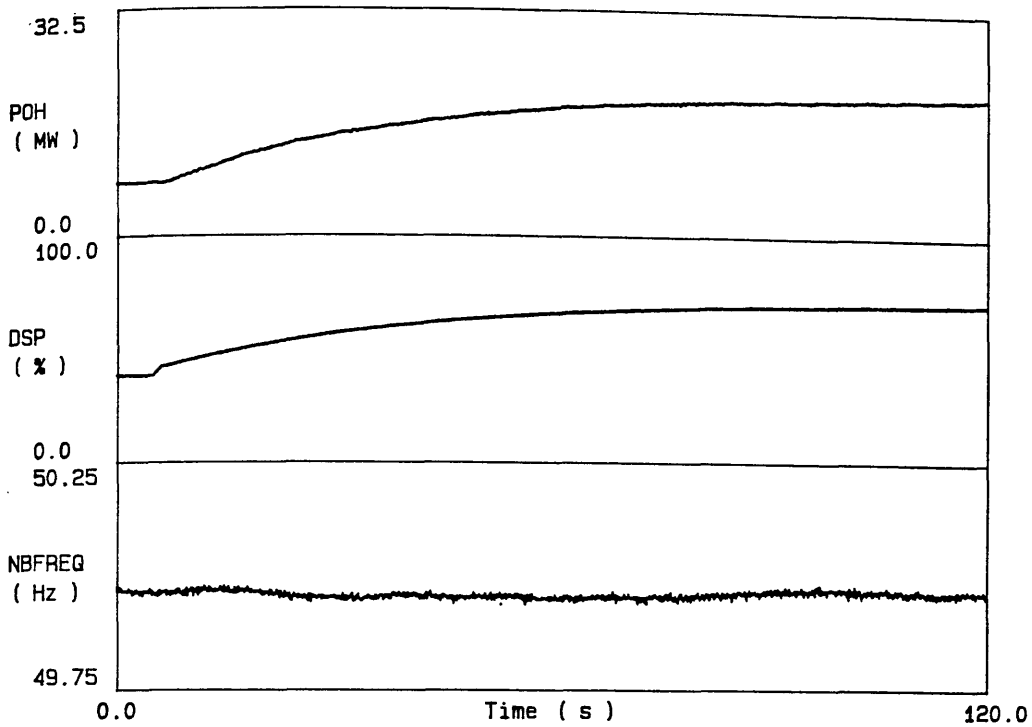


Figure 4.1 Test signal injection on electronic governor

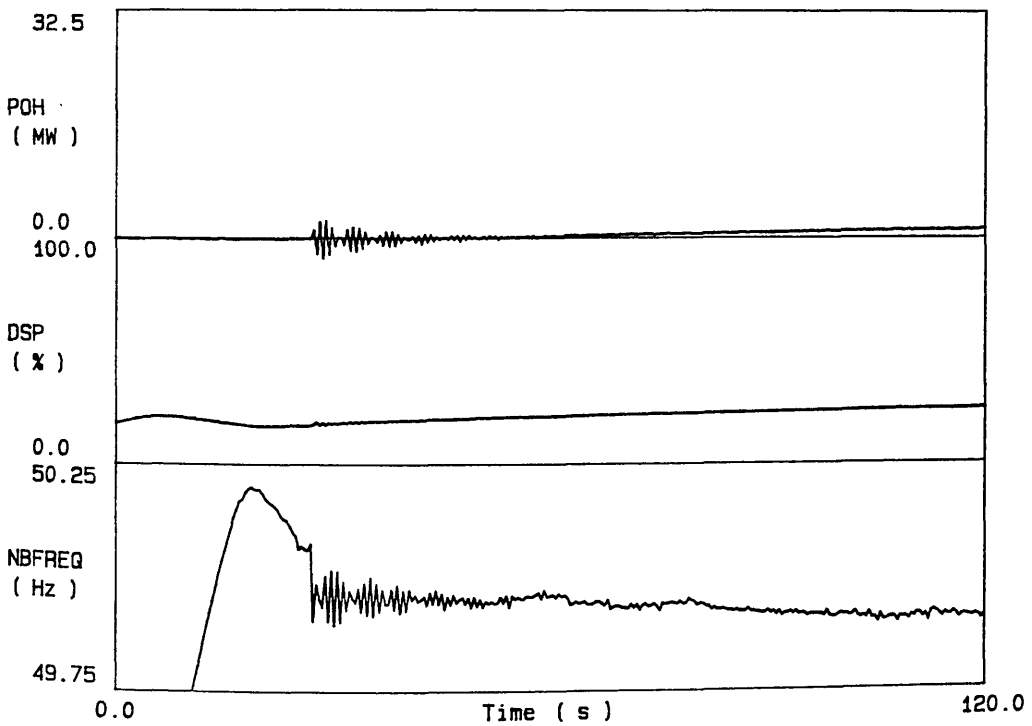


Figure 4.2 Generator synchronisation with electronic governor

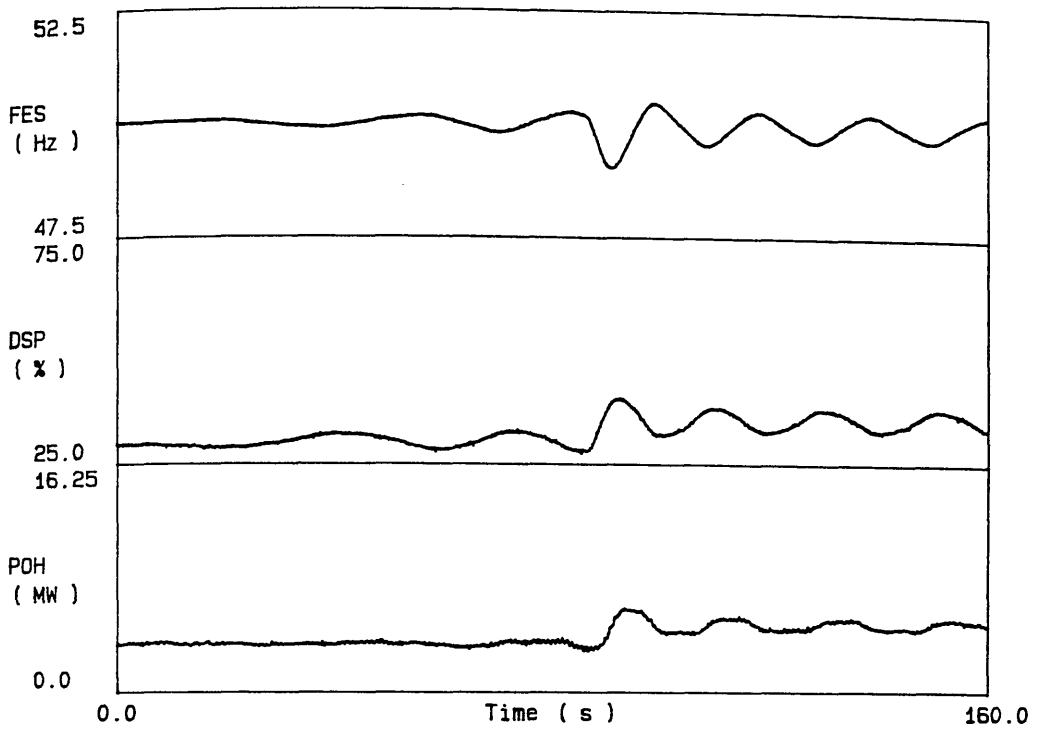


Figure 4.3 Isolated load test with electronic governor

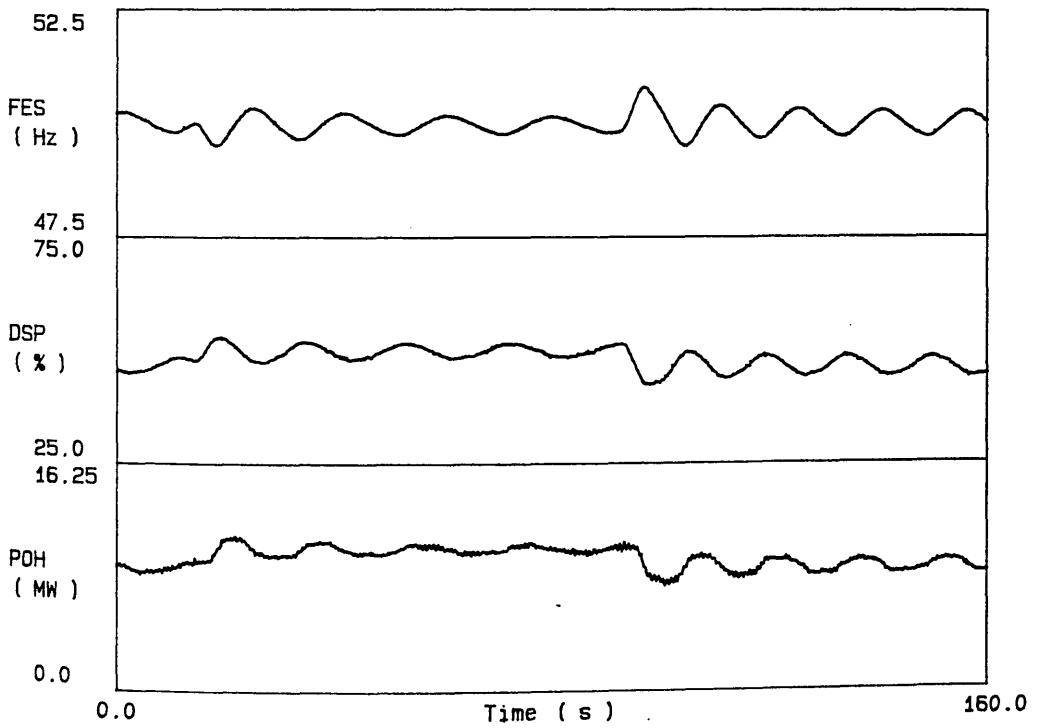


Figure 4.4 Isolated load test with electronic governor

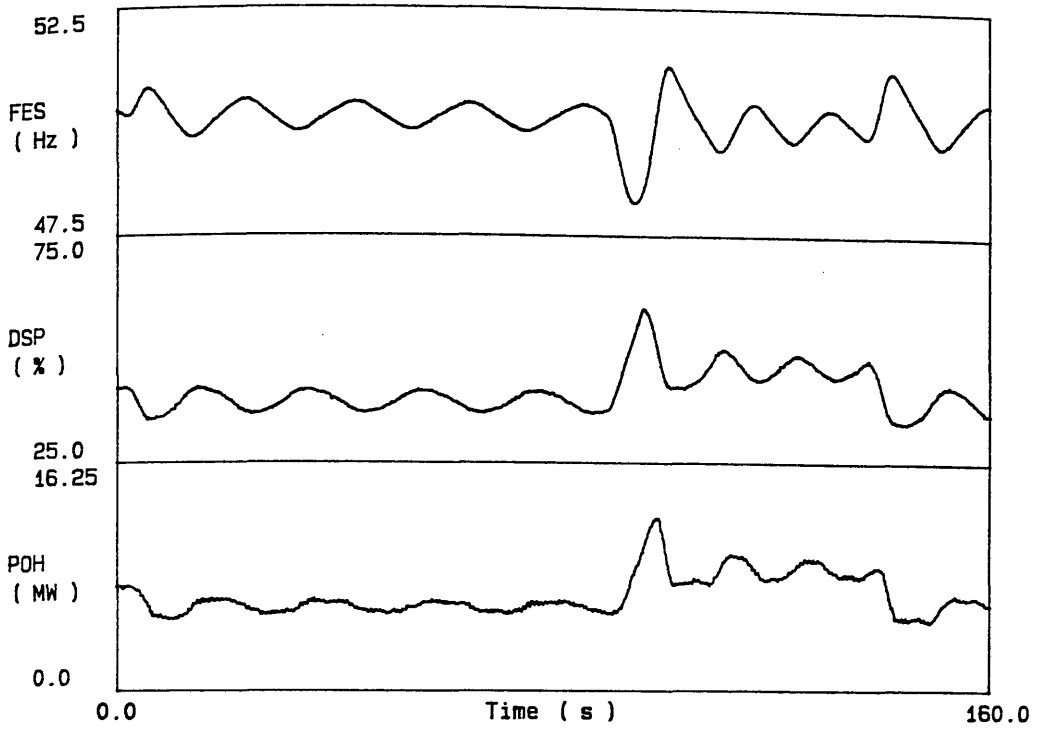


Figure 4.5 Isolated load test with electronic governor

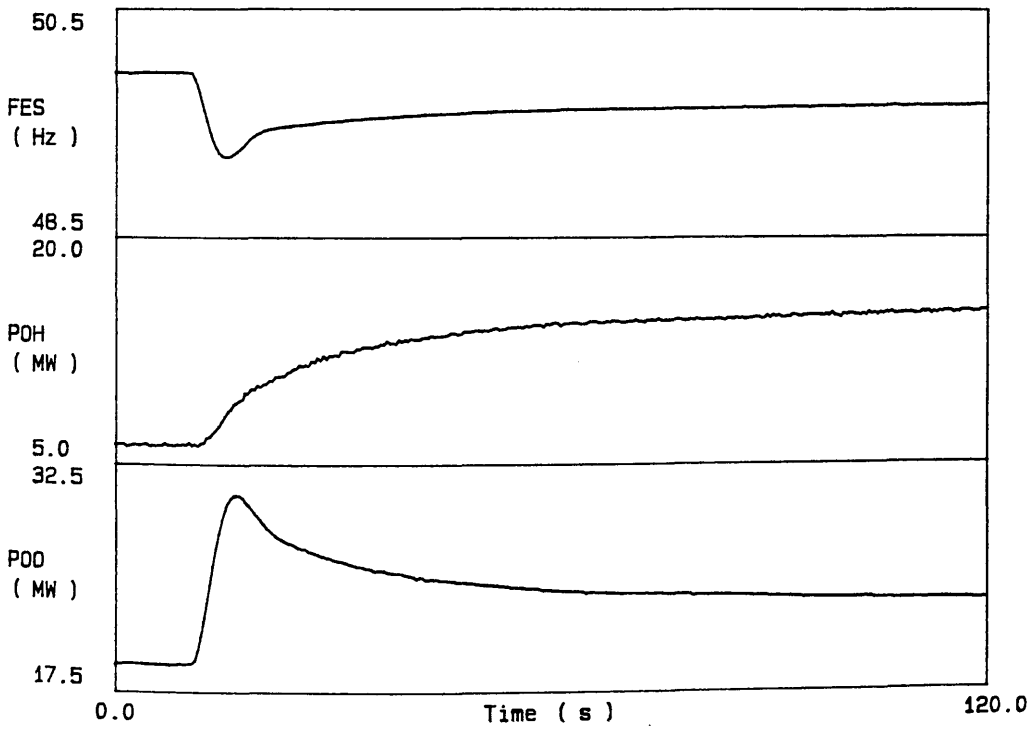


Figure 4.6 Mixed system test with electronic governor

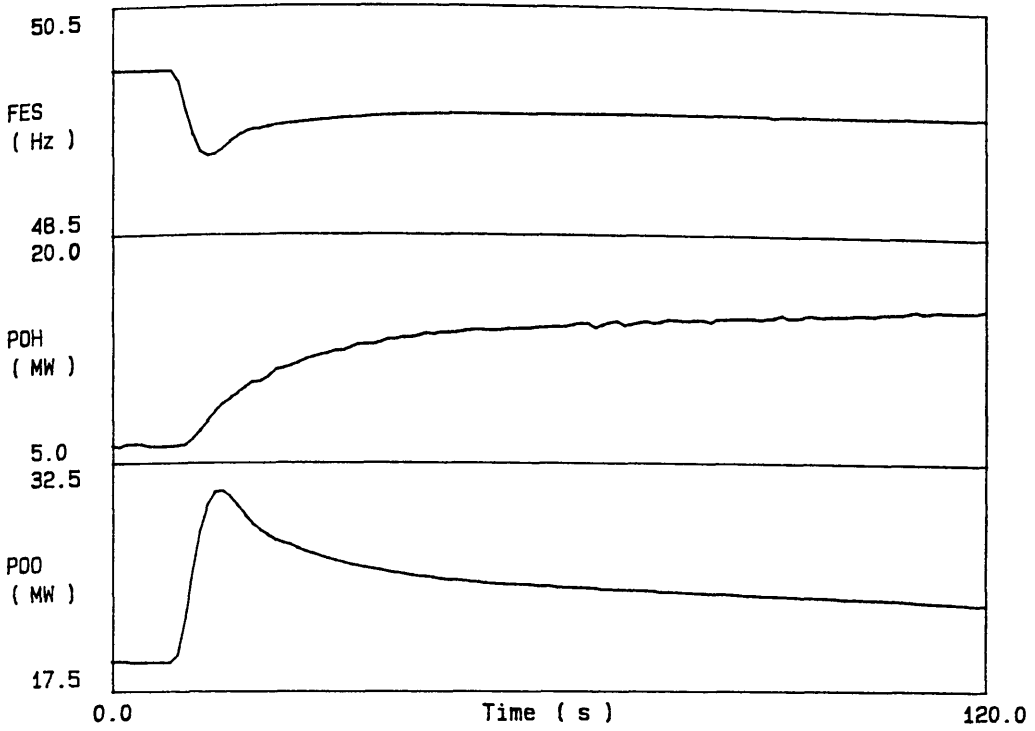


Figure 4.7 Mixed system test with electronic governor (longer fuel feed time constant)

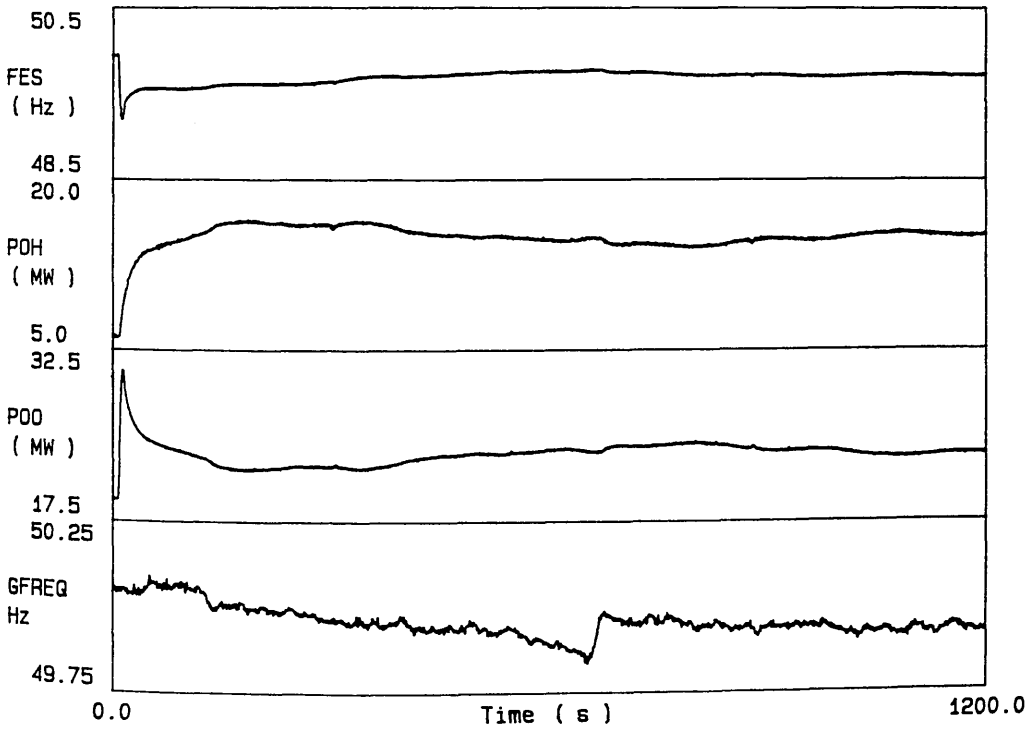


Figure 4.8 Mixed system test with electronic governor (longer fuel feed time constant)

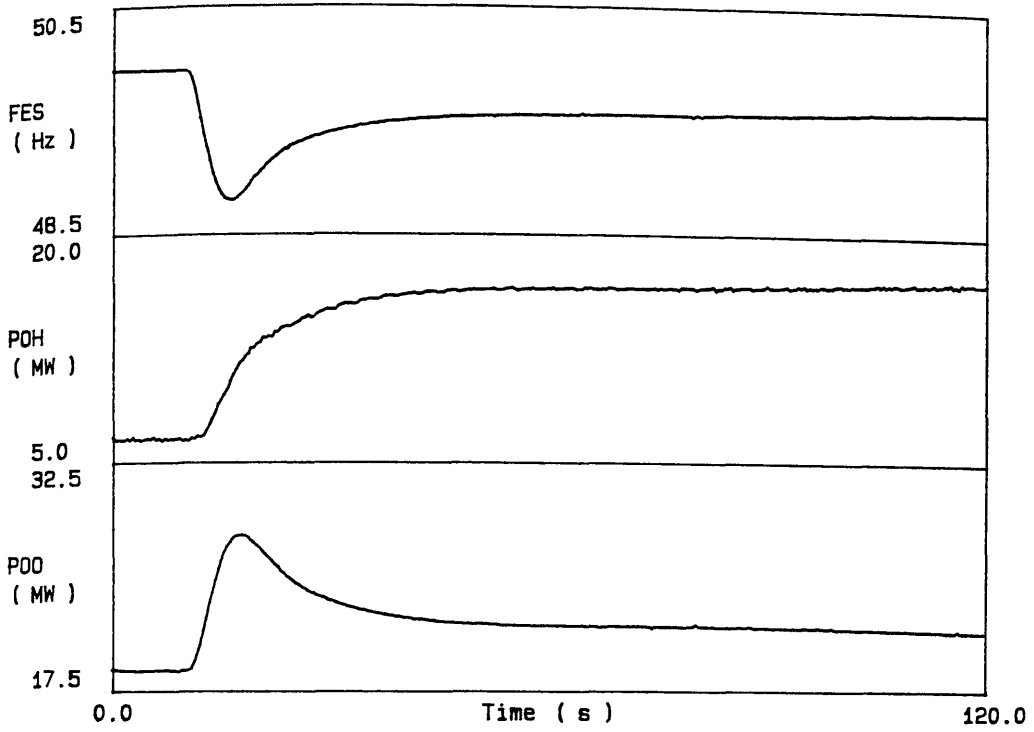


Figure 4.9 Mixed system test with electronic governor
(higher thermal plant droop)

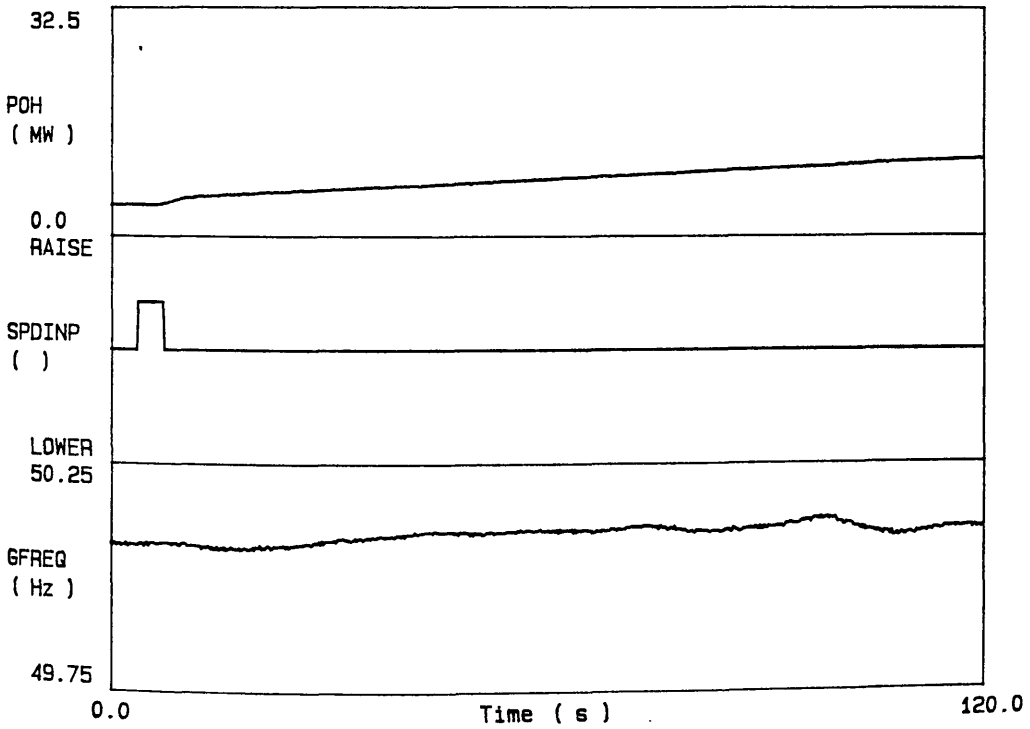


Figure 4.10 Speeder motor injection on hydraulic governor

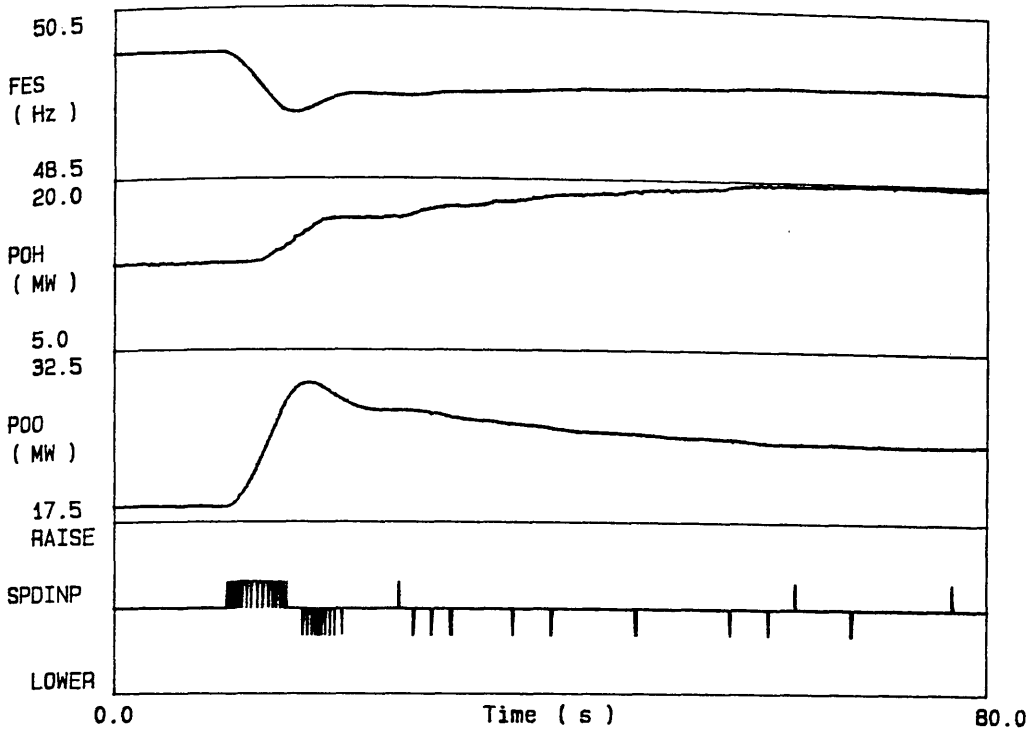


Figure 4.11 Mixed system test with hydraulic governor

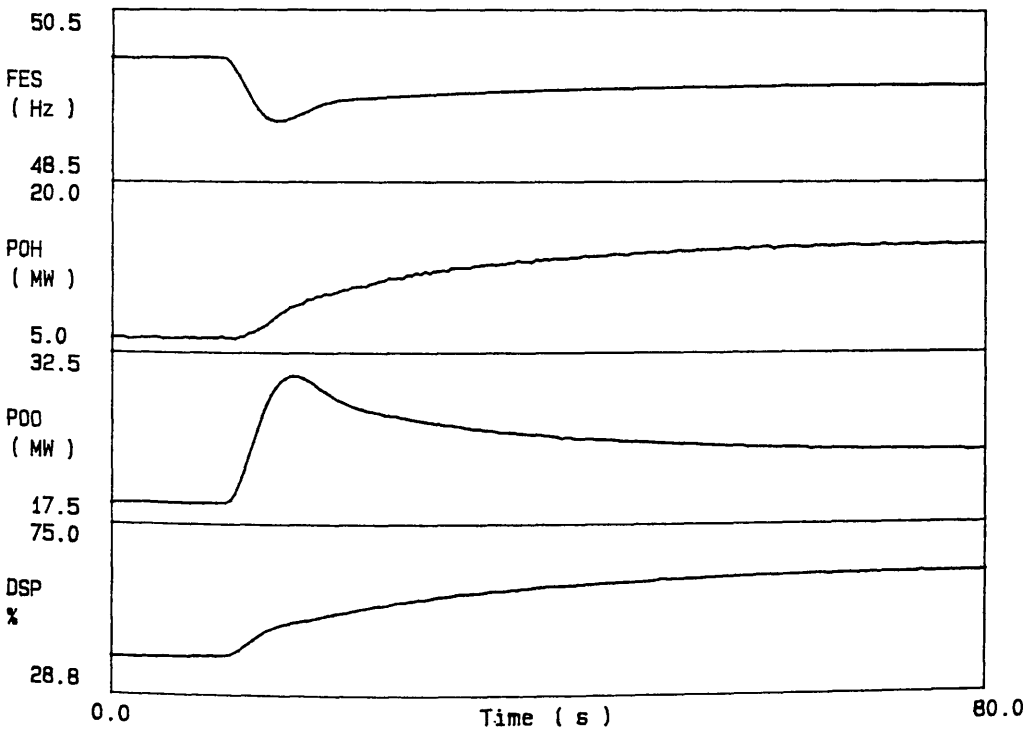


Figure 4.12 Mixed system test with electronic governor

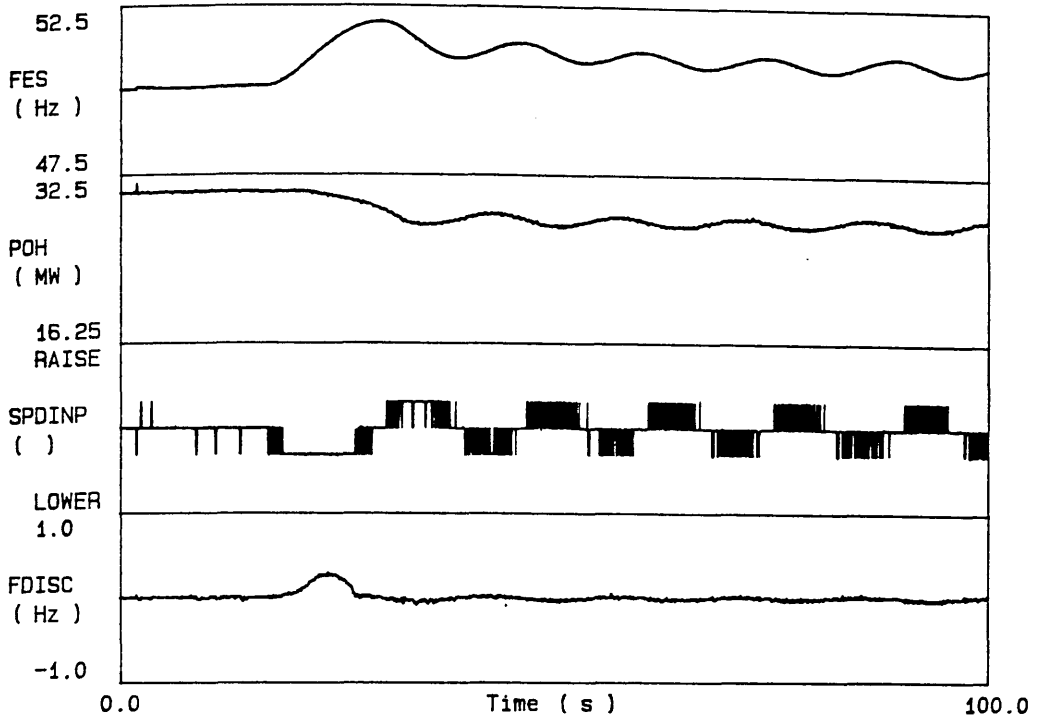


Figure 4.13 Isolated load test with hydraulic governor

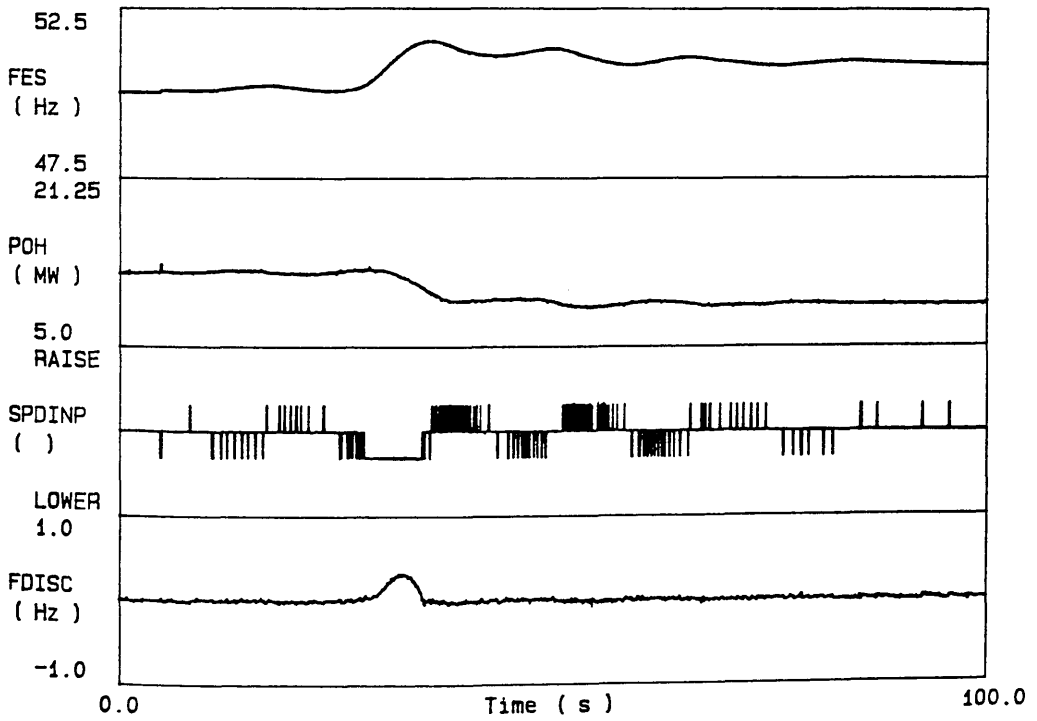


Figure 4.14 Isolated load test with hydraulic governor

CHAPTER 5

A MULTIPROCESSOR SIMULATOR

At various stages in the development of the power system simulator, the hardware resources of one single-board computer became insufficient. Additional digital input and output (I/O) was required to drive raise/lower control relays when the simulator was adapted to use speeder motor injection; extra memory was required to implement a delay subroutine for a second thermal plant model; and additional analog I/O was needed to output variables internal to the simulation. It was also anticipated that the processing power of a single 8086/8087 combination would become insufficient to complete numerical solution of all the components of the power system model in real time.

The computational load on the hardware would increase dramatically if a large number of prime mover models were required in the simulation. It would also increase if the integration interval had to be reduced to accommodate short term effects that had to be included when tests were performed on particularly responsive plant. In order to accommodate growth of the model used in the power system simulator, the feasibility of a multiprocessor version was investigated. The inherent parallelism at several levels of the system dynamics made decomposition of the problem reasonably straightforward.

For many years, combined analog and digital 'hybrid' computers were used to speed up the solution of large simulation problems.⁸² The system differential equations were solved in parallel by analog circuits under the control of the digital computer. With a sufficiently large number of analog modules, the

solution rate was independent of the size of the simulated system. By replacing the analog components with microprocessors, the resulting parallel computer can retain a high speed of solution but add the flexibility, reliability and ultimately lower cost of a digital implementation.¹²⁷ The selection of parameters and configurations in software is much more convenient than the patch panels and potentiometers used in analog computers.

This chapter reviews the application of multiprocessor systems to real-time simulation and describes how Intel single board computers can be used to implement such a system. Software development aspects are discussed with particular reference to interprocessor communication and decomposition of the power system model for allocation to individual processors. The specific implementation of a model with two boiler-turbine units will be described. Finally, possible alterations to achieve higher performance will be outlined.

5.1 MULTIPROCESSOR SYSTEMS

A particularly suitable form of parallel processor for real-time simulation is the multiprocessor. A multiprocessor is a single computer with multiple processing units each of which is capable of independent operation. In a true multiprocessor, the processors have common access to memory and input/output channels and are controlled by a single operating system.¹²⁸ Some authors insist that all memory in a multiprocessor must be addressable by every processor¹²⁹, but this is neither required nor helpful in many practical applications. The individual processors in a multiprocessor system need not be identical but they will usually have comparable performance. Frequently, the processors will not be equivalent because their I/O configurations are different.

The simplest multiprocessor systems use a time-shared bus to connect the processors and common memory, although more elaborate schemes can provide higher performance when large amounts of data must be transferred between processors.¹²⁸ Data written to common memory by a particular processor is then available to that or any other processor in the system. Access to the common memory is controlled by hardware arbitration logic which interfaces the common and local buses. From a software point of view, common memory is identical to local memory and both are accessed by a single read or write instruction.¹³⁰ Since the common memory is only used for data transfer, interference is kept to a minimum.

Networks of microcomputers loosely coupled by serial or parallel I/O channels are not strictly multiprocessor systems because they have no shared memory. Strongly connected multiprocessor systems are more suitable when high processing speeds are needed for dedicated tasks.^{130,131} Expansion is also simpler in a common memory system and the number of processors can be readily altered to suit the application.

5.2 SOME APPLICATIONS OF MULTIPROCESSOR SYSTEMS

Multiple processor systems of various types have been applied to power system problems,^{86,132,133} particularly in the areas of transient stability^{129,133,134,135,136} and load flow calculations.¹³⁵ However, they have not yet been used in the simulation of system response to loading disturbances.

Real-time multiprocessor systems are commonly used in operator training simulators for nuclear and fossil-fired power plant,^{103,137} and in the aerospace industry for pilot training simulators and aircraft^{138,139} or jet engine¹⁴⁰ design studies.

Multiprocessor systems based on microprocessors have been

developed for control and simulation applications^{103,130,141,142} and used to study the control of high-voltage d.c. transmission¹⁴³ and for the real-time simulation of an internal combustion engine.^{144,145}

5.3 PARALLEL PROCESSING IN THE MULTIBUS ENVIRONMENT

A number of Multibus boards could have been used to provide additional resources for the power system simulator. An SBC 517 I/O expansion board was set up in the laboratory to drive the relays controlling the speeder motor on hydraulic governors. However, two 88/25 single-board computers (based on the 8088 microprocessor) were available and the intention was to use these to increase the computational capability of the real-time simulator. Consequently, a multiprocessor system was established using the 86/14 and one 88/25 board to provide additional I/O facilities. Dual-port RAM on the 86/14 could be accessed not only from the on-board processor's local bus, but also from the system Multibus and so this memory could be used for interprocessor communication.^{146,147,148} An 8087 numeric coprocessor and two 8kbyte RAM chips were added to each 88/25 to expand their capability.

In the first implementation of the multiprocessor system, the 88/25 merely collected values for output from the 86/14 and carried out the appropriate I/O functions, although, at one stage, it also carried out the grid frequency measurement described in Section 2.3, passing the result to the 86/14.

Unfortunately, the 86/14 board became unreliable because of faulty operation of its multibus interface circuitry and had to be removed from the system. The fault was intermittent in nature and may have been due to a cracked track in the multi-layer printed

circuit board.

The arrangement of the hardware for the multiprocessor system was then as shown in Figure 5.1. There are two SBC 88/25 processor boards, each with local memory for program and data storage and one SBC 032 common memory board for shared data and control flags. All I/O is local to one or other of the processor boards so the common bus is not used to access I/O devices. The single-board computers use their own local bus and memory for code and data and they can, therefore, execute their programs in parallel without accessing the global bus.

In-circuit emulation (ICE) facilities were not available for the 8088 and so this powerful debugging tool could not be used when the 86/14 was no longer functional. However, a new debugging program, which ran on an IBM PC, provided some of the facilities of the in-circuit emulator.

5.4 BUS ACCESS ARBITRATION

Whether it is on the Multibus or in the form of dual-port RAM on one of the single board computers, the common memory appears in part of each processors memory map. Whenever the arbitration logic detects that the processor wishes to access a memory (or I/O) address that does not exist on the local bus, it claims use of the Multibus if it is free or if the current user has a lower priority. The buffers between the common and private buses are then enabled and the memory cycle is completed. During this process, and if the Multibus is not immediately available, the memory cycle of the microprocessor is extended by inserting extra clock cycles, called 'wait states'. The whole process is transparent to the processor.

System arbitration mechanisms are included to accomodate

conflicts over the use of a particular common bus cycle. A hardware mechanism assigns each processor a priority based on its physical bus position.

A serial priority resolution technique can be implemented by chaining the bus priority signals from one bus arbiter to the next. This 'daisy-chained' arbitration scheme was used for the power system simulator and is suitable for use on systems with up to three processors, or more if the frequency of the system bus clock is reduced. If the simulator were to be expanded beyond this number of processors, gate propagation delays would preclude this serial arbitration scheme, with the standard 10MHz bus clock,¹⁴⁹ and centralised parallel resolution would have to be implemented.¹⁵⁰ Whichever scheme is used, an arbiter gaining priority over another must wait until the present occupant completes its access cycle so that transfer integrity is ensured. This is achieved with another control line.¹⁵¹

In a parallel resolution scheme, a separate bus request line from each arbiter on the bus must be taken to centralised logic which activates the bus priority line connected to the highest priority requesting arbiter.¹⁴⁹ Up to 16 processors can be used with a parallel scheme, but above this number, signal loadings may become significant.¹⁵¹

5.5 A PROGRAMMING LANGUAGE FOR THE MULTIPROCESSOR

As with many hardware advances, the development of supporting software has not kept pace with the application of multiprocessors. High level languages for multiprocessors should allow the program to reflect the structure of the problem and not that of the hardware.¹⁴⁰ In a simulator, the program should itself be a good expression of the underlying physical reality. A number

of high level languages have features that go some way towards this goal. For example, the 'task' and 'package' constructs of Ada support simultaneous execution and data transfer with a 'rendezvous' to provide synchronisation and the programmer is freed of the need to effect bus communication directly.¹⁴⁰ However, while useful high level language structures have been established, a general method of mapping program code to different hardware configurations has not yet been developed.

Although the Intel Fortran compiler offered no particular features for multiprocessor systems, it was found to be adequate for generating code for the system used here. Shared data items could be located in common memory by placing them in COMMON blocks and then using the locator utility software to position the COMMON blocks at addresses corresponding to part of the Multibus RAM board. Semaphore handling routines were written in assembly language and these could be linked easily with the main Fortran program.

5.6 AN OPERATING SYSTEM FOR THE MULTIPROCESSOR

The requirements of an operating system for a dedicated real-time application are quite different from those of a general-purpose multiprocessor system.¹³⁰

The term 'parallel processing' is often applied to both multiprocessing and multiprogramming which is unfortunate because they are entirely different. Multiprocessing supports the simultaneous execution of two or more tasks, whereas multiprogramming only provides interleaved execution on a single processor i.e. 'concurrent' execution.¹²⁸ However, many of the software techniques used in uniprocessor operating systems can be applied to multiprocessors.

For most multiprocessors, the master-slave operating system is the most readily implemented and this configuration was used here. The master processor generates signals to activate the slaves and synchronise them with the real-time clock. Although symmetrical and independent operation of processors offers advantages in certain applications and achieves greater utilisation of resources,¹²⁸ the extra programming effort required is not usually worthwhile for dedicated systems unless graceful degradation is important. Master-slave configurations have been used in other real-time simulators using multiprocessors.^{103,137,142}

Data exchange is controlled by the master and the resulting rigid synchronisation avoids conflicts of access to memory and deadlock situations. Only items of data that have to be transferred are held in common memory. This keeps interference to a minimum.

5.7 MUTUAL EXCLUSION

In a multiprocessor system, it must be ensured that two processors cannot access a particular item in common memory at the same time. For example, if one processor reads sequentially the four bytes of a real number, then the value obtained will be corrupted if another processor starts to change the number before the first has finished.

Semaphores can be used to prevent memory access conflicts. The semaphore, in its simplest form, as used here, is a flag bit or byte in the shared memory that indicates whether or not a particular variable is available for access. Before entering a program section that must access a variable in common memory, a processor inspects a semaphore to determine whether it can access

that variable. At the same time, it sets the semaphore anyway, claiming access to the variable. These two operations must be performed indivisibly to avoid the possibility of two processors inspecting the semaphore and finding it clear before either can set it. If it turns out that the semaphore was already set, no harm is done by setting it again. In this application, the processor waits until the semaphore is reset but it could, if desired, execute some other code and return later. When the processor finds the semaphore clear, it accesses the shared data, resetting the semaphore when it has finished. Semaphores with no associated data can be used to achieve synchronisation of processors.¹⁵⁰

Mutual exclusion can, in fact, be implemented entirely in software using variables which can be read or written in single, indivisible operations,^{152,153} but a much more convenient approach is possible with semaphores and a 'test and set' instruction. The 8086 and 8088 microprocessors provide this operation in the form of a locked exchange instruction. The LOCK prefix byte activates a hardware signal from the processor which ensures that control of the local and system buses is not lost before the exchange operation is completed. The exchange instruction swaps the contents of a designated register and the semaphore byte in memory.¹⁵⁰ In this application, there is no need to implement the more elaborate forms of semaphores which are used to control the execution of tasks with 'wait' and 'signal' procedures.^{151,154}

Putting the common data, the associated semaphores and the procedures for accessing them in a single program unit called a 'monitor' eliminates a potential source of error by removing the responsibility for mutual exclusion from the programmer to the

compiler.¹⁵⁴ However, this approach is more appropriate to multitasking environments where program code is shared between processors or tasks and it was not used here.

5.8 INITIAL SYNCHRONISATION OF THE PROCESSORS

Before discussing methods for mutual exclusion, most authors make assumptions about the initial state of semaphores in the common memory area. Few describe how to start up the system. One specifically designated processor can initialise the common memory while the other processors are delayed for a sufficient time either artificially or by their own initialisation.¹⁵¹ When appropriate links are fitted to the master board, it is also possible to lock the system bus from an I/O port and this facility can be used during initialisation.

Neither of these schemes were used here. Instead, an explicit synchronisation method was established. Following operation of the central reset button on the system, the master processor initialises the common memory communication flags and then repeatedly sets and resets a synchronisation flag. Before it executes any other code, the slave processor waits until it sees the synchronisation flag in the common memory changing state. It then sets another flag indicating that it is ready to proceed and enters a waiting loop where it performs background I/O tasks. When the master processor sees that the slave is ready to proceed, it leaves its set and reset loop and continues with the initialisation of the system. The use of the dynamic scheme where the slave processor waits for a flag to change state guards against the possibility of the common memory flag being in the active state when the system is first switched on. A synchronisation scheme depending on a static value will fail in

this situation. The dynamic scheme can easily be extended to a system with more than one slave processor.

5.9 DEADLOCK AVOIDANCE

Deadlock occurs in a multiprocessor when one processor is waiting for data from a second processor while the second is waiting for the first. Three or more processors can be involved in a 'circular wait'. Deadlock can generally be avoided by careful programming and is not a problem in the power system simulator because the interaction between processors is entirely pre-determined.

5.10 DECOMPOSITION OF THE POWER SYSTEM MODEL

The partitioning of the power system model follows physical rather than purely mathematical lines. The models of the plant components are distributed according to their physical grouping in the real plant. This not only makes the software organisation of the models very clear but also minimises the data transfer between the processors.

Physically-based partitioning of simulation models normally results in a communication overhead which is insignificant compared to the overall computation time and an intuitive allocation of tasks is adequate.^{134,144} This approach has the advantage that communicated variables have physical meaning and program design and testing are simplified. Physical partitioning is a 'top-down' approach and, therefore, has all the advantages of top-down techniques in software development. The method is problem-dependent but its simplicity far outweighs this disadvantage.

A distinction can be made between parallel and cascade decomposition.^{144,148} In a system response simulation, separating

the prime mover models is parallel decomposition whereas a cascade decomposition would allocate a boiler model to one processor and a turbine model to another.

5.11 SCHEDULING OF TASKS

In parallel computers, it is important to utilise each processor evenly and to minimise degradation in system throughput due to excessive interprocessor communication.

Effective use of multiprocessors in general purpose computers requires dynamic scheduling because the executed tasks are of indeterminate length and sequence. However, in a dedicated system, the execution time and required sequence of tasks is known in advance and static scheduling is appropriate.¹³⁰ Task execution control can be permanently embodied in the operating system software and the elaborate scheduling and multi-user facilities of 'real-time executives' like RMX¹⁵⁵ are not required.

Mathematical methods are available for the allocation of tasks to processors in a real-time application,^{156,157,158,159} but these are more applicable to networks of computers where it is very important to minimise interprocessor communication. An ad-hoc approach was found to be quite satisfactory for the power system simulator. If the multiprocessor is operating at the limits of its computational power, then the allocation of model sections will become critical. However, it is probably more cost-effective to add another processor board than to attempt to use elaborate methods to achieve the highest possible utilisation of the existing hardware.

5.12 IMPLEMENTATION OF A POWER SYSTEM MODEL ON THE MULTIPROCESSOR

To demonstrate the application of the multiprocessor system to the real-time simulation of a power system, a model with two

coal-fired boiler-turbine units was established. Some of the results reported in Chapter 6 were obtained with this multiprocessor simulator. The flow diagram shown in Figure 5.2 outlines the organisation of the programs for the master and slave processors. One thermal plant model is allocated to each processor and the master also solves the single alternator model.

Following synchronisation of the two processors as described in Section 5.8, the slave processor enters a waiting loop where it performs background I/O tasks, transferring data between the common memory and its I/O ports. The master processor performs its own initialisation and proceeds through the operator dialogue, placing data for the slave processor in common memory. The slave is then re-activated to copy its data from the common memory and to calculate the initial conditions of its model. Once both processors have calculated the initial conditions of their models, the master processor starts the real-time clock.

At each integration interval, the master commands the slave to perform one step of its thermal plant model and then processes its own model equations. When both processors have finished the step, the master collects the slave's power output value and performs one step of the single alternator model, putting the resulting system frequency value in common memory. After the master has sent the injection and logging signals for output, it returns to a loop and waits for the next time interval. While the slave is waiting to execute its thermal plant model, it performs background I/O tasks.

The interrupts for turbine power and grid frequency measurement processed in the single processor implementation are handled in the same way by the master in the multiprocessor

configuration.

The control flags used in this implementation are single byte variables and, in fact, neither these nor the shared data need be protected by semaphores because the interaction of the two processors is fully determined in advance. At all points of interaction, one processor waits for the other and there is no possibility of data corruption.

In an alternative system, the slave processor could be allowed to run asynchronously to the master processor while using its own timer to provide real-time execution. In this case, the shared data would have to be protected by semaphores.

At one stage, the slave processor was used to provide additional analog outputs for the simulator so that a larger number of internal simulation variables could be recorded in the data logger. The slave processor was not solving any model equations and so it was not synchronised to the master processor. The two-byte integer values transferred to the slave were, therefore, protected by semaphores.

5.13 SEMI-AUTOMATIC DECOMPOSITION

Writing separate programs for each processor is a direct but cumbersome approach. Although this method was used here, a means of writing the multiprocessor software as a single program would be extremely useful. Such systems have been developed for other multiprocessors^{130,137,140} and would be straightforward to implement for the power system simulator. A text translating package such as STAGE 2B could be employed to separate the sections of source code for each processor and add these to an appropriate operating software and synchronisation kernel. Directives to the translator could be included in the comment

lines of the source code which could then be linked with different libraries to run without alteration on a uniprocessor. This type of facility would reduce the scope for programming errors that exists when two or more interacting programs have to be constructed directly.

5.14 ALTERNATIVE CONFIGURATIONS

The modular nature of multiprocessor systems is a major advantage because it makes expansion relatively easy.

With the 8086/8088-based Multibus systems, there is the possibility of improving the performance by using single board computers based on the more powerful 80286 or 80386 microprocessors. These microprocessors are code compatible with the 8086 and the 8088 and so performance improvements can be obtained without any great need for re-coding.

A synchronous execution procedure has the disadvantage that for a large number of processors working on a particular problem, there may be a time in the simulation cycle when there is a particularly heavy load on the common bus. This tends to lead to a degradation in performance because the system is delayed while the data transfers take place. Allowing the processors to communicate asynchronously has the advantage that they could run at different rates and the communication load would be more evenly distributed in time.¹⁶⁰ However, the communications protocol is more involved and more complex programming is necessary.

The two-processor system described here has sufficient computational power to solve at least six of the thermal plant models in real-time. If more detailed models were used, requiring a shorter integration interval for some components, it would be advantageous to use a multiple rate integration scheme. This

would most easily be implemented by solving the fastest components on the master processor, because the D/A convertors would normally be updated at the fastest integration rate. The slower components would be simulated on the slave processor (or processors) with its own real-time clock. The two processors would run asynchronously so the shared data would require protection by semaphore.

5.15 DEGRADATION IN PERFORMANCE DUE TO BUS CONTENTION

Frequently, the addition of extra processors does not achieve the expected performance improvement,¹²⁹ because of the overhead introduced by communication and synchronisation.

A number of authors have described methods to estimate the degradation in the performance of multiprocessors due to common memory access contention and other factors.^{161,162} Grasso et al.¹⁶³ studied the memory interference in multiprocessor systems for control and simulation applications. When processors are added to a system, a point is reached where adding a processor does not increase the overall throughput of the system. The number of processors at which this occurs depends on the fraction of time each processor requires the common bus.

The smallest fraction considered by Grasso et al. was 4% and, for this value, no degradation in performance was observed with eight processors, the maximum number investigated. Inspection of the program code for the power system simulator, suggests that the corresponding fraction for the simulator is certainly less than 1%. It should, therefore, be possible to expand the system to the full sixteen processor configuration supported by the Multibus hardware, without encountering significant common bus interference.

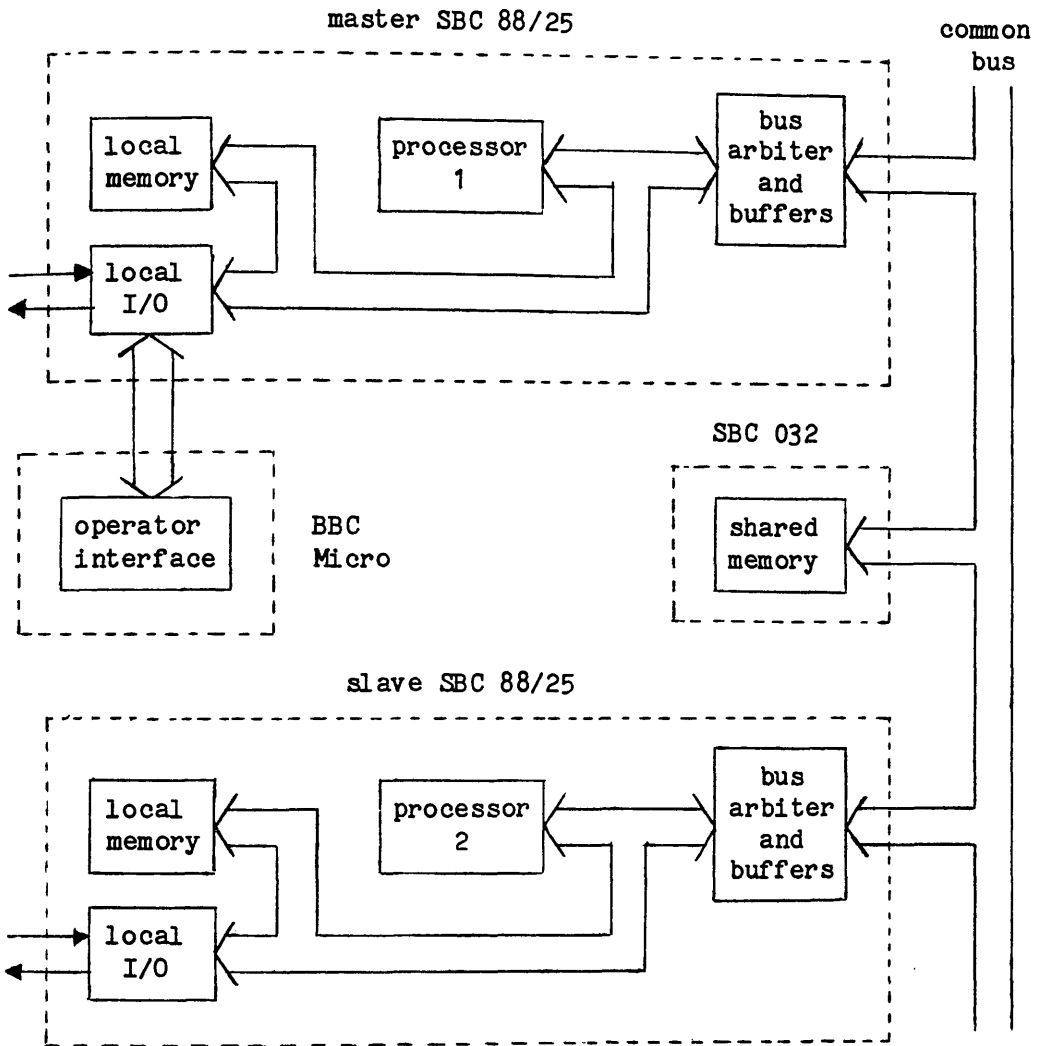


Figure 5.1 Arrangement of the multiprocessor hardware

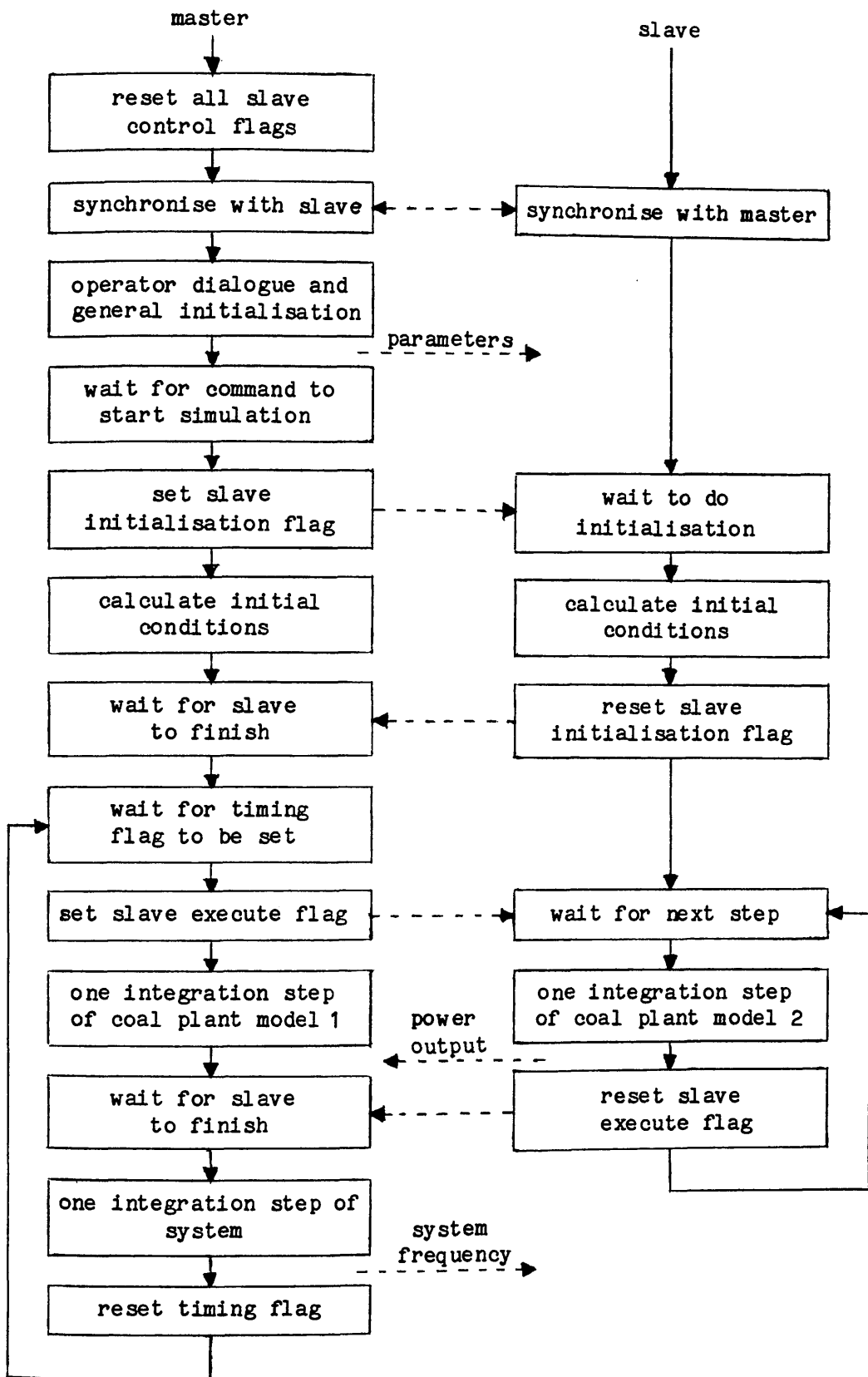


Figure 5.2 Organisation of the master and slave programs

CHAPTER 6

DETAILED TESTS OF A MIXED HYDRO-THERMAL SYSTEM

After various improvements had been made to the power system simulator, further tests were conducted at Loch Sloy Power Station on No.3 machine with its microprocessor governor and No.2 machine with its mechanical-hydraulic governor. These tests used a more realistic thermal plant model based on that used by the CEGB in off-line system response studies^{2,44} and described in detail in Chapter 3. The simulator implementation also included a mechanism to compensate for grid frequency movements occurring in the course of a test. A range of operating situations were investigated by changing the key parameters of the simulation and the effects of variation in the following areas were considered: Characteristics of the thermal plant; relative proportions of generating plant types; operation of the hydro-turbine at a different load level; proportion of non-regulating plant on the system and the amount of spinning reserve held on the steam plant.

A dual-processor simulator had been established (Chapter 5) and this had been used to implement a power system model consisting of two blocks of thermal generation whose parameters could be selected independently during the operator dialogue. This was used to investigate the operation of two steam units of different configuration in a mixed hydro-thermal system.

Using the speeder motor injection technique, some of the tests were repeated on No.2 machine with its hydraulic temporary droop governor.

Some of the tests were re-run and this confirmed the repeatability of the results which are presented in this chapter.

In all the systems studied, the MW ratings of the thermal units vary according to their size relative to the real 32.5MW hydro-turbine. For example, in a system with 90% thermal and 10% hydro-electric generation, the rating of the thermal unit will be 292.5MW. The total MW capacity of the system will, therefore, also vary depending on the proportion of the system constituted by the real hydro-turbine. It would be possible to keep the system size constant at, say, 1000MW and consider the rating of the hydro-turbine to change merely by altering the values on the plot axes. The frequency transients and plant responses would essentially be the same in a 1000MW or a 10,000MW system with proportionate plant mixes and generation/load imbalances. In all of the plotted responses, the hydro-turbine power output is scaled over a 15MW range which corresponds to about 46% m.c.r. (maximum continuous rating). The thermal plant responses are plotted over the same percentage range but as the generation mix changes, the end-point values in MW must also change.

All of the tests reported in this chapter used simulated step changes in demand of 10% of the total generating capacity on the system. Although all the tests involved increases in demand, there is no reason why results could not be obtained for reductions. It is convenient to remove an increase in demand before stopping a test run, but this will not give accurate results for a decrease in demand because the boiler model will not have returned to a steady state. To study this type of incident, the simulator should be restarted with a negative step selected so that the boiler model is re-initialised.

For all of the tests described in this chapter, the parameters of the thermal models were as given in Section 3.6.6;

in particular, the droop was 4% ($b_p=0.04$) and the fuel feed delay, T_d was 60s. These values are appropriate to a coal-fired unit. The response of an oil-fired unit could be investigated if desired but this was not done here. The reheater time constant, T_r and the operating point of the thermal plant model were changed for some of the tests. As discussed in Section 3.8.1, 20s is a reasonable figure for the system alternator time constant, T_a , and this value was used for all of the tests.

6.1 ELECTRONIC GOVERNOR IN A MIXED SYSTEM WITH ONE THERMAL UNIT

The starting point for the series of tests with the coal-fired plant model was, as in the preliminary tests with the oil-fired plant model, a system with two equally-sized generation blocks. One of these was the real hydro-turbine with its electronic double derivative governor and the other was the simulated coal-fired boiler-turbine unit. The reheater time constant, T_r was 10s. The hydro-turbine output power was initially 10MW (31% m.c.r.) and the coal-fired plant was operating at 80% m.c.r. The response of this system to a 10% step increase in consumer demand is shown in Figure 6.1. This test may be regarded as a base case for comparison with the results presented in the following sections.

After the step change in load, the system frequency falls rapidly until it is brought up at about 49.39Hz by the operation of the governor on the thermal unit. For this size of disturbance, the steam valves reach their fully open position causing a 'knee' in the generated power trajectory where the rate of increase in power output is reduced. The power output continues to rise as the extra steam appears at the IP and LP turbines. When the frequency rises again, the governor valves move off their end-stop and the

power output falls sharply. By this time, the thermal energy stored in the boiler is becoming depleted, reducing the drum pressure and tending to reduce the power output from the steam turbine until the fuel feed to the furnace can be increased. The hydro-turbine does not respond as rapidly as the steam turbine but its change in output is sustained. The ability of the hydro-turbine to complement the thermal plant by providing power when the thermal energy reserves are depleted is of great importance.

6.1.1 Operation with Non-reheat Plant

If the time constant, T_p , of the first-order lag representing steam storage in the reheater is reduced from 10s to 2s, the model behaves like non-reheat plant and this has a significant effect on the response (Figure 6.2). Increases in steam flow through the HP turbine stage can immediately feed through to the IP and LP stages which, in total, constitute 80% of the capacity of the turbine. This means that non-reheat plant can respond more rapidly to loading disturbances, at least while boiler pressure is maintained. A more rapid thermal plant response and a correspondingly reduced frequency swing to about 49.53Hz can be seen in Figure 6.2. This type of behaviour was typical of steam plant about 30 years ago before construction of plant for the reheat cycle became economic. The hydro-turbine is not required to respond as rapidly although it eventually reaches the same load level as in Figure 6.1. The states of the systems are the same at 120s with a frequency of 49.85Hz showing that the longer term response is determined by the dynamics of the boiler rather than those of the turbine.

6.1.2 Variation of Plant Proportions

A system with 50% thermal and 50% conventional and pumped-storage hydro-electric generation, as used in the above tests, is most unlikely to occur in the UK system as a whole. At the most, the proportion of hydro plant could reach 10% if abnormal conditions arose at a time of low demand during a summer night. However, if all or part of the Scottish system were to become disconnected, much higher proportions of hydro-electric generation could occur, particularly if more pumped-storage plant were to be built in Scotland.

The succession of responses shown in Figures 6.1, 6.3 and 6.4 illustrates the effect of varying the relative proportions of hydro and thermal plant on the system. For these tests, a reheat turbine model was used ($T_p=10s$). With a 50% hydro component (Figure 6.1), the frequency transient is large, reaching 49.39Hz, and the hydro-turbine makes a large initial contribution driven by this swing. If, instead, the system has 20% hydro and 80% coal-fired plant (Figure 6.3), the initial frequency swing is reduced, reaching 49.51Hz, because more stored thermal energy is available. However, the frequency at 120s falls from 49.85 (Figure 6.1) to 49.79Hz because there is less hydro plant to provide a response in the mid term. Reducing the hydro component further to 10% (Figure 6.4) results in a further reduced frequency transient (49.55Hz), but, again, the frequency at 120s is lower at 49.77Hz. As the proportion of hydro-electric plant decreases, the shape of its response changes considerably. The initial increase in output is smaller but there is a gradual climb to a load level that is higher when the hydro-turbine is a smaller proportion of the system.

This sequence illustrates a problem that may arise if the Scottish system is required to operate in isolation from the rest of the national grid. The proportionate reduction in plant providing a response in the first 5s or so of a disturbance may lead to large frequency swings with consequent shedding of load by protective relays. However, the results illustrate the ability of hydro-turbines to complement the response of thermal plant by providing power in the mid-term period when the steam turbines are suffering from a drop in boiler pressure.

The small deviation in the hydro-turbine power output in Figure 6.3 is caused by a fault in the microprocessor governor which causes an occasional glitch on the governor output.

The system alternator time constant, T_a was kept at 20s for all of these tests, although it would be reasonable to reduce it somewhat for a system with a high proportion of hydro plant. A value of 16s would be suitable for a 50% hydro system. Reducing the alternator time constant would increase the size of the initial frequency swings and produce slightly more oscillatory behaviour. The effects of variation in this parameter could be investigated if desired but this was not done here.

6.1.3 Variation in Hydro-turbine Operating Point

When tests are repeated at different hydro-turbine operating points, the responses obtained are slightly different. Figures 6.5 and 6.6 correspond directly with Figures 6.1 and 6.4 except that the initial power output of the hydro-turbine was 24MW (74% m.c.r.) rather than 10MW (31% m.c.r.). When the hydro-turbine is 50% of the generating plant on the system (Figures 6.1 and 6.5), there is a noticeable difference in the form of the initial frequency transient. The initial swing is larger when the hydro-

turbine is at a higher load level, reaching 49.34 rather than 49.39Hz, and the behaviour as a whole is slightly more oscillatory. This is the result of two features: The increase in the pipeline water time constant, T_w with increasing load and the increase in the effective gain of the hydro-turbine governor associated with the non-linear relationship between valve position and water flow rate. The overall increase in power output from the hydro-turbine is also slightly larger (0.25MW) in Figure 6.5 due to the increase in gain which, in fact, reaches a maximum at about 80% m.c.r.^{39,108} If the hydro-turbine is a smaller proportion of the system as in Figures 6.4 and 6.6, then these factors have less effect. Generally, the margin of stability of the mixed hydro-thermal system decreases as the hydro content increases. The initial dip in the hydro-turbine response caused by the pipeline effect is quite evident in Figure 6.5. This dip becomes more pronounced at higher loads as the pipeline water time constant, T_w increases.

If the hydro-turbines in a power station are supplied from a single high pressure pipeline, the water inertia time constant also changes if other sets are running. With more plant generating, T_w is larger which leads to a reduction in the stability of the sets. However, this effect is usually less pronounced than the variation of T_w with load on a particular machine because only part of the pipeline is shared between the turbines. The running of other sets at Sloy in the station was found to have very little effect on the response of the test turbine in the hydro-thermal system configurations used here. If the stability of the system was marginal, the effect would be more important.

6.1.4 Increased Base Load Capacity

The response shown in Figure 6.7 is for a system with 50% thermal (reheat), 20% hydro and 30% base load (non-regulating) plant and that in Figure 6.8 is for 50% thermal, 10% hydro and 40% base load. There are two effects here: As the proportion of nuclear or other base load plant increases, the magnitude of the initial frequency swing becomes larger, reaching 49.25Hz in Figure 6.7 and 49.20Hz in Figure 6.8. The swing is considerably extended in comparison with Figure 6.1 where the frequency fell to 49.39Hz. As a result of the large frequency swing, the steam valves stay fully open for longer, changing the shape of the thermal plant response. The second effect is the increasing activity of the hydro plant as it is reduced from 50% to 20% and then 10% as a proportion of the overall system. As the amount of base load capacity increases and the hydro-turbine becomes a smaller proportion of the system, the frequency at 120s drops from about 49.83Hz (Figure 6.1) to 49.72Hz (Figure 6.7) and 49.63Hz (Figure 6.8).

Figures 6.4 and 6.8 are both for systems with 10% hydro and comparison of these shows the effect of an increase in non-regulating capacity while the proportion of hydro remains the same. In Figure 6.4 with 90% thermal plant (regulating), the system frequency is about 49.78Hz at 120s.

6.1.5 Larger Reserve on Thermal Plant

When a larger reserve is maintained on the thermal plant, the behaviour of the system is rather different. Figure 6.9 corresponds to Figure 6.8 except that the thermal plant is initially operating at 70% rather than 80% m.c.r. The generation deficit is then not sufficiently large to take the governor valve

to its fully open position and the thermal plant is able to contain the disturbance more readily. The frequency swing is held to 49.40Hz and the hydro-turbine is not called upon to make such a large contribution. The system frequency at 120s is not changed much by the increase in spinning reserve because the same change in boiler firing is required.

6.2 ELECTRONIC GOVERNOR IN A MIXED SYSTEM WITH TWO THERMAL UNITS

Using the dual-processor simulator, tests were conducted on a system consisting of two blocks of thermal generation, some non-regulating capacity i.e. either nuclear or base-load hydro or thermal generation, and the real hydro-turbine. Both the thermal units were represented using the model described in Chapter 3 and used in the studies already reported in this chapter. Throughout all of the tests described in this section, the thermal units were each 25% of the total system capacity.

An initial test with the base case parameters confirmed that this version of the simulator produced results that were identical to those obtained with the single thermal plant model (Figure 6.1). The result of this test has been plotted (Figure 6.10) to facilitate comparison with the tests of different configurations described in the following sections.

6.2.1 Different Thermal Plant Operating Points

If one thermal unit is operating at 90% and the other at 70% of full load when a 10% generation deficit occurs (Figure 6.11), the frequency transient is little different from that obtained if both units are operating at 80%. This shows that even though the individual responses are quite different, the aggregated response is similar to the individual responses if both units are operating at 80% load (Figure 6.10) or the response of a single unit

operating at 80% m.c.r. (Figure 6.1). If the operating points of the thermal plant are split in such a way that the amount of spinning reserve is the same, the output from the more efficient unit can be increased without greatly affecting the system's ability to deal with a disturbance.

6.2.2 Operation With Non-reheat Plant

If one of the thermal units has a non-reheat turbine (Figure 6.12) with a consequently faster response, the frequency swing is reduced, reaching 49.48 rather than 49.38Hz, and this initiates a smaller hydro-turbine contribution. As in Figure 6.2, the state of the system at 120s is not affected by the change in reheater time constant. By operating the non-reheat plant at 70% and the reheat plant at 90% of full load, the disturbance to the reheat plant can be considerably reduced (Figure 6.13) although the frequency transient is unaffected. This illustrates the advantage of allocating immediate reserve duties to generally older and lower merit non-reheat plant allowing the efficient reheat plant to operate continuously at or near maximum output. If the thermal plant operating points are interchanged, the frequency swing is slightly increased, reaching 49.41 rather than 49.46Hz, and there is more disturbance to all the plant including the hydro-turbine (Figure 6.14).

6.2.3 Increased Base Load Capacity

Figure 6.15 corresponds to Figure 6.8 but the former was obtained with the dual coal plant model. The hydro-turbine was also operating at a higher load level (20MW, 62% m.c.r.). Both of these responses are for systems with 50% thermal, 10% hydro and 40% base load capacity. The responses show the larger and longer frequency deviation associated with an increase in non-regulating

capacity and the increasing activity of the hydro-turbine as it becomes a smaller part of the system.

6.3 OPERATION OF THE GRID FREQUENCY CORRECTION MECHANISM

Figure 6.16 shows the simulated system frequency, injected frequency and real grid frequency signals for the test shown in Figure 6.15 plotted over a longer time scale. The injected signal is offset to compensate for the grid frequency disturbance occurring towards the end of the test. There is no sign of a deviation in the turbine power output and this shows the effectiveness of the grid frequency correction mechanism. Note that the grid frequency and injected signals are plotted on a different scale.

6.4 HYDRAULIC GOVERNOR IN A MIXED SYSTEM WITH TWO THERMAL UNITS

Following the tests with the dual coal plant model simulator on No.3 machine with its electronic governor, similar studies were performed on the hydraulic temporary droop governor on No.2 machine. (No.1 machine had been used in earlier tests of this type, reported in Section 4.2, but it was not available at this time.) The test signal was injected via the raise/lower controls as described in Sections 2.2 and 4.2. The calibration figure for the speeder motor on this set was measured to be 8s for a full-load change in output i.e. a 3% change in frequency.

The simulated system was provided with 10% hydro plant in the form of the real hydro-turbine, two regulating (4% droop) reheat thermal units of equal capacity and some base load plant. The thermal unit capacities were reduced together in accordance with the amount of non-regulating plant selected. One thermal unit was operating at 90% and the other at 70% m.c.r. and the initial power output from the hydro-turbine was 10MW.

Figures 6.17, 6.18 and 6.19, for 0, 20 and 40% base load respectively, show the responses of the system to 10% increases in demand applied through a first-order lag. This lag had a time constant of 2.5s and was used, as described in Section 2.5, to avoid the rate-limiting effect of the speeder motor injection technique. As the amount of base load capacity is increased, the frequency swing becomes larger and the hydro-turbine is called upon to provide more of the deficit. The minimum system frequencies are about 49.61, 49.48 and 49.28Hz for the systems with 0, 20 and 40% base load respectively. The simulated system frequency plots appear quantised because they had to be reconstructed from the record of the pulses applied to the raise/lower controls.

Figure 6.20 shows a repeat of the temporary droop governor test with 40% base load (Figure 6.19) at a higher load level. In this test, the initial power output from the hydro-turbine was 20MW. It can be seen that, as with the electronic governor tests, the frequency swing is slightly larger at the higher load level, reaching 49.23Hz. This is due to the increased pipeline time constant. Note that Figures 6.19 and 6.20 have been plotted over different time scales. A second run of this test with the same parameters and initial conditions confirmed the repeatability of the results obtained using the speeder motor injection technique.

6.5 A COMPARISON OF THE TWO GOVERNOR TYPES

In order to make a comparison between the responses of the double derivative and temporary droop governors, one of the previous tests on the electronic governor on No.3 machine had used a lagged demand transient with a time constant of 2.5s. The result of this test is shown in Figure 6.21 and the form of the demand

disturbance is shown in Figure 6.22. The system composition was 50% thermal in the form of two units at different operating points, 40% base load and 10% hydro. The initial power output from the hydro-turbine was 20MW and the response is, therefore, directly comparable with the test of the temporary droop governor shown in Figure 6.20. (Figure 6.15 shows the corresponding double derivative response for a step increase in demand.)

These two tests show clearly that the type of governor affects the shape of the hydro-turbine power trajectory. It can be seen that the double derivative governor has a more rapid and sustained response. With the temporary droop governor, the hydro power output tends to fall back slightly after the thermal plant has restored the system frequency to a reasonably steady value. The minimum system frequency is only slightly improved from 49.23 to 49.28Hz, but, considering the small relative capacity of the hydro-turbine, the improvement in the system frequency at 120s from 49.43Hz (Figure 6.20) to 49.55Hz (Figure 6.21) is very significant. The reduction in disturbance to the thermal plant is also worthwhile.

6.6 CONCLUSION

The results presented in this chapter have illustrated a number of the features of the behaviour of a nuclear-hydro-thermal power system. More importantly, they have demonstrated the ability of the power system simulator to investigate the response of mixed system to loading disturbances and to establish the merits of particular governor configurations on a real hydro-turbine. The use of a multiprocessor simulation vehicle to relieve constraints on the problem size has also been demonstrated in the environment of on-line tests at a power station.

Labels for Figures 6.1 to 6.22

- FES - simulated system frequency
- POH - hydro-turbine power output
- POC - coal-fired plant power output
- POC1 - coal-fired plant 1 power output
- POC2 - coal-fired plant 2 power output
- FESCR - simulated system frequency corrected for grid frequency
deviations
- GFREQ - real grid frequency
- PD - consumer demand

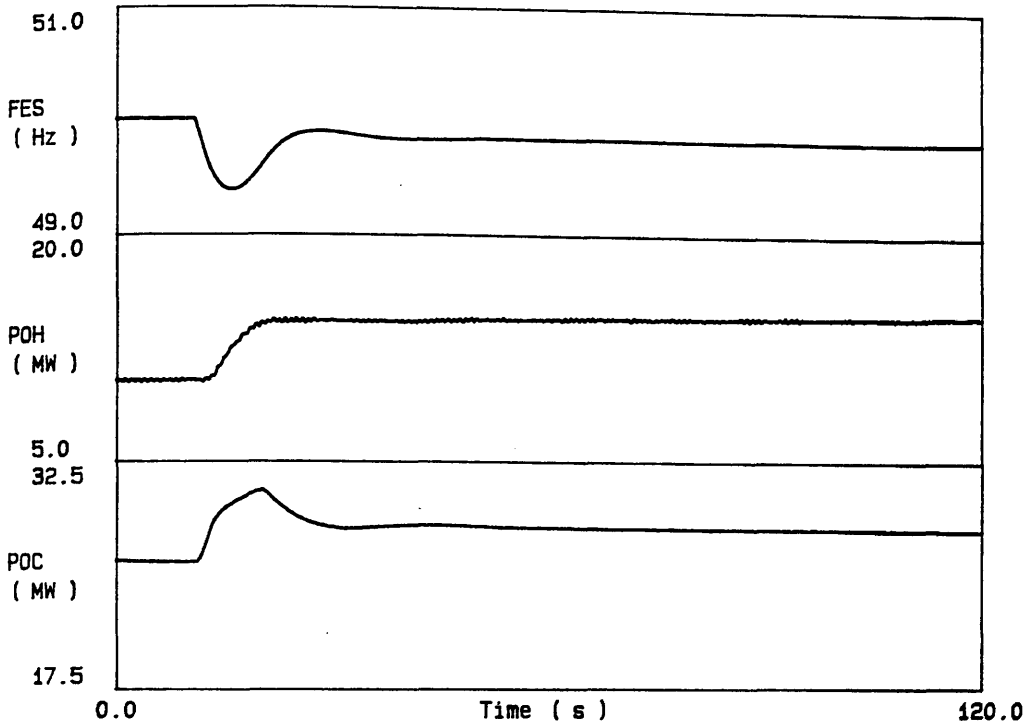


Figure 6.1 Mixed system test with electronic governor
(reheat plant, 50% hydro)

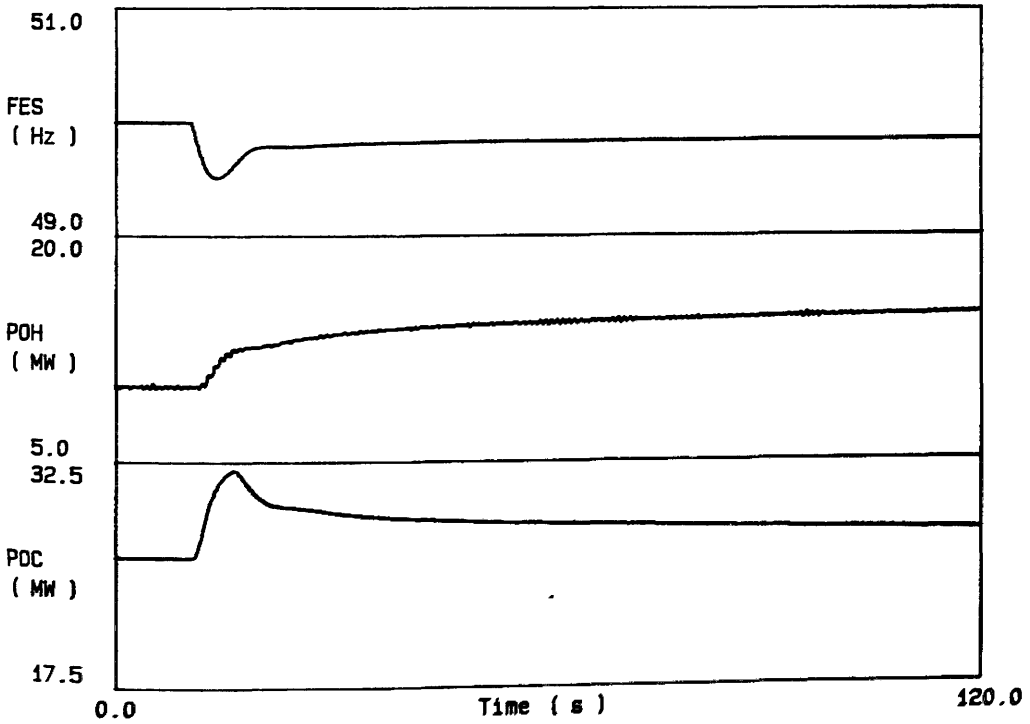


Figure 6.2 Mixed system test with electronic governor
(non-reheat plant, 50% hydro)

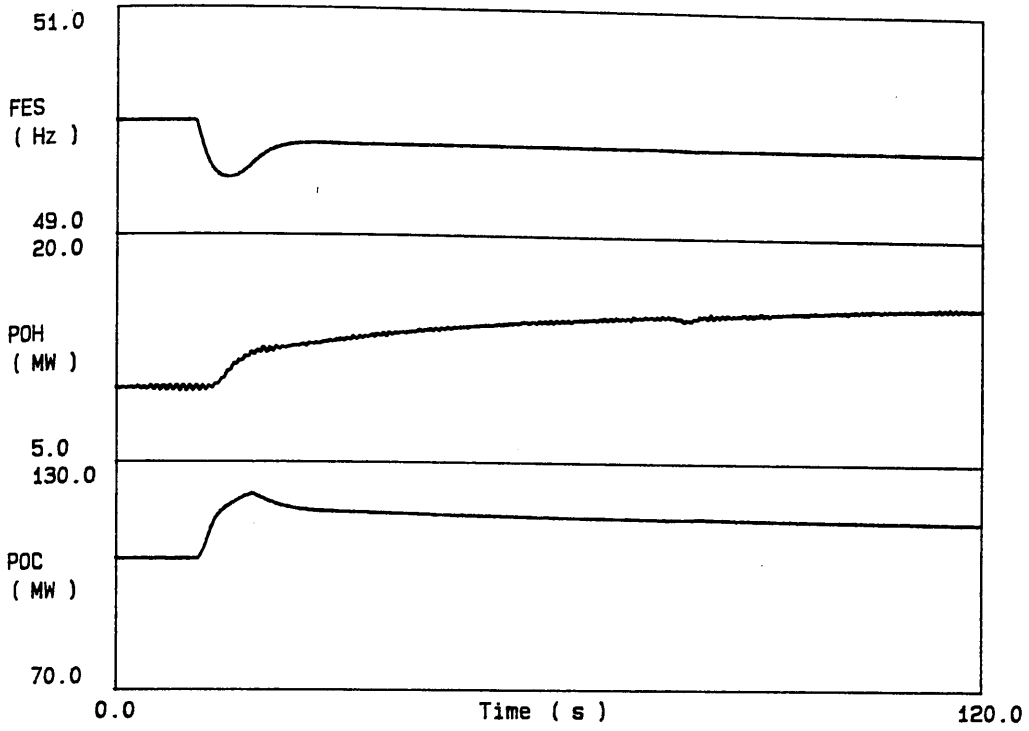


Figure 6.3 Mixed system test with electronic governor (20% hydro, 80% thermal)

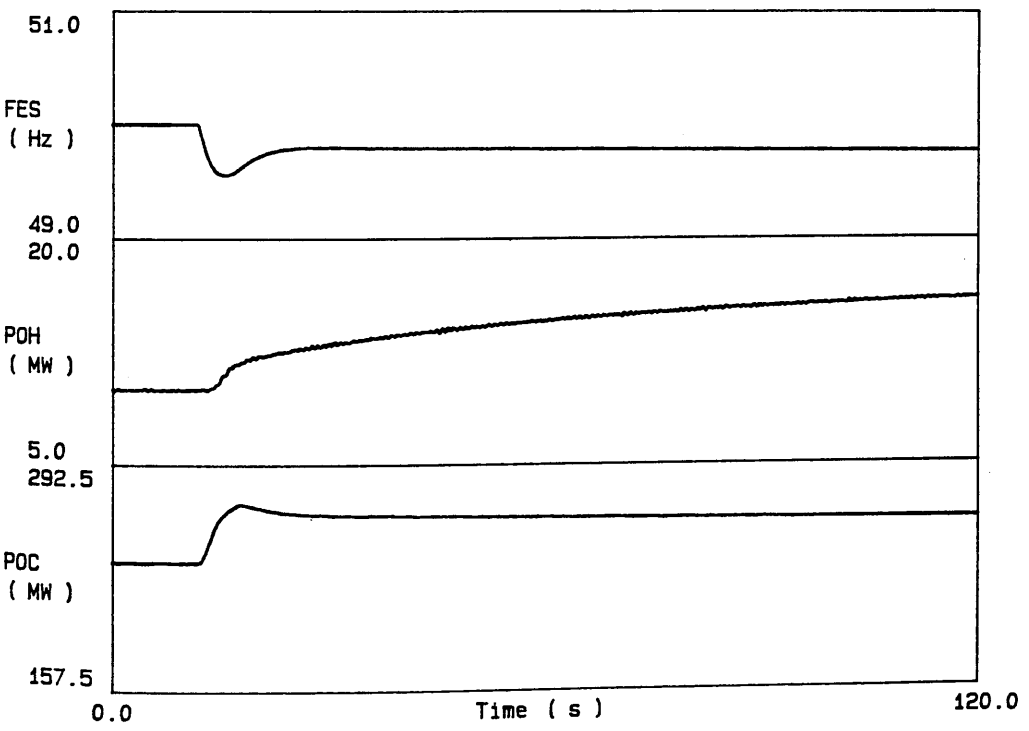


Figure 6.4 Mixed system test with electronic governor (10% hydro, 90% thermal)

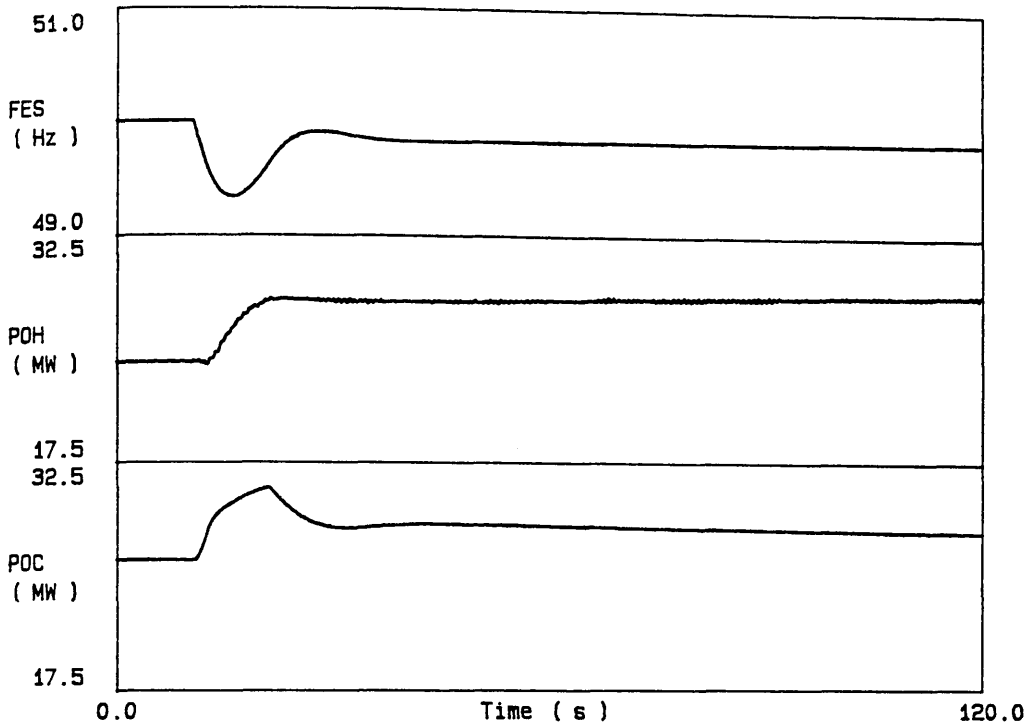


Figure 6.5 Mixed system test with electronic governor (reheat plant, 50% hydro, higher hydro operating point)

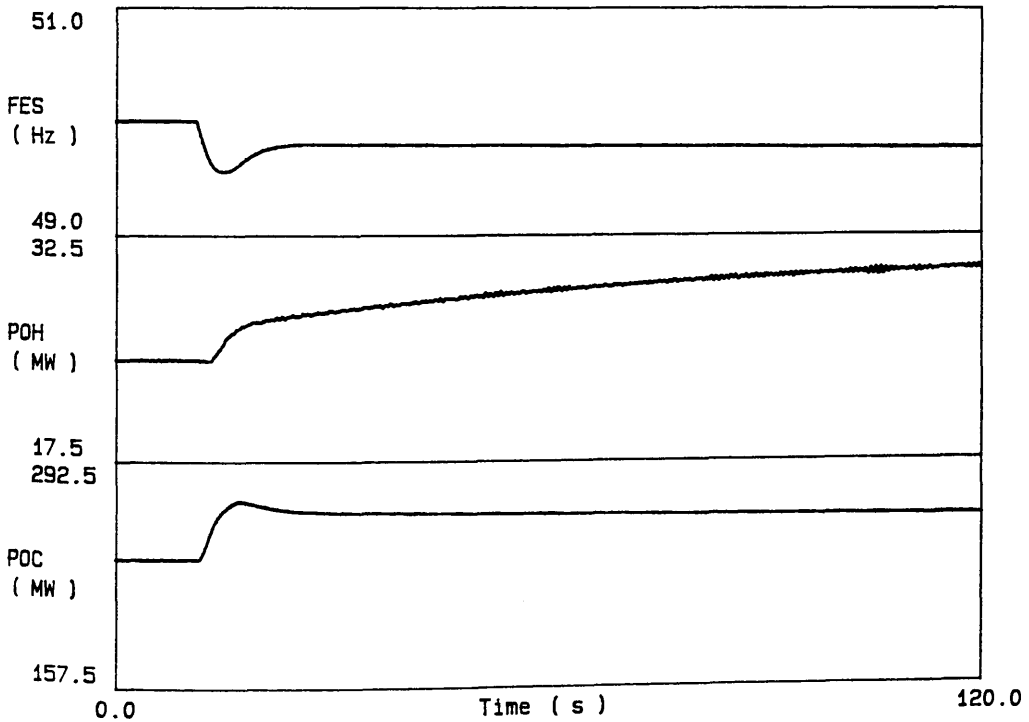


Figure 6.6 Mixed system test with electronic governor (10% hydro, 90% thermal, higher hydro operating point)

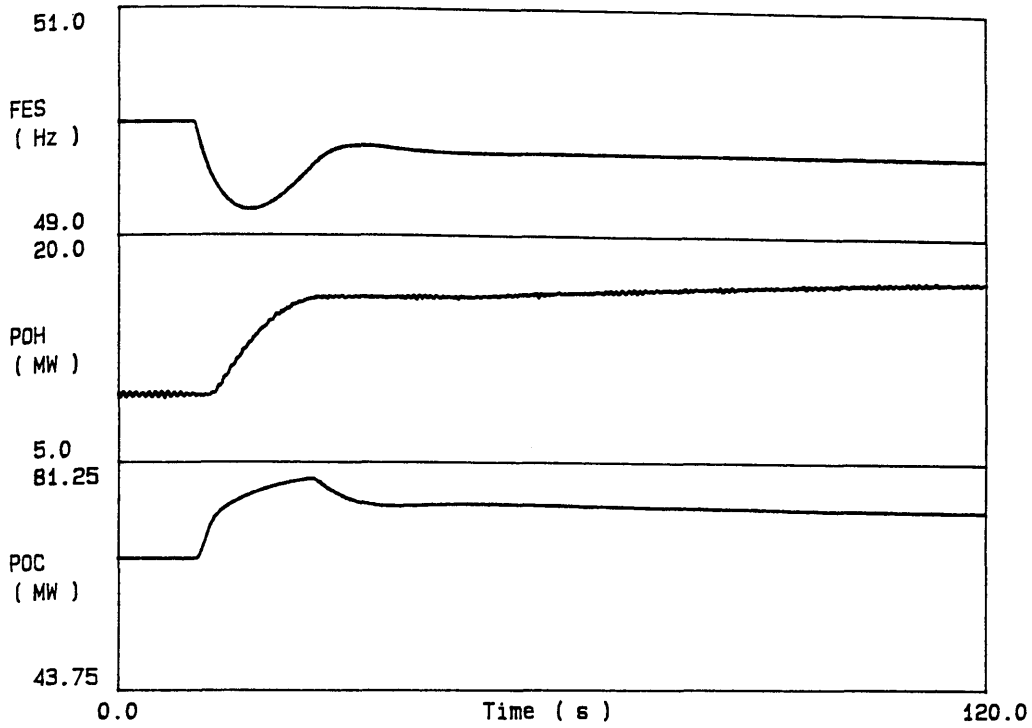


Figure 6.7 Mixed system test with electronic governor
(50% thermal, 20% hydro, 30% base load)

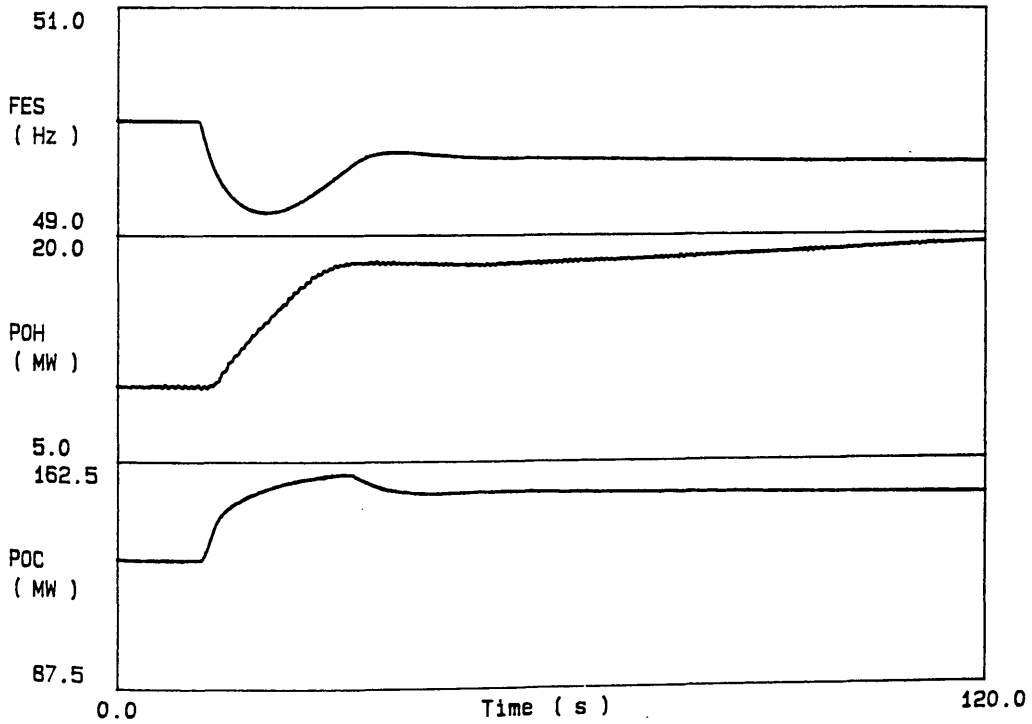


Figure 6.8 Mixed system test with electronic governor
(50% thermal, 10% hydro, 40% base load)

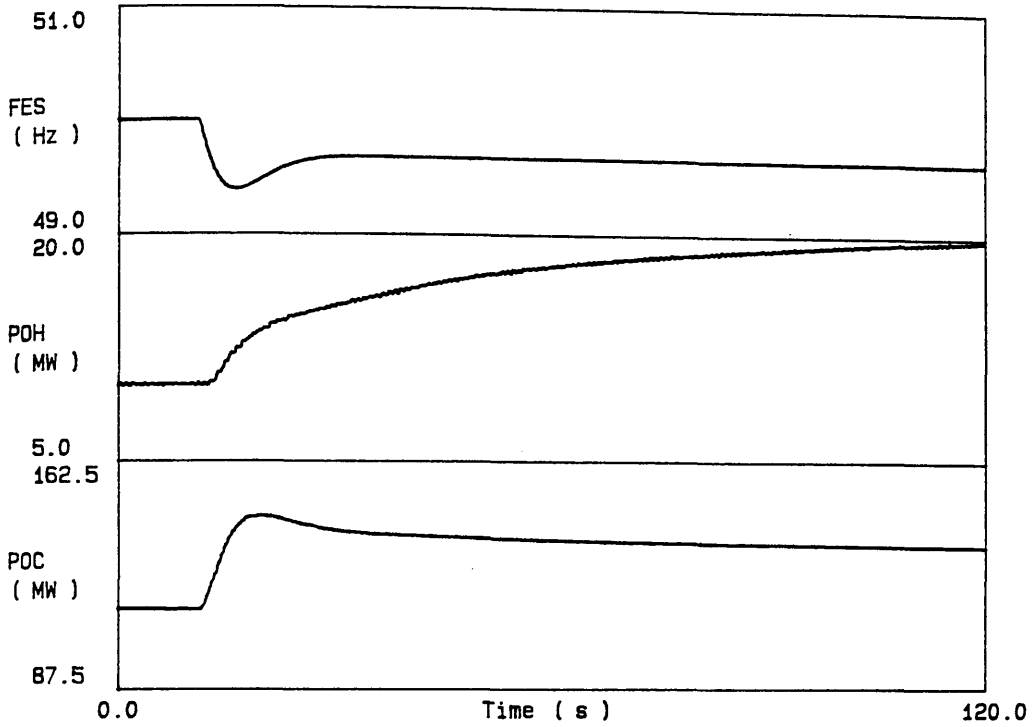


Figure 6.9 Mixed system test with electronic governor
(50% thermal, 10% hydro, 40% base load, larger reserve)

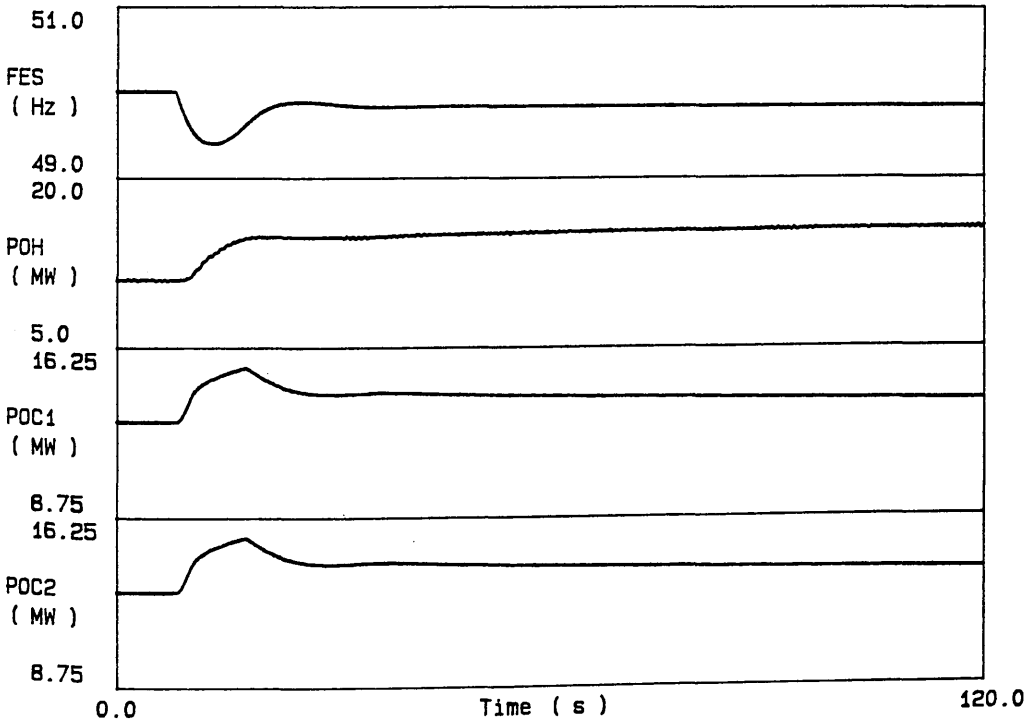


Figure 6.10 Mixed system test with two thermal units
(50% hydro)

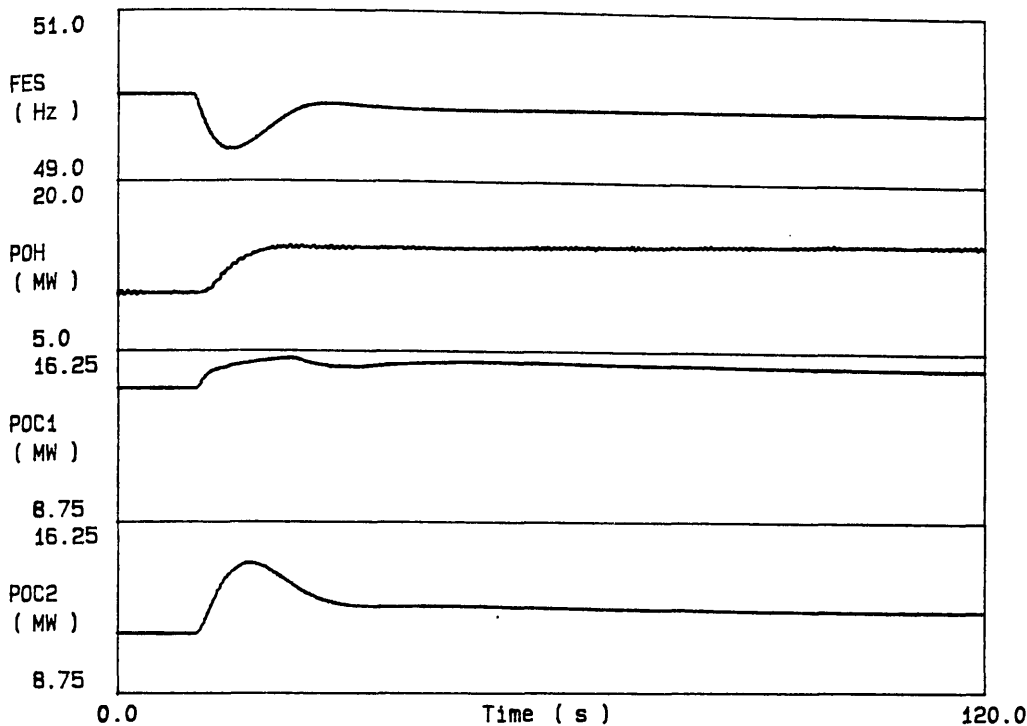


Figure 6.11 Mixed system test with two thermal units (different operating points)

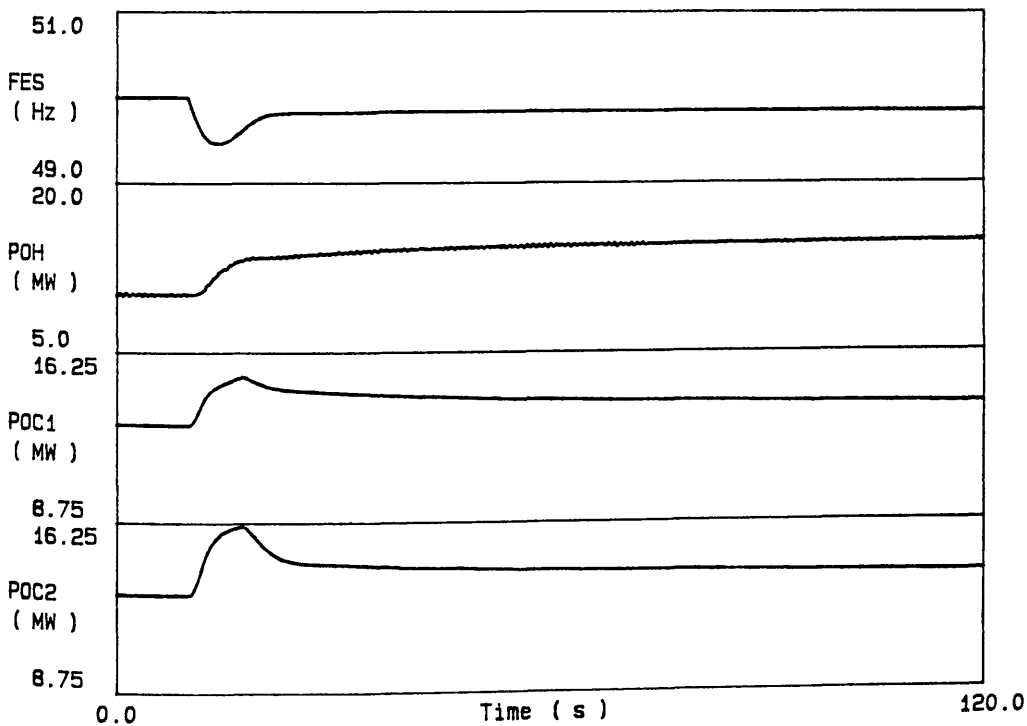


Figure 6.12 Mixed system test with two thermal units (some non-reheat plant)

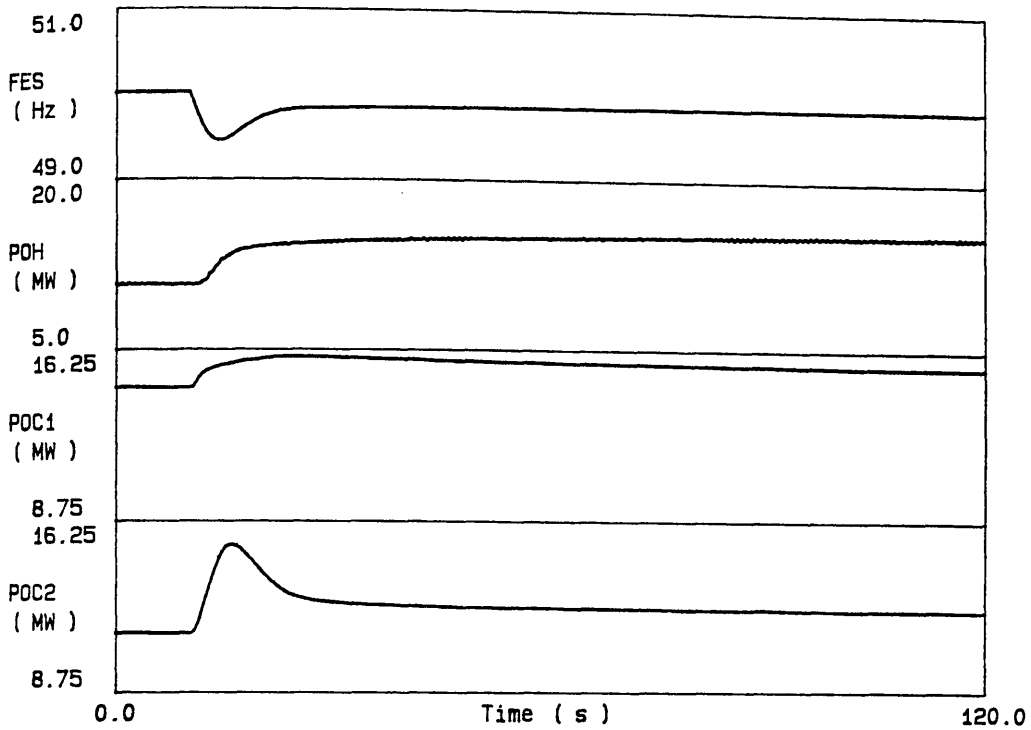


Figure 6.13 Mixed system test with two thermal units (some non-reheat plant, different operating points)

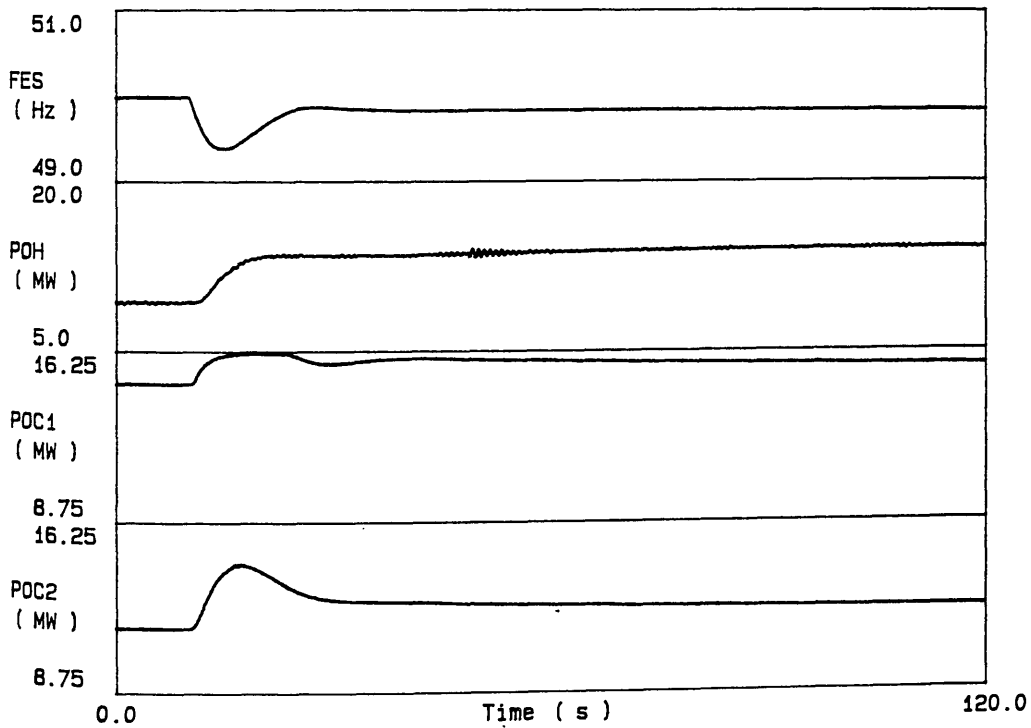


Figure 6.14 Mixed system test with two thermal units (some non-reheat plant, interchanged operating points)

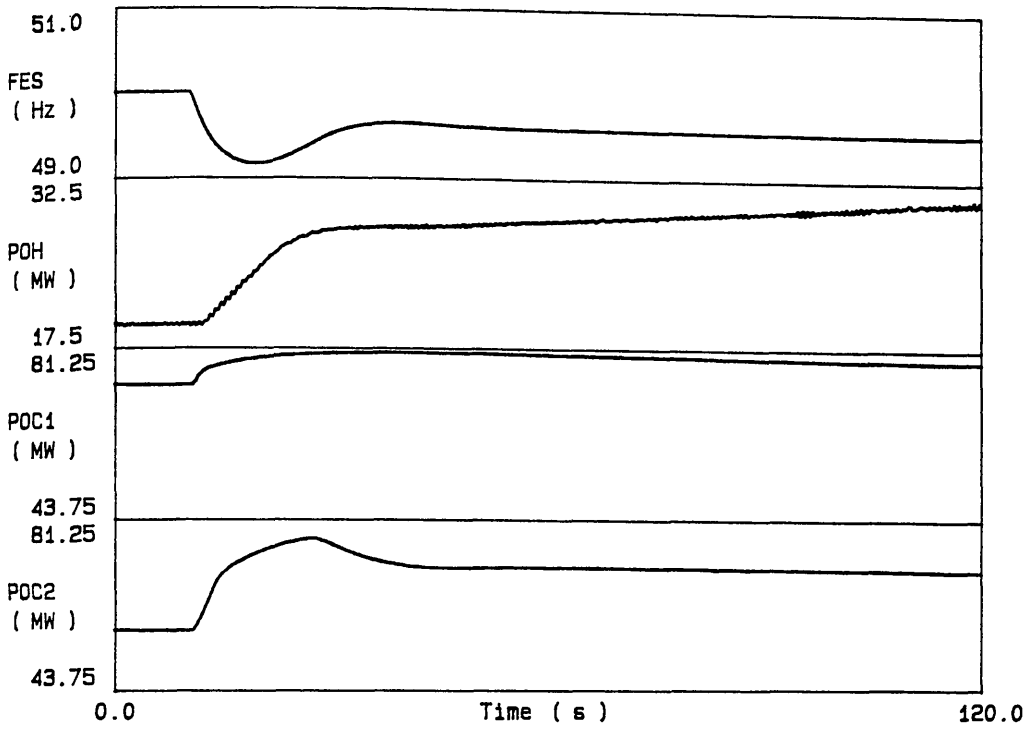


Figure 6.15 Mixed system test with two thermal units (50% thermal, 10% hydro, 40% base load)

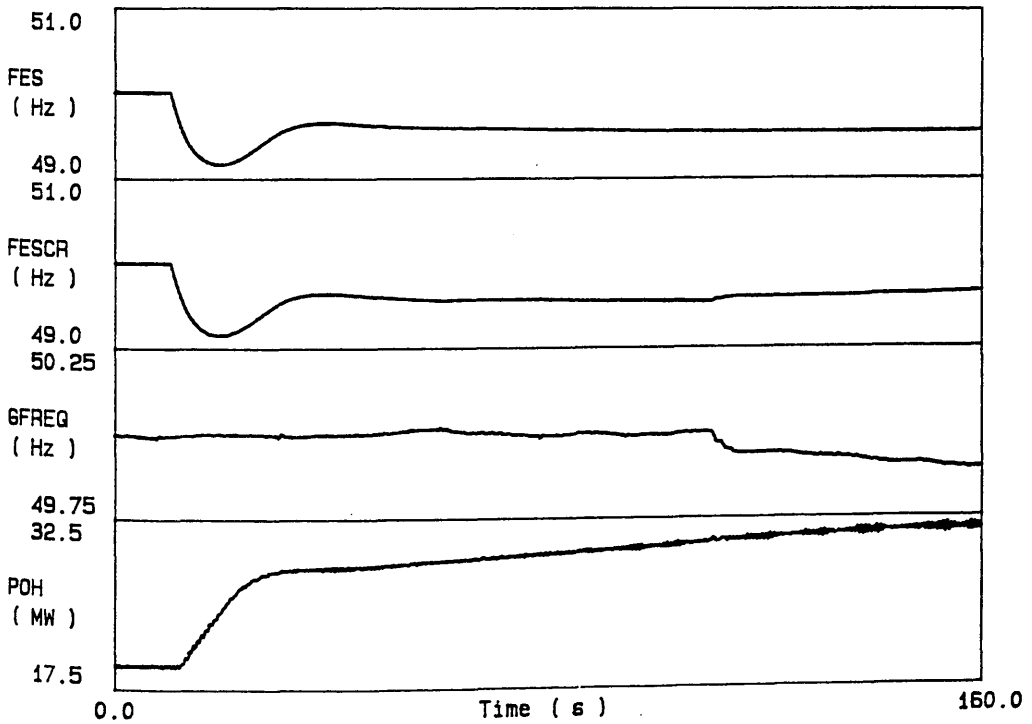


Figure 6.16 Operation of the grid frequency correction mechanism

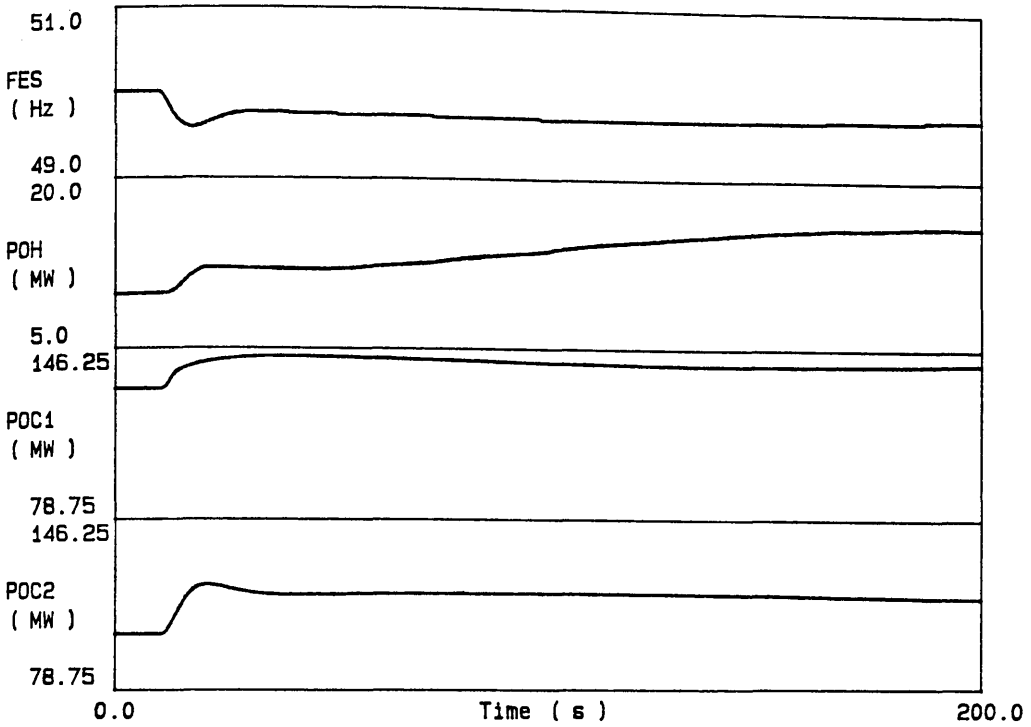


Figure 6.17 Mixed system test with hydraulic governor (10% hydro, 90% thermal, no base load)

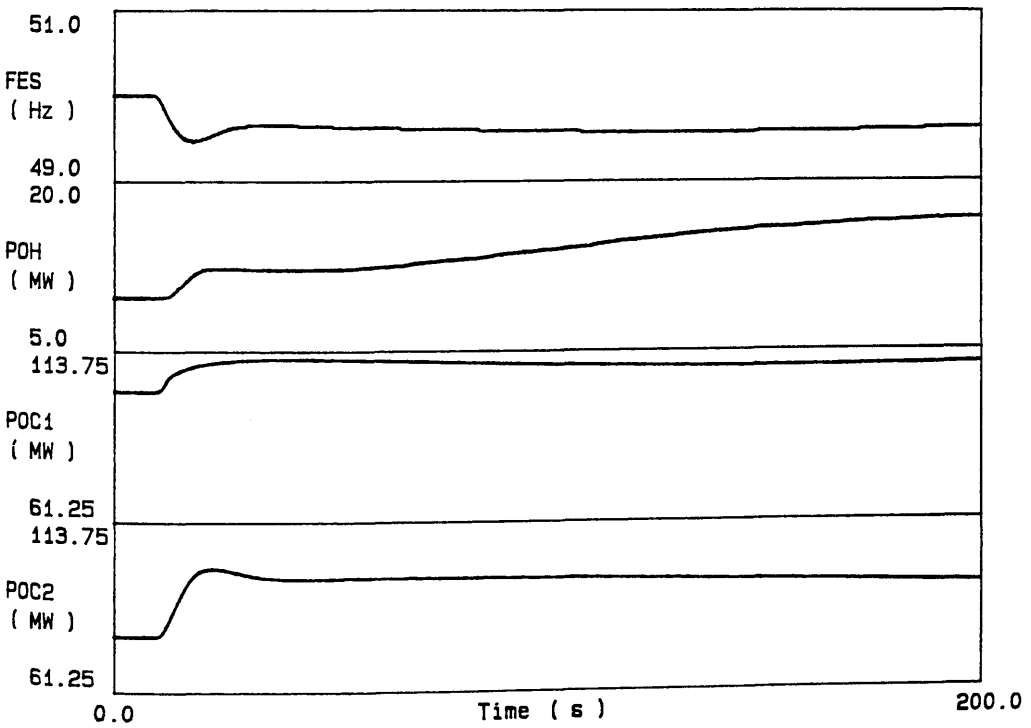


Figure 6.18 Mixed system test with hydraulic governor (10% hydro, 70% thermal, 20% base load)

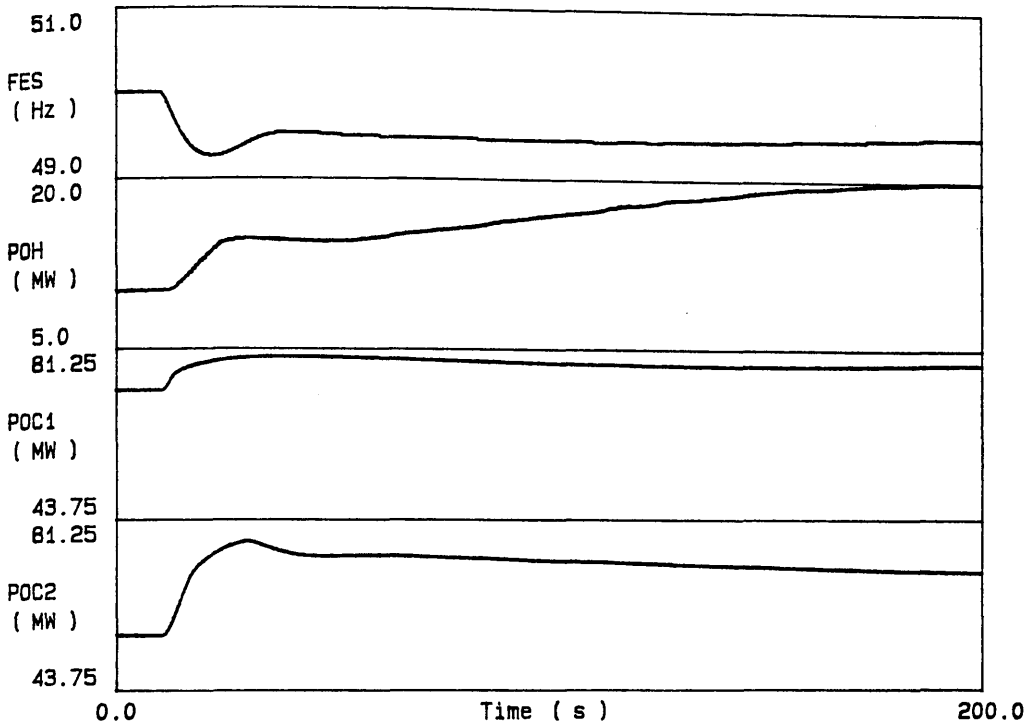


Figure 6.19 Mixed system test with hydraulic governor (10% hydro, 50% thermal, 40% base load)

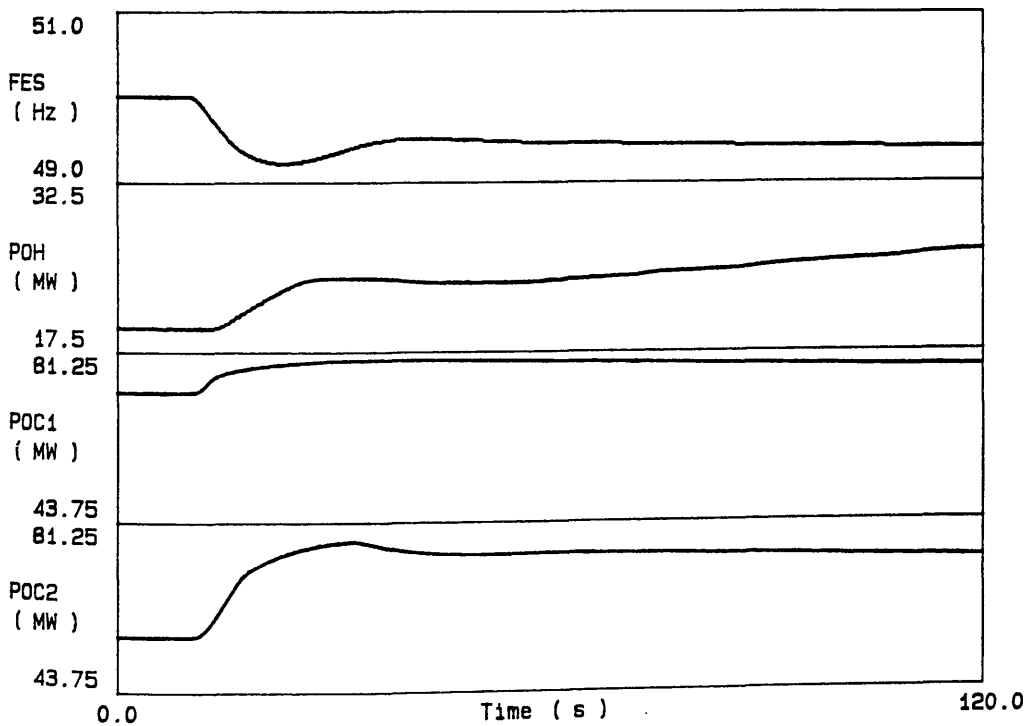


Figure 6.20 Mixed system test with hydraulic governor (10% hydro, 50% thermal, 40% base load)

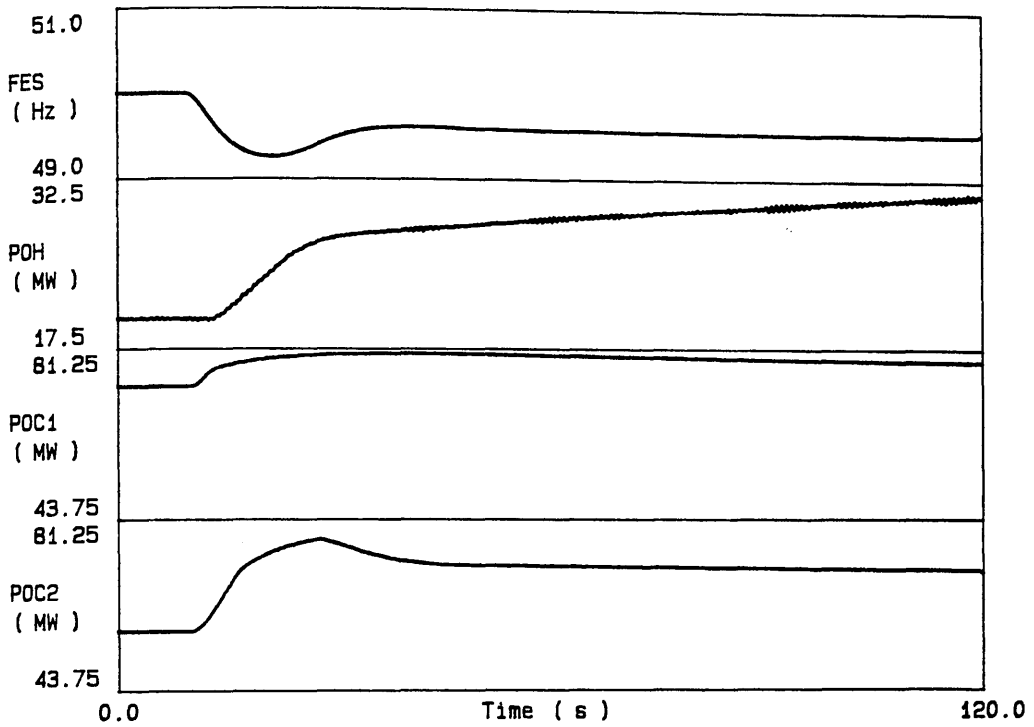


Figure 6.21 Mixed system test with electronic governor
(10% hydro, 50% thermal, 40% base load)

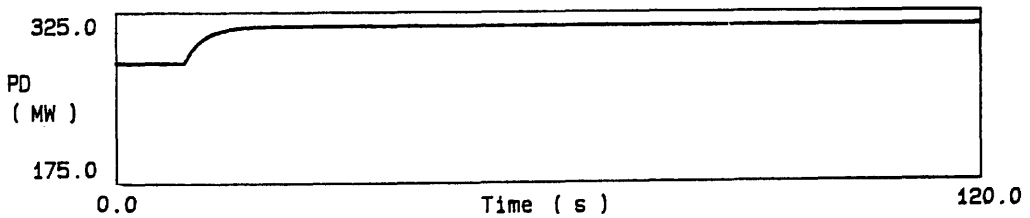


Figure 6.22 Form of demand disturbance used in some of the tests

CHAPTER 7

APPLICATION OF THE TECHNIQUE TO DIESEL ENGINES IN AN ISOLATED POWER SYSTEM

Previous chapters have described the development, testing and subsequent use of the real-time power system simulator on hydro-turbine generators at Loch Sloy Power Station. These generators have a rating of 32.5MW which is small in the context of the national grid (maximum demand over 40GW⁸⁷). Consequently, generator output variations in the course of a test with the simulator have only a negligible effect on the frequency of the grid system. The running of a test does not itself alter the real system conditions seen by the governor. For convenience, the effects of unrelated grid frequency disturbances can be nullified by offsetting the injected test signal by an appropriate amount. This is not absolutely essential because the likelihood of the grid frequency remaining reasonably constant during a test is fairly high and any affected tests can be repeated.

However, these favourable conditions would not be encountered if the power system simulator were to be used on larger hydro-turbines such as those in the pumped-storage stations at Foyers (150MW generators), Dinorwig (300MW) or the proposed Craig Royston scheme, or if on-line tests were to be performed on steam plant at Peterhead (660MW), for example. Changes in output from generators of this size have an appreciable effect on the national grid and the resulting changes in system frequency would be seen by the governor. In effect, there is a feedback coupling from the governor test input causing the change in power output, through the real power system to a change in frequency seen at the governor summing junction. Some of the effect of the test input

signal is undone by a change in the real system conditions and the power system simulator would have to contend with this feedback coupling. Grid frequency disturbances during test runs would no longer be a matter of chance, they would be a certainty. In this situation, some mechanism to correct for these disturbances would be essential in order to isolate the plant under test from the effects of its own actions on the real system.

Although Peterhead and Foyers were considered for tests with the power system simulator, in the event, neither of these were available. However, a similar situation was encountered when the simulator was applied to diesel engine generators at Stornoway Power Station in the Western Isles of Scotland. These machines operate in a power system isolated from the mainland grid and so the generator under test was supplying a significant proportion of the load. At times, the test machine constituted as much as 50% of the generating plant on the island system. This situation presented difficulties for the simulator technique of greater severity than would be expected if the equipment was used for tests on any mainland generation. This chapter describes how these difficulties were overcome, insofar as this was possible, and how the technique was applied to the study of a wind-diesel system.

7.1 THE BENEFIT OF ON-LINE TESTS OF DIESEL ENGINE RESPONSE

Diesel generators are an appropriate application of the power system simulator because the dynamics of the engines and their governors are not particularly well known.^{164,165} Very little has been published on the dynamic modelling of this type of plant, although some authors have used computer simulation of the thermodynamic cycle in the design process.¹⁶⁶ Manufacturers have available empirical steady-state models which can be used to calculate various outputs for a given set of inputs but provide no

indication of how the plant will move from one state to another. Such a model has been incorporated in system simulation studies with some success¹⁶⁴ and others have introduced a form of lagged behaviour by interpolating linearly between initial and predicted final states over a suitable time interval.¹⁶⁷

Some identification studies have been carried out on one of the Stornoway diesel engines (No.3),^{168,169} but one of these¹⁶⁸ was intended for performance monitoring and the resulting model is only valid for small a.c. signals of frequency greater than about 0.5Hz. It also does not include an observed pure time delay. The outcome of the other study was a non-linear difference equation model relating fuel rack position to engine torque,¹⁶⁹ but documentation of this model is not complete. Knowledge gained during the tests described here suggests that models based on identification work on one particular machine may not be typical of the rest of the engines. Certainly, the electronic governor on No.3 engine can be very much more responsive than the mechanical governors used on the other sets. Experience also shows that no two diesel engines have quite the same behaviour and also that even this dissimilar behaviour of an engine changes with time in some relation to the number of hours run since its last overhaul and to its long-term maintenance history.

As a consequence of these factors, use of the power system simulator should provide further insight into the response of power systems incorporating diesel plant. It allows studies to be performed where the dynamics of a real diesel engine and its governor are coupled into a system response study thus obviating the need for a model of this component of the system. Although the engine used in the study will provide only an example of the behaviour, the results obtained should still be more realistic

than those obtained off-line with existing models. Experience shows that the conditions encountered by a control system on real plant are almost invariably more onerous than first analysis would suggest and on-line tests display features of behaviour not predicted by off-line simulation.

7.2 THE WESTERN ISLES POWER SYSTEM

Along with the Shetland Islands, the Outer Hebrides are not connected to the mainland electricity supply, although the laying of a submarine cable link is proposed. Lewis and Harris are supplied by nine diesel engines at Stornoway Power Station with a total installed capacity of 30.4MW and, at Chliostair and Gisla, three small hydro-electric generators totalling 2.16MW. Two 11MW gas turbines are available but are not normally used for long periods. The ratings and inertia constants of the individual machines are as follows: (There is no longer a No.4 machine at Stornoway.)

	Rating (MW)	H constant (s)
Stornoway No.1	2.0	1.73
Stornoway No.2	2.0	1.73
Stornoway No.3	4.6	2.00
Stornoway No.5	3.0	1.60
Stornoway No.6	2.0	1.73
Stornoway No.7	3.5	1.74
Stornoway No.8	3.5	1.74
Stornoway No.9	4.6	2.00
Stornoway No.10	5.2	2.00
Chliostair No.1	0.81	0.847 (induction)
Chliostair No.2	0.81	0.847 (induction)
Gisla	0.54	0.549 (synchronous)

Using Equation 3.47, the overall inertia constant was calculated to be 1.78s. Without the hydro plant, the value is 1.85s.

The frequency of the Western Isles system is much less tightly controlled than that of the mainland system. Figure 7.7 shows a log of the system frequency during a period of relatively

close regulation. In contrast, the effect of the switching of large industrial loads can be seen in Figure 7.8. A log of the mainland system frequency is also shown for comparison (Figure 7.9).

7.3 SIMPLE DIESEL ENGINE MODELS FOR PRELIMINARY STUDIES

Woodward¹⁷⁰ has suggested that diesel engine governors may be represented by a transfer function equivalent to that shown in Figure 7.1 and that the majority of speed governors used are of the hydraulic type with a temporary droop characteristic as shown. The mechanical governors installed on the Stornoway diesels are of this type.¹⁷¹ T_y is determined by the servo geometry and is not adjustable. b_t and T_d are the temporary droop or 'compensating' feedback gain and time constant respectively and are adjusted at no load with the generator unsynchronised. By closing a needle valve, T_d is increased until stable operation is obtained for the minimum possible value of b_t . In the absence of any other information, the engine itself can be represented by a first-order lag with time constant, T_e .

Values of these parameters were indicated by Woodward.¹⁷⁰ For the arrangement shown in Figure 7.1, these were: $T_y=0.025s$, $b_t=0.1$ and $T_d=1.0s$. An engine time constant, T_e of $0.1s$ ¹⁷⁰ was used, supported by a values of $0.064s$ at full load and $0.117s$ at no load found by Goodwin and Ng¹⁷² on a 200kW diesel engine.

One of the Stornoway diesels (No.3) has an electronic governor with the arrangement shown in Figure 7.2. The frequency and power measurement lags, T_1 and T_2 and the actuator lag, T_3 are 0.073 , 0.60 and $0.12s$ respectively. The other parameters are given by

$$g = 128 (1-a)$$

7.1

$$2\% \omega = \frac{0.85}{a(1-a)} + \frac{1.47}{1-b} \quad 7.2$$

$$\alpha = \frac{68}{1-b} \quad 7.3$$

$$\omega^2 = \frac{1.13}{a(1-a)(1-b)} \quad 7.4$$

The constants, a and b are determined by the gain and reset potentiometer settings respectively. The values of these constants were not known but reasonable behaviour in off-line simulation was obtained with a and b both equal to 0.2.

7.4 TEST SIGNAL INJECTION POSSIBILITIES

The original intention was to carry out tests on No.3 engine with its electronic governor which had provision for the injection of a test frequency signal in much the same way as the Sloy microprocessor governor. Measurements of the real and reactive power outputs from Sets 3 and 9 were also available in the form of d.c. voltages. However, two problems arose that prevented the use of the set in conjunction with the power system simulator.

No.9 engine was used to make a slow change to the system frequency of about 0.4Hz and the change in power output from No.3 was measured. The steady-state droop of the electronic governor on No.3 machine was then calculated to be about 4% using the machine rating given in Section 7.2. Average frequency and power values were used by working from a data logger plot. When the load on No.3 was changed, the droop of the hydraulic governor on No.9 engine was found to be around 5%.

In accordance with the usual on-site procedure, a variable d.c. voltage source was applied to the test signal injection point in order to confirm its operation and to measure its gain. When a step change in voltage was applied to this input, considerable ringing was observed on the the power output trace. Figure 7.10 shows the effect of a 2V step. The discontinuous input causes a

severe oscillation at about 2Hz but only a small steady-state change. Application of the same voltage change in the form of a ramp over about 4s caused no ringing. Even with a responsive frequency measurement with a rise time of about 0.1s, the system frequency trace shows no sign of any oscillation. However, the power output on No.9 machine rings in anti-phase with the No.3 signal. This suggests that rotor angle oscillation is taking place with the generators exchanging energy along the 11kV busbar. At no stage were inter-machine swings excited by speeder motor action on any of the machines.

Arrangements were made to log the governor output during the transient and some sign of the oscillation was seen. Although the reliability of the signal was doubtful, the observed oscillation was probably the governor's response to the rotor angle swings appearing as a speed oscillation at its input. The speed signal is derived locally to the generator and so the oscillation is seen by the governor while it is absent from the system frequency measurement which is obtained from a 240V a.c. supply electrically remote from the generator.

The test frequency input was calibrated during these tests by calculating the apparent change in frequency at the summing junction in the governor. This is the sum of two parts: The frequency change required to produce the observed change in power, with a droop of 4%; and the observed system frequency deviation caused by the power change. (When the test signal is applied, some of its effect is undone by a change in frequency on the island system as the engine takes up or reduces load. This effect must be taken into account when the sensitivity of the test input is calculated.) Following gain adjustment, the scaling of the input was established to be 0.5HzV^{-1} .

At this stage, it was apparent that No.3 engine was very much more responsive than No.9. Figure 7.11 shows the response of the two machines on reconnection of the 33kV line to Harris. Some rotor angle oscillation is again evident, but it is quite clear that No.3 engine provides a very much greater contribution. Unfortunately, no system frequency log was obtained for this event.

7.5 OPERATION OF THE GRID FREQUENCY CORRECTION MECHANISM

In order to observe more clearly the effects on the system as a whole, the first tests on No. 3 set were attempted during night-time low-load conditions when No. 9 engine was the only other plant running. This also meant that the inconvenience to islanders would be minimised in the event of untoward happenings. With only two sets on, the engine under test constituted 50% of the system generation and the 'grid' frequency correction term was incorporated in the simulator in order to isolate the simulated system from frequency changes in the real system. The block diagram shown in Figure 7.3 depicts the coupling of the real and simulated power systems.

G_c is a constant with a value between 0.0 and 1.0 specified in the simulator. This determines the extent of correction for real system frequency deviations with a value of 1.0 giving full compensation. Use of this correction mechanism has some destabilising effect on the grid. If $G_c=1.0$, the engine under test no longer contributes to the regulation of the real system and the remaining plant must perform this task alone. For this reason, a G_c value of 0.8 or 0.9 was used throughout these tests, although operation with $G_c=1.0$ should be possible. For the tests on the Stornoway diesel engines, the correction was only applied if the system frequency remained between 49.6 and 50.4Hz.

Immediately following the start of a run, when the simulator is given control of the governor and engine, the injected signal, initially zero volts, should change only by an amount necessary to compensate for any deviation of the system frequency from its value at the start of the test. If the simulated system demand is not changed, the simulator should hold the test engine's output constant, irrespective of real system frequency changes (within certain limits).

7.6 SIMULATION OF ISOLATED OPERATION WITH THE ELECTRONIC GOVERNOR

Despite the difficulties with rotor angle oscillations excited by the injection of step voltages, an attempt was made to simulate, on-line, isolated load conditions on No.3 set using the test equipment. The simulator would not normally inject step disturbances; rather, its output would change at a finite rate determined by the inertia of the simulated system, although increasing with the size of the generation/load imbalance. As long as the maximum rate of injection was less than about 1Vs^{-1} , serious rotor angle oscillation would not occur.

When simulator runs were attempted on No.3 set, it was found that the mechanical governor on No.9 machine was not sufficiently responsive to regulate the real system within acceptable limits. Even before the application of any step, No.9 engine was not able to cope with the power changes in the real system associated with the extremely rapid behaviour of No.3 engine in the simulated system. The fluctuations on the island system frequency were unacceptably large. Simulation of isolated operation was not possible on No.3 set even with an unrealistically large inertia time constant, T_a of 20s.

7.7 TESTS OF A MIXED DIESEL-THERMAL SYSTEM

In view of this difficulty with testing on No.3 engine, a decision was made to change to No.9 and use the speeder motor injection technique described in Chapter 2. The responsive governor on No.3 was then available to regulate the real system and absorb changes in generation while tests were carried out on the other machine.

After the interface relay box had been connected appropriately, the speeder motor characteristics were measured. By controlling the speeder motor from switches connected to the data logger, pulses of measurable length, T , were applied and the change in power output, ΔP , observed. As with the calculation of the test input sensitivity, it is necessary to take into account the change in system frequency, Δf , caused by the action. The effective change in power output, $\Delta P'$ is

$$\Delta P' = \Delta P + \frac{\Delta f P_o}{f_o b_p} \quad 7.5$$

where P_o is the generator rating, f_o is the rated system frequency (50Hz) and b_p is the governor droop (0.05pu). The pulse length for a full load change is

$$T_{fl} = \frac{P_o T}{\Delta P'} \quad 7.6$$

It was found that the speeder motor would require a raise or lower of about 10s duration to provide a full load change i.e. an apparent change of frequency of 5% if this is the measured value of droop.

Before isolated load simulation was attempted on No.9 engine, tests were first carried out with the simulator configured with the coal-fired thermal plant model described in Chapter 3. A mixed diesel-thermal system is of little practical interest in the UK, although such systems do occur on larger island systems

overseas. However, the availability of a contribution from simulated plant eased the difficulty of coupling a real diesel engine into a simulated system response test. Operating alongside a coal-fired boiler-turbine unit of equal size, the diesel engine was relieved of the need to meet the load exactly. The confusion of limit cycle oscillation was, therefore, eliminated and a technique for tests could be developed.

Figure 7.12 shows the response of a 50% diesel/50% thermal system to a 20% step reduction in load. It can be seen that No.9 engine is quite heavily damped in this configuration. Operation of the grid frequency correction mechanism is also evident here. The injected signal is larger than the simulated system frequency in order to compensate for the fall in real system frequency caused by the reduction in output from the diesel engine. G_c was 0.8 for this test.

7.8 SIMULATION OF ISOLATED OPERATION WITH THE HYDRAULIC GOVERNOR

Following the success of the diesel-thermal system tests, the possibility of isolated load simulation on No.9 engine was investigated. Figure 7.13 shows a run where the alternator time constant was 20s. Limit cycle oscillation can be seen at the start of the trace followed by the response to a 10% step increase in load. The oscillation caused by the disturbance is only lightly damped. Although the stability of No.9 engine on isolated load is certainly marginal, it is unlikely that this severe oscillation is a true picture of the machine's behaviour, rather it is the effect of additional lag and rate limiting associated with the speeder motor injection technique.

Attempts to reduce the alternator time constant towards the more realistic value of 4s resulted in sustained or growing oscillation. Examination of an auxiliary signal produced by the

simulator showed a gradual increase in the error involved in the speeder motor injection technique. As the oscillation grows, the speeder motor is unable to keep up with the rapid changes in frequency, and the resultant lag further increases the instability.

7.9 THE INTEGRATION OF WIND ENERGY CONVERSION SYSTEMS

In recent years, attention has focussed on large-scale power generation from 'renewable' sources such as wind, wave, tidal and solar energy. Wind power is probably the most readily utilised for bulk electricity production and, although it will never be practicable to supply the UK entirely from this source, several wind-turbines of moderate (250kW) to large (3MW) size have been installed around the British Isles.

Wind energy conversion systems are being constructed in a number of countries and studies of various aspects have been reported. Many of these wind turbines operate in conjunction with diesel engine generators^{173,174,175,176,177} in remote, isolated power systems ranging in size from about 100MW maximum demand (in Crete)¹⁷⁴ down to a few kilowatts (on remote telecommunications sites).^{175,177} Some of these systems include oil-fired steam plant¹⁷⁴ or solar power.^{175,177}

The NSHEB, in particular, operate wind-turbines in Orkney¹⁷⁸ and Shetland, and there are possible sites in the Western Isles. The installation of aero-generators inevitably has an effect on the long-term stability of these remote, and in the case of Shetland and the Western Isles, isolated power systems. Temporary isolation of the Orkney Islands also occurs in the event of a fault on its submarine cable.

Two questions arise: Will the system as a whole always be able to accommodate the fluctuating output of the aero-generator

and will a reduction in conventional regulating plant capacity associated with a significant penetration of wind-turbine plant degrade the response of the system to generation/load disturbances? Generally, the wind turbines will be operating in partnership with diesel generators and so the acceptability of the wind power depends on the ability of the engines to absorb the variability of the wind-generated contribution. In fact, if its control system is carefully designed, the wind turbine may actually improve the frequency regulation of the system,¹⁷⁸ without the need to resort to fast-switched dump loads.^{165,179}

7.10 SIMULATION STUDIES OF WIND-DIESEL SYSTEMS

Off-line simulation studies of wind-energy integration have been reported by a number of authors^{179,180,181,182,183,184} including the NSHEB¹⁶⁴, although not all of these consider plant dynamics and system control issues. Some use an hour-by-hour simulation to assess the economic benefit of wind energy utilisation^{180,181} or to evaluate the reliability of the mixed generation system.^{182,183} Apart from the simple model of a wind-turbine with an induction generator used by Bossanyi,¹⁸¹ these latter studies do not include the dynamics of the system.

Some investigations of wind-diesel system control use a periodic function or a random time series rather than a dynamic model to represent the aero-generator power output.^{164,184} A wind-turbine's sensitivity to system frequency deviations either through its mechanical transmission or its control system cannot be represented in this way.

Computer simulation has been widely used in the design of aero-generators worldwide and, consequently, a wide range of models have been published, see, for example, References 185, 186, 187, 188, 189, 190 and 191, although some of these¹⁹¹ are not

sufficiently detailed for system response studies. Implementation of wind-turbine models is relatively straightforward, and, in contrast to diesel engines, the dynamics of the aero-generators are not particularly time-dependent so the accuracy of the simulation should be high.

Wind turbines intended for operation on a large power system can use cage induction generators, possibly with fixed-pitch turbines, allowing significant cost savings.¹⁹² However, on smaller systems, it is desirable for the wind turbines to contribute to system voltage and frequency control and so synchronous generators are normally preferred.¹⁹³ The Orkney machines are of this type and so simulation models of induction aero-generators, such as described in References 165 and 192, are not appropriate for a study of isolated wind-diesel systems in the UK.

Interest was shown in the possibility of programming the power system simulator with a suitable wind-turbine dynamic model and using it to incorporate a real diesel engine in a study of the behaviour of a wind-diesel system.

7.11 FEATURES OF WIND TURBINE DYNAMICS

The design of wind-turbine generators has ranged widely throughout their development. However, all designs attempt to decouple the generator from wind speed fluctuations by absorbing the resulting short-term blade torque fluctuations in the gearbox and coupling between the rotor and the generator.¹⁹³

In some designs, the casing of the gearbox is free to rotate over a limited angle against springs and dampers in order to introduce some compliance into the transmission.¹⁹⁴ This 'soft shaft' configuration is widely used with synchronous generators.¹⁹³

It is possible to use a fixed pitch turbine and a synchronous generator with static rectifier/inverter frequency conversion^{194,195} to allow the turbine speed to vary, but this option tends to be expensive¹⁸⁹ and is not well suited to operation in an isolated system.

Only one simulation model was implemented since the objective of the work reported here was to establish whether the power system simulator could be applied to this problem; a comparison of wind-turbine control/coupling designs being outwith the scope of this thesis. The example chosen was the 3MW, 60m diameter aero-generator¹⁸⁹ installed on Orkney and due to be commissioned in 1987. This machine utilises a novel form of mechanical power transmission and its size is typical of recently constructed wind-turbines throughout the world. In view of the small size of the Orkney and Western Isles power systems (minimum demand around 4MW¹⁷⁸), the 3MW rating of the installation would represent a very significant penetration of wind-turbine plant in the event of separation from the national grid.

7.12 A SIMULATION MODEL OF THE 3MW WIND TURBINE

In this design, the synchronous generator is directly connected to the grid and is driven by the turbine through a differential gearbox. The third shaft of the gearbox is coupled to a variable speed 'reaction machine' which is supplied from a variable frequency rectifier/inverter. The reaction machine acts as a torque controller and turbine torque fluctuations are accommodated by allowing the turbine shaft speed to deviate from the generator shaft speed. The generator torque is determined by the reaction machine torque.

7.12.1 Torque Transmission System

A mathematical model of the transmission system and its control was available¹⁸⁹ and a block diagram describing the transient behaviour is shown in Figure 7.4. This model describes the behaviour for perturbations about an operating point i.e. the steady-state values of the variables are zero. The following parameter values, provided by GEC Energy Systems Ltd., were used in the model:

High rate torque control constant	$K_{c1} = 2400 \text{ Nmsrad}^{-1}$
Low rate torque control constant	$K_{c0} = 150 \text{ Nmsrad}^{-1}$
Turbine shaft inertia	$J_b = 3144 \text{ kgm}^2$
Reaction machine inertia	$J_m = 338 \text{ kgm}^2$
Inertia compensation constant	$K_j = 313 \text{ kgm}^2$

All of these are values referred to the generator shaft (1500rpm, 157.08rads^{-1}). The inertia of the synchronous generator is 195kgm^2 which can be used with Equation 3.36 to calculate the generator H constant as 0.802s.

The gearbox system can be described by the following equations:

$$\frac{d\omega}{dt}_b = (T_{ow} - T_{og}) / J_b \quad 7.7$$

$$\omega_m = \omega_b - 157.08 (f_s - 1) \quad 7.8$$

$$\frac{d\omega}{dt}_{m1} = (\omega_m - \omega_{m1}) / T_c \quad 7.9$$

where ω_b and ω_m are the turbine shaft and reaction machine speeds (rads^{-1}), T_{ow} and T_{og} are the turbine and generator torques (Nm), f_s is the simulated system frequency and ω_{m1} is an intermediate variable. A suitable value for T_c was found to be 0.1s using off-line simulation. This time constant is only introduced to make the derivative term realisable and to provide some filtering and its value is not critical.

The generator torque is

$$T_{og} = \frac{J'_m}{T_c} \omega_m + \left(K_c - \frac{J'_m}{T_c} \right) \omega_{m1} \quad 7.10$$

and the per unit generator power is

$$P_{ow} = f_s \left(O_{wt} + \frac{T_{og}}{T_{ofl}} \right) \quad 7.11$$

where K_c is the torque control gain and O_{wt} is the per unit operating point of the wind turbine and T_{ofl} is the full load generator torque (19098.6Nm). The absolute generator torque is

$$T_e = O_{wt} T_{ofl} + T_{og} \quad 7.12$$

In order to compensate for the inertia of the reaction machine, additional torque is generated proportional to the reaction machine acceleration. The effective reaction machine inertia is then

$$J'_m = J_m - K_j \quad 7.13$$

The torque control algorithm for the reaction machine is shown diagrammatically in Figure 7.5. Reaction machine torque and thus generator torque is controlled as a function of reaction machine speed. When the turbine speed lies between the lines $\omega_5\omega_7$ and $\omega_6\omega_8$, a change in turbine speed (i.e. a change in reaction machine speed) causes the torque to change according to the low value torque/speed constant, K_{c0} . Wind gusts or troughs, or cyclic variations, tend to accelerate or decelerate the turbine and the generator torque is maintained substantially constant. When a drop in wind speed and hence turbine torque causes the turbine speed to drop below that defined by the characteristic $\omega_5\omega_7$, the reaction machine torque is reduced in sympathy, according to a gradually increasing torque/speed gain. If the turbine speed reaches that defined by $\omega_1\omega_3$, the reaction machine torque is reduced according to the high value torque/speed constant, K_{c1} . The torque

controller behaves in the same manner for increases in reaction machine speed except that the generator torque is increased rather than reduced.

The torque control algorithm can be implemented as follows:

$$\omega_{kc} = \omega_m + (T_{of1} - T_e) / K_{c1}$$

$$K_{cd} = K_{c0} \quad \text{for } \omega_5 < \omega_{kc} < \omega_6$$

$$K_{cd} = K_{c0} + (\omega_5 - \omega_{kc}) K_{cgrad} \quad \text{for } \omega_1 < \omega_{kc} < \omega_5$$

$$K_{cd} = K_{c1} \quad \text{for } \omega_{kc} < \omega_1$$

$$K_{cd} = K_{c0} + (\omega_{kc} - \omega_6) K_{cgrad} \quad \text{for } \omega_2 > \omega_{kc} > \omega_6$$

$$K_{cd} = K_{c1} \quad \text{for } \omega_{kc} > \omega_2 \quad 7.14$$

where

$$K_{cgrad} = \frac{K_{c1} + K_{c0}}{\omega_5 - \omega_1} = \frac{K_{c1} + K_{c0}}{\omega_2 - \omega_6} \quad 7.15$$

The selected value of K_{cd} is filtered with a first-order lag to obtain K_c :

$$\frac{dK_c}{dt} = (K_{cd} - K_c) / T_{kc} \quad 7.16$$

The first-order lag is used to smooth out the effects of the discontinuities caused by switching K_{cd} . Using off-line simulation, a suitable value of T_{kc} was found to be 1s.

Unfortunately, neither the characteristics of the turbine blades nor the details of the tip-blade pitch angle control system on this turbine had been published. GEC were not in a position to provide exact details of these components. However, a reasonable substitution was made using the corresponding information for the American DOE/NASA 2.5MW (MOD-2) wind-turbine.^{187,188} Although it employs a more conventional design of soft transmission, this is a comparable machine which has been used as the basis for a control system study.¹⁹³

7.12.2 Turbine Blade Characteristics

The turbine blades were not modelled individually and so wind shear and tower turbulence effects were not included. Oscillation of the driving force at a frequency corresponding to twice rotor speed is, therefore, not modelled. The yaw control system was not of interest here and was not included either.

Imperial units were used in the documentation of this model¹⁸⁷ and so wind velocity is measured in miles per hour rather than metres per second although the value in the SI unit will be given in brackets in the following sections.

The turbine characteristics are non-linear so an absolute model is used and the turbine shaft speed must be referred from 1500rpm (157.08rads^{-1}) to 17.55rpm (1.8378rads^{-1}) in absolute form:

$$\omega_{bb} = \left(1 + \frac{\omega_b}{157.08}\right) 1.8378 \quad 7.17$$

The tip speed ratio, γ is then given by

$$\gamma = \frac{V_w}{\omega_{bb}} \quad 7.18$$

where V_w is the wind speed (mph), and the power coefficient is

$$C_p = 0.5 (\gamma - 0.022B^2 - 5.6) e^{-0.17\gamma} \quad 7.19$$

where B is the blade angle.

The torque generated by the rotor is

$$T'_{ow} = 0.0001372 V_w^2 C_p \gamma \quad 7.20$$

where T'_{ow} is a normalised variable with a value of 1.0 giving full load output. For Equation 7.7, T_{ow} is calculated from

$$T_{ow} = T_{ofl} (T'_{ow} - 0_{wt}) \quad 7.21$$

For this wind-turbine, 'cut-in' wind speed is 13mph (5.8ms^{-1}) and full-load output is reached with a wind speed of 45mph (20.1ms^{-1}).

7.12.3 Tip-blade Pitch Control

In the absence of more exact information, the tip-blade control system shown in Figure 7.6 was used in the simulation. The controller was described by the following equations:

$$P_{err} = (f_s - f_{ref}) / b_p + P_{ow} - P_{ref} \quad 7.22$$

$$\frac{dx_1}{dt} = P_{err} \quad 7.23$$

where P_{ref} is the power output set-point, b_p is desired droop, f_{ref} is a frequency reference and x_1 is an intermediate variable used to implement the integrator. The pitch angle demand, B_d is given by the expression

$$B_d = K_p P_{err} + K_i x_1 \quad 7.24$$

Using an off-line simulation, suitable values of the proportional and integral gains, K_p and K_i were found to be 2.0 and 0.2 respectively. These settings were chosen to make the pitch control very slow, forcing the reaction machine to accommodate as much as possible of any disturbance.

The pitch actuator was described by the differential equation

$$\frac{dB}{dt} = (B_d - B) / T_p \quad 7.25$$

where the pitch servo time constant, T_p was taken to be 59ms, this being the value for a 100kW wind turbine of similar design¹⁸⁶ supported by a value of 50ms for a 6MW machine.¹⁹⁰ Limits of ± 10 degrees/sec were imposed on the rate of blade pitch movement¹⁹⁰, although the value of ± 8 degrees/sec used by Hwang¹⁸⁶ is slightly more restrictive. The blade angle position was limited to the range 0 to 90 degrees.

7.13 ON-LINE TESTS WITH THE WIND TURBINE MODEL

The wind turbine model described above was implemented in the simulator. The equations and data are listed in Appendix 4. Three types of tests were performed with this simulation in conjunction

with Stornoway No.9 engine. The combined wind-diesel system was perturbed with step increases in wind speed, wind gusts and generation deficit incidents. In each type of test, all the disturbances used were of the same sign i.e. wind speed reduction and excess generation incidents were not investigated. This was only due to lack of time on-site and there is no reason why such perturbations could not be used.

7.13.1 Response to a Step Change in Wind Speed

This type of disturbance was investigated first because it produces the most easily analysed responses. Although a step change in wind speed is not a realistic perturbation, it is an approximation to a change in mean wind speed and the combined system must be able to cope with such a disturbance. For these tests, the simulator was configured for equal proportions of diesel and wind plant. This is appropriate because the 3MW wind turbine could conceivably provide half of the generation of an isolated system the size of Orkney or the Western Isles. This choice of plant proportions also simplifies the interpretation of the preliminary tests reported here.

The response of the wind-diesel system to a step change in wind speed from 30mph (13.4ms^{-1}) to 32.5mph (14.5ms^{-1}) is shown in Figure 7.14. The wind turbine is initially able to absorb some of the extra energy by allowing the rotor and reaction machine to accelerate. The power output increases relatively slowly at this stage. However, once the reaction machine speed approaches its limit, the extra torque must be transferred to the generator by increasing the torque control gain, K_c . Acting more slowly, the tip-blade pitch angle control increases the blade angle in order to return gradually the turbine output to its set point which will be temporarily reduced by the high system frequency following the

wind step. The diesel engine's output is reduced to compensate for the increase in power from the wind turbine.

Although the simulated system remained in a reasonably steady state after the start of the run shown in Figure 7.14, it was much more common in the wind/diesel system tests for limit cycle oscillations to build up almost immediately. The wind turbine initially contributes very little to the system control because the torque control gain, K_c is set to its low value making the power output insensitive to reaction machine speed and hence system frequency. Consequently, the diesel engine is effectively operating in isolated conditions and limit cycle oscillations caused by backlash in the fuel rack linkages and elsewhere build up rapidly as soon as there is a slight perturbation from the real or simulated systems.

This situation can be seen in Figure 7.15 where large amplitude oscillation and a downward drift of the diesel engine output and simulated system frequencies is evident. This downward drift occurred in all runs where sustained oscillation occurred. To investigate this, a series of alternate raise and lower pulses of length, T , each separated by the same time, T , was applied to the speeder motor on the test machine for about four minutes. With 0.5s pulses, this produced a downward drift of about 1.3kWs^{-1} even though the system frequency drifted down with the decline in generation at about 0.30mHzs^{-1} . (The system frequency would have to rise to produce a downward drift.) With $T=0.1\text{s}$, the minimum duration of pulse generated by the simulator, a downward drift of about 1.1kWs^{-1} took place with a frequency decline of 0.26mHzs^{-1} . This experiment was not repeated, so it is not certain that the shorter pulses would always produce a slower drift.

It is clear that the speeder motor travels more rapidly in

the lower direction, but it is not clear why longer pulses should produce a faster rate of drift. It may be that there is a second effect where the speeder motor accelerates more rapidly in the raise direction and which will be more pronounced for a train of shorter pulses thus reducing the rate of drift. Notice that in Figure 7.15, the rapid drift occurs with pulses of about 4s duration closely spaced whereas there is no drift at the start of Figure 7.12 even though the raise and lower controls are being operated frequently with short pulses. Complete and conclusive explanation of this effect requires further investigation. However, it seems that a lower pulse on this particular relay box and speeder motor combination is a few percent more effective than a raise pulse. A similar but less pronounced effect had, in fact, been observed at Sloy during the tests described in Section 4.2.1.

Whatever the explanation, this drift interferes with the test. As the diesel power output drifts downwards so too does the simulated system frequency and the wind turbine reaction machine speed increases until a point is reached where the wind turbine torque control becomes more active and contributes to the system frequency regulation and reduces the limit cycle oscillation. If the wind speed step is now applied as in Figure 7.15, the wind turbine is unable to absorb any of the extra energy because the reaction machine speed is already high following the drift. The test is, therefore, not a true indication of the wind-diesel system's response.

To avoid this problem, the wind speed step must be applied before the system has had a chance to drift. Figure 7.16 shows the response of the system to a wind speed step from 30mph (13.4ms^{-1}) to 32.5mph (14.5ms^{-1}) applied during the period of limit cycle oscillation. Point-of-wave switching was used to obtain a

repeatable response of reasonable clarity. The step was applied when the diesel engine output was at the bottom of a downswing. This point, which is the opposite of the usual procedure, was used because the absorption of the initial part of the wind speed step causes a delay of about half the limit cycle oscillation period before a large change in output appears from the wind turbine.

A limit cycle oscillation regime of smaller amplitude and longer period is evident after the step has been applied and the wind turbine has been moved to a region of its characteristic where it contributes significantly to system regulation. If the test were run for a sufficiently long time, the pitch control of the wind turbine would operate to bring the reaction machine speed back to zero and the turbine to a new steady state suited to the changed wind speed. With operator action on the diesel engine to bring the simulated system frequency back to 50Hz, the behaviour would eventually return to the initial regime of large amplitude limit cycle oscillations.

This test was repeated with a 5mph (2.2ms^{-1}) wind speed step (Figure 7.17). The ability of the reaction machine to absorb the extra wind energy is now rapidly exceeded and the change in turbine output and the resulting frequency swing are much larger. The diesel engine has to make a much larger change in output to control the system.

7.13.2 Response to a Wind Gust

The effect of a gust on the wind-diesel system was also investigated. The following equation^{186,187,188} was used to generate the wind speed

$$V_w = V_{wm} + \frac{A}{2} \left(1 - \cos \frac{2\pi t}{T} \right) \quad 0 < t < T \quad 7.26$$

where the gust is initiated by a switch. A and T are the amplitude and duration respectively. Before and after the gust, the wind

speed is constant at the mean level, V_{wm} .

Figure 7.18 shows the response of the 50% diesel/ 50% wind system to a gust from 30mph (13.4ms^{-1}) to 35mph (15.6ms^{-1}) of 10s period. As with the wind speed step, point-of-wave switching was used to obtain the clearest response. It can be seen that the wind turbine is able to absorb some of the gust until the reaction machine approaches its speed limit and further excess energy must be transferred to the system.

With a 10mph (4.4ms^{-1}) gust of 7.5s period (Figure 7.19), which contains more energy, the disturbance is greater with a larger frequency swing requiring more regulation from the diesel engine.

The amplitudes and periods of the gusts used in these tests were chosen to exercise the wind turbine-diesel engine system and to illustrate various features of their behaviour. They were not intended to represent any particular recorded data. Hwang,^{186,187} in fact, used shorter gusts of larger amplitude.

7.13.3 Response to a System Load Increase

The third type of disturbance considered was a generation/load imbalance in the wind-diesel system. The wind turbine control system design reported in Reference 189 is intended for operation on a large power system. If the aerogenerator was to be used in an isolated system, some changes would be necessary. In particular, the reaction machine cannot itself distinguish between a rise in rotor speed caused by a wind speed increase and a fall in generator speed caused by a generation deficit. In the former case, the control system should attempt to keep the generator torque constant whereas in the latter, it should be increased.

If the wind turbine controller is provided with a measurement

of system frequency, perhaps using the method outlined in Section 2.3, a scheme could be devised to recognise a system frequency disturbance and change the torque control gain, K_c in a manner to respond to the load change by drawing stored energy out of the rotor. Implementation would be straightforward because the controller is microprocessor-based. Such a scheme was not used here, but K_c was held at its high value to obtain the maximum response from the wind turbine throughout the system disturbance tests described in this section.

Figures 7.20, 7.21 and 7.22 show the response to a 5% increase in demand for systems with 50% diesel/50% wind, 80% diesel/20% wind and 90% diesel/ 10% wind respectively. The demand step was applied through a first-order lag as described in Section 2.5 with a time constant of 1.0s for the first two and 2.0s for the third run.

With 20% wind turbine penetration, limit cycle oscillation of the diesel engine begins to predominate. Tests with smaller proportions of wind turbine plant were attempted but as the diesel engine approached isolated operating conditions, difficulties were encountered due to the test signal injection method being used (as described in Section 7.8).

Two measurements of the speeder motor characteristic at this point produced average values of 5.9 and 7.3s for the raise time for full load change and 5.6 and 6.9s for the corresponding lower time. This is much lower than the value used by the simulator to calculate the injected signal and, to some extent, accounts for the instability of isolated load simulation.

It is not clear why the speeder motor characteristics should change from one measurement to the next. However, a slip coupling is provided between the speeder motor shaft and the 'synchroniser'

(summing junction) adjusting gear on the governor. This friction coupling allows the synchroniser to be adjusted on the governor itself and prevents damage to the motor when the speed setting stops are reached.¹⁷¹ It may be that the degree of slip in this connection is rather variable which would explain the inconsistency in the speeder motor rate measurement. It is also possible that minor adjustments to the engine between one measurement and the next may have inadvertently altered the characteristics of the set.

7.14 PARAMETERS FOR THE DIESEL ENGINE AND GOVERNOR MODEL

The diesel-thermal system test shown in Figure 7.12 was reproduced in detail using off-line simulation and the parameters of the temporary droop governor and diesel engine model were altered to obtain a close fit to the experimental data. The responses of No.3 and No.9 engines to the reconnection of the Harris line (Figure 7.11) were also used. It was also required that the chosen parameters should predict the instability of isolated load simulation using the speeder motor injection technique for inertia time constants less than about 10s.

Although a range of parameters provided a reasonable fit to the data, it was found that the best representation of the overall behaviour was obtained with $T_y=0.025s$, $b_t=0.8$ and $T_d=0.5s$. The engine was represented by a first-order lag with a time constant of 0.1s, a delay of 0.5s and a backlash of 2%.

7.15 CONCLUSION

Despite the problems with speeder motor calibration and asymmetry, the work on the Stornoway diesel engine has proved that the power system simulator can be used on a system where the test machine is a significant proportion of the generating plant. A means of injecting a test signal has been established and although

isolated load tests were not very successful, useful results were obtained with a mixed diesel-thermal system configuration. The use of the technique to investigate the behaviour of an isolated wind-diesel power system has also been demonstrated. If a rotational position transducer was fitted to the reference dial on the mechanical governor and used to provide a feedback signal to the simulator, it might be possible to eliminate the uncertainty associated with the open loop nature of the speeder motor injection technique.

Although no simulator tests were completed successfully using direct injection on the electronic governor on No.3 engine, this approach merits further investigation. If tests were performed during heavier load conditions where No.3 set was only, say, 25% of the generating plant on the Western Isles system, then the other plant might well be able to regulate the system adequately. The tests reported in this chapter were carried out on two different occasions and it was found on the second visit that, following overhaul, the electronic governor was very much less responsive than previously. This improves the potential for successful tests because the mechanical governors will be able to keep up with the electronic governor during tests.

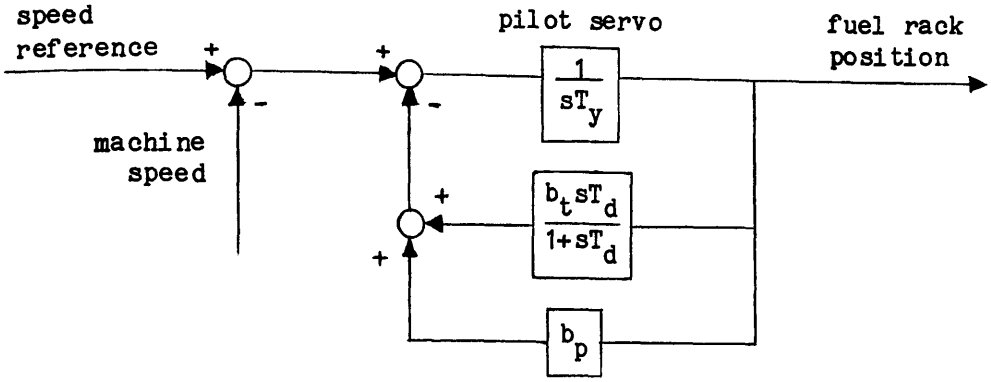


Figure 7.1 Mechanical-hydraulic governor

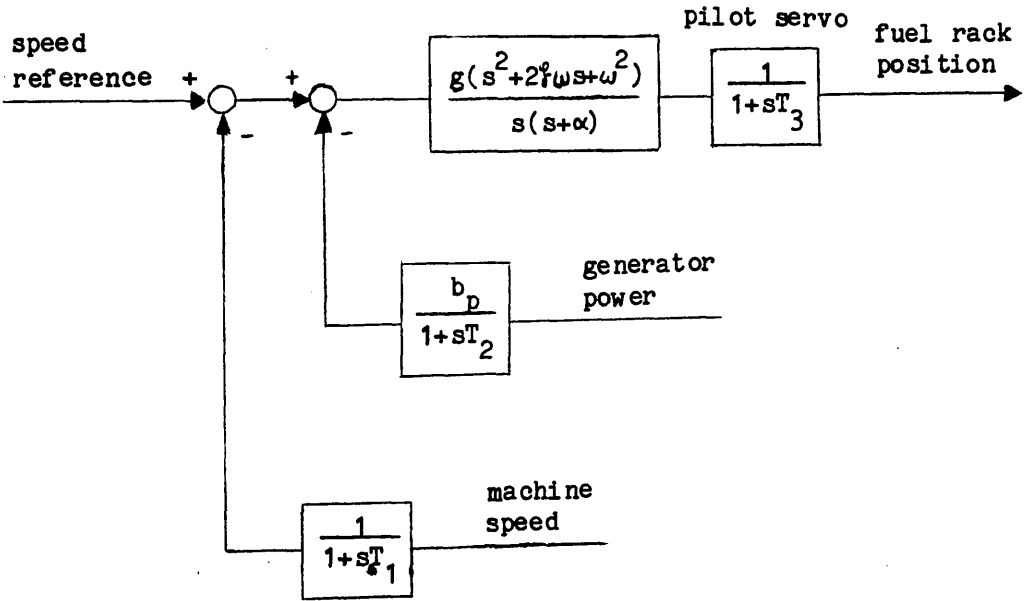


Figure 7.2 Electronic governor

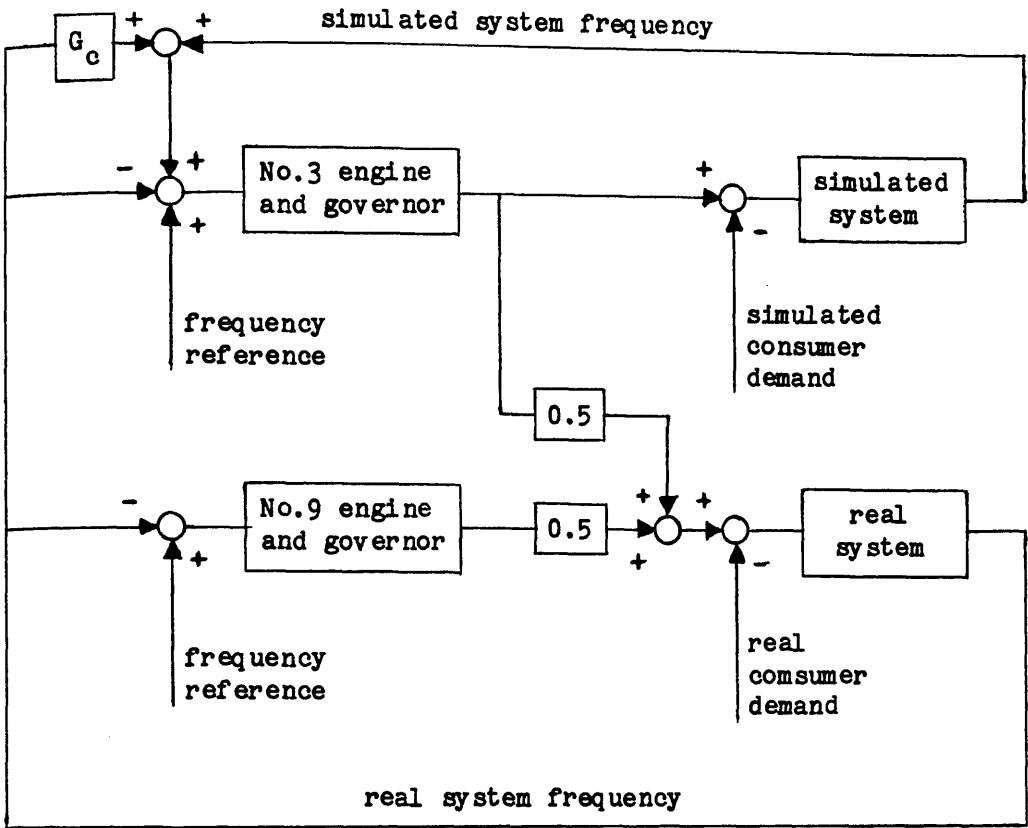


Figure 7.3 Coupling of the real and simulated power systems

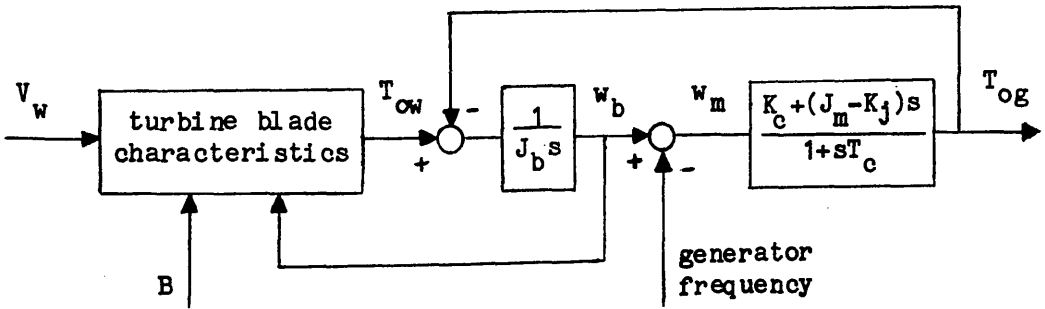


Figure 7.4 Torque transmission system for the 3MW wind turbine

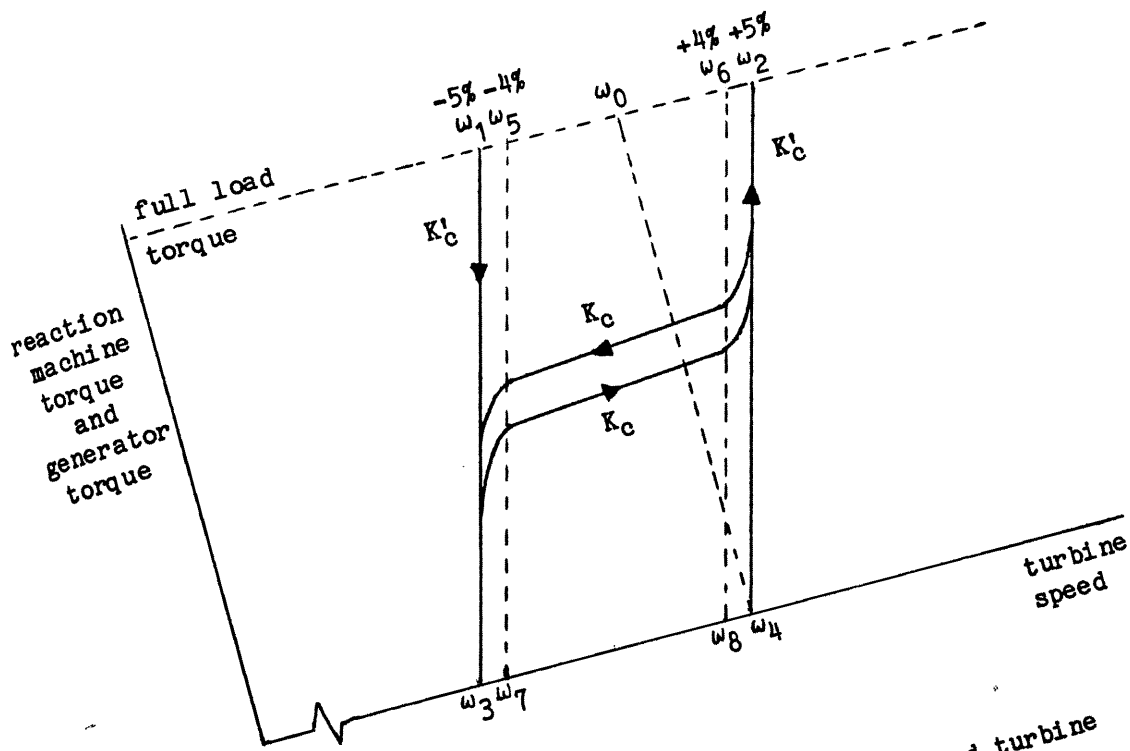


Figure 7.5 Torque control algorithm for the wind turbine

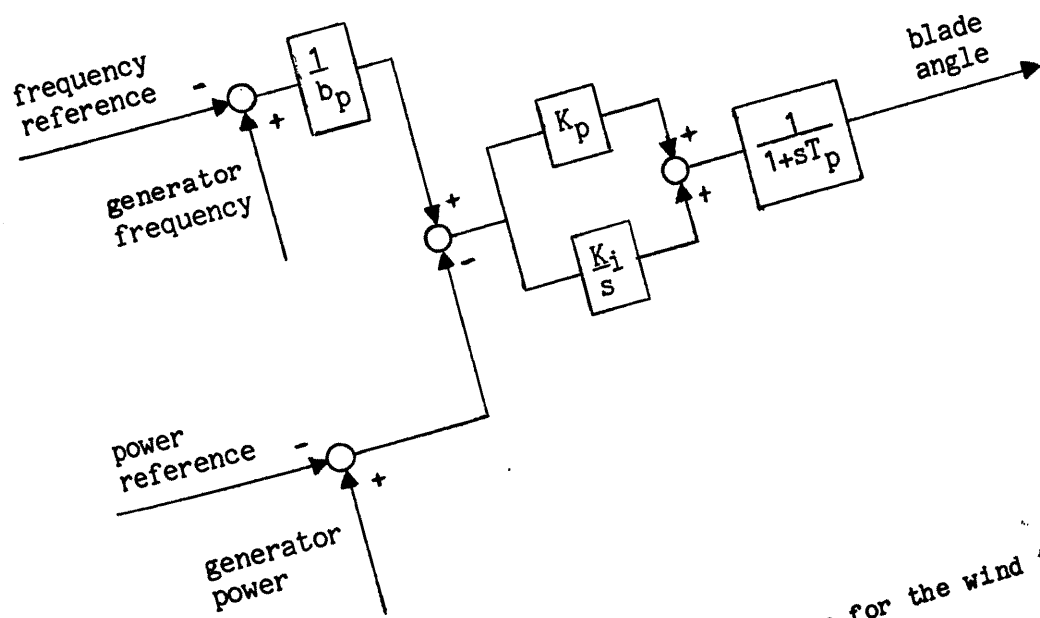


Figure 7.6 Tip-blade pitch control system for the wind turbine

Labels for Figures 7.7 to 7.22

GFREQ - real grid frequency
POD3 - No.3 engine power output
POD9 - No.9 engine power output
FES - simulated system frequency
POD - diesel engine power output
POC - coal-fired plant power output
FESCR - simulated system frequency corrected for grid frequency
deviations
SPDINP - speeder motor pulses
FTRACK - injected frequency signal
POW - wind turbine power output
TOW - wind turbine rotor torque
WB - wind turbine rotor speed
WM - wind turbine reaction machine speed
KC - wind turbine torque control gain
B - wind turbine tip-blade pitch angle
VW - wind speed
PD - consumer demand

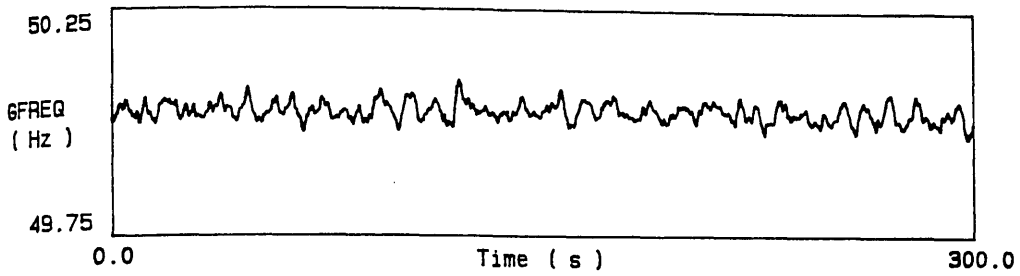


Figure 7.7 Western Isles system frequency

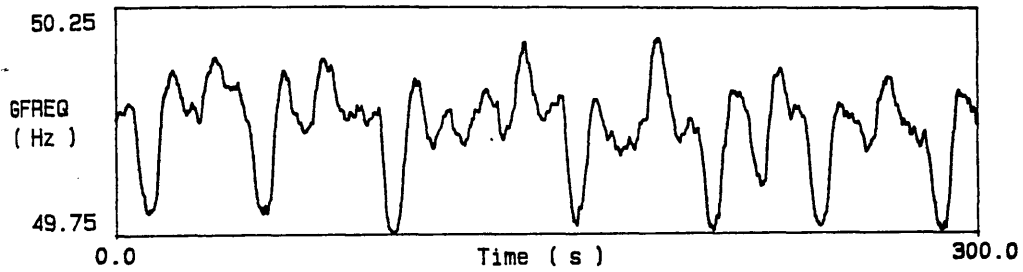


Figure 7.8 Western Isles system frequency

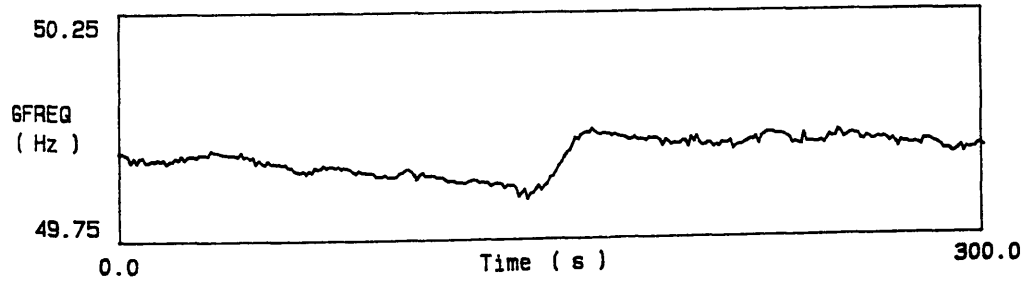


Figure 7.9 Mainland system frequency

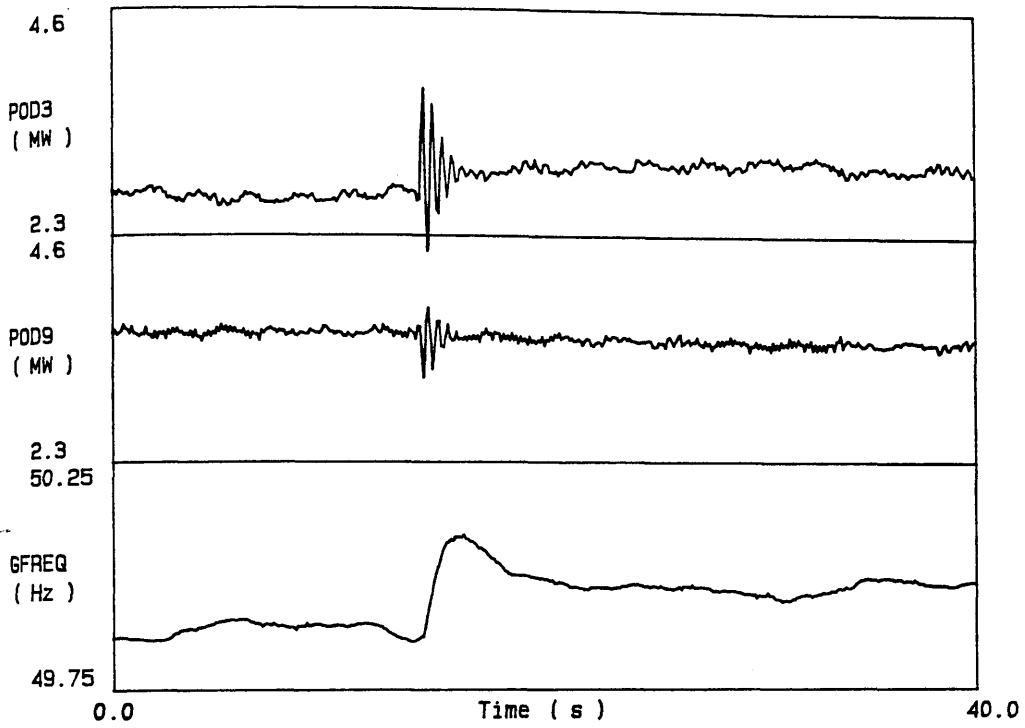


Figure 7.10 Test signal injection on electronic governor

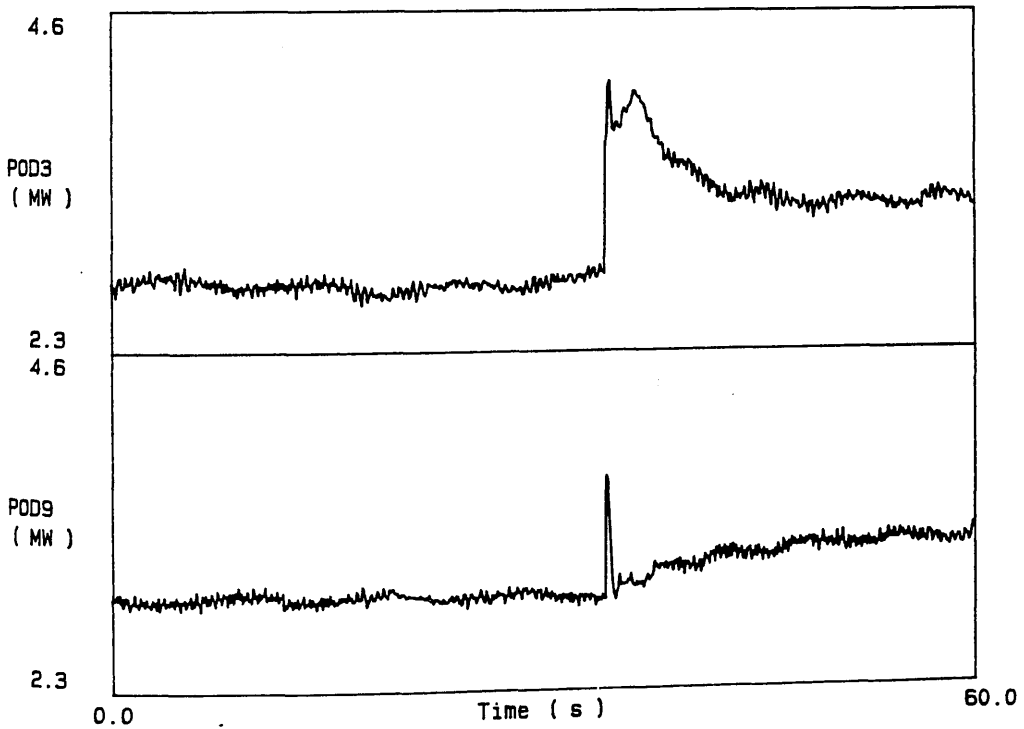


Figure 7.11 Reconnection of Harris line

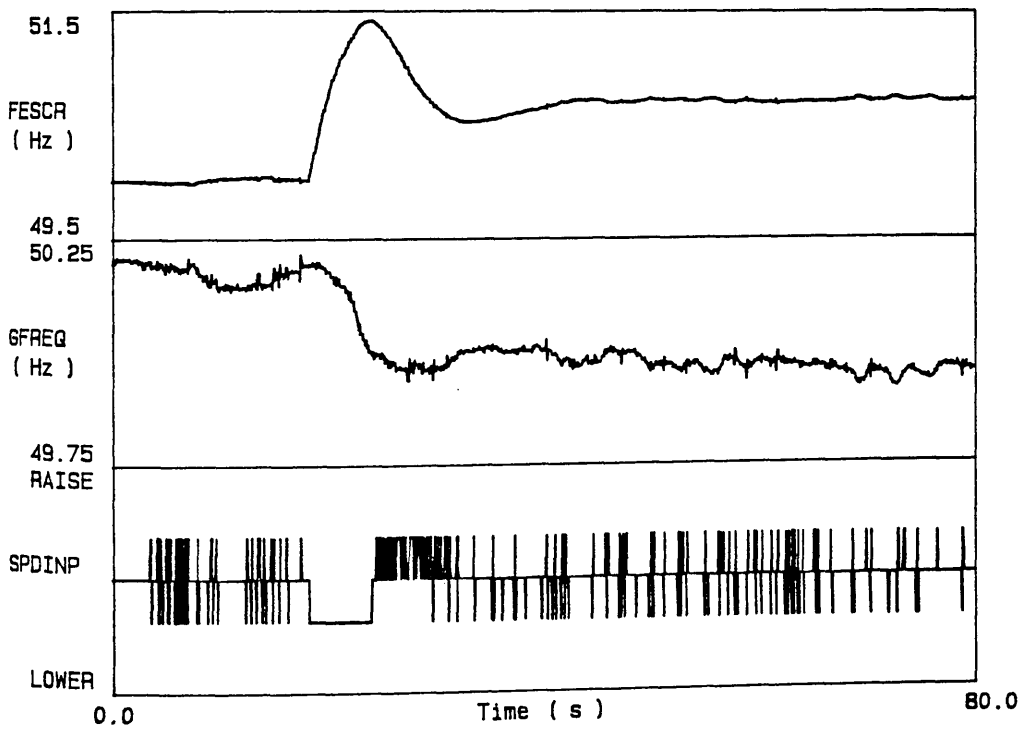
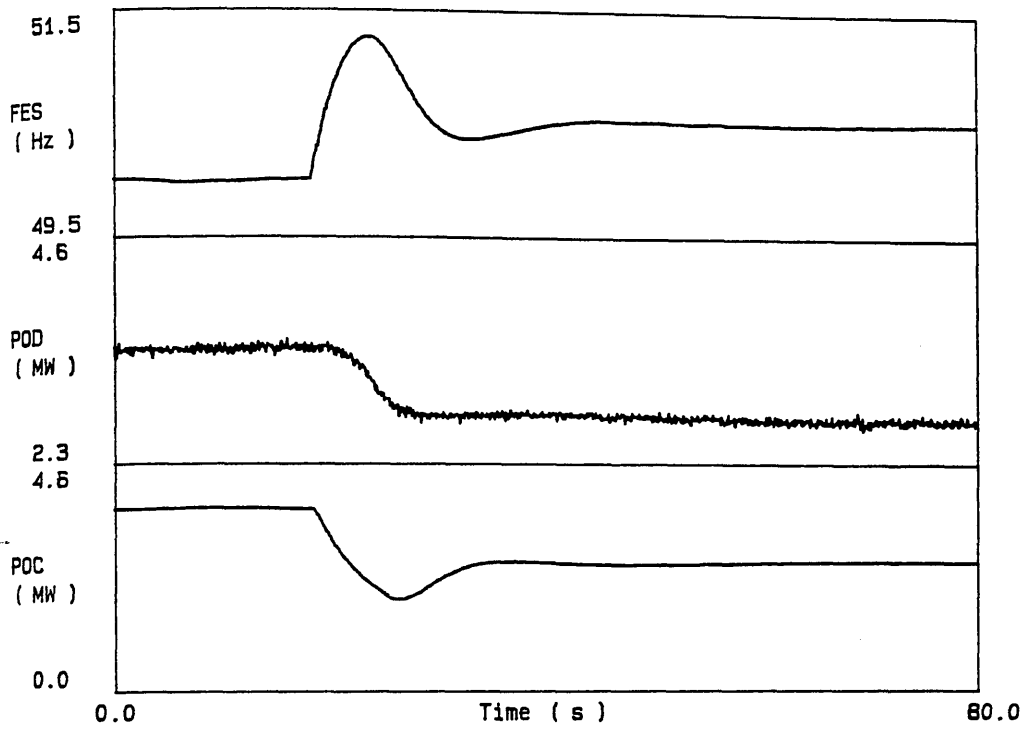


Figure 7.12 Diesel-thermal system test with hydraulic governor

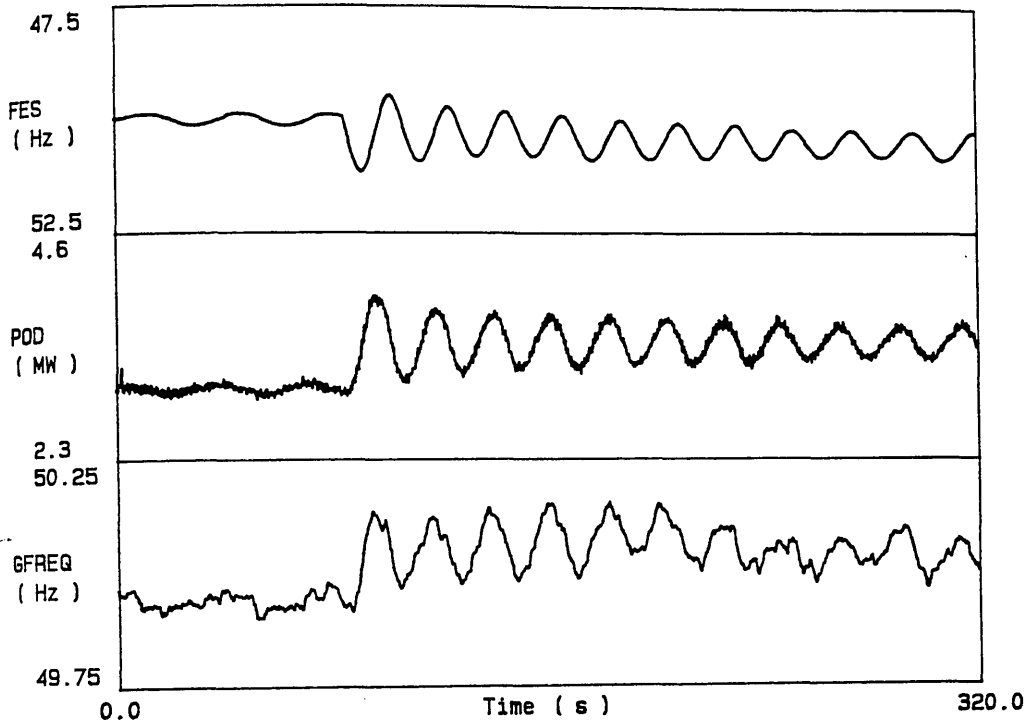


Figure 7.13 Isolated load test with hydraulic governor

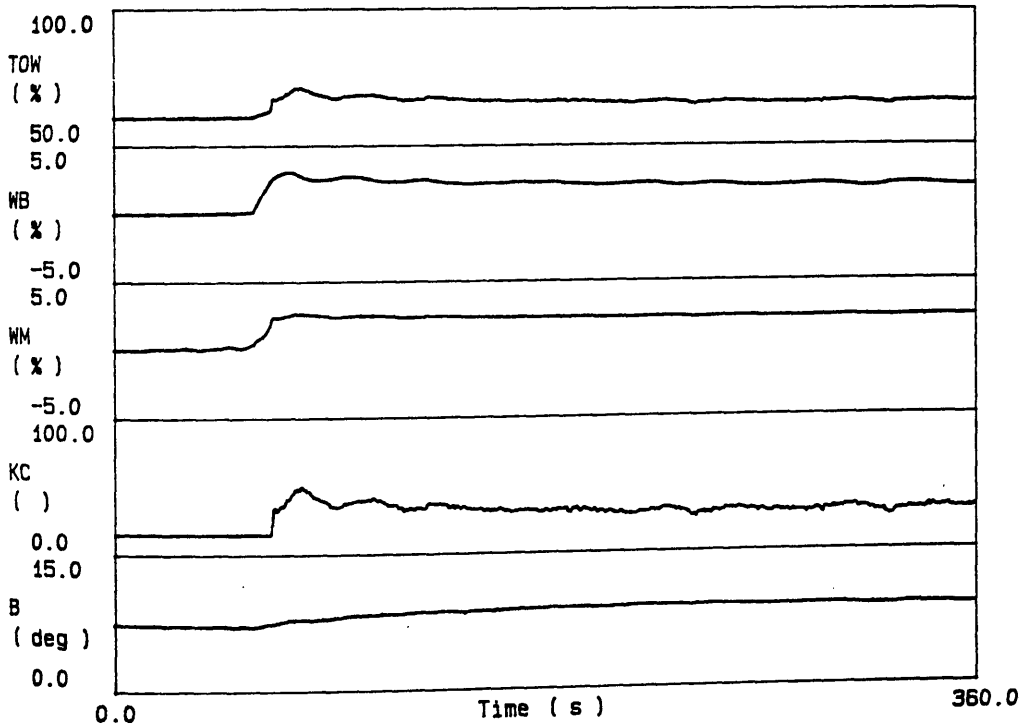
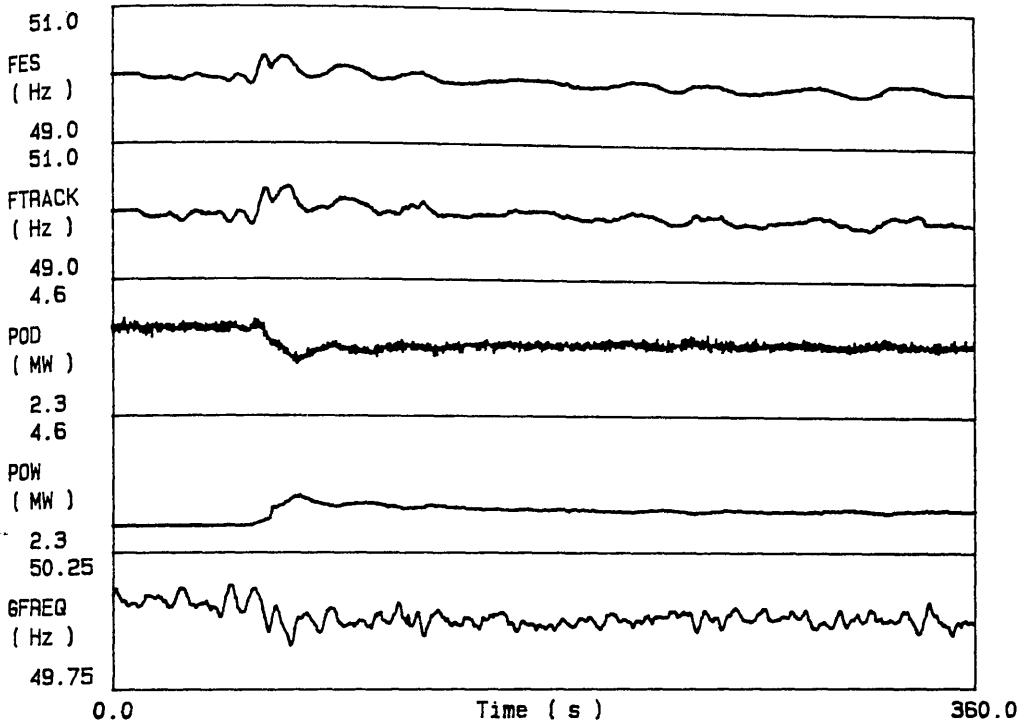


Figure 7.14 Wind-diesel system
(2.5mph wind speed step)

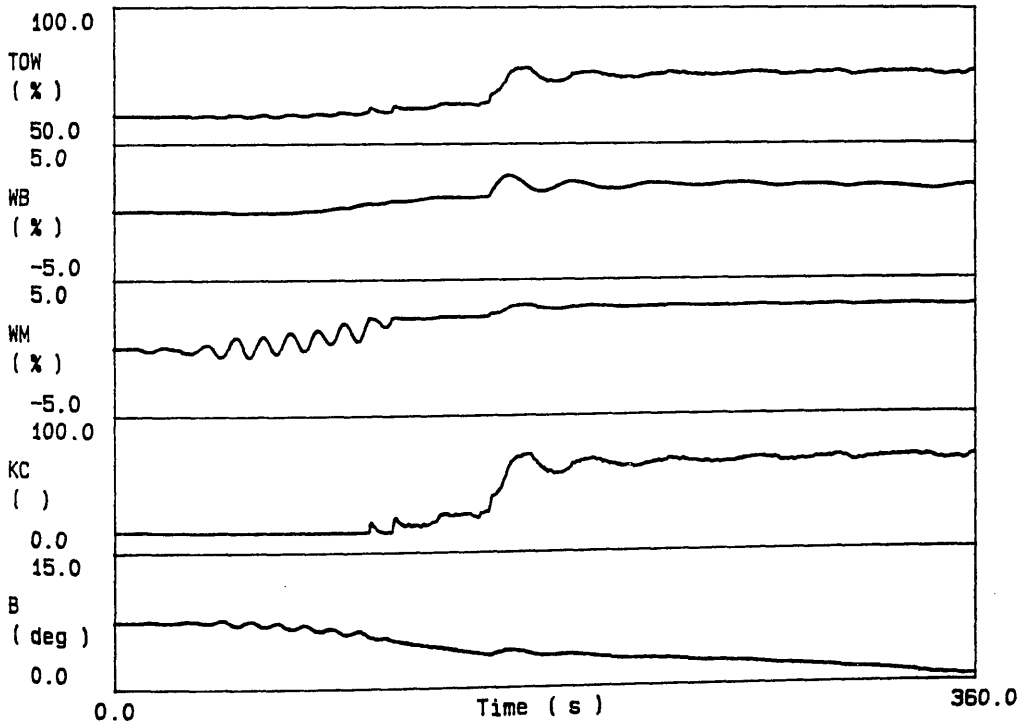
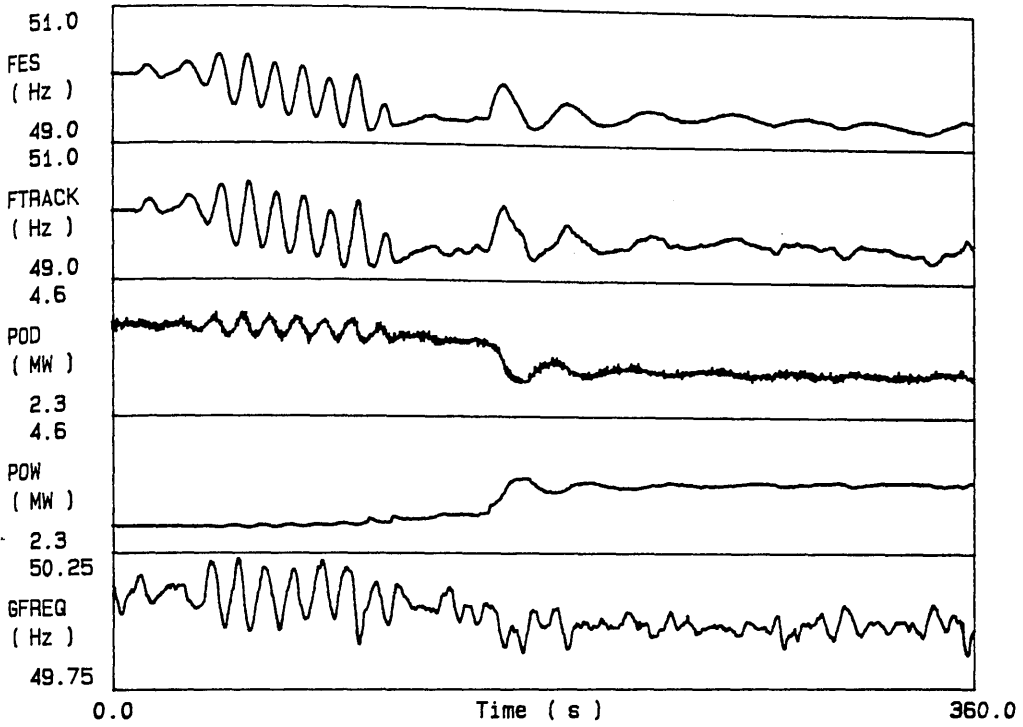


Figure 7.15 Wind-diesel system
(2.5mph wind speed step)

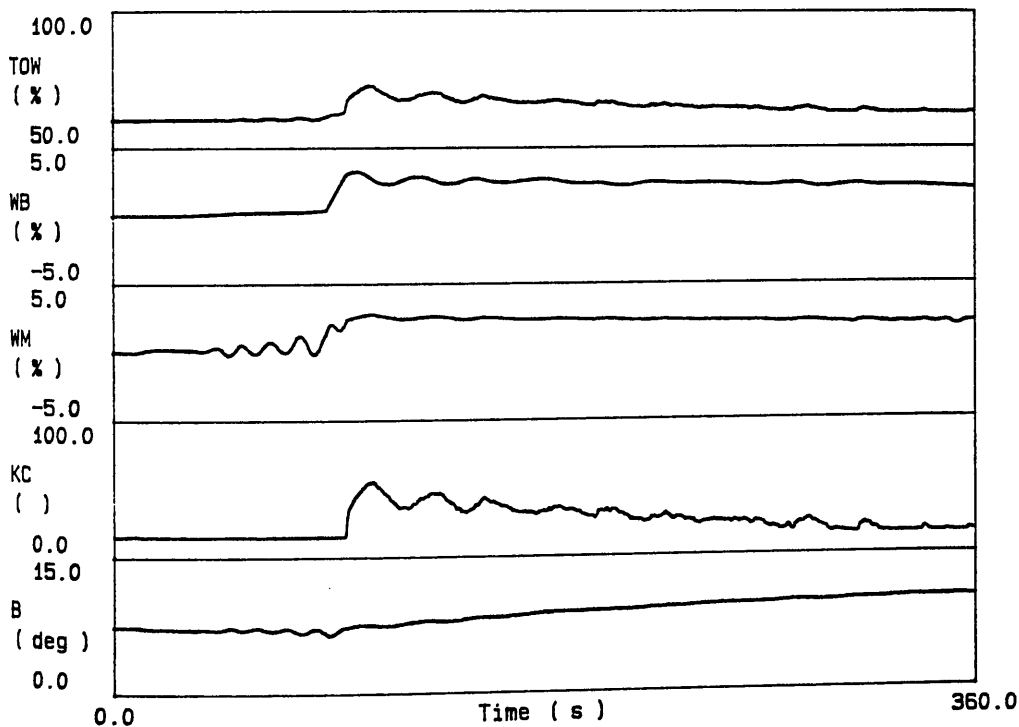
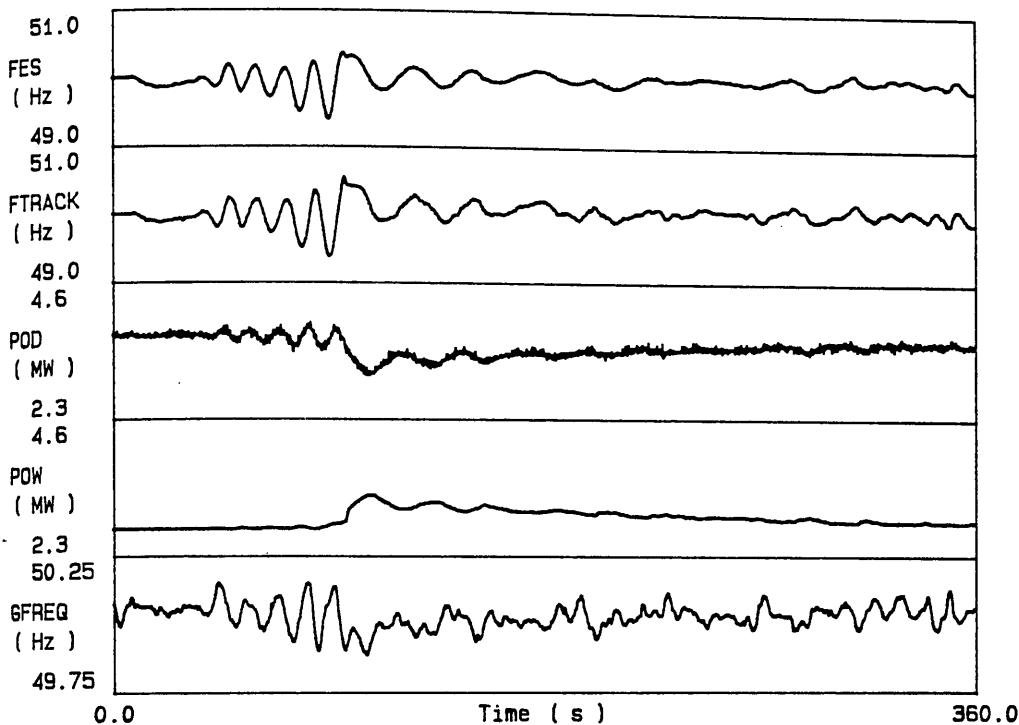


Figure 7.16 Wind-diesel system
 (2.5mph wind speed step)

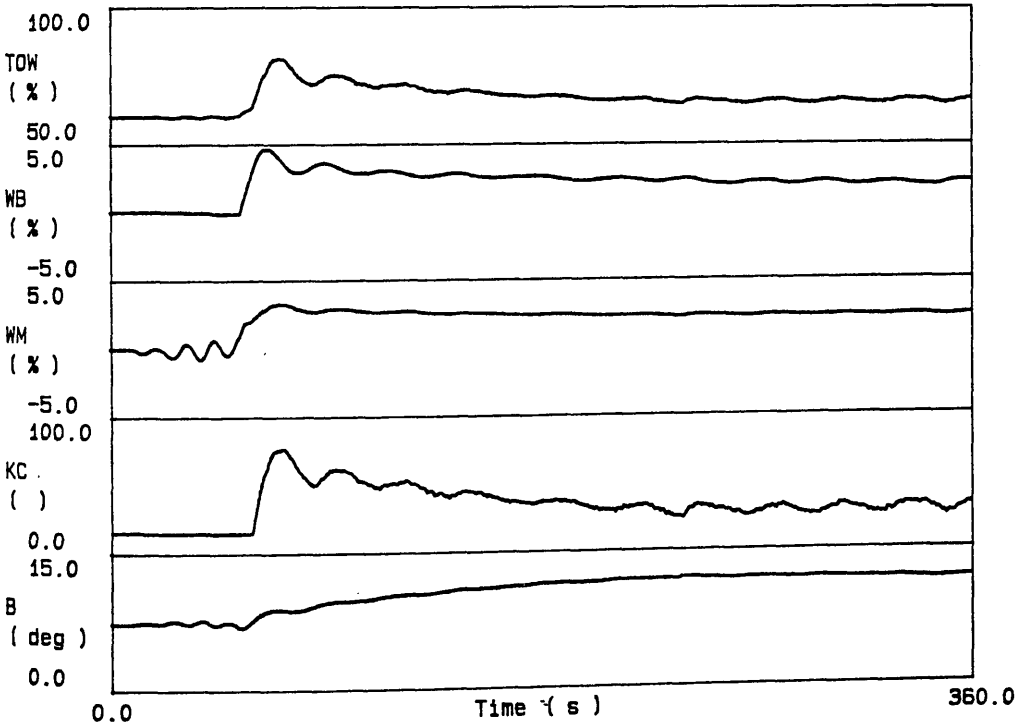
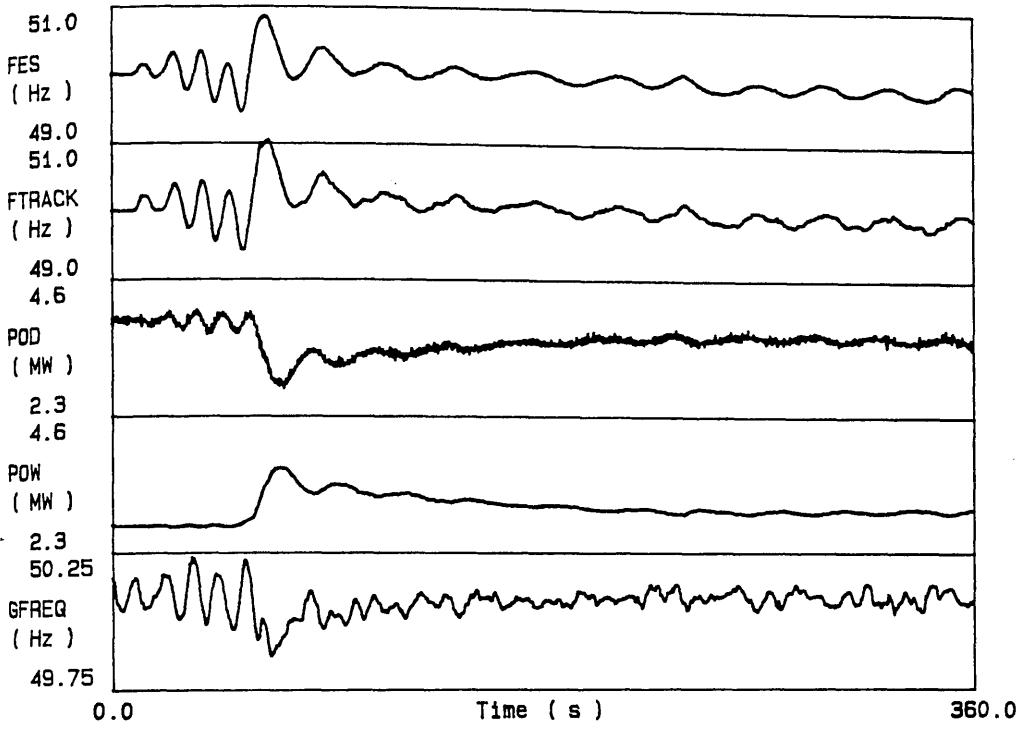


Figure 7.17 Wind-diesel system
(5mph wind speed step)

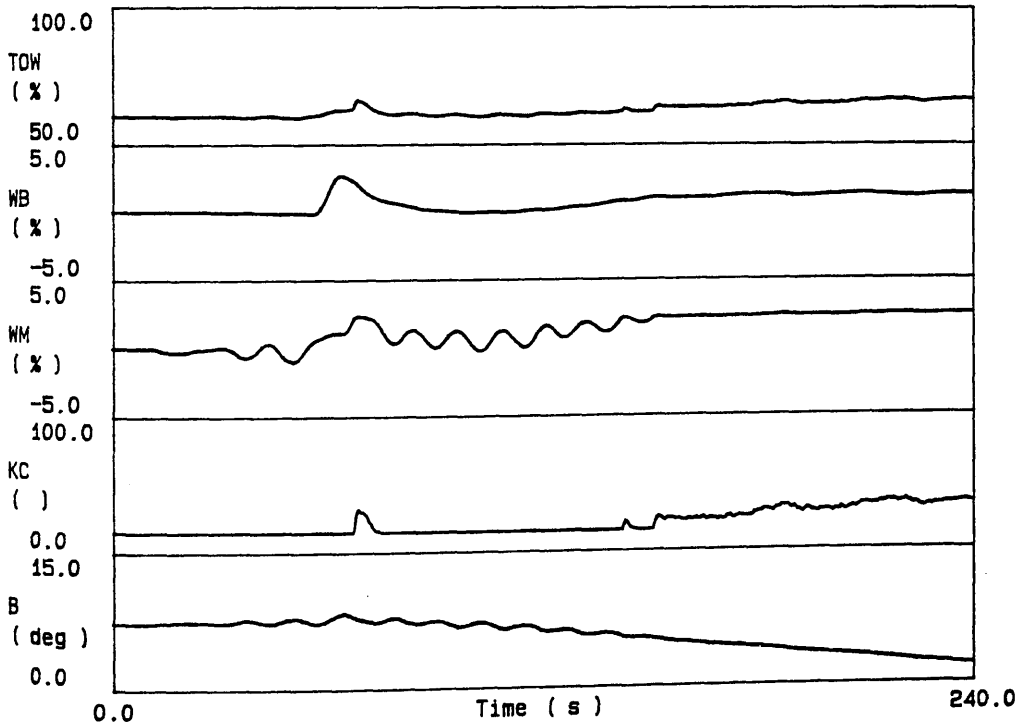
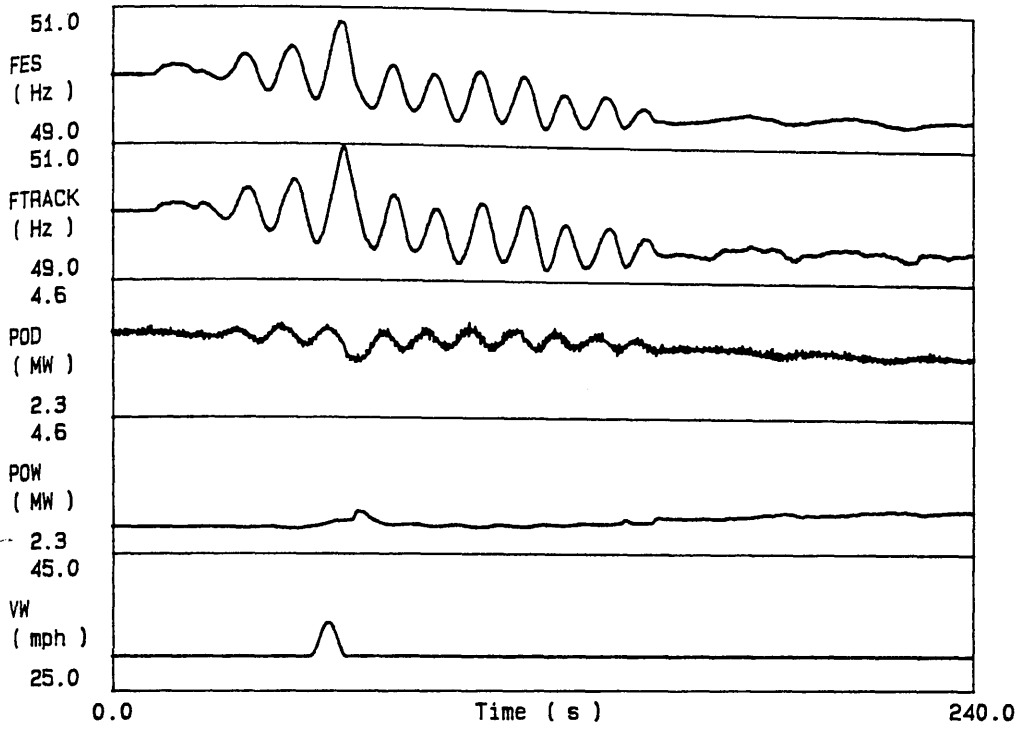


Figure 7.18 Wind-diesel system
(5mph wind gust lasting 10s)

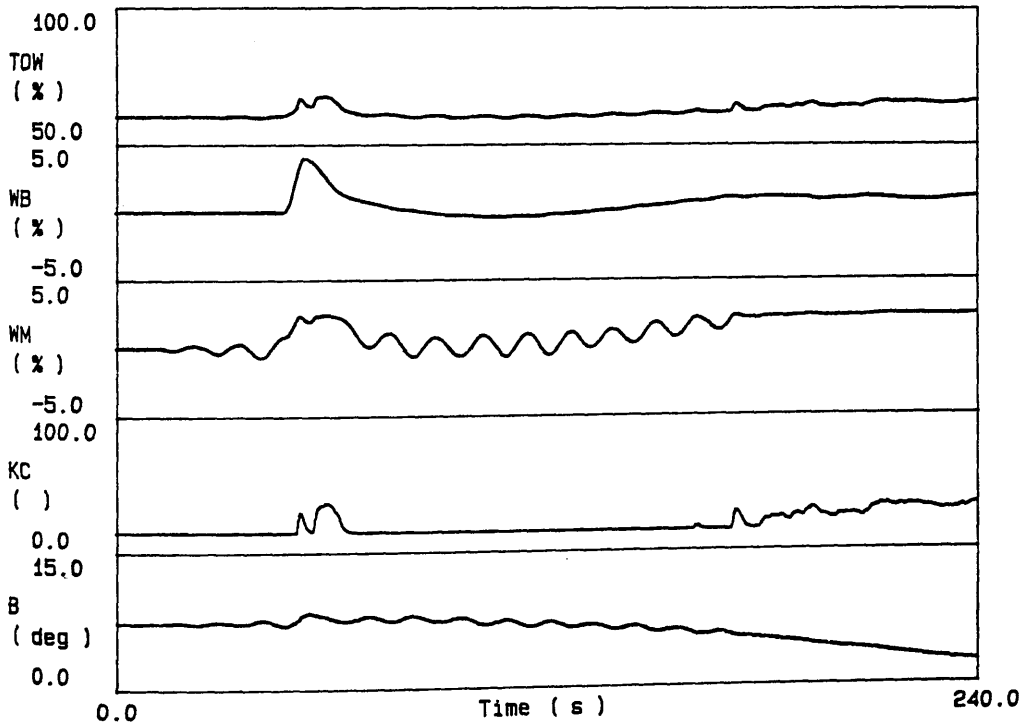
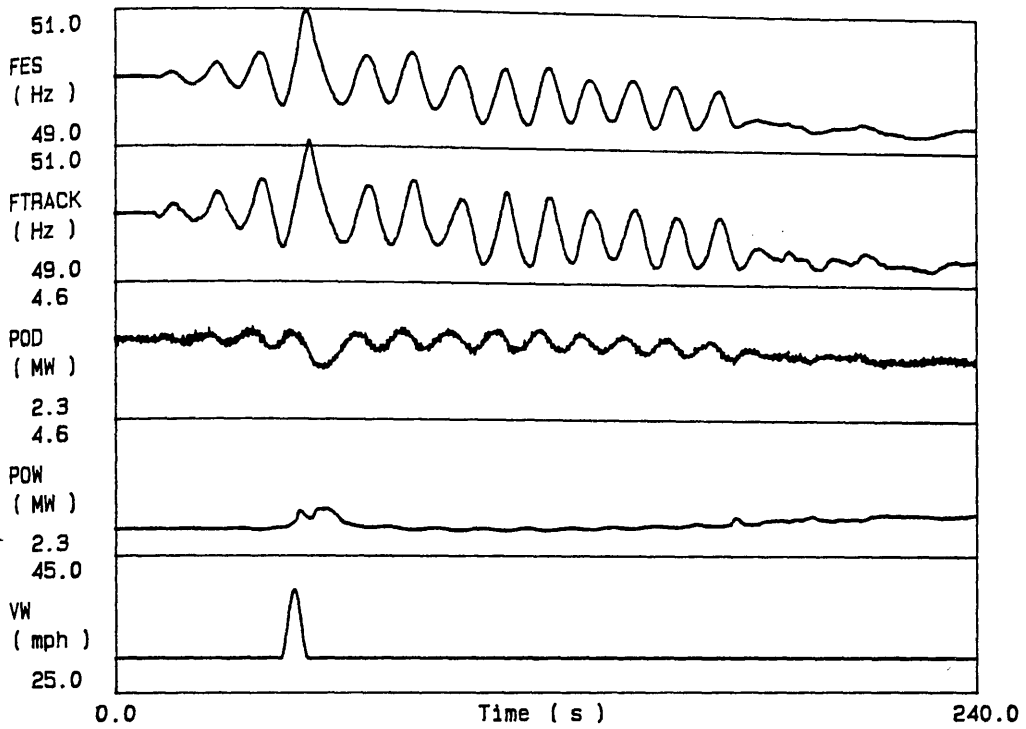


Figure 7.19 Wind-diesel system
 (10mph wind gust lasting 7.5s)

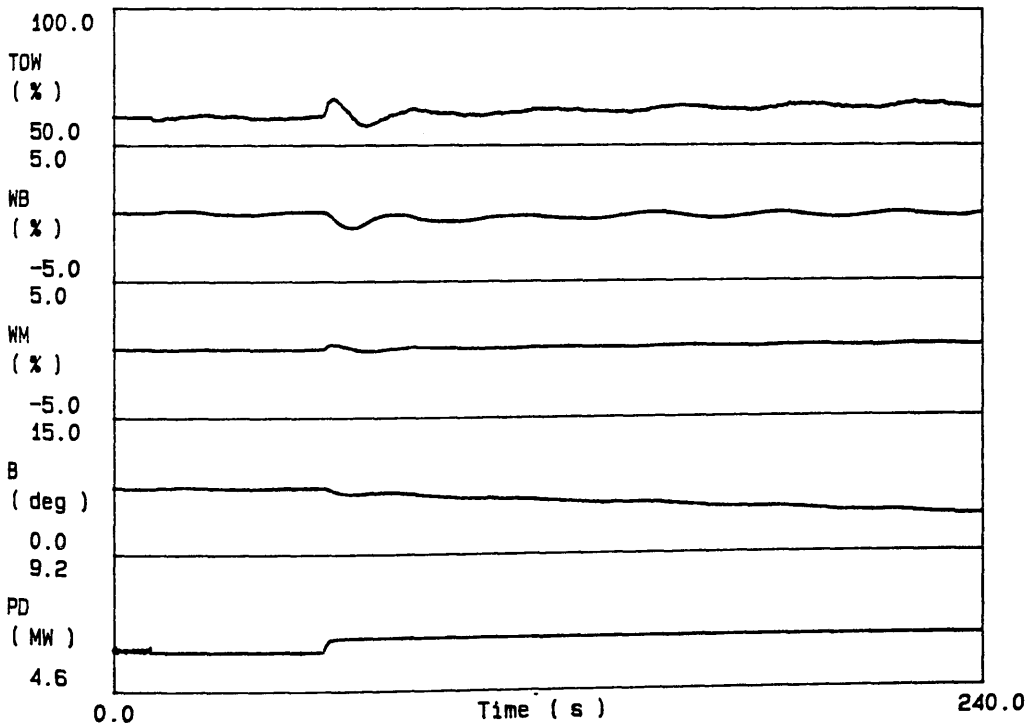
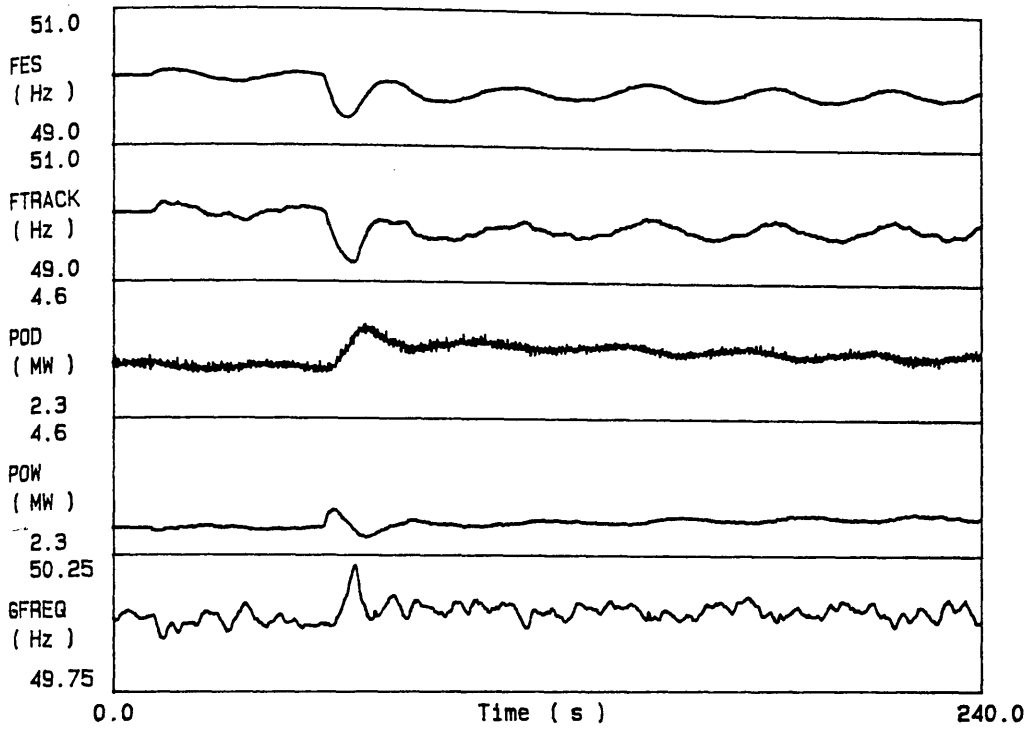


Figure 7.20 Wind-diesel system
 (50% wind, 50% diesel, 5% increase in consumer demand)

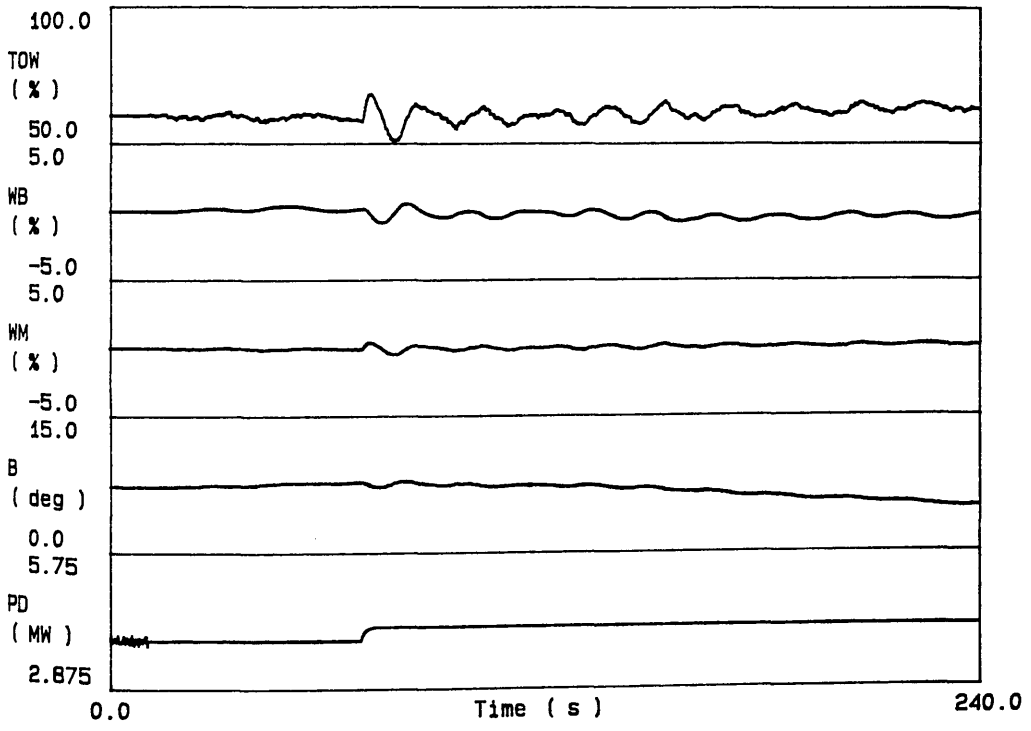
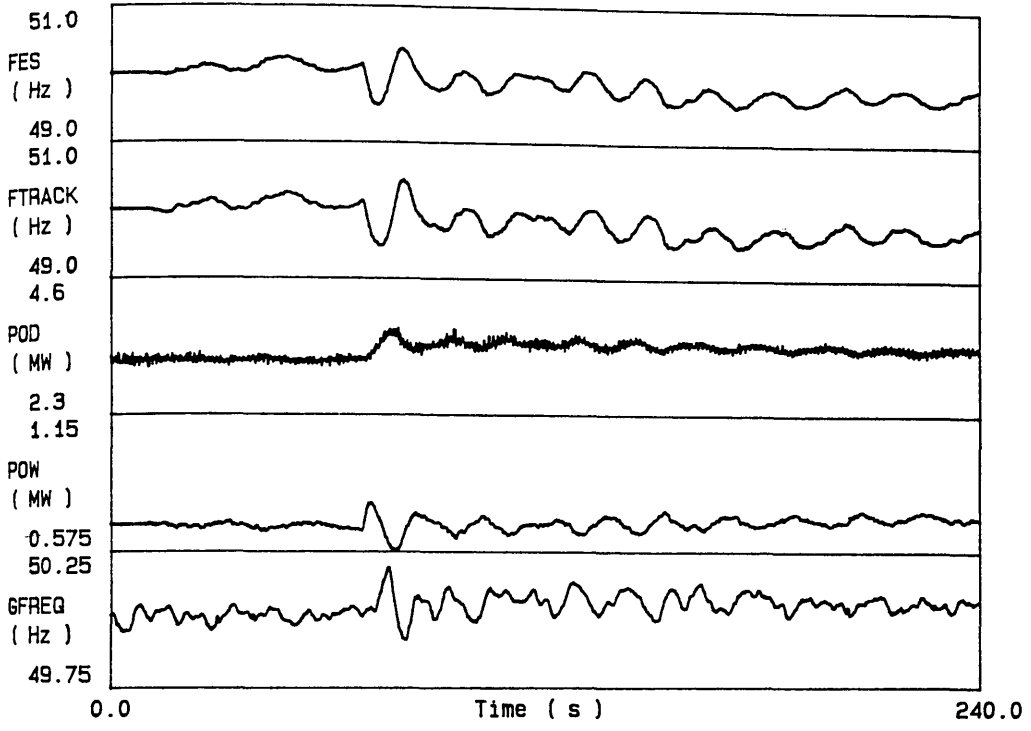


Figure 7.21 Wind-diesel system
 (20% wind, 80% diesel, 5% increase in consumer demand)

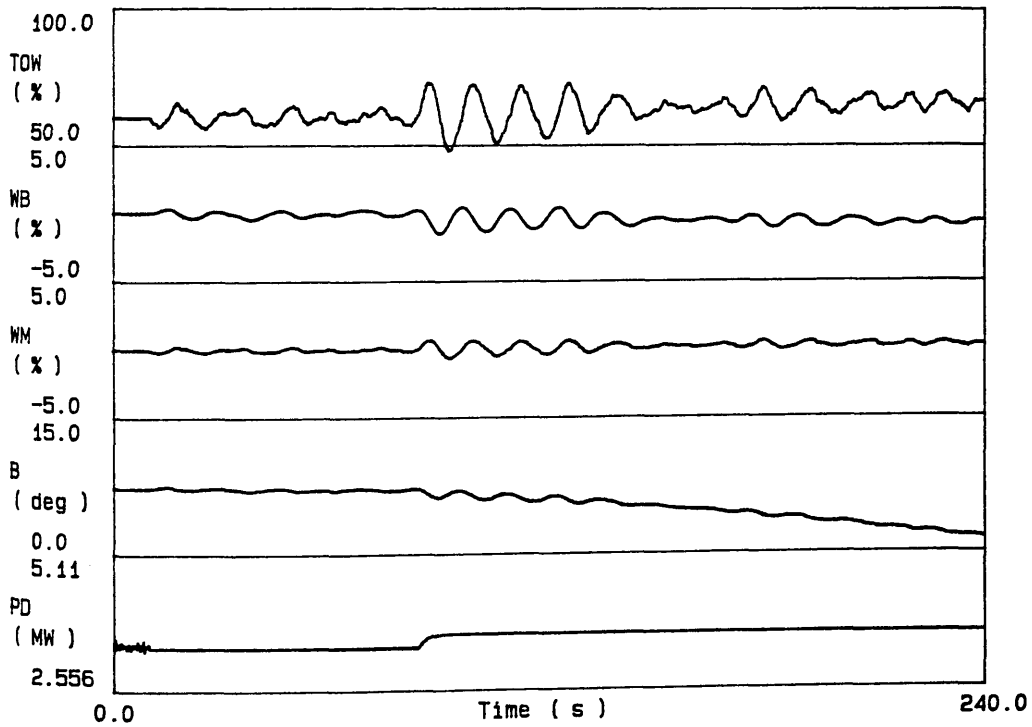
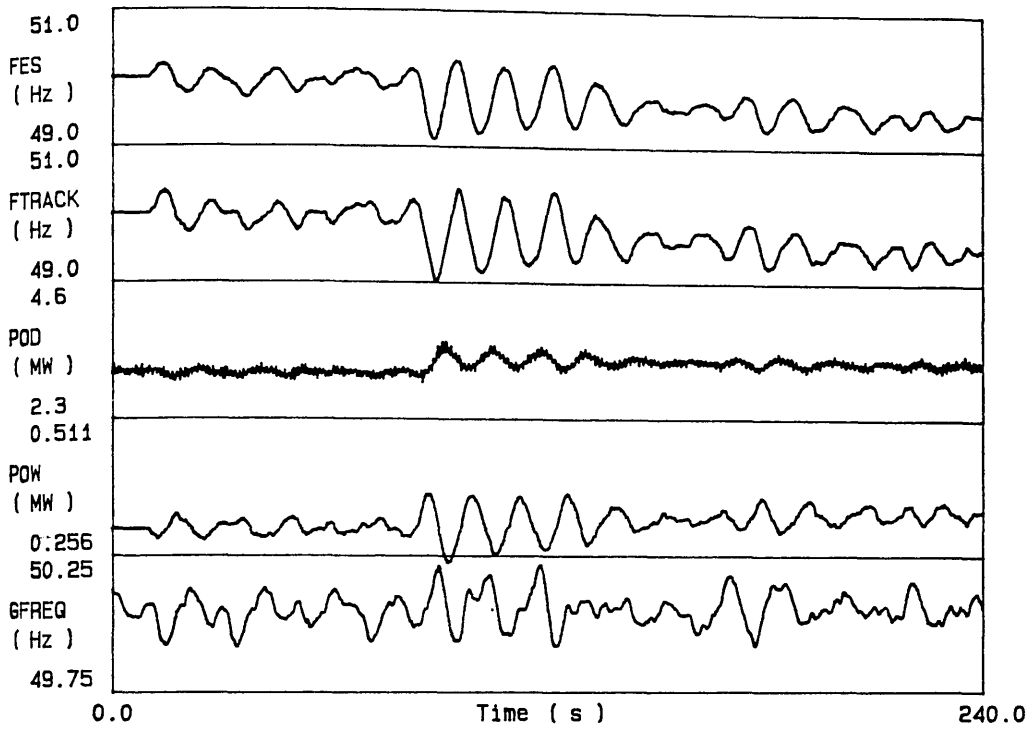


Figure 7.22 Wind-diesel system
 (10% wind, 90% diesel, 5% increase in consumer demand)

CHAPTER 8

A DEVICE TO ENHANCE THE PERFORMANCE OF EXISTING HYDRO-TURBINE GOVERNORS

The advantages of electronic governors for large hydro-electric installations have been widely established^{23,24,26} and such equipment has been used in recently constructed plant. Governor characteristics of greater complexity, such as the PID or double-derivative algorithms, can be used with electronic implementation to provide a faster response to system disturbances. Microprocessor governors, in particular, allow straightforward implementation of adaptive algorithms where the governor parameters are matched to the operating point of the turbine in order to compensate for non-linear plant characteristics and provide good performance at all load levels.

However, the NSHEB operates about 60 hydro-turbines of 5 to 50MW capacity which still employ the original hydraulic governors fitted when the schemes were constructed around 30 years ago. Regular maintenance has ensured that the governor components are, in general, mechanically sound and operate according to their design, albeit with a correspondingly slow response to system disturbances.

In view of the small size of these hydro-turbines, and the considerable plant modification that would be required, it is difficult to justify the fitting of the electro-hydraulic actuators necessary for the installation of electronic governing whether of analog or microprocessor form. The benefit of improved control during operation on the national grid cannot be presented easily in terms of a cost-saving.

Consequently, interest lies in any electronic control device that can be connected easily to a hydraulic governor and provide an improvement in response. The only existing electrical route into a hydraulic governor is via the speeder motor which positions the governor speed/load reference (a mechanical component). The power system simulator was used to investigate the performance of a device using this route to enhance the response of a governor and the results are presented in this chapter.

8.1 POSSIBLE ADJUSTMENTS TO HYDRAULIC GOVERNORS

It is possible to improve the grid-connected response of hydraulic governors by reducing either or both of the temporary and permanent droop feedback gains. The temporary droop feedback can be reduced to zero, by holding open the dashpot bypass valve, giving a purely proportional governor. Although hydro-turbines have been operated with no temporary droop feedback for long periods, such operation is unsatisfactory, particularly for plant in thinly connected areas of the power system.^{17,29} The necessary adjustments are mechanical in nature and can only be made on the governor equipment itself. If the turbine is unexpectedly required to operate in isolation from at least the major part of the national grid, then it will be unstable and an operator in a control room, possibly at a remote site, will be quite unable to reset the governor parameters to their original values.

8.2 A HYDRO-TURBINE LOAD CONTROLLER

During earlier work at Glasgow University, Davie and Clink¹⁹⁶ developed a hydro-turbine load controller which was subsequently tested with success at Sloy, Fasnakyle and Torr Achilty Power Stations. By driving the raise/lower controls to the speeder motor with appropriate pulses, this computer-based device implements

power output changes under automatic control using feedback from a measurement of generator power output. Loading changes can be provided either as quickly as possible or at a specified rate. This device was intended for use in the remote operation of hydro-electric power stations from centralised control rooms. The load controller employs a fairly elaborate algorithm in order to cope with the saturation effect present in most hydraulic governor designs incorporated to provide fast loading.

Examples of the load controller's operation are shown in Figure 8.2, where it has been commanded to increase the power output from 10 to 30MW as quickly as possible, and Figure 8.3 where the power is to be ramped down from 27 to 5MW over a 100s period. The effect of saturation in the temporary droop feedback term can be seen in Figure 8.2 where the power output, after increasing gradually, suddenly breaks away and climbs rapidly. It is this feature that makes precise and rapid control of the turbine output difficult both for an automatic load controller and an operator using the raise/lower controls directly.

As originally conceived, the load controller is not a frequency sensitive device but rather an aid to an operator in a remote control room with a large number of turbines to control. However, by adapting it to respond to grid frequency changes, a device is obtained which can be fitted very simply to a hydraulic governor and provide improvements in response to system disturbances. The processing power required is not great and it would be possible for one computer to operate several turbines. Improvements in response could, therefore, be obtained for only a small outlay per set and no modifications to the hydraulic components would be necessary. In the event of a malfunction of

the equipment or isolated operation of the turbine, the standard governor would still be available.

8.3 A GOVERNOR ENHANCEMENT DEVICE USING THE LOAD CONTROLLER

In utilising the load controller as the basis of a device to enhance the performance of an existing hydraulic governor, the load controller itself was taken as a functional unit and not altered in any way. Frequency sensitivity was provided by a component driving the target power level input to the load controller.

The load controller's function is to regulate the turbine-generator output to a target power setting and to provide the basic operations shown in Figures 8.2 and 8.3, the target level is held constant or changed to a new value either instantaneously or at a finite rate. However, the load controller is quite capable of accepting a continuously varying target level input although it will not necessarily be able to make the generator output track a rapidly changing signal. This robust behaviour allows freedom of choice in the frequency-to-target algorithms preceding the load controller.

Two frequency-to-target characteristics were investigated. In the first, the target power was held constant until the grid frequency fell below a certain value, at which time, the load controller was commanded to increase the output power by a predetermined amount. The second algorithm provided a form of continuous control where the target level was varied in accordance with the variations in grid frequency.

As indicated above, the load controller was taken as a given functional unit and no attempt was made to tune its parameters to the frequency algorithm in use. The load controller is normally

tuned over step and ramp targets and there is no particular reason to re-tune it for other input types.

The effects of these governor enhancement devices on a mixed hydro-thermal power system were investigated using off-line simulation and the established algorithms were tested on Sloy No.2 machine using the real-time power system simulator. The arrangement of the various items of equipment is outlined in Figure 8.1.

In all of the tests, the hydro-electric plant controlled by the device was 10% of the simulated system; the remainder being a mix of thermal and base load plant. Satisfactory operation of the devices would be difficult to achieve on plant constituting more than 10% of the system generation.

For some of the tests, the two thermal units in the system were set at different load levels. Operating the two equal components at 90% and 70% m.c.r. rather than both at 80% m.c.r. has little effect on the behaviour of the system.

8.4 A LOW FREQUENCY RELAY DEVICE

The first type of frequency driven load controller is intended to mimic the operation of Dinorwig pumped-storage units in their low frequency relay activated loading.⁸ While the NSHEB turbines cannot be dewatered and spun in air to provide an economic spinning reserve state, they can be maintained at a low power level and then moved to a higher power when a specified low frequency is detected. This type of operation is similar to one mode of the Dinorwig machines. NSHEB turbines controlled in this way would provide spinning reserve at greater running cost than Dinorwig, but their contribution would be of significance when circumstances reduce the overall system regulation. Such a mode of

operation could be very desirable in the event of transmission circuit failures causing separation of the SSEB and NSHEB systems from the CEGB.

Figure 8.4 illustrates the behaviour of a system with 90% thermal and 10% hydro generation where the hydro component (Sloy No.2 machine) is provided with a low frequency relay driven load controller set at 49.75Hz with a subsequent load increment of 50% m.c.r. corresponding to a 1% droop.

Increasing the base load capacity to 40% (Figure 8.5) increases the overall droop of the system and the frequency deviation is larger, particularly in the initial transient where the hydro-turbine is not yet contributing to the response. The hydro power output trajectory is unchanged from Figure 8.4 because this load controller device is not sensitive to system frequency after it has been triggered and before it has been reset.

If a frequency driven load controller were to be permanently installed on a hydro-turbine, the machine frequency drive would not be removed from the governor. The turbine would, therefore, respond to frequency transients with contributions from both the load controller and the governor itself. It is not possible to induce the governor's own contribution when testing a frequency-driven load controller on a real hydro-turbine. The load controller requires exclusive use of the speeder motor and the simulator is unable to inject a simulated frequency signal. However, the governor's own contribution is quite small and its absence does not greatly affect the behaviour of the complete system. Any action taken by the governor itself is eventually undone by the load controller regulating the turbine output to a target power.

Off-line simulation shows that the governor's effect is, in fact, beneficial in that it causes the hydro contribution to appear slightly earlier. The performance of the enhanced governor for a real system disturbance would, therefore, be slightly better than the tests with the simulator suggest.

The load controller's use of the speeder motor also prevented the correction of grid frequency fluctuations during a test but a measurement of grid frequency was logged along with the other signals of interest. This was then checked for deviations large enough to have interfered with the test which could then be re-run if necessary. A visual check could also be maintained on a digital grid frequency meter.

8.5 A CONTINUOUS FREQUENCY DEVICE

An alternative frequency-to-target scheme which can provide a continuous action is obtained if the target level input to the load controller is made proportional to the deviation of the system frequency from 50Hz. In this way, the effective droop of the hydro-turbine can be increased and the load controller can be used to overcome the temporary droop feedback which normally dominates the plant's response. In contrast to the low-frequency relay device, a proportional scheme causes the hydro plant to assist more effectively with the regulation of the system when the frequency remains close to 50Hz. A deadband could, however, be incorporated so that the device was inactive when the frequency deviation was less than a certain value. The droop could also be made dependent on the size of the frequency error in order to produce a contribution greater than pro-rata for a larger deviation.

The behaviour of this type of enhancement device differs from

that of the low frequency relay in that the control is continuously active and the device will respond to the effects of its own actions. In view of this closed-loop situation, fully stable operation of the hydro-turbine is not guaranteed. The succession of Figures 8.6, 8.7 and 8.8 show results obtained with a device driving a load controller on Sloy No.2 machine in direct proportion to the simulated frequency signal provided by the power system simulator. The configuration is once again a 90%/10% mix of generation types with a thermal droop of 4%. The frequency-to-target droop is 2% in Figure 8.6, 1.5% in 8.7 and 1% in 8.8. As expected, the reductions in droop increase the hydro-turbine response with a correspondingly improved post-transient frequency value. Unfortunately, limit cycle oscillations also become prevalent indicating an imprudent choice of gain and causing unacceptable continuous operation of the speeder motor.

With a frequency-to-target droop of 2%, the effect of an increase in the proportion of base load (non-regulating) capacity with a corresponding reduction in regulating thermal plant was investigated. Figures 8.9, 8.10 and 8.11 are for base load capacities of 0, 20 and 40% respectively. In the arguably more realistic situation of a significant proportion of non-regulating plant causing a larger initial frequency swing following the disturbance, the overshoot in the hydro-turbine power output becomes quite marked. In fact, during the test with 40% base load, the turbine relief valve operated when the water control valve was closed rapidly by the governor, following the overshoot, indicating the strenuous nature of the response. As with the reduced droop tests, the reduction in system regulation in these tests leads to the appearance of limit cycle oscillations in

Figures 8.10 and 8.11. These results indicate that operation with a droop of 2% may not be satisfactory.

Figures 8.12 and 8.13 are for 3% droop with 20 and 40% base load capacity respectively. The hydro-turbine's behaviour is no longer so lively and the onset of limit cycle oscillation has receded to a higher base load capacity.

The addition of a derivative term to the proportional frequency-to-target algorithm was investigated by off-line simulation but the effect was not found to be beneficial.

The limit cycle oscillation of the continuous frequency device for low droop values was not predicted by off-line simulation. This illustrates the ability of the power system simulator to show up problems with a control scheme which only become evident on the real plant.

8.6 COMPARISON WITH THE BASIC GOVERNOR TYPES

In order to compare the performance of the two enhancement devices with that of the basic governor types, responses were obtained for a system with 40% base load generation and a 10% step increase in load applied through a first-order lag with a time constant of 2.5s. Figure 8.14 is for the low frequency relay and Figure 8.15 for the continuous device with a 3% droop. For convenience, the corresponding responses for the temporary droop (Figure 6.20) and double derivative (Figure 6.21) governors have been replotted here with a change of scale as Figures 8.16 and 8.17 respectively.

Very good performance is obtained with the low frequency relay device. Although the magnitude of the initial frequency swing is not much reduced, the frequency is much closer to 50Hz after the transient. This is due to the 1% droop setting of the

relay device.

A degree of overshoot is evident on the power output response with the continuous frequency device but the frequency trace is still much improved over that obtained with the temporary droop governor alone. Although the overall droop of the turbine is still 3%, the device is able to overcome the effect of the temporary droop feedback and provide a fast response. The overshoot is not in itself important and steam turbines are regularly expected to follow this shape of power output trajectory. If the hydro-electric plant controlled by this type of device was less than 10% of the system, it would be possible to use a lower droop value. The continuous frequency device achieves a response that is comparable to that of the double derivative governor although it does not maintain isolated load stability.

8.7 CONCLUSION

The investigation reported in this chapter has established the potential of electronic devices to improve the response of hydraulic temporary droop governors for system operation. The low frequency relay device would appear to be the most practicable. This scheme could be used to obtain a much greater contribution to system response from existing hydro-turbine plant. The investigation has also illustrated the use of the power system simulator to demonstrate the advantages of a novel governor design.

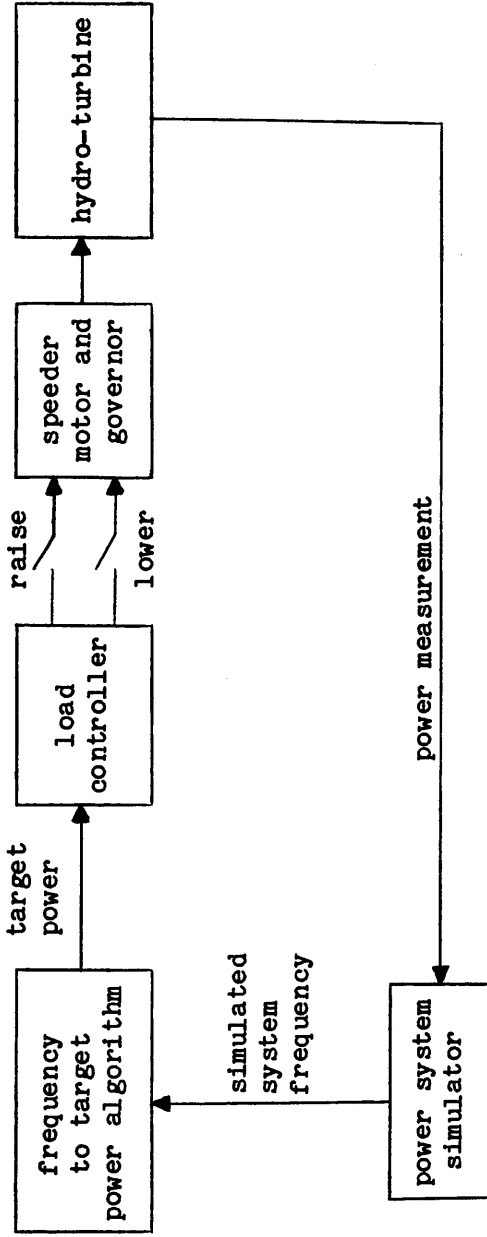


Figure 8.1 Arrangement of the simulator and load controller for on-line tests

Labels for Figures 8.2 to 8.17

- SPDINP - speeder motor pulses
- POH - hydro-turbine power output
- FES - simulated system frequency
- POC1 - coal-fired plant 1 power output
- POC2 - coal-fired plant 2 power output

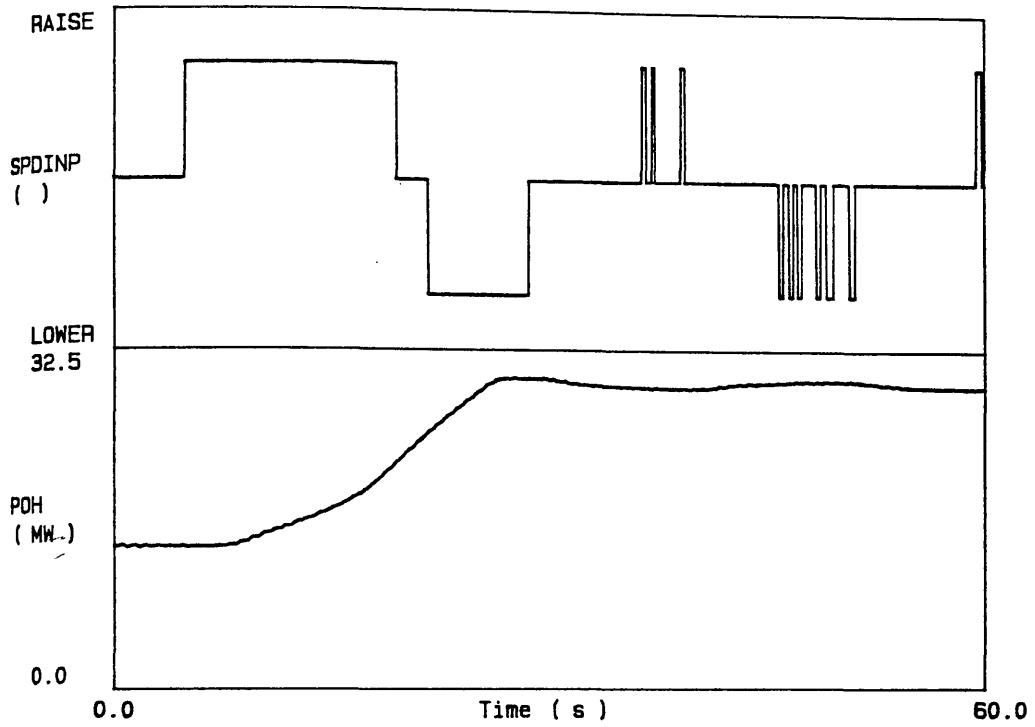


Figure 8.2 Load controller operation for step increase in power

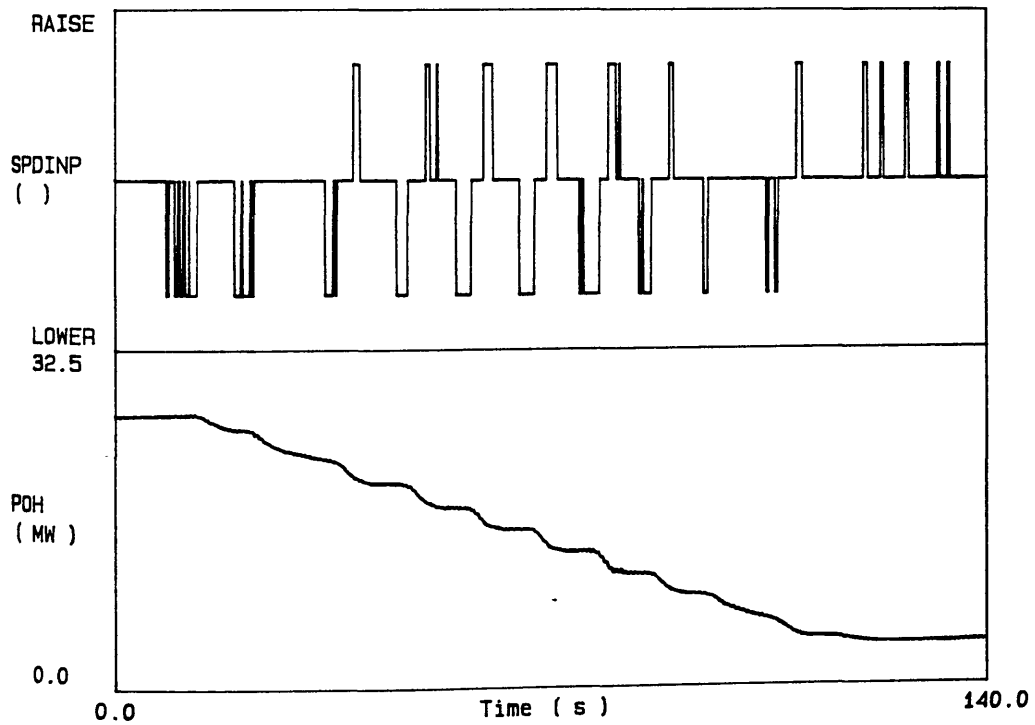


Figure 8.3 Load controller operation for ramp decrease in power

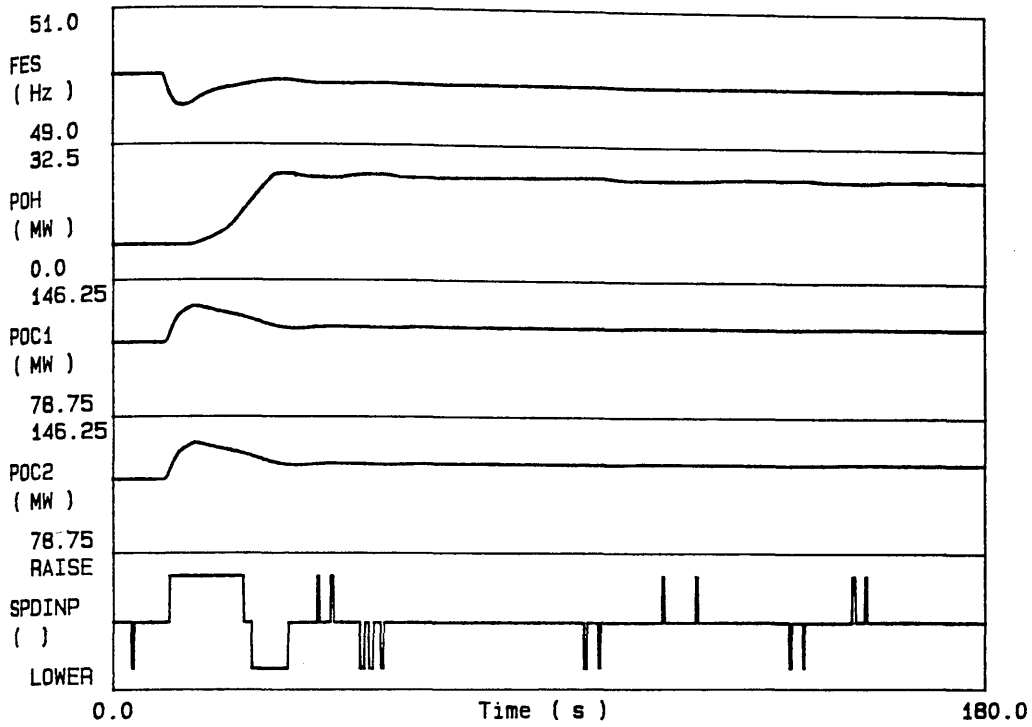


Figure 8.4 Mixed system test with low frequency relay device (1% droop, no base load)

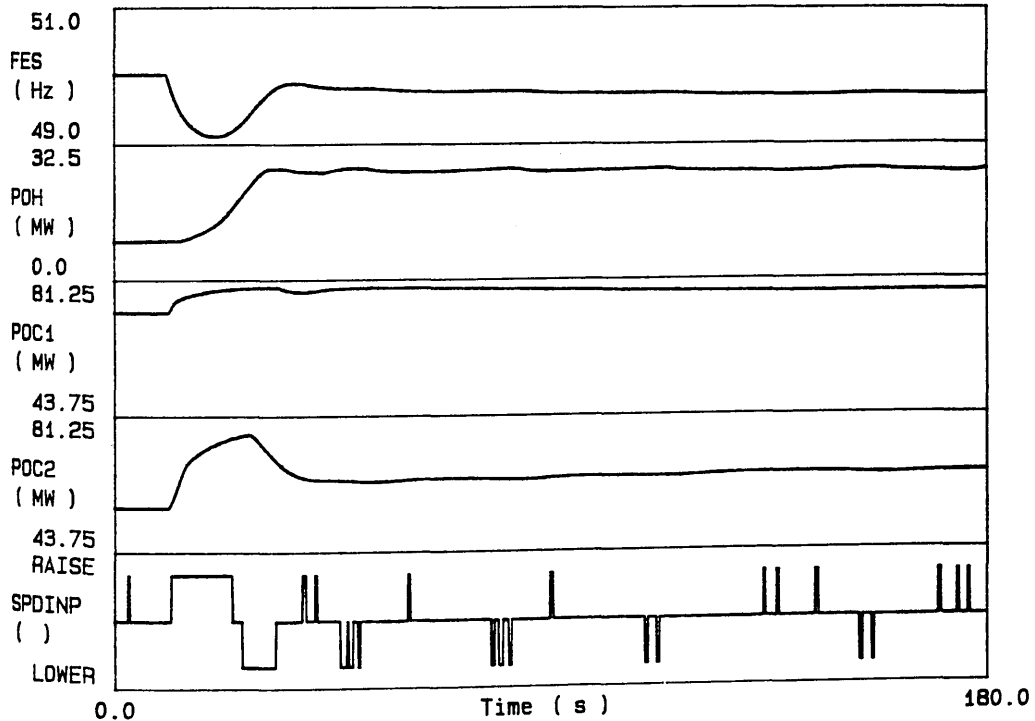


Figure 8.5 Mixed system test with low frequency relay device (1% droop, 40% base load)

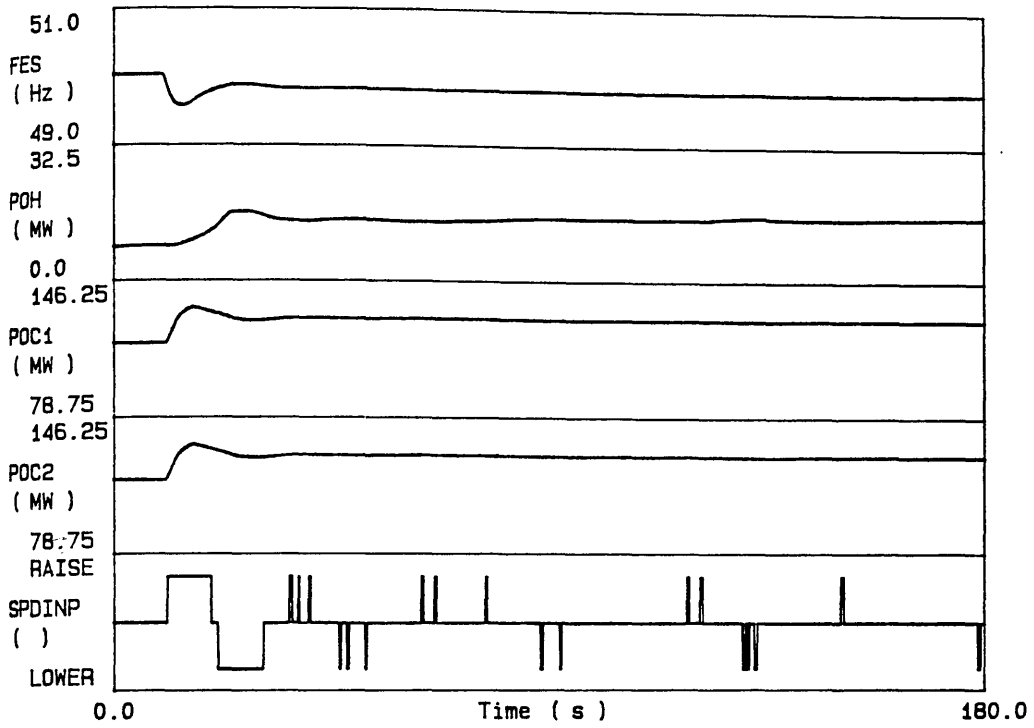


Figure 8.6 Mixed system test with continuous frequency device (2% droop, no base load)

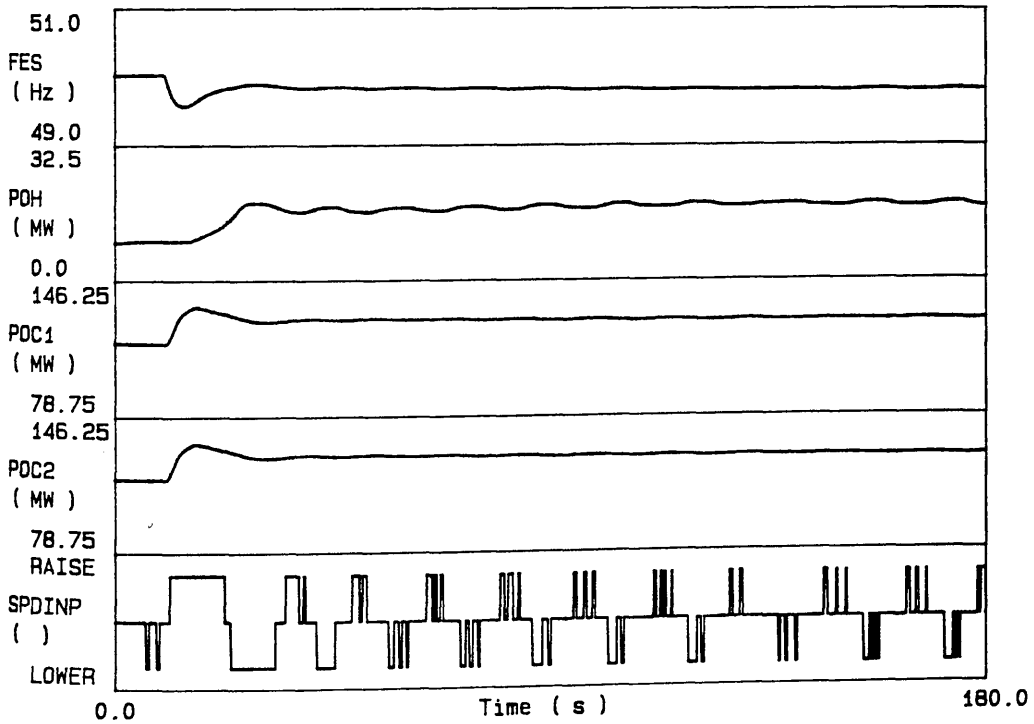


Figure 8.7 Mixed system test with continuous frequency device (1.5% droop, no base load)

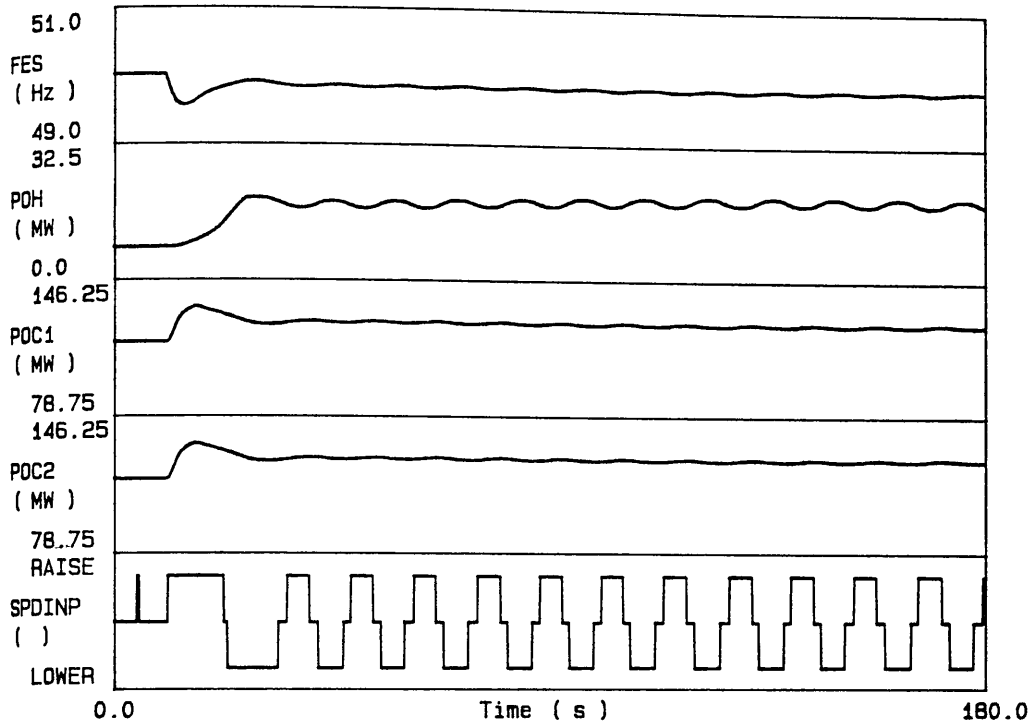


Figure 8.8 Mixed system test with continuous frequency device (1% droop, no base load)

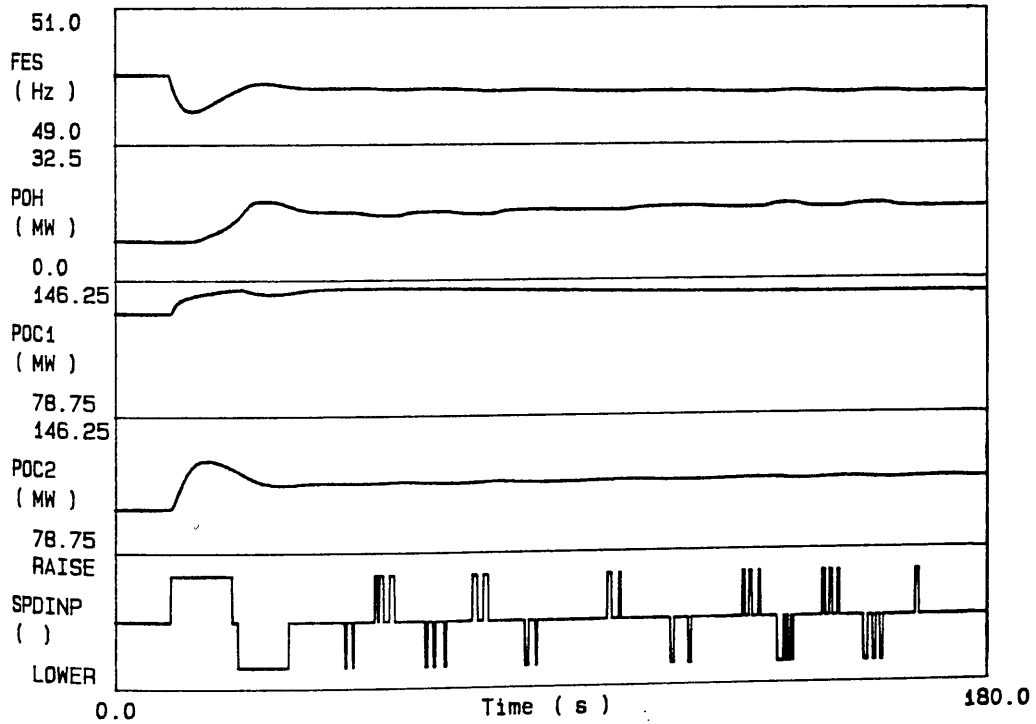


Figure 8.9 Mixed system test with continuous frequency device (2% droop, no base load)

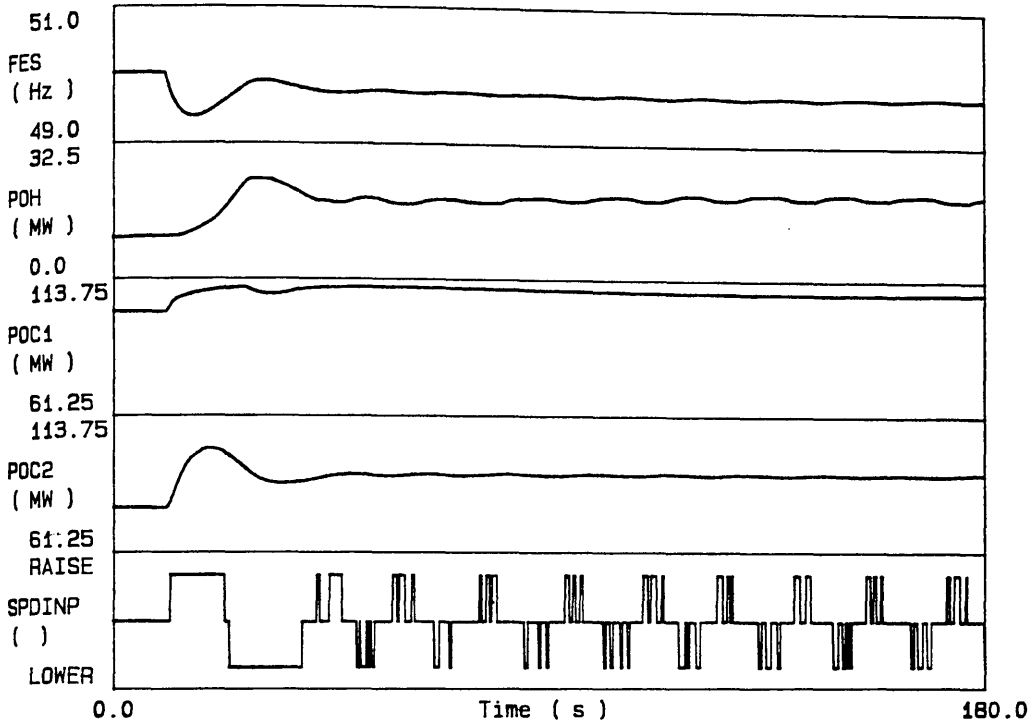


Figure 8.10 Mixed system test with continuous frequency device (2% droop, 20% base load)

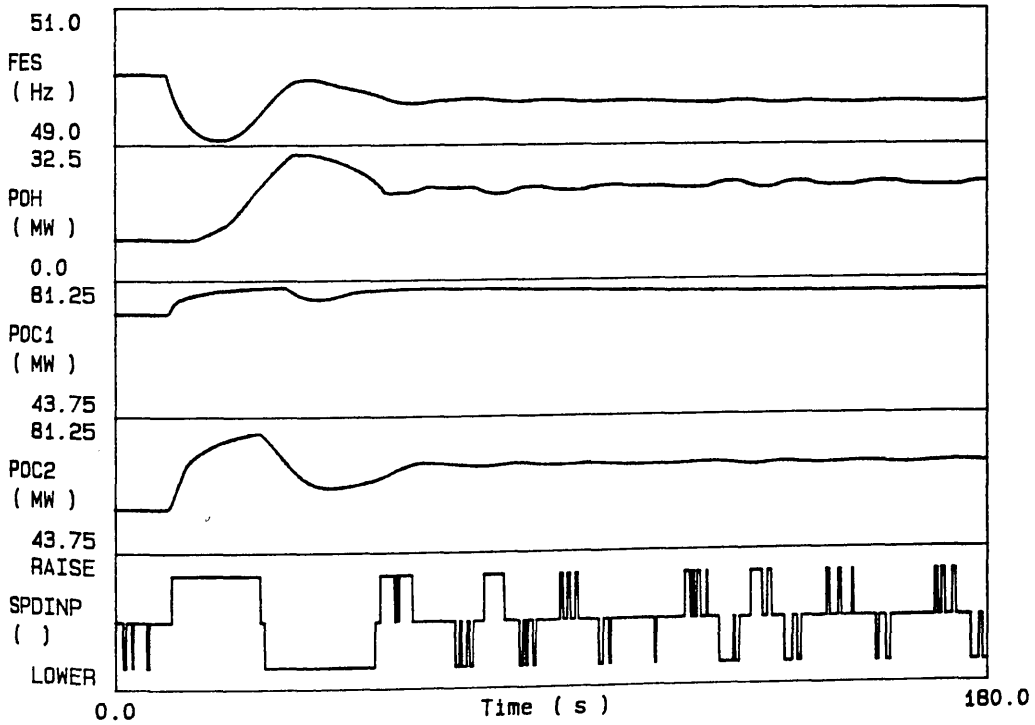


Figure 8.11 Mixed system test with continuous frequency device (2% droop, 40% base load)

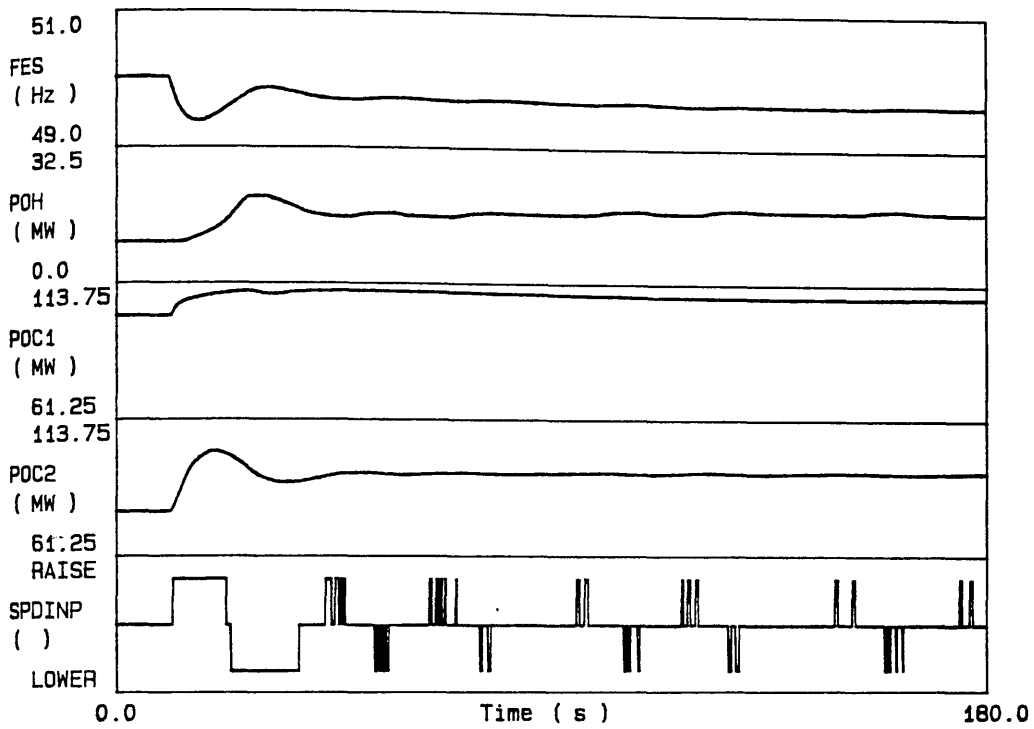


Figure 8.12 Mixed system test with continuous frequency device (3% droop, 20% base load)

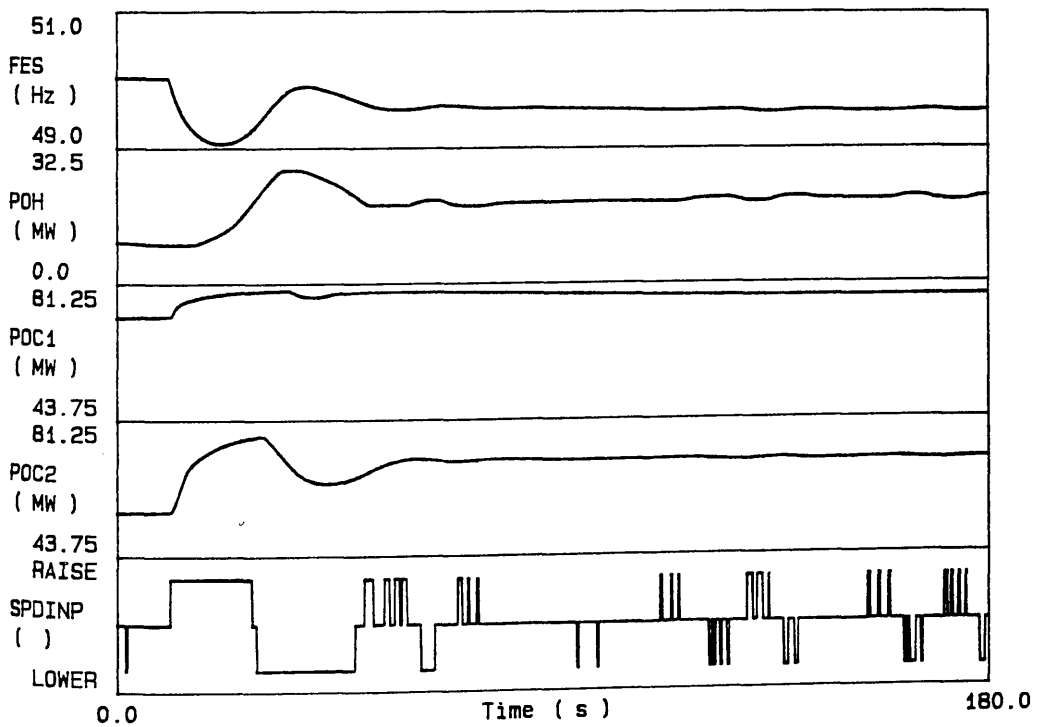


Figure 8.13 Mixed system test with continuous frequency device (3% droop, 40% base load)

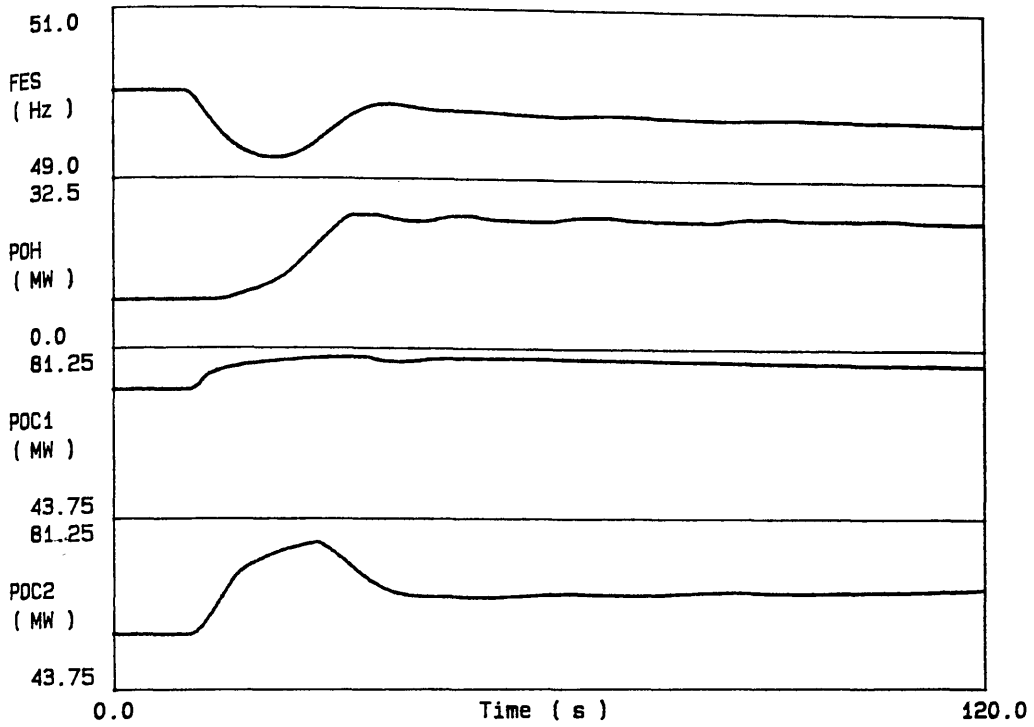


Figure 8.14 Mixed system test with low frequency relay device (1% droop, 40% base load)

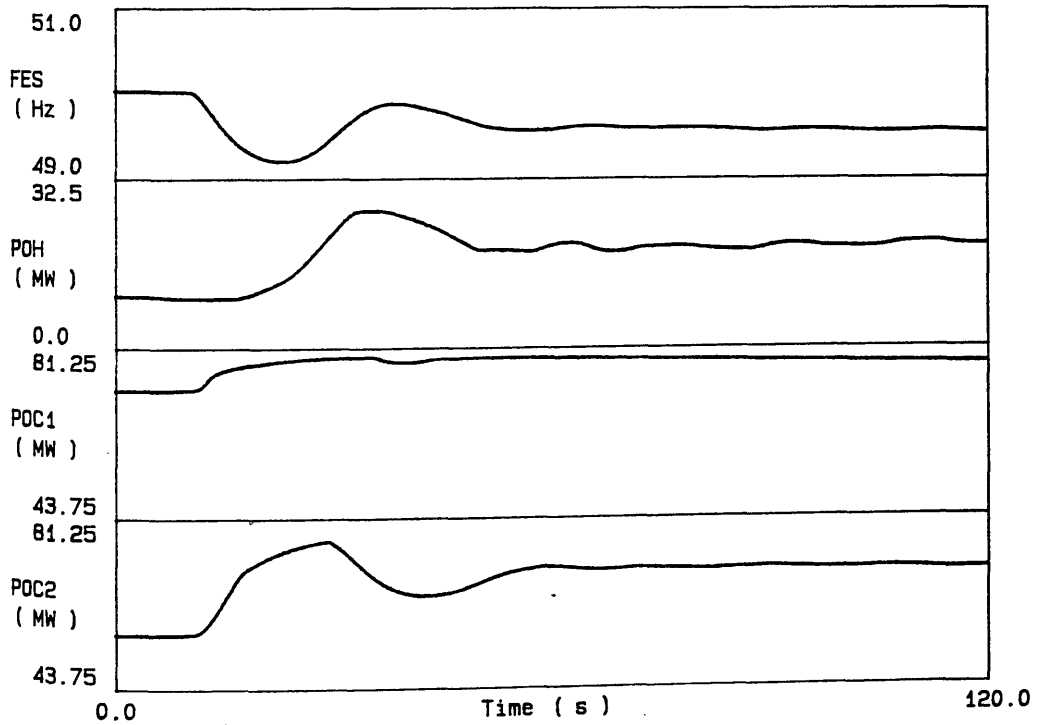


Figure 8.15 Mixed system test with continuous frequency device (3% droop, 40% base load)

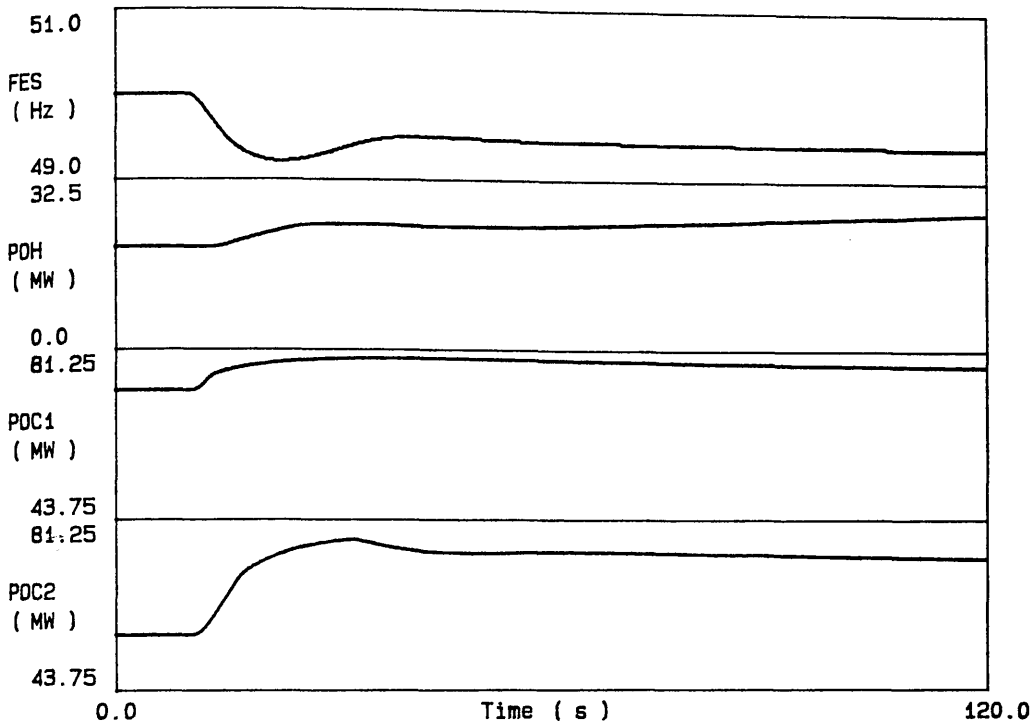


Figure 8.16 Mixed system test with hydraulic governor (3% droop, 40% base load)

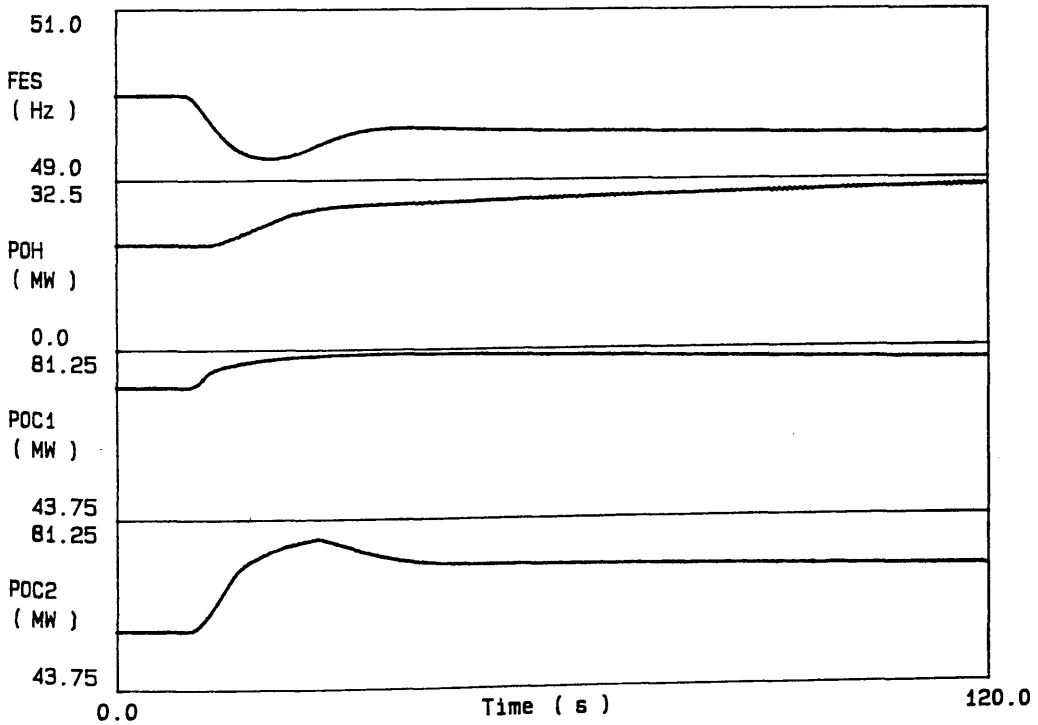


Figure 8.17 Mixed system test with electronic governor (3% droop, 40% base load)

CHAPTER 9

CONCLUSIONS AND RECOMMENDATIONS FOR FURTHER WORK

A power system simulator has been developed to investigate the response of generating plant to loading disturbances on an interconnected power system. On-site tests at Loch Sloy Power Station have established the potential of the equipment for real plant tests. Methods of injecting the test signal have been developed which allow the simulator to be used with the majority of hydro-turbines and other generating plant. More extensive investigations are possible with electronic governors, but useful results can also be obtained for mechanical-hydraulic equipment.

Tests with a coal-fired plant model have illustrated a number of the features of the behaviour of a nuclear-hydro-thermal power system. More importantly, they have demonstrated the ability of the power system simulator to investigate the response of a mixed system and to establish the merits of particular governor configurations on a real hydro-turbine. The use of a multiprocessor simulation vehicle to relieve constraints on the problem size has also been demonstrated in the environment of on-line tests at a power station.

Application of the technique to a Stornoway diesel engine has proved that the power system simulator can be used on a system where the test machine is a significant proportion of the generating plant. Useful results were obtained with a mixed diesel-thermal system configuration and the technique was used to investigate the behaviour of an isolated wind-diesel power system.

A further investigation on hydro-turbine plant has established the potential of electronic devices to improve the

response of hydraulic temporary droop governors for system operation. This investigation has illustrated the use of the power system simulator in the development of a novel controller design.

9.1 FURTHER WORK

The potential of the simulator has been displayed on small to medium sized plant. It is not anticipated that any major modifications would be required if the technique were to be applied to large turbines such as those at Foyers (2x150MW) or Dinorwig (6x300MW), but this supposition could usefully be substantiated. Tests were proposed for Foyers, but these could not be carried out due to plant availability constraints. Such tests would demonstrate the application of the power system simulator to large plant and might indicate possible improvements to the governor settings.

REFERENCES

1. Booth, E.S.
The electricity supply industry - yesterday, today and tomorrow
Proc. IEE, Vol.124, No.1, January 1977, pp.1-16
2. Symons, O.C., Ward, R.J.S.
Power System Disturbances
20th Universities Power Engineering Conf., Huddersfield Polytechnic, 1985, pp.321-324
3. Waddington, J., Maples, G.C.
The control of large coal- and oil-fired generating units
Power Engineering Journal, Vol.1, No.1, January 1987, pp.25-34
4. Elgerd, O.I.
Electric Energy Systems Theory
McGraw-Hill, London, 1983
5. Booth, E.S.
Whither Nuclear Power?
Proc. IEE, Vol.118, No.9, September 1971, pp.1215-1226
6. Carvalho, F.L.
Nuclear Power Plant Performance in Power System Control
Int. Conf. on Large High Voltage Electric Systems, CIGRE, 1986
7. Fairney, W., Newman, V.G., Harman, R.D.
The CEBG requirement for Dinorwig Power Station
The Dinorwig Power Station Symposium, I.Mech.E., 1985, pp.1-12
8. Wallis, E.A.
Operation of Dinorwig pumped storage station on the CEBG system
The Dinorwig Power Station Symposium, I.Mech.E., 1985, pp.221-230
9. Fulton, A.A.
The Cruachan Pumped-storage Development
Electronics and Power, Vol.12, No.7, July 1966, pp.220-224
10. Miller, D.J., Murray, A.T.L., Marshall, C.C., Argent, G.C.R.
Foyers pumped-storage project
Proc. IEE, Vol.122, No.11, November 1975, pp.1222-1234
11. Davidson, D.R., Ewart, D.N., Kirchmayer, L.K.
Long Term Dynamic Response of Power Systems: An Analysis of Major Disturbances
IEEE Trans. PAS, Vol.94, No.3, May/June 1975, pp.819-826
12. Benko, G.B.
Governing turbines for transient loads
Int. Water Power & Dam Construction, Vol.33, No.4, April 1981, pp.38-42

13. Bryce, G.W., Agnew, P.W., Foord, T.R., Winning, D.J.,
Marshall, A.G.
On-site investigation of electrohydraulic governors for water
turbines
Proc. IEE, Vol.124, No.2, February 1977, pp.147-153
14. Mawer, W.T., Queen, B.B., Hooper, P.N.
The hydraulic design
The Dinorwig Power Station Symposium, I.Mech.E., 1985,
pp.25-35
15. Undrill, J.M., Strauss, W.
Influence of Hydro Plant Design on Regulating and Response
Capacity
IEEE Trans. PAS, Vol.93, No.4, July/Aug 1974, pp.1192-1200
16. Bryce, G.W., Agnew, P.W., Foord, T.R., Winning, D.J.,
Marshall, A.G.
In reply to discussion on Reference 13
Proc. IEE, Vol.124, No.9, September 1977, pp.768-770
17. Schleif, F.R., Wilbor, A.B.
The Coordination of Hydraulic Turbine Governors for Power
System Operation
IEEE Trans. PAS, Vol.85, No.7, July 1966, pp.750-758
18. Woodward, J.L.
Hydraulic-turbine Transfer Function for Use in Governing
Studies
Proc. IEE, Vol.115, No.3, March 1968, pp.424-426
19. Paynter, H.M.
The Analog in Governor Design, I - A Restricted Problem
A Palimpsest on the Electronic Analog Art, G.A. Philbreck
Researches Inc., Boston, Mass., USA, 1960, p.228
20. Schleif, F.R., Bates, C.G.
Governor Characteristics for 820,000 Horsepower Units for
Grand Coulee Third Power Plant
IEEE Trans. PAS, Vol.90, No.2, March/April 1971, pp.882-890
21. Schleif, F.R.
Governor Characteristics for Large Hydraulic Turbines
Report REC-ERC-71-14, Electric Power Branch, Engineering and
Research Center, Denver, Colorado, 1971
22. Briggs, D.A.
Discussion on Reference 13
Proc. IEE, Vol.124, No.9, September 1977, pp.768-770
23. Eilts, L.E., Schleif, F.R.
Governing Features and Performance of the First 600MW
Hydrogenerating Unit at Grand Coulee
IEEE Trans. PAS, Vol.96, No.2, March/April 1977, pp.457-466
24. Richards, K.H.
Control and instrumentation concepts and reliability
The Dinorwig Power Station Symposium, I.Mech.E., 1985,

25. Briggs, D.A.
Dinorwic Power Station. Theoretical Study of ASEA Governor System Dynamics
CEGB Generation Development and Construction Division Report No. PED/SES/CPK/29, 1976
26. Findlay, D., Davie, H., Foord, T.R., Marshall, A.G., Winning, D.J.
Microprocessor-based adaptive water-turbine governor.
IEE Proc., Vol.127, Pt.C, No.6, November 1980, pp.360-369
27. Grant, N.F.
A Microprocessor Based Controller Applied to a Hydro-turbine
Ph.D. Thesis, University of Glasgow, 1980
28. Findlay,
Microprocessor Governors for Hydro-turbine Generators
Ph.D. Thesis, University of Glasgow, 1980
29. Hovey, L.M.
Optimum Adjustment of Hydro Governors on Manitoba Hydro System
AIEE Trans., Vol.81, Part III, December 1962, pp.581-587
30. Chaudry, M.H.
Governing stability of a hydroelectric power plant
Water Power, Vol.22, No.4, April 1970, pp.131-136
31. Thorne, D.H., Hill, E.F.
Field Testing and Simulation of Hydraulic Turbine Governor Performance
IEEE Trans. PAS, Vol.93, No.4, July/Aug 1974, pp.1183-1191
32. Thorne, D.H., Hill, E.F.
Extensions of Stability Boundaries of a Hydraulic Turbine Generating Unit
IEEE Trans. PAS, Vol.94, No.4, July/Aug 1975, pp.1401-1409
33. Phi, D.T., Bourque, E.J., Thorne, D.H., Hill, E.F.
Analysis and Application of the Stability Limits of a Hydro-generating Unit
IEEE Trans. PAS, Vol.100, No.7, July 1981, pp. 3203-3212
34. Dhaliwal, N.S., Wichert, H.E.
Analysis of PID Governors in Multimachine System
IEEE Trans. PAS, Vol.97, No.2, March/April 1978, pp.456-463
35. Hagihara, S., Yokota, H., Goda, K., Isobe, K.
Stability Analysis of Hydraulic Turbine Generating Unit Controlled by PID Governor.
IEEE Trans. PAS, Vol.98, No.6, Nov/Dec 1979, pp.2294-2298
36. Stein, T.
Frequency control under isolated network conditions
Water Power, Vol.22, No.9, September 1970, pp.320-324
37. Fasol, K.H.
Economical dynamic governor tests in power stations
Water Power, Vol.25, No.4, April 1973, pp.129-134

38. Undrill, J.H., Woodward, J.L.
Nonlinear Hydro Governing Model and Improved Calculation for
Temporary Droop
IEEE Trans. PAS, Vol.86, No.4, April 1967, pp.443-453
39. Schleif, F.R., Angell, R.R.
Governor Tests by Simulated Isolation of Hydraulic Turbine
Units
IEEE Trans. PAS, Vol.87, No.5, May 1968, pp.1263-1269
40. Causon, G.J.
Governing a Hydro-electric System
Int. Assoc. for Hydraulic Research, 7th Int. Symposium,
Vienna, 1974, pp.X/2/1-13
41. Brown, P.A.N., Willing, B.C.
Development and Use of a Machine Isolation Simulator for
Testing Hydraulic Turbine Governor Systems
Inst. Eng. Aust. Electr. Eng. Trans., Vol.14, No.1, 1978,
pp.20-24
42. de Mello, R.W., Parkinson, D.W., Wode, S.L., McDonnell, J.R.,
Gay, J.W.
Digital Simulator for the Checkout of Advanced Boiler and
Turbine Controls
IEEE Trans. PAS, Vol.102, No.6, June 1983, pp.1505-1509
43. Fischetti, A., Ormelli, L., Petrioli, G.
In-line Simulation of Turbine Generator Units for Testing
Electro-hydraulic Control Systems
AICA Symposium on Hybrid Computation in Dynamic Systems
Design, Rome, 1974
44. Ashmole, P.H., Battlebury, D.R., Bowdler, R.K.
Power system model for large frequency disturbances
Proc. IEE, Vol.121, No.7, July 1974, pp.601-608
45. Chan, M.L., Dunlop, R.D., Schweppe, F.
Dynamic Equivalents for Average System Frequency Behaviour
Following Major Disturbances
IEEE Trans. PAS, Vol.91, No.4, July/Aug 1972, pp.1637-1642
46. Fraser, D.K.S., Davie, H., Macauley, M.W.S.
On-line Study of a Mixed Hydro-thermal Power System
21st Universities Power Engineering Conf., Imperial College,
London, 1986, pp.238-241
47. Fraser, D.K.S., Davie, H., Macauley, M.W.S.
A Real-time Power System Simulator for Hydro-turbine Plant
Tests
2nd Int. Conf. on Simulators, University of Warwick, 1986,
pp.113-118
48. Fraser, D.K.S., Davie, H., Macauley, M.W.S., Johnson, P.M.
System response studies incorporating real plant
Power Engineering Journal, Vol.1, No.2, March 1987,
pp.101-107

49. Ewart, D.N., deMello, F.P.
FACE - A Digital Dynamic Analysis Program
Power Industry Computer Applications Conf., 1967, pp.83-94
50. Verleye, S.
Using the iRMX 86 Operating System
Intel Application Note AP86, 1980
51. Humpage, W.D., Wong, K.P., Lee, Y.W.
Numerical integration algorithms in power system dynamic
analysis
Proc. IEE, Vol.121, No.6, June 1974, pp.467-473
52. Dickie, A.A., Ricketts, I.W.
A Comparison of Thirteen Numerical Integration Routines
UKSC Conf. on Computer Simulation, 1978, pp.307-311
53. Hall, G., Watt, J.M.
Modern Numerical Methods for Ordinary Differential Equations
Clarendon, Oxford, 1976
54. Gear, C.W.
Numerical Initial Value Problems in Ordinary Differential
Equations
Prentice-Hall, Englewood Cliffs, New Jersey, USA, 1971
55. Stroud, A.H.
Numerical Quadrature and Solution of Ordinary Differential
Equations
Springer-Verlag, New York, USA, 1974
56. Press, W.H., Flannery, B.P., Teukolsky, S.A., Vetterling,
W. T.
Numerical Recipes - The Art of Scientific Computing
Cambridge University Press, London, 1986
57. Taylor, C.W., Cresap, R.L.
Real-time Power Sytem Simulation for Automatic Generation
Control
IEEE Trans. PAS, Vol.95, No.1, Jan/Feb 1976, pp.375-384
58. Rafian, M., Irving, M.R., Sterling, M.J.H.
A Real-time Power System Simulator
2nd. Int Conf. on Simulators, University of Warwick, 1986,
pp.219-225
59. Hemmaplardh, K., Manke, J.W., Pauly, W.R., Lamont, J.W.
Considerations for a Long Term Dynamics Simulation Program
IEEE Trans. FWRS, Vol.1, No.1, February 1986, pp.129-136
60. Manke, J.W., Pauly, W.R., Hemmaplardh, K.
Long-term System Dynamics Simulation Methods
EPRI-EL-3894 RP-1469-1 Final Report, 1985
61. Arrillaga, J., Arnold, C.P.
Computer Modelling of Electrical Power Systems
Wiley, Chichester, 1983

62. Bui, T.D.
Solving stiff differential equations in the simulation of
physical systems
Simulation, Vol.37, No.2, August 1981, pp.37-46
63. Enwright, W.H., Hull, T.E., Linberg, B.
Comparing Numerical Methods for Stiff Systems of O.D.E.s
BIT, Vol.15, No.1, 1975, pp.10-48
64. Rodriguez, G., Kuhlmann, F., Castelazo, I.A., Fernandez del
Busto, R., Torres, M.A., Gonzalez, S.
On the Real-time Simulation of Large-scale Dynamic Systems
Using Multirate Integration Methods
Thirteenth Annual Pittsburgh Conf.on Modeling and Simulation,
Pittsburgh, PA, USA, 1982, pp.1603-1608
65. Raghavendra Rao, K., Jenkins, L., Parthasarathy, K.,
Balasubramanian, R.
Multi-time scale analysis applied to long time simulation of
power systems
Int. J. Electrical Power and Energy Systems, Vol.7, No.1,
January 1985, pp.7-12
66. Cate, E.G., Hemmaplardh, K., Manke, J.W., Gelopoulos, D.P.
Time Frame Notion and Time Response of the Models in
Transient, Mid-term and Long-term Stability Programs
IEEE Trans. PAS, Vol.103, No.1, January 1984, pp.143-151
67. Lewis, E.J.
A Revised Transient Stability Program, RASM05
CEGB Sstem Technical Branch Report PL-ST/27/72, 1973
68. Carlsen, K., Carroll, D.P., Gareis, G.E., Krause, P.C.,
Nozari, F., Ong, C.M., Triezenberg, D.M.
Design of a Power System Simulator
IEEE PES Winter Meeting, New York, USA, 1978
69. Ewart, D.N., Schulz, R.P.
FACE Multi-machine Power System Simulator Program
Power Industry Computer Applications Conf., 1969, pp.133-153
70. Ham, P.A.L.
Turbine and Governor Modelling
Symposium on Power System Dynamics, UMIST, 1973
71. Dy Liacco, T.E., Schoeffler, J.D., Quanda, J.J., Rosa, D.L.,
Jurkoshek, C.W., Anderson, M.D.
Considerations in Developing and Utilising Operator Training
Simulators
IEEE Trans. PAS, Vol.102, No.11, November 1983, pp.3672-3679
72. Shiota, H., Tamenaga, Y., Tsuji, T., Dan, K.
Development of Training Simulator for Power System Operators
IEEE Trans. PAS, Vol.102, No.10, October 1983, pp.3439-3445

73. Metcalfe, M.J.
Real Time Simulation of Severe Disturbances for System
Control Engineer Training
Int. Conf. on Power System Monitoring and Control, London,
1980, pp.165-169
74. Laubli, F., Le Febve, D., Palanikumar, P.
Dynamics of Output Primary Grid Frequency Controls in Steam
Power Units
Sulzer Research Number 1973, pp.40-49
75. Luini, J.F., Schulz, R.P, Turner, A.E.
A Digital Computer Program for Analyzing Long Term Dynamic
Response of Power Systems
Power Industry Computer Applications Conf., New Orleans,
1975, pp.136-143
76. Taylor, C.W., Lee, K.Y., Dave, D.P.
Automatic Generation Control Analysis with Governor Deadband
Effects
IEEE Trans. PAS, Vol.98, No.6, Nov/Dec 1979, pp.2030-2036
77. Smith, L.M., Fink, L.H., Schulz, R.P.
Use of Computer Model of Interconnected Power System to
Assess Generation Control Strategies
IEEE Trans. PAS, Vol.94, No.5, Sept/Oct 1975, pp.1835-1842
78. IEEE Working Group on Power Plant Response to Load Changes
MW Response of Fossil Fueled Steam Units
IEEE Trans. PAS, Vol.92, No.2, March/April 1973, pp.455-463
79. Bowdler, R.K.
Linear and Non-linear Turbine Governing Models: Stage 1
CEGB Report, London, 1970
80. Battlebury, D.R.
Comparison of SYRES01U program results with system test
results
CEGB System Technical Branch Report No.STB/16/71, 1971
81. Young, C.C.
Equipment and System Modeling for Large-scale Stability
Studies
Power Industry Computer Applications Conf., 1971, pp.163-172
82. Ott, G.E., Walker, L.N., Wong, D.T.Y.
Hybrid Simulation for Long Term Dynamics
IEEE Trans. PAS, Vol.96, No.3, May/June 1977, pp.907-913
83. Dunlop, R.D., Ewart, D.N., Schulz, R.P.
Use of Digital Computer Simulations to Assess Long-term Power
System Dynamic Response
IEEE Trans. PAS, Vol.94, No.3, May/June 1975, pp.850-857
84. Frowd, R.J., Giri, J.C., Podmore, R.
Transient Stability and Long-term Dynamics Unified
IEEE Trans. PAS, Vol.101, No.10, October 1982, pp.3841-3850

85. Concordia, C., deMello, F.P., Kirchmayer, L.K., Schulz, R.P.
Prime-mover response and system dynamic performance
IEEE Spectrum, Vol.3, No.10, October 1966, pp.106-111
86. Dwarakanath, M.H., Dembart, R., Erisman, A.M., Hemmaplardh,
K., Manke, J.W.
A Generalized Methodology for Modeling System Components in
Power System Dynamics Simulation
IEEE Trans PAS, Vol.101, No.1, January 1982, pp.136-146
87. CEGB
Handbook of Electricity Supply Statistics
CEGB, London, 1983
88. Levy, A.
Statistical Analysis of System Frequency Variations
7th Universities Power Engineering Conference, University of
Bradford, 1972, pp.43-48
89. Di Lascio, M.A., Moret, R., Poloujadoff, M.
Reduction of Program Size for Long-term Power System
Simulation with Pressurized Water Reactor
IEEE Trans. PAS, Vol.102, No.3, March 1983, pp.745-751
90. Jolley, W.P.
Steam Turbine Control
Inst. M.C. Symposium: Turbine and Compressor Control, 1972,
pp.27-39
91. Battlebury, D.R.
Total Power System Model
7th Universities Power Engineering Conf., University of
Bradford, 1972, pp.17-22
92. Ham, P.A.L.
Control Requirements for Large Turbines
Inst. M.C. Symposium: Turbine and Compressor Control, 1972,
pp.40-47
93. IEEE Working Group on Power Plant Response
Guidelines for Enhancing Power Plant Response to Partial Load
Rejections
IEEE Trans. PAS, Vol.102, No.6, June 1983, pp.1501-1504
94. Ham, P.A.L., Jenkins, K., Mikhail, S.E.
Performance and control capabilities of electro-hydraulic
governing systems for steam turbine-generators
Reyrolle Parsons Review, Vol.2, No.5, 1976
95. Gorzegno, W.P., Guido, P.V.
Load Rejection Capability for Large Steam Generators
IEEE Trans. PAS, Vol.102, No.3, March 1983, pp.548-557
96. Park, R.H.
Fast Turbine Valving
IEEE Trans. PAS, Vol.92, No.3, May/June 1973, pp.1065-1073

97. Rampton, R.
An Analog Study of Turbine and Boiler Control Systems
CEGB Generation Design Department, Control and
Instrumentation Design Report, 1970
98. Kwan, H.W., Anderson, J.H.
A mathematical model of a 200MW boiler
Int. J. Control, Vol.12, No.6, 1970, pp.977-998
99. Armor, A.F., Shor, S.W.W., DiDomenico, P.N., Bennett, W.E.,
Smith, L.P.
Dynamic Performance of Fossil-fueled Power Plants
IEEE Trans. PAS, Vol.101, No.10, October 1982, pp.4136-4146
100. Bollinger, K.E., Snowden, H.R.
The Experimental Determination of Coal Mill Models
IEEE Trans. PAS, Vol.102, No.6, June 1983, pp.1473-1477
101. Sutherland, P.
Dynamic Response of Feed Water System at Ferrybridge 'C'
Power Station
CEGB Report SSD/NE/N80, 1973
102. Davison, A.
Fundamentals of Boiler Modelling
Conf. on the Application of Simulation to Power Units and
Systems, Huddersfield Polytechnic, 1972
103. O'Kelly, P.A., Tendulkar, G.A.
Multi-microprocessor Based Simulators for Fossil-fired Power
Stations
2nd Int. Conf. on Simulators, University of Warwick, 1986,
pp.119-124
104. Dalpiaz, C.P.
Cost-effective Digital Enhancement of an Analog Steam
Operator Training Simulator
IEEE Trans. PAS, Vol.102, No.11, November 1983, pp.3516-3521
105. Anderson, P.M., Nanakorn, S.
An Analysis and Comparison of Certain Low-order Boiler Models
ISA Trans., Vol.14, No.1, 1975, pp.17-23
106. Astrom, K.J., Eklund, K.
A simplified non-linear model of a drum boiler-turbine unit
Int. J. Control, Vol.16, No.1, 1972, pp.145-169
107. Thompson, E.C.
A Digital Simulation of a Boiler and Turbine in Conjunction
with a Model Power System
Ph.D. Thesis, University of Glasgow, 1976
108. Aitken, K.H.
Development of a Simulation Language in Conjunction with
Hydro-turbine Modelling
Ph.D. Thesis, University of Glasgow, 1982

109. Waddington, J.
Load-controller design for a regulating coal-fired unit
Proc. IEE, Vol.126, No.5, May 1979, pp.439-445
110. Jolley, W.P.
A General Purpose Turbine Model
Conf. on the Application of Simulation to Power Units and
Systems, Huddersfield Polytechnic, 1972
111. Hughes, F.M.
Improvement of turbogenerator transient performance by
control means
Proc. IEE, Vol.120, No.2, February 1973, pp.233-240
112. Maples, G.C.
A Non-linear Model of a Drum-type Boiler-turbine Unit
CERL Laboratory Note No. RD/L/N 16/70, 1970
113. Rogers, G.F.C., Mayhew, Y.R.
Engineering Thermodynamics, Work and Heat Transfer
Longman, London, 1980
114. IEEE Committee Report
Dynamic Models for Steam and Hydro Turbines in Power System
Stability Studies
IEEE Trans. PAS, Vol.92, No.6, Nov/Dec 1973, pp.1904-1915
115. Anderson, P.M.
Discussion on Reference I1
116. Metcalfe, M.J., Waddington, J., Wilson, R.G.
Operational experience with fossil-fired generating plant
under automatic load control
Proc. IEE, Vol. 126, No.4, April 1979, pp.327-332
117. Weissberger, J.
Discussion on Reference I1
118. Bauman, H.A., Hahn, G.R., Metcalf, C.N.
The Effect of Frequency Reduction on Plant Capacity and on
System Regulation
AIEE Trans. PAS, Vol.73, February 1955, pp.1632-1637
119. Metcalfe, M.J.
The Preliminary Design of a Pressure-governing Control System
for Regulating Coal-fired Plant
CERL Report RD L R 1884, 1974
120. Delfino, B., Denegri, G.B., Massucco, S., Pinceti, P.,
Schiappacasse, A.
Dynamic Response of Power Systems in the Mid-term Period
20th Universities Power Engineering Conf., Huddersfield
Polytechnic 1985, pp.412-415
121. Kent, M.H., Schmus, W.R., McCrackin, F.A., Wheeler, L.M.
Dynamic Modeling of Loads in Stability Studies
IEEE Trans. PAS, Vol.88, No.5, May 1969, pp.756-763

122. Ashmole, P.H., Farmer, E.D., Myerscough, C.J.
The Dynamic Response of the Load to Changes in System Frequency
7th Universities Power Engineering Conf., University of Bradford, 1972, pp.36-42
123. Berg, G.J.
Power system load representation
Proc. IEE, Vol.120, No.3, March 1973, pp.344-348
124. Berg, G.J.
System and load behaviour following loss of generation
Proc. IEE, Vol.119, No.10, October 1972, pp.1483-1486
125. Ashmole, P.H., Myerscough, C.J., Symons, O.C.
Measurements and Simulations of Power System Inertia
5th Universities Power Engineering Conf., London 1975
126. Symons, O.C., Bowdler, R.K.
System Frequency Response to Loading Disturbances
Simulation of Cellerhead Test No.6 using RASMO4
CEGB System Technical Branch Report No. PL-ST/22/71, 1971
127. Day, A.L., Graham, H.L., Walker, L.N., Leavene, R.W.
Parallel Digital Simulation of Power Systems
Summer Computer Simulation Conf., Los Angeles, CA, USA, 1978,
pp.372-376
128. Enslow, P.H.
Multiprocessor Organisation - A Survey
Computing Surveys, Vol.9, No.1, March 1977, pp.103-129
129. Durham, I., Dugan, R.C., Jones, A.K., Talukdar, S.N.
Power System Simulation on a Multiprocessor
IEEE PES Summer Meeting, Vancouver, Canada, 1979
130. Grasso, P.A., Forward, K.E., Dillon, T.S.
Operating system for a dedicated common memory multiprocessor system
IEE Proc., Vol.129, Pt.E, No.5, September 1982, pp.200-206
131. Bertora, F., De Cena, C., Di Manzo, M., Micheli, C.
Multiprocessor Architectures for Control Applications
Microprocessing and Microprogramming, Vol.7, No.3, March 1981, pp.169-176
132. Happ, H.H.
Parallel Processing in Power Systems
Seventh Power System Computation Conf., Lusanne, Switzerland, July 1981, pp.9-16
133. Taoka, H., Abe, S., Takeda, S.
Fast Transient Stability Solution Using an Array Processor
IEEE Trans. PAS, Vol.102, No.12, December 1983, pp.3835-3841

134. Johnson, R.B.I., Short, M.J.
A Multiple Microprocessor Simulator for Dynamical Power Systems
2nd Int. Conf. on Simulators, University of Warwick, 1986,
pp.44-48
135. Talukdar, S.N., Carey, M., Pyo, S.S.
Multiprocessors for Power Systems - Some Programming and
Research Issues
IFAC Symposium on Theory and Application of Digital Control,
New Delhi, India, 1982, pp.133-138
136. Schmidt, K., Leonhard, W.
Simulation of Electric Power Systems by Parallel Computation
ISA Transactions, Vol.21, No.4, 1982, pp.15-22
137. Garibay, D.T., Sinencio, I.C.
Executive Control of a Real Time Power Plant Simulator in a
Multiprocessor Environment
14th Annual Pittsburgh Conf. on Modeling and Simulation,
Pittsburgh, PA, USA, 1983, pp.201-207
138. Klein, D., Parrish, E.A.
A Reconfigurable Multiprocessor System for Real-time
Simulation
Southeastcon '80, Nashville, TN, USA, 1980, pp.331-334
139. Gilbert, E.O., Howe, R.M.
Design considerations in a multiprocessor computer for
continuous system simulation
AFIPS Conf. Procs. 1978 National Computer Conf., Anaheim, Ca,
USA, 1978, pp.385-393
140. Feyock, S., Collins, W.R.
Ada and Multi-microprocessor Real-time Simulation
16th Annual Simulation Symposium, Tampa, FL, USA, 1983,
pp.211-228
141. Grasso, P.A., Forward, K.E., Dillon, T.S.
Theoretical and Experimental Investigation of Multi-
Microprocessor Systems
I.E. Aust. Conf. on Microprocessor Systems, Melbourne,
Australia, 1979, pp.63-67
142. Grasso, P.A., Forward, K.E., Dillon, T.S.
Hardware Design of a Parallel Processor for Control
Applications,
I.E. Aust. Conf. on Digital System Design, Sydney, Australia,
1980, pp.38-41
143. Arrillaga, J., Graham, J.C., Hisha, H.
Microprocessor-controlled HVDC simulator
IEE Proc., Vol.131, Pt.C., No.5, September 1984, pp.197-203
144. Pimentel, J.R.
Real-time simulation using multiple microcomputers
Simulation, Vol.40, No.3, March 1983, pp.93-104

145. Pimentel, J.R., Loeffler, M.T.
A Multiple Microcomputer System for Real-Time Engine Simulation
IEEE Workshop on Automotive Applications of Microprocessors,
Dearborn, MI, USA, 1982, pp.52-56
146. Johnson, J., Kinnie, C., Maerz, M.
Triple-bus architecture on a single-board microcomputer
Electronic Design 15, July 19, 1978, Intel AR-65
147. Kinnie, C., Maerz, M.
Dual-port RAM Hikes Throughput in Input-output Controller Board
Electronics, August 17, 1978, Intel AR-69
148. Barthmaier, J.P.
Multiprocessing System Mixes 8- and 16-bit Microcomputers
Computer Design, February 1980, Intel AR-133
149. Nadir, J., McCormick, B.
Bus Arbiter Streamlines Multiprocessor Design
Computer Design, June 1980, Intel AR
150. Alexy, G., Katz, B.J.
Multiprocessing increases power of inexpensive uP-based designs
EDN, May 20, 1980, Intel AR
151. Adams, G., Rolander, T.
Design Motivations for Multiple Processor Microcomputer Systems
Computer Design, March 1978, Intel AR-55
152. Dijkstra, E.W.
Solution of a Problem in Concurrent Programming Control
Communications of the ACM, Vol.8, No.9, September 1965, p.569
153. Shastry, S.K.
A Control Structure for Parallel Processing
Sagamore Computer Conf. on Parallel Processing, 1974,
pp.134-147
154. Lister, A.M.
Fundamentals of Operating Systems
Macmillan, London, 1984
155. Anderson, P.
Multiprocessing Extensions for the RMX/80 Real-Time Executive
Intel Application Note AP-88, 1980
156. Ma, P.R., Lee, E.Y.S., Tsuchiya, M.
A Task Allocation Model for Distributed Computing Systems
IEEE Trans. C, Vol.31, No.1, January 1982, pp.41-47
157. Gylys, V.B., Edwards, J.A.
Optimal Partitioning of Workload for Distributed Systems
COMPCON '76, 1976, pp.353-357

158. Buckles, B.P., Hardin, D.M.
Partitioning and Allocation of Logical Resources in a
Distributed Computing Environment
General Research Corporation Report, Huntsvill, Alabama, 1979
159. Stone, H.S.
Multiprocessor Scheduling with the Aid of Network Flow
Algorithms
IEEE Trans. SE, Vol.3, No.1, January 1977, pp.85-93
160. Talukdar, S.N., Pyo, S.S., Giras, T.C.
Asynchronous Procedures for Parallel Processing
IEEE Trans. PAS, Vol.102, No.11, November 1983, pp.3652-3659
161. Lin, E.K., Jen, C.L.
Contention Problem of a Multiprocessor Simulator
16th Annual Simulation Symposium, Tampa, FL, USA, 1983,
pp.229-238
162. Cho, C.K., Lin, E.K., Jen, C.L.
On Performance Evaluation of Multiprocessor Systems for Real-
time Simulation
17th Annual Simulation Symposium, Tampa, FL, USA, 1984,
pp.209-225
163. Grasso, P.A., Dillon, T.S., Forward, K.E.
Memory interference in multimicroprocessor systems with a
time-shared bus
IEE Proc., Vol. 131, Pt.E, No.2, March 1984, pp.61-68
164. Sulley, J.L., Moffatt, A.M.
Isolated diesel system simulation - a design/operation
facility
17th Universities Power Engineering Conf., UMIST, 1982
165. Tsitsovits, A.J., Freris, L.L.
Dynamics of an isolated system supplied from diesel and wind
IEE Proc., Vol.130, Pt.A, No.9, December 1983, pp.587-595
166. Garg, R.D., Agarwal, K.K., Desikachari, R.
Computer Simulation of a Diesel Engine
J. Inst. Eng. (India), Mech. Eng. Div., November 1974, Vol.55,
ME-2, pp.67-75
167. Douglas, J.D., Beams, R.
The maritime simulation centre at Warsash
2nd Int. Conf. on Simulators, University of Warwick, 1986,
pp.138-143
168. Whittingdon, H.W., Jordan, J.R., Paterson, N., Johnson, P.M.
Performance monitoring of diesel electricity generation
IEE Proc., Vol.133, Pt.B, No.3, May 1986, pp.149-154
169. Billings, S.A., Fadzil, M.B., Sulley, J.L., Johnson, P.M.
Identification of a Nonlinear Difference Equation Model of an
Industrial Diesel Generator
To be published

170. Woodward, J.L.
Impact of Large Chip Mill Loads on Diesel-Powered Systems
IFAC Symposium, Melbourne, Australia, 1977, pp.424-428
171. Woodward Governor Company
UG32 & UG40 Governors
Woodward Governor Company, Bulletin 03014H, Slough, England
172. Goodwin, G.C., Ng, T.S.
Identification of Systems Operating in Closed Loop with
Application to a 200kW Diesel Generating Plant
IFAC Symposium, Melbourne, Australia, 1977, pp.480-484
173. Magnusson, R.
A Wind-Diesel Energy System for Grimsey, Iceland
Wind Engineering, Vol.6, No.4, October 1982, pp.185-192
174. Tsitsovits, A.J., Freris, L.L.
A statistical method for optimising wind power contribution
in a diesel supplied network
IEE Proc., Vol.132, Pt.C, No.6, November 1985, pp.269-276
175. Losie, B.J., Steeves, J.G.
Case Study of a Hybrid Wind/Photovoltaic/Diesel Power System
at a Radio Repeater Site
INTELEC '84, Sixth Int. Telecommunications Energy Conf., New
Orleans, LA, USA, 1984, pp.159-165
176. Stiller, P.H., Scott, G.W., Shaltens, R.K.
Measured Effect of Wind Generation on the Fuel Consumption
of an Isolated Diesel Power System
IEEE Tans. PAS, Vol.102, No.6, June 1983, pp.1788-1792
177. Tipney-Hicks, A.D., Attwood, R.
Hybrid Schemes for Remote Power Systems
INTELEC '84, Sixth Int. Telecommunications Energy Conf., New
Orleans, LA, USA, 1984, pp.166-169
178. Sulley, J.L., Moffatt, A.M., Barlow, J.M.
Technical aspects of integrating wind and wave generation
sources into small island systems
Fourth Int. Conf. on Energy Options: The Role of Alternatives
in the World Energy Scene, London, 1984, pp.207-210
179. Leung, K.S., Stronach, A.F.
Integration of wind turbine generators into small diesel-
based power systems
Fourth Int. Conf. on Energy Options: The Role of Alternatives
in the World Energy Scene, London, 1984, pp.151-154
180. Bossanyi, E.
Use of a Grid Simulation Model for Longer-Term Analysis of
Wind Energy Integration
Wind Engineering, Vol.7, No.4, 1983, pp.233-246
181. Bossanyi, E.A., Whittle, G.E., Lipman, N.H., Musgrove, P.J.
Wind Turbine Response and System Integration
Third Int. Conf. on Future Energy Concepts, London, 1981,
pp.296-302

182. Desrochers, G.
Simulation of a Mixed Wind Turbine Diesel Power System
Operation
10th Annual Eng. Conf. on Reliability, Availability and
Maintainability for the Electric Power Industry, 1983,
pp.270-275
183. Traca de Almeida, A., Martins, A. Jesus, H., Climaco, J.
Source Reliability in a Combined Wind-Solar-Hydro System
IEEE Trans. PAS, Vol.102, No.6, June 1983, pp.1515-1520
184. Curtice, D.H., Reddoch, T.W.
An Assessment of Load Frequency Control Impacts Caused by
Small Wind Turbines
IEEE Trans. PAS, Vol.102, No.1, January 1983, pp.162-170
185. Hwang, H.H., Guo, T-H.
Digital Simulation of Dynamics of Wind Turbine Generators
21 Midwest Symposium on Circuits and Systems, Ames, IA,
USA, 1978, pp.634-638
186. Hwang, H.H., Gilbert, L.J.
Synchronisation of Wind Turbine Generators Against an
Infinite bus Under Gusting Wind Conditions
IEEE Trans. PAS, Vol.97, No.2, March/April 1978, pp.536-544
187. Hwang, H.H., Zhuang, X.F.
Digital Simulation of Second Generation Wind Turbine
Generators Connected to Power Systems
Proc. 18th Intersociety Energy Conversion Engineering Conf.,
Orlando, FL, USA, 1983, Vol.3, pp.1367-1372
188. Anderson, P.M., Bose, A.
Stability Simulation of Wind Turbine Systems
IEEE Trans. PAS, Vol.102, No.12, December 1983, pp.3791-3795
189. Law, H., Doubt, H.A., Cooper, B.J.
Power control systems for the Orkney wind-turbine generators
GEC Engineering, No.2, 1984, pp.19-28
190. Murdoch, A. Winkelman, J.R., Javid, S.H., Barton, R.S.
Control Design and Performance Analysis of a 6MW Wind
Turbine-Generator
IEEE Trans. PAS, Vol.102, No.5, May 1983, pp.1340-1347
191. Power, H.M.
A Simulation Model for Wind Turbines
Applied Energy, Vol.6, No.5, September 1980, pp.395-399
192. Swansborough, R.H., Ballard, L.J.
Rotational Dynamics of Wind Turbine Generators
Third Int. Conf. on Future Energy Concepts, London, 1981,
pp.357-360
193. Hinrichsen, E.N.
Controls for Variable Pitch Wind Turbine Generators
IEEE Trans. PAS, Vol.103, No.4, April 1984, pp.886-892

194. Cooper, B.J.
Control System for the 20m 250kW W.T.G. for Orkney
Colloquium on Energy Generating Systems for Wind Power,
1982, pp.2/1-6
195. Raina, G., Malik, O.P.
Variable Speed Wind Energy Conversion Using Synchronous
Machine
IEEE Trans. AES, Vol.21, No.1, January 1985, pp.100-105
196. Clink, J.
Optimal Computer Control of a Group of Interacting Hydro
Electric Power Stations
Ph.D. Thesis, University of Glasgow, 1986

APPENDIX 1

A NON-LINEAR HYDRO-TURBINE AND PIPELINE MODEL

$$\frac{dQ}{dt} = (1 - H_T) / T_W \quad \text{A1.1}$$

$$H_T = Q^2 / C^2 \quad \text{A1.2}$$

$$P = Q H_T \quad \text{A1.3}$$

Q - volumetric flow

H_T - pressure head at the turbine

T_W - full load water inertia time constant

C - valve position

P - power output

Reference:

Wylie, E.B., Streeter, V.L.
Fluid Transients
McGraw-Hill, London, 1978

Sloy values:

$$T_W = 1.1s$$

Rate of change of C limited to -0.25pus^{-1} to 0.05pus^{-1}

Sloy temporary droop governor:

$$T_y = 0.3s, b_t = 0.25, T_d = 16s, b_p = 0.03$$

Temporary droop feedback limited to $\pm 0.015\text{pu}$

Sloy double derivative governor:

$$T_1 = 0.3s, T_2 = 0.3s, K_1 = 3.0, K_2 = 2.3, b_p = 0.03, T_y = 1s$$

APPENDIX 2

EQUATIONS AND DATA FOR THE OIL-FIRED PLANT MODEL

$$\frac{dp}{dt} = -a_1 (w_S p^{0.625} - a_4) + a_2 u_1 - a_3 u_3 \quad A2.1$$

$$\frac{dx_1}{dt} = p_{ref} - p \quad A2.2$$

$$\frac{du_1}{dt} = (K_1 (p_{ref} - p) + K_1 K_2 x_1 - u_1) / T_2 \quad A2.3$$

$$\frac{du_3}{dt} = (u_3 - w_s) / T_1 \quad A2.4$$

$$\frac{dx_2}{dt} = d_{ref} - d \quad A2.5$$

$$\frac{du_3}{dt} = (K_3 (d_{ref} - d) + K_3 K_4 x_2 - u_3) / T_3 \quad A2.6$$

$$a_1=0.00545, a_2=0.00506, a_3=0.00162, p_{ref}=1, d_{ref}=1$$

$$a_4=0.370, T_1=10.0s, T_2=10.0s, T_3=24.0s$$

$$K_1=5.0, K_2=0.002, K_3=0.1, K_4=0.001$$

$$w_S = (17.39 (p - p_V))^{0.5} \quad A2.7$$

$$P_{HP} = v_G P_V \quad A2.8$$

$$w_{HP} = 1.113 (P_{HP}^2 - P_R^2)^{0.5} \quad A2.9$$

$$w_{LP} = 3.521 P_R \quad A2.10$$

$$\frac{dv_G}{dt} = (G_1 (f_{ref} - f_s) - v_G) / T_G \quad A2.11$$

$$\frac{dp_V}{dt} = (w_S - w_{HP}) / T_S \quad A2.12$$

$$\frac{dp_R}{dt} = (w_{HP} - w_{LP}) / T_R \quad A2.13$$

$$P_{OHP} = 1.087 w_{HP} (1 - (P_R/P_{HP})^{0.23}) \quad A2.14$$

$$P_{OLP} = 2.173 w_{LP} (1 - (P_A/P_R)^{0.115}) \quad A2.15$$

$$P_{oo} = P_{OHP} + P_{OLP} \quad A2.16$$

$$G_1=25.0, T_G=0.1$$

$$T_S=1.11s, T_R=7.41s, P_A=0.0077$$

p - boiler pressure

d - boiler drum level

u₁ - fuel feed flow

u₃ - feed water flow

x₁ - intermediate state variable

x₂ - intermediate state variables

w_S - superheater steam flow

P_V - pressure at turbine stop valve
 P_{HP} - high pressure stage inlet pressure
 P_R - reheater pressure
 P_A - condenser vacuum pressure
 w_{HP} - HP turbine steam flow
 w_{LP} - IP/LP turbine steam flow
 P_{OHP} - HP turbine power
 P_{OLP} - IP/LP turbine power
 P_{oo} - total turbine power
 v_G - governor valve position
 f_s - simulated system frequency

All variables except steam pressures are normalised with respect to full load values. Pressures are normalised with respect to normal boiler pressure.

APPENDIX 3

EQUATIONS AND DATA FOR THE COAL-FIRED PLANT MODEL

$$P_e = P_s - P_b \quad A3.1$$

$$\frac{dy}{dt} = k_1 p_e \quad A3.2$$

$$M = y + k_2 p_e \quad A3.3$$

M is limited to 0.2 to 1.2pu

$$E_m = M e^{-sT_d} \quad A3.4$$

E_m is limited to 0.001 to 1.05pu

$$\frac{dF_i}{dt} = (E_m - F_i) / T_c \quad A3.5$$

$$\frac{dF_d}{dt} = (F_i - Q_i) / T_m \quad A3.6$$

F_d is limited to 0.001 to 1.05pu

$$Q_i = M F_d \quad A3.7$$

$$\frac{dp_b}{dt} = (Q_i - W_1) / T_b \quad A3.8$$

$$P_s=1, k_1=0.015, k_2=5.0$$

$$T_d=60s, T_c=45s, T_m=2s, T_b=240s$$

$$\frac{da_x}{dt} = (f_{ref} - f) / b_p - a_x) / T_g \quad A3.9$$

a_x is limited to 0.001 to 1.0pu

$$\frac{da_2}{dt} = (a_x - a_2) / T_{gv} \quad A3.10$$

$$b_p=0.04, T_g=0.1s, T_{gv}(\text{opening})=0.1s, T_{gv}(\text{closing})=0.7s$$

$$P_1 = a_2 P_b \quad A3.11$$

$$W_1 = P_1 \frac{\left[1 - R \left(\frac{P_2}{P_1} \right)^2 \right]^{\frac{1}{2}}}{1 - R^2} \quad A3.12$$

$$P_{m1} = K_4 W_1 \frac{1 - R \left(\frac{P_2}{P_1} \right)^{0.231}}{1 - R^{0.231}} \quad A3.13$$

$$\frac{dp_2}{dt} = (W_1 - W_2) / T_r \quad A3.14$$

$$W_2 = P_2 \quad A3.15$$

$$P_{m2} = (1 - K_4) W_2 \quad A3.16$$

$$P_{oc} = P_{m1} + P_{m2} \quad A3.17$$

$R=0.35$, $K_u=0.2$, $T_r=10.0s$

P_b - boiler drum pressure

p_e - boiler pressure error

y - intermediate variable

M - master firing signal

E_m - fuel feed rate to mill

F_i - fuel pick up

F_d - fuel density

Q_1 - heat input to boiler

W_1 - HP turbine steam flow

W_2 - LP turbine steam flow

a_x - governor output

a_2 - governor valve position

P_1 - HP turbine inlet pressure

p_2 - IP/LP turbine inlet (reheater) pressure

P_{m1} - HP turbine power

P_{m2} - IP/LP turbine power

P_{oc} - total turbine power

All variables are normalised with respect to full load values.

APPENDIX 4

EQUATIONS AND DATA FOR THE WIND TURBINE MODEL

$$\frac{d\omega}{dt}^b = (T_{ow} - T_{og}) / J_b \quad A4.1$$

$$\omega_m = \omega_b - 157.08 (f_s - 1) \quad A4.2$$

$$\frac{d\omega}{dt}^{m1} = (\omega_m - \omega_{m1}) / T_c \quad A4.3$$

$$T_{og} = \frac{J'_m}{T_c} \omega_m + (K_c - \frac{J'_m}{T_c}) \omega_{m1} \quad A4.4$$

$$P_{ow} = f_s (O_{wt} + \frac{T_{og}}{T_{ofl}}) \quad A4.5$$

$$T_e = O_{wt} T_{ofl} + T_{og} \quad A4.6$$

$$J'_m = J_m - K_j \quad A4.7$$

$$\omega_{kc} = \omega_m + (T_{ofl} - T_e) / K_{c1}$$

$$K_{cd} = K_{c0} \quad \text{for } \omega_5 < \omega_{kc} < \omega_6$$

$$K_{cd} = K_{c0} + (\omega_5 - \omega_{kc}) K_{cgrad} \quad \text{for } \omega_1 < \omega_{kc} < \omega_5$$

$$K_{cd} = K_{c1} \quad \text{for } \omega_{kc} < \omega_1$$

$$K_{cd} = K_{c0} + (\omega_{kc} - \omega_6) K_{cgrad} \quad \text{for } \omega_2 > \omega_{kc} > \omega_6$$

$$K_{cd} = K_{c1} \quad \text{for } \omega_{kc} > \omega_2 \quad A4.8$$

$$K_{cgrad} = \frac{K_{c1} + K_{c0}}{\omega_5 - \omega_1} = \frac{K_{c1} + K_{c0}}{\omega_2 - \omega_6} \quad A4.9$$

$$\frac{dK}{dt}^c = (K_{cd} - K_c) / T_{kc} \quad A4.10$$

$$K_{c1} = 2400 \text{ Nmsrad}^{-1}, K_{c0} = 150 \text{ Nmsrad}^{-1}, J_b = 3144 \text{ kgm}^2, J_m = 338 \text{ kgm}^2$$

$$K_j = 313 \text{ kgm}^2, H = 0.802 \text{ s}, T_{kc} = 1 \text{ s}, T_c = 0.1 \text{ s}, T_{ofl} = 19098.6 \text{ Nm}$$

$$\omega_1 = -0.05, \omega_2 = 0.05, \omega_5 = -0.04, \omega_6 = 0.04$$

$$\omega_{bb} = (1 + \frac{\omega_b}{157.08}) 1.8378 \quad A4.11$$

$$\gamma = \frac{V_w}{\omega_{bb}} \quad A4.12$$

$$C_p = 0.5 (G - 0.022B^2 - 5.6) e^{-0.17\gamma} \quad A4.13$$

$$T'_{ow} = 0.0001372 V_w^2 C_p \gamma \quad A4.14$$

$$T_{ow} = T_{ofl} (T'_{ow} - O_{wt}) \quad A4.15$$

$$P_{err} = (f_s - f_{ref}) / b_p + P_{ow} - P_{ref} \quad A4.16$$

$$\frac{dx_1}{dt} = P_{err} \quad A4.17$$

$$B_d = K_p P_{err} + K_i x_1 \quad A4.18$$

$$\frac{dB}{dt} = (B_d - B) / T_p \quad A4.19$$

$$K_p=2.0, K_i=0.2, T_p=59ms$$

Rate limits of ± 10 degrees/sec are imposed on B

B is limited to 0 to 90 degrees.

ω_b - turbine shaft speed

ω_m - reaction machine speed

T_{ow} - turbine torque

T_{og} - generator torque

P_{ow} - per unit generator power

f_s - simulated system frequency

ω_{m1} - intermediate variable

K_{cd} - desired value of torque control gain

K_c - torque control gain

ω_{bb} - absolute turbine shaft speed

T'_{ow} - per unit turbine torque

O_{wt} - per unit operating point

V_w - wind speed

χ - tip speed ratio

C_p - power coefficient

T_e - absolute generator torque

P_{ref} - power output set-point

b_p - pitch controller droop

f_{ref} - pitch controller frequency reference

x_1 - intermediate variable

B_d - desired pitch angle

B - tip-blade pitch angle



A POWER SYSTEM SIMULATOR FOR
ON-LINE TESTS OF GENERATING PLANT

David K.S. Fraser

PROGRAM LISTINGS

FROM THE UNIVERSITY, GLASGOW.

NOT TO BE ACCESSED WITHOUT PERMISSION
OF DR D K S FRASER OR DR H DAVIE
FOR A PERIOD OF 3 YEARS

Master processor code for hydro-thermal system tests
(electronic injection)

```

C     MIXED SYSTEM SIMULATOR USING COAL FIRED PLANT MODEL
C     REQUIRES BBC TERMINAL
C     USES EULER
C     INCORPORATES AVERAGING OF TURBINE POWER MEASUREMENT
C     VERSION FOR ELECTRONIC GOVERNOR
C     MULTIPROCESSOR VERSION WITH GRID FREQUENCY ADJUSTMENT
C     CODE FOR PROCESSOR 1

EXTERNAL NUMIN,NUMOUT,BYTIN,BYTOU,SCANIN,ANINIT,ANIN,ANOUT
EXTERNAL CYCLE,SAMPLE,GETSEM,GIVSEM
REAL*4 DELAY,LIMIT
REAL*4 H
REAL*4 READMW,TIMSCL,PWSCL,FESSCL,POSCL,POH5V,FGSCL
REAL*4 PD,PL,PON,POC,POH,FG,GFRLML,GFRLMH
REAL*4 POC2,TD2,TR2,BPC2
REAL*4 QN,QC1,QC2,QH,TA,PDSTEP,PDRATE,PDL,PDH,PDTRIG,TDEM
REAL*4 FREQ,FES,FESCOR,GFREQ,GFREQI
REAL*4 DFREQ,DPD
REAL*4 TG,PREF,K1,K2,TC,TM,R,KH,KL,TB,FREF,TD,TR,BPC
REAL*4 POHMCR,POC1MCR,POC2MCR,PONMCR,TOTMCR,W1ML,PM1ML
REAL*4 AX,Y2,FI,FD,AXV,P2,PB
REAL*4 DAX,DY2,DF1,DFD,DAXV,DP2,DPB
REAL*4 PERR,MX,EM,QI,TGV,P1,W1,W2,PM1,PM2
INTEGER*1 INTCT1,INTCT2,PORTA,PORTB,PORTC,PRTCTL
INTEGER*1 TIMER0,TIMER1,TIMCTL,T1LOB,T1HOB
INTEGER*1 CTLIN,CTLOUT
INTEGER*1 FSAMPL,ICNSMP,NSAMPL,NCOUNT,KSIM,ISPCTL,IPDCTL,IPDSW
INTEGER*2 I,CNSAMP(50),TOLAST,IPD,IPOC,IPOH,IFES,IFESCR,IGFREQ
INTEGER*4 CNTSUM,IPOHSM
LOGICAL*1 LGFROK,LGFRCR,LGFRLM,LRISEG,LRISE,LFALLG,LFALL,LAGDEM
LOGICAL*1 SYNC,P2RDY,P2INIT,P2EX,LSTART
LOGICAL*1 LFLAG3,LFLAG4,LFLAG5,LFLAG6
COMMON/SAMPL1/NSAMPL,NCOUNT,KSIM
COMMON/SAMPL2/IPOHSM
COMMON/SAMPL3/FSAMPL,ICNSMP,TOLAST,LGFROK,CNSAMP
COMMON/SYSTEM/H
COMMON/PRL1/ISPCTL,IPDSW,LGFRLM,LFLAG3,LFLAG4,LFLAG5,LFLAG6
COMMON/PRL2/SYNC,P2RDY,P2INIT,P2EX
COMMON/PRL3/POC2,TD2,TR2,BPC2,FREQ
COMMON/PRL4/LSTART
PARAMETER(INTCT1=#0C0H,INTCT2=#0C2H)
PARAMETER(PORTA=#0C8H,PORTB=#0CAH,PORTC=#0CCH,PRTCTL=#0CEH)
PARAMETER(TIMER0=#0D0H,TIMER1=#0D2H,TIMCTL=#0D6H)

C     DISABLE PROCESSOR INTERRUPTS
C     CALL DSABLE

C     INITIALISE MULTIPROCESSOR CONTROL FLAGS
C     P2EX=.FALSE.
C     P2RDY=.FALSE.
C     P2INIT=.FALSE.

C     RESET SPARE ERROR INDICATIONS
C     LFLAG3=.FALSE.
C     LFLAG4=.FALSE.
C     LFLAG5=.FALSE.
C     LFLAG6=.FALSE.

C     SYNCHRONISE PROCESSORS
3     CONTINUE

```

```
SYNC=.FALSE.
SYNC=.TRUE.
IF(.NOT.P2RDY) GOTO 3

C 30 SAMPLES PER 0.05 SECOND INTEGRATION INTERVAL
H=0.05
T1LOB=0
T1HOB=1

C SET UP DAC AND INITIALISE CHANNELS TO 0 VOLTS
CALL ANINIT(7)
DO 5 I=0,7
CALL ANOUT(I,2048)
5 CONTINUE

C SET UP FREQUENCY MEASUREMENT
LGFROK=.FALSE.
FSAMPL=25
TOLAST=0
ICNSMP=FSAMPL

C SET UP FREQUENCY FILTER
DO 10 I=1,FSAMPL
CNSAMP(I)=1.0
10 CONTINUE

C SET UP FREQUENCY SCALING CONSTANTS
TIMSCL=FLOAT(FSAMPL)*1228800.0/50.0
FGSCL=4096.0/(1.005-0.995)

C SET UP INTERRUPT CONTROLLER
CALL OUTPUT(INTCT1,#13H)
CALL OUTPUT(INTCT2,#20H)
CALL OUTPUT(INTCT2,#0DH)

C SET UP TIMER 0
CALL OUTPUT(TIMCTL,#34H)
CALL OUTPUT(TIMER0,0)
CALL OUTPUT(TIMER0,0)

C SET UP VECTOR AND UN-MASK FOR MAINS CROSS-OVER INTERRUPTS
CALL SETINT(#20H,CYCLE)
CALL OUTPUT(INTCT2,#0FEH)

C RE-ENABLE PROCESSOR INTERRUPTS
CALL ENABLE

C SET UP SBC 86/14 PARALLEL PORTS
CALL OUTPUT(PRTCTL,#0A6H)
CALL OUTPUT(PRTCTL,#0DH)
CALL OUTPUT(PRTCTL,#05H)

C OUTPUT PULSE TO SET UP INPUT PORT
CALL OUTPUT(PRTCTL,#03H)
CALL OUTPUT(PRTCTL,#02H)

C ESTABLISH COMMUNICATION WITH BBC
40 CALL BYTIN(CTLIN)
IF(CTLIN.NE.#10H) GOTO 40
CTLOUT=#11H
```

```

CALL BYTOUT(CTLOUT)

70  CONTINUE

C    SET UP GRID FREQUENCY CORRECTION LIMITS
    LGFRLM=.FALSE.
    GFRLML=0.996
    GFRLMH=1.004

C    SET UP AVERAGING OF TURBINE POWER OUTPUT
    NSAMPL=30
    NCOUNT=0
    KSIM=0

C    SEND SWITCH STATUS
    IPDCTL=IPDSW
    CALL BYTOUT(IPDCTL)

C    LOAD PROPORTION OF NUCLEAR PLANT
    CALL NUMIN(QN)

C    LOAD PROPORTIONS OF COAL PLANT
    CALL NUMIN(QC1)
    CALL NUMIN(QC2)

C    LOAD PROPORTION OF HYDRO PLANT
    CALL NUMIN(QH)

C    LOAD COAL FIRED PLANT OPERATING POINTS
    CALL NUMIN(POC)
    CALL NUMIN(POC2)

C    LOAD FUEL FEED DELAYS
    CALL NUMIN(TD)
    CALL NUMIN(TD2)

C    LOAD REHEATER TIME CONSTANTS
    CALL NUMIN(TR)
    CALL NUMIN(TR2)

C    LOAD COAL FIRED PLANT DROOPS
    CALL NUMIN(BPC)
    CALL NUMIN(BPC2)

C    LOAD ALTERNATOR TIME CONSTANT
    CALL NUMIN(TA)

C    LOAD DEMAND STEP SIZE
    CALL NUMIN(PDSTEP)

C    ESTABLISH TYPE OF DEMAND TRANSIENT
    CALL BYTIN(CTLIN)
    IF(CTLIN.EQ.#4CH) THEN
        LAGDEM=.TRUE.
    ELSE
        LAGDEM=.FALSE.
    ENDIF

C    LOAD DEMAND TRANSIENT PARAMETERS
    IF(LAGDEM) CALL NUMIN(TDEM)

```

```

C      DECIDE ON USE OF GRID FREQUENCY CORRECTION
      CALL BYTIN(CTLIN)
      IF(CTLIN.EQ.#59H) THEN
        LGFRCR=.TRUE.
      ELSE
        LGFRCR=.FALSE.
      ENDIF

C      COAL FIRED MODEL CONSTANTS
      FREF=1.0+BPC*POC
      TG=0.1
      PREF=1.0
      K1=0.015
      K2=5.0
      TC=45.0
      TM=2.0
      R=0.35
      KH=0.2
      KL=0.8
      TB=240.0
      W1ML=1.0/(1.0-R*R)
      PM1ML=1.0/(1.0-R**0.231)

C      SYSTEM CONSTANTS
      PON=1.0

C      CALCULATE PLANT MAXIMUM CONTINUOUS RATINGS
      POHMCR=32.5
      TOTMCR=POHMCR/QH
      POC1MCR=QC1*TOTMCR
      POC2MCR=QC2*TOTMCR
      PONMCR=QN*TOTMCR

C      SET UP DEMAND STEP CONTROL
      LRISEG=.TRUE.
      LRISE=.FALSE.
      LFALLG=.FALSE.
      LFALL=.FALSE.

C      ANALOG OUTPUT SCALING CONSTANTS
      FESSCL=4096.0/(1.05-0.95)
      POSCL=(4096.0-2048.0)/(1.0-0.0)

C      CALCULATION AND AVERAGING OF GRID FREQUENCY VALUE
75     CONTINUE
      IF(.NOT.LGFROK) GOTO 75
      CNTSUM=0
      DO 77 I=1,FSAMPL
        CALL DSABLE
        CNTSUM=CNTSUM+INT4(CNSAMP(I))
        CALL ENABLE
77     CONTINUE
      GFREQI=TIMSCL/FLOAT(CNTSUM)

C      OUTPUT INITIAL FREQUENCY DEVIATION
      IFES=2048
      CALL ANOUT(0,IFES)

C      OUTPUT INITIAL CORRECTED FREQUENCY DEVIATION

```

```

IFESCR=2048
CALL ANOUT(4,IFESCR)

C   OUTPUT INITIAL GRID FREQUENCY
    IGFREQ=2048+NINT(FGSC*(GFREQI-1.0))
    IF(IGFREQ.GT.4095) IGFREQ=4095
    IF(IGFREQ.LT.0) IGFREQ=0
    CALL ANOUT(6,IGFREQ)

C   LOAD MW METER READING
    CALL NUMIN(READMW)

C   CALCULATE HYDRO OPERATING POINT
    POH=READMW/POHMCR

C   MEASURE AVERAGE VALUE OF TURBINE OUTPUT POWER
    IPOHSM=0
    DO 20 I=1,NSAMPL
    CALL ANIN(1,IPOH)
    IPOHSM=IPOHSM+INT4(IPOH)
20  CONTINUE

C   ANALOG INPUT SCALING CONSTANTS
    PWSCL=(POH-0.0)/(FLOAT(IPOHSM)-2048.0*FLOAT(NSAMPL))
    POH5V=2048.0*PWSCL*FLOAT(NSAMPL)

60  CONTINUE

C   CALCULATION AND FILTERING OF GRID FREQUENCY VALUE
    CNTSUM=0
    DO 65 I=1,FSAMPL
    CALL DSABLE
    CNTSUM=CNTSUM+INT4(CNSAMP(I))
    CALL ENABLE
65  CONTINUE
    GFREQI=TIMSCL/FLOAT(CNTSUM)

C   MEASURE AVERAGE VALUE OF TURBINE OUTPUT POWER
    IPOHSM=0
    DO 90 I=1,NSAMPL
    CALL ANIN(1,IPOH)
    IPOHSM=IPOHSM+INT4(IPOH)
90  CONTINUE
    POH=PWSCL*FLOAT(IPOHSM)-POH5V
    IPOHSM=0

C   CALCULATE INITIAL DEMAND VALUE
    PD=QN*PON+QC1*POC+QC2*POC2+QH*POH

C   SET UP DEMAND STEP PARAMETERS
    PDL=PD
    PDH=PD+PDSTEP
    PDTRIG=PDL

C   OUTPUT INITIAL COAL TYPE 1 POWER OUTPUT
    IPOC=2048.0+NINT(POSCL*POC)
    IF(IPOC.GT.4095) IPOC=4095
    IF(IPOC.LT.2048) IPOC=2048
    CALL ANOUT(1,IPOC)

```

```

95  IF(P2INIT) GOTO 95

C   RESET START FLAG
    LSTART=.FALSE.

C   SET UP TIMER 1
    CALL OUTPUT(TIMCTL,#74H)
    CALL OUTPUT(TIMER1,T1LOB)
    CALL OUTPUT(TIMER1,T1HOB)

C   SET UP VECTOR AND UN-MASK FOR TIME INTERRUPTS
    CALL SETINT(#24H,SAMPLE)
    CALL OUTPUT(INTCT2,#0EEH)

C   WAIT FOR INTERRUPTS
30  CONTINUE
    IF(KSIM.NE.1) GOTO 30

C   START PROCESSOR 2
    P2EX=.TRUE.

C   SET PC4
    CALL OUTPUT(PRTCTL,#0BH)

C   CALCULATION AND FILTERING OF GRID FREQUENCY VALUE
    CNTSUM=0
    DO 100 I=1,FSAMPL
        CALL DSABLE
        CNTSUM=CNTSUM+INT4(CNSAMP(I))
        CALL ENABLE
100  CONTINUE
    GFREQ=TIMSCL/FLOAT(CNTSUM)

C   CALCULATE TURBINE OUTPUT POWER
    CALL DSABLE
    POH=PWSCL*FLOAT(IPOHSM)-POH5V
    IPOHSM=0
    CALL ENABLE

C   MASTER PRESSURE CONTROLLER
    PERR=PREF-PB
    DY2=K1*PERR
    MX=Y2+K2*PERR
    MX=LIMIT(MX,0.2,1.2)

C   FUEL FEED SYSTEM
    EM=DELAY(MX,TD,MX)
    EM=LIMIT(EM,0.001,1.05)
    DF1=(EM-F1)/TC
    DFD=(F1-Q1)/TM
    FD=LIMIT(FD,0.001,1.05)
    Q1=MX*FD

C   GOVERNOR
    DAX=((FREF-FREQ)/BPC-AX)/TG
    AX=LIMIT(AX,0.001,1.0)

C   STEAM VALVE
    IF(AX.GT.AXV) THEN
        TGV=0.7
    
```

```

C      OUTPUT INITIAL HYDRO PLANT POWER OUTPUT
      IPOH=2048.0+NINT(POSCL*POH)
      IF(IPOH.GT.4095) IPOH=4095
      IF(IPOH.LT.2048) IPOH=2048
      CALL ANOUT(2,IPOH)

C      OUTPUT INITIAL DEMAND VALUE
      IPD=2048+NINT(POSCL*PD)
      IF(IPD.GT.4095) IPD=4095
      IF(IPD.LT.2048) IPD=2048
      CALL ANOUT(5,IPD)

C      OUTPUT INITIAL GRID FREQUENCY
      IGFREQ=2048+NINT(FGSCL*(GFREQI-1.0))
      IF(IGFREQ.GT.4095) IGFREQ=4095
      IF(IGFREQ.LT.0) IGFREQ=0
      CALL ANOUT(6,IGFREQ)

C      OUTPUT INITIAL COAL TYPE 2 POWER OUTPUT
      IPOC=2048.0+NINT(POSCL*POC2)
      IF(IPOC.GT.4095) IPOC=4095
      IF(IPOC.LT.2048) IPOC=2048
      CALL ANOUT(7,IPOC)

C      ECHO PARAMETERS TO BBC
      CALL NUMOUT(PD)
      CALL NUMOUT(PD*TOTMCR)
      CALL NUMOUT(PON)
      CALL NUMOUT(PON*PONMCR)
      CALL NUMOUT(POC)
      CALL NUMOUT(POC*POC1MCR)
      CALL NUMOUT(POC2)
      CALL NUMOUT(POC2*POC2MCR)
      CALL NUMOUT(POH)
      CALL NUMOUT(POH*POHMCR)

C      LOOK FOR COMMAND TO START SIMULATION
      CALL BYTIN(CTLIN)
      IF(CTLIN.NE.#53H) GOTO 60

C      SET START FLAG FOR DELAY FUNCTIONS ETC
      LSTART=.TRUE.

C      SET FLAG FOR PROCESSOR 2 INITIALISATION
      P2INIT=.TRUE.

C      INITIAL CONDITIONS
      AX=POC
      Y2=POC
      FI=POC
      QI=POC
      FD=1.0
      AXV=POC
      P2=POC
      PB=1.0
      FREQ=1.0
      MX=Y2
      EM=DELAY(MX,TD,MX)

C      WAIT FOR PROCESSOR 2 TO FINISH INITIALISATION

```

```

ELSE
  TGV=0.1
ENDIF
DAXV=(AX-AXV)/TGV

C   TURBINE
    P1=AXV*PB
    W1=P1*SQRT(ABS((1-(P2*R/P1)**2.0)*W1ML))
    W2=P2
    DP2=(W1-W2)/TR
    PM1=KH*W1*(1.0-(P2*R/P1)**0.231)*PM1ML
    PM2=KL*W2
    POC=PM1+PM2

C   BOILER
    DPB=(QI-W1)/TB

C   NUMERICAL INTEGRATION
    AX=AX+H*DAX
    Y2=Y2+H*DY2
    FI=FI+H*DFI
    FD=FD+H*DFD
    AXV=AXV+H*DAXV
    P2=P2+H*DP2
    PB=PB+H*DPB

C   WAIT FOR PROCESSOR 2 TO FINISH
120  IF(P2EX) GOTO 120

C   SYSTEM
    PL=PD*FREQ
    DFREQ=((QN*PON+QC1*POC+QC2*POC2-PL)/FREQ+QH*POH/GFREQ)/TA
    FREQ=FREQ+H*DFREQ

C   COLLECT DEMAND CONTROL
    IPDCTL=IPDSW

C   CALCULATE DEMAND VALUE
    IF(LRISEG.AND.IPDCTL.EQ.#00H) THEN
      PDTRIG=PDH
      LRISEG=.FALSE.
      LFALLG=.TRUE.
    ENDIF
    IF(LFALLG.AND.IPDCTL.EQ.#01H) THEN
      PDTRIG=PDL
      LFALLG=.FALSE.
      LRISEG=.TRUE.
    ENDIF
    IF(LAGDEM) THEN
      DPD=(PDTRIG-PD)/TDEM
      PD=PD+H*DPD
    ELSE
      PD=PDTRIG
    ENDIF

C   TEST FREQUENCY INPUT
    FES=1.0-FREQ
    IF(LGFRCR) THEN
      FESCOR=FES+GFREQ-GFREQI
    ELSE

```

```

        FESCOR=FES
    ENDIF
    IF(GFREQ.LT.GFRLML.OR.GFREQ.GT.GFRLMH) LGFRLM=.TRUE.

C      OUTPUT FREQUENCY DEVIATION
        IFES=2048+NINT(FESSCL*FES)
        IF(IFES.GT.4095) IFES=4095
        IF(IFES.LT.0) IFES=0
        CALL ANOUT(0,IFES)

C      OUTPUT COAL TYPE 1 POWER OUTPUT
        IPOC=2048.0+NINT(POSCL*POC)
        IF(IPOC.GT.4095) IPOC=4095
        IF(IPOC.LT.2048) IPOC=2048
        CALL ANOUT(1,IPOC)

C      OUTPUT HYDRO PLANT POWER OUTPUT
        IPOH=2048+NINT(POSCL*POH)
        IF(IPOH.GT.4095) IPOH=4095
        IF(IPOH.LT.2048) IPOH=2048
        CALL ANOUT(2,IPOH)

C      OUTPUT CORRECTED FREQUENCY DEVIATION IF GRID FREQUENCY OK
        IF(.NOT.(LGFRLM.AND.LGFRCR)) THEN
            IFESCR=2048+NINT(FESSCL*FESCOR)
            IF(IFESCR.GT.4095) IFESCR=4095
            IF(IFESCR.LT.0) IFESCR=0
            CALL ANOUT(4,IFESCR)
        ENDIF

C      OUTPUT DEMAND VALUE
        IPD=2048+NINT(POSCL*PD)
        IF(IPD.GT.4095) IPD=4095
        IF(IPD.LT.2048) IPD=2048
        CALL ANOUT(5,IPD)

C      OUTPUT GRID FREQUENCY
        IGFREQ=2048+NINT(FGSCCL*(GFREQ-1.0))
        IF(IGFREQ.GT.4095) IGFREQ=4095
        IF(IGFREQ.LT.0) IGFREQ=0
        CALL ANOUT(6,IGFREQ)

C      OUTPUT COAL TYPE 2 POWER OUTPUT
        IPOC=2048.0+NINT(POSCL*POC2)
        IF(IPOC.GT.4095) IPOC=4095
        IF(IPOC.LT.2048) IPOC=2048
        CALL ANOUT(7,IPOC)

C      RESET 0.1S FLAG
        KSIM=0

C      RESET PC4
        CALL OUTPUT(PRTCTL,#0AH)

C      LOOK FOR COMMAND TO FINISH SIMULATION
        CALL SCANIN(CTLIN)
        IF(CTLIN.NE.#46H) GOTO 30

C      IF FINISHED DISABLE PROCESSOR INTERRUPTS AND RESTART
        CALL DSABLE
    
```

GOTO 70

END

\$INTERRUPT

SUBROUTINE SAMPLE
 EXTERNAL ANIN
 INTEGER*1 INTCT1,PRCTL
 INTEGER*1 NSAMPL,NCOUNT,KSIM
 INTEGER*2 IPOH
 INTEGER*4 IPOHSM
 COMMON/SAMPL1/NSAMPL,NCOUNT,KSIM
 COMMON/SAMPL2/IPOHSM
 PARAMETER(INTCT1=#0C0H,PRCTL=#0CEH)

C RE-ENABLE PROCESSOR INTERRUPTS
 CALL ENABLE

C SET PC4
 CALL OUTPUT(PRTCTL,#09H)

C MEASURE TURBINE POWER OUTPUT
 CALL ANIN(1,IPOH)
 IPOHSM=IPOHSM+INT4(IPOH)

C INTEGRATION CONTROL
 NCOUNT=NCOUNT+1
 IF(NCOUNT.EQ.NSAMPL) THEN
 NCOUNT=0
 KSIM=1
 ENDIF

C RESET PC4
 CALL OUTPUT(PRTCTL,#08H)

C SEND EOI TO PIC
 CALL OUTPUT(INTCT1,#64H)

RETURN
 END

\$INTERRUPT

SUBROUTINE CYCLE
 EXTERNAL TIMCNT,ANOUT
 INTEGER*1 INTCT1,INTCT2,PRCTL
 INTEGER*2 TOLAST,ICOUNT
 INTEGER*2 CNSAMP(50)
 INTEGER*1 FSAMPL,I,ICNSMP
 LOGICAL*1 LGFROK
 COMMON/SAMPL3/FSAMPL,ICNSMP,TOLAST,LGFROK,CNSAMP
 PARAMETER(INTCT1=#0C0H,INTCT2=#0C2H,PRCTL=#0CEH)

C SET PC5
 CALL OUTPUT(PRTCTL,#0BH)

C READ TIMER

```
CALL TIMCNT(TOLAST,ICOUNT)
IF(ICOUNT.GT.24699) ICOUNT=24699
IF(ICOUNT.LT.24454) ICOUNT=24454
```

```
C SEND COUNT VALUE TO FILTER
CNSAMP(ICNSMP)=ICOUNT
ICNSMP=ICNSMP-1
IF(ICNSMP.EQ.0) THEN
  ICNSMP=FSAMPL
  LGFROK=.TRUE.
ENDIF
```

```
C RESET PC5
C CALL OUTPUT(PRTCTL,#0AH)
```

```
C SEND EOI TO PIC
CALL OUTPUT(INTCT1,#60H)
```

```
RETURN
END
```

```
REAL*4 FUNCTION DELAY(VAL,TD,STRVAL)
INTEGER*2 I
INTEGER*2 NSTRCL,STPTR1,STPTR2
REAL*4 VAL,TD,STRVAL
REAL*4 STORE(1200)
REAL*4 H
LOGICAL*1 LSTART
COMMON/SYSTEM/H
COMMON/PRL4/LSTART
IF(LSTART) THEN
  NSTRCL=NINT(TD/H)
  DO 10 I=1,NSTRCL
    STORE(I)=STRVAL
10 CONTINUE
  STPTR1=0
  STPTR2=1
ELSE
  STPTR1=STPTR1+1
  IF(STPTR1.GT.NSTRCL) STPTR1=1
  STPTR2=STPTR2+1
  IF(STPTR2.GT.NSTRCL) STPTR2=1
  STORE(STPTR1)=VAL
  DELAY=STORE(STPTR2)
ENDIF
RETURN
END
```

```
C LIMIT FUNCTION
REAL*4 FUNCTION LIMIT(VAL,BTMLIM,TOPLIM)
REAL*4 VAL,BTMLIM,TOPLIM
IF(VAL.LE.BTMLIM) LIMIT=BTMLIM
IF(VAL.GT.BTMLIM) LIMIT=VAL
IF(VAL.GE.TOPLIM) LIMIT=TOPLIM
RETURN
END
```

Master processor code for hydro-thermal system tests
(speeder motor injection)

```

C      MIXED SYSTEM SIMULATOR USING COAL FIRED PLANT MODEL
C      REQUIRES BBC TERMINAL
C      USES EULER
C      INCORPORATES AVERAGING OF TURBINE POWER MEASUREMENT
C      VERSION FOR SPEEDER MOTOR INJECTION
C      MULTIPROCESSOR VERSION WITH GRID FREQUENCY ADJUSTMENT
C      CODE FOR PROCESSOR 1

EXTERNAL NUMIN,NUMOUT,BYTIN,BYTOUT,SCANIN,ANINIT,ANIN,ANOUT
EXTERNAL CYCLE,SAMPLE,GETSEM,GIVSEM
REAL*4 DELAY,LIMIT
REAL*4 H
REAL*4 READMW,TIMSCL,PWSCL,FESSCL,POSCL,POH5V,FGSCL
REAL*4 PD,PL,PON,POC,POH,FG,GFRLML,GFRLMH
REAL*4 POC2,TD2,TR2,BPC2
REAL*4 QN,QC1,QC2,QH,TA,PDSTEP,PDRATE,PDL,PDH,PDTRIG,TDEM
REAL*4 FREQ,FES,FESCOR,GFREQ,GFREQI
REAL*4 DFREQ,DPD
REAL*4 TG,PREF,K1,K2,TC,TM,R,KH,KL,TB,FREF,TD,TR,BPC
REAL*4 POHMCR,POC1MCR,POC2MCR,PONMCR,TOTMCR,W1ML,PM1ML
REAL*4 AX,Y2,FI,FD,AXV,P2,PB
REAL*4 DAX,DY2,DFI,DFD,DAXV,DP2,DPB
REAL*4 PERR,MX,EM,QI,TGV,P1,W1,W2,PM1,PM2
REAL*4 SPRS,HFSPRS,FDSCLM,FREFI,FRFLML,FRFLMH,FRFSNL
REAL*4 FDISC,FREFH,FTRACK
INTEGER*1 INTCT1,INTCT2,PORTA,PORTB,PORTC,PRTCTL
INTEGER*1 TIMER0,TIMER1,TIMCTL,T1LOB,T1HOB
INTEGER*1 CTLIN,CTLOUT
INTEGER*1 FSAMPL,ICNSMP,NSAMPL,NCOUNT,KSIM,ISPCTL,IPDCTL,IPDSW
INTEGER*2 I,CNSAMP(50),TOLAST,IPD,IPOC,IPOH,IFES,IFESCR,IGFREQ
INTEGER*2 IFDISC,ISDPIP,NPULSE,IFTRACK,ISPCNT
INTEGER*4 CNTSUM,IPOHSM
LOGICAL*1 LGFROK,LGFRCR,LGFRLM,LRISEG,LRISE,LFALLG,LFALL,LAGDEM
LOGICAL*1 SYNC,P2RDY,P2INIT,P2EX,LSTART
LOGICAL*1 LLTSNL,LDODGY,LSPRLM
COMMON/SAMPL1/NSAMPL,NCOUNT,KSIM
COMMON/SAMPL2/IPOHSM
COMMON/SAMPL3/FSAMPL,ICNSMP,TOLAST,LGFROK,CNSAMP
COMMON/SYSTEM/H
COMMON/PRLL1/ISPCTL,IPDSW,LDODGY,LGFRLM,LSPRLM,LLTSNL
COMMON/PRLL2/SYNC,P2RDY,P2INIT,P2EX
COMMON/PRLL3/POC2,TD2,TR2,BPC2,FREQ
COMMON/PRLL4/LSTART
PARAMETER(INTCT1=#0C0H,INTCT2=#0C2H)
PARAMETER(PORTA=#0C8H,PORTB=#0CAH,PORTC=#0CCH,PRTCTL=#0CEH)
PARAMETER(TIMER0=#0D0H,TIMER1=#0D2H,TIMCTL=#0D6H)

C      DISABLE PROCESSOR INTERRUPTS
C      CALL DSABLE

C      CLEAR RAISE/LOWER CONTROL
C      ISPCTL=#03H

C      INITIALISE MULTIPROCESSOR CONTROL FLAGS
C      P2EX=.FALSE.
C      P2RDY=.FALSE.
C      P2INIT=.FALSE.

C      RESET SPARE ERROR INDICATIONS
C      LFLAG3=.FALSE.

```

```

C     LFLAG4=.FALSE.
C     LFLAG5=.FALSE.
C     LFLAG6=.FALSE.

C     SYNCHRONISE PROCESSORS
3     CONTINUE
      SYNC=.FALSE.
      SYNC=.TRUE.
      IF(.NOT.P2RDY) GOTO 3

C     30 SAMPLES PER 0.05 SECOND INTEGRATION INTERVAL
      H=0.05
      T1LOB=0
      T1HOB=1

C     SET UP DAC AND INITIALISE CHANNELS TO 0 VOLTS
      CALL ANINIT(7)
      DO 5 I=0,7
      CALL ANOUT(I,2048)
5     CONTINUE

C     SET UP FREQUENCY MEASUREMENT
      LGFROK=.FALSE.
      FSAMPL=25
      TOLAST=0
      ICNSMP=FSAMPL

C     SET UP FREQUENCY FILTER
      DO 10 I=1,FSAMPL
      CNSAMP(I)=1.0
10    CONTINUE

C     SET UP FREQUENCY SCALING CONSTANTS
      TIMSCL=FLOAT(FSAMPL)*1228800.0/50.0
      FGSC=4096.0/(1.005-0.995)

C     SET UP INTERRUPT CONTROLLER
      CALL OUTPUT(INTCT1,#13H)
      CALL OUTPUT(INTCT2,#20H)
      CALL OUTPUT(INTCT2,#0DH)

C     SET UP TIMER 0
      CALL OUTPUT(TIMCTL,#34H)
      CALL OUTPUT(TIMER0,0)
      CALL OUTPUT(TIMER0,0)

C     SET UP VECTOR AND UN-MASK FOR MAINS CROSS-OVER INTERRUPTS
      CALL SETINT(#20H,CYCLE)
      CALL OUTPUT(INTCT2,#0FEH)

C     RE-ENABLE PROCESSOR INTERRUPTS
      CALL ENABLE

C     SET UP SBC 86/14 PARALLEL PORTS
      CALL OUTPUT(PRTCTL,#0A6H)
      CALL OUTPUT(PRTCTL,#0DH)
      CALL OUTPUT(PRTCTL,#05H)

C     OUTPUT PULSE TO SET UP INPUT PORT
      CALL OUTPUT(PRTCTL,#03H)

```

```

CALL OUTPUT(PRTCTL,#02H)

C   ESTABLISH COMMUNICATION WITH BBC
40  CALL BYTIN(CTLIN)
    IF(CTLIN.NE.#10H) GOTO 40
    CTLOUT=#11H
    CALL BYTOUT(CTLOUT)

70  CONTINUE

C   RESET RAISE/LOWER CONTROL
    ISPCNT=1
    ISPCTL=#03H
    NPULSE=0
    FDSCLM=0.01
    LDOOGY=.FALSE.
    LSPRLM=.FALSE.
    LLTSNL=.FALSE.
    FRFLML=0.955
    FRFLMH=1.095
    FRFSNL=1.006

C   SET UP GRID FREQUENCY CORRECTION LIMITS
    LGFRM=.FALSE.
    GFRLML=0.996
    GFRLMH=1.004

C   SET UP AVERAGING OF TURBINE POWER OUTPUT
    NSAMPL=30
    NCOUNT=0.
    KSIM=0

C   SEND SWITCH STATUS
    IPDCTL=IPDSW
    CALL BYTOUT(IPDCTL)

C   LOAD PROPORTION OF NUCLEAR PLANT
    CALL NUMIN(QN)

C   LOAD PROPORTIONS OF COAL PLANT
    CALL NUMIN(QC1)
    CALL NUMIN(QC2)

C   LOAD PROPORTION OF HYDRO PLANT
    CALL NUMIN(QH)

C   LOAD COAL FIRED PLANT OPERATING POINTS
    CALL NUMIN(POC)
    CALL NUMIN(POC2)

C   LOAD FUEL FEED DELAYS
    CALL NUMIN(TD)
    CALL NUMIN(TD2)

C   LOAD REHEATER TIME CONSTANTS
    CALL NUMIN(TR)
    CALL NUMIN(TR2)

C   LOAD COAL FIRED PLANT DROOPS
    CALL NUMIN(BPC)

```

```

CALL NUMIN(BPC2)

C   LOAD ALTERNATOR TIME CONSTANT
    CALL NUMIN(TA)

C   LOAD DEMAND STEP SIZE
    CALL NUMIN(PDSTEP)

C   ESTABLISH TYPE OF DEMAND TRANSIENT
    CALL BYTIN(CTLIN)
    IF(CTLIN.EQ.#4CH) THEN
        LAGDEM=.TRUE.
    ELSE
        LAGDEM=.FALSE.
    ENDIF

C   LOAD DEMAND TRANSIENT PARAMETERS
    IF(LAGDEM) CALL NUMIN(TDEM)

C   DECIDE ON USE OF GRID FREQUENCY CORRECTION
    CALL BYTIN(CTLIN)
    IF(CTLIN.EQ.#59H) THEN
        LGFRCR=.TRUE.
    ELSE
        LGFRCR=.FALSE.
    ENDIF

C   SPEEDER MOTOR CONSTANTS
    SPRS=0.1*0.03/8.0
    HFSPRS=SPRS/2.0

C   COAL FIRED MODEL CONSTANTS
    FREF=1.0+BPC*POC
    TG=0.1
    PREF=1.0
    K1=0.015
    K2=5.0
    TC=45.0
    TM=2.0
    R=0.35
    KH=0.2
    KL=0.8
    TB=240.0
    W1ML=1.0/(1.0-R*R)
    PM1ML=1.0/(1.0-R**0.231)

C   SYSTEM CONSTANTS
    PON=1.0

C   CALCULATE PLANT MAXIMUM CONTINUOUS RATINGS
    POHMCR=32.5
    TOTMCR=POHMCR/QH
    POC1MCR=QC1*TOTMCR
    POC2MCR=QC2*TOTMCR
    PONMCR=QN*TOTMCR

C   SET UP DEMAND STEP CONTROL
    LRISEG=.TRUE.
    LRISE=.FALSE.
    LFALLG=.FALSE.

```

```

LFALL=.FALSE.

C   ANALOG OUTPUT SCALING CONSTANTS
    FESSCL=4096.0/(1.05-0.95)
    POSCL=(4096.0-2048.0)/(1.0-0.0)

C   CALCULATION AND AVERAGING OF GRID FREQUENCY VALUE
75  CONTINUE
    IF(.NOT.LGFROK) GOTO 75
    CNTSUM=0
    DO 77 I=1,FSAMPL
    CALL DSABLE
    CNTSUM=CNTSUM+INT4(CNSAMP(I))
    CALL ENABLE
77  CONTINUE
    GFREQI=TIMSCL/FLOAT(CNTSUM)

C   OUTPUT INITIAL FREQUENCY DEVIATION
    IFES=2048
    CALL ANOUT(0,IFES)

C   OUTPUT INITIAL CORRECTED FREQUENCY DEVIATION
    IFESCR=2048
    CALL ANOUT(4,IFESCR)

C   OUTPUT INITIAL GRID FREQUENCY
    IGFREQ=2048+NINT(FGSCL*(GFREQI-1.0))
    IF(IGFREQ.GT.4095) IGFREQ=4095
    IF(IGFREQ.LT.0) IGFREQ=0
    CALL ANOUT(6,IGFREQ)

C   LOAD MW METER READING
    CALL NUMIN(READMW)

C   CALCULATE HYDRO OPERATING POINT
    POH=READMW/POHMCR

C   MEASURE AVERAGE VALUE OF TURBINE OUTPUT POWER
    IPOHSM=0
    DO 20 I=1,NSAMPL
    CALL ANIN(1,IPOH)
    IPOHSM=IPOHSM+INT4(IPOH)
20  CONTINUE

C   ANALOG INPUT SCALING CONSTANTS
    PWSCS=(POH-0.0)/(FLOAT(IPOHSM)-2048.0*FLOAT(NSAMPL))
    POH5V=2048.0*PWSCS*FLOAT(NSAMPL)

60  CONTINUE

C   CALCULATION AND FILTERING OF GRID FREQUENCY VALUE
    CNTSUM=0
    DO 65 I=1,FSAMPL
    CALL DSABLE
    CNTSUM=CNTSUM+INT4(CNSAMP(I))
    CALL ENABLE
65  CONTINUE
    GFREQI=TIMSCL/FLOAT(CNTSUM)

C   MEASURE AVERAGE VALUE OF TURBINE OUTPUT POWER

```

```

IPOHSM=0
DO 90 I=1,NSAMPL
CALL ANIN(1,IPOH)
IPOHSM=IPOHSM+INT4(IPOH)
90 CONTINUE
POH=PWSCL*FLOAT(IPOHSM)-POH5V
IPOHSM=0

C CALCULATE INITIAL DEMAND VALUE
PD=QN*PON+QC1*POC+QC2*POC2+QH*POH

C SET UP DEMAND STEP PARAMETERS
PDL=PD
PDH=PD+PDSTEP
PDTRIG=PDL

C OUTPUT INITIAL COAL TYPE 1 POWER OUTPUT
IPOC=2048.0+NINT(POSCL*POC)
IF(IPOC.GT.4095) IPOC=4095
IF(IPOC.LT.2048) IPOC=2048
CALL ANOUT(1,IPOC)

C OUTPUT INITIAL HYDRO PLANT POWER OUTPUT
IPOH=2048.0+NINT(POSCL*POH)
IF(IPOH.GT.4095) IPOH=4095
IF(IPOH.LT.2048) IPOH=2048
CALL ANOUT(2,IPOH)

C OUTPUT INITIAL DEMAND VALUE
IPD=2048+NINT(POSCL*PD)
IF(IPD.GT.4095) IPD=4095
IF(IPD.LT.2048) IPD=2048
CALL ANOUT(5,IPD)

C OUTPUT INITIAL GRID FREQUENCY
IGFREQ=2048+NINT(FGSCLE*(GFREQ1-1.0))
IF(IGFREQ.GT.4095) IGFREQ=4095
IF(IGFREQ.LT.0) IGFREQ=0
CALL ANOUT(6,IGFREQ)

C OUTPUT INITIAL COAL TYPE 2 POWER OUTPUT
IPOC=2048.0+NINT(POSCL*POC2)
IF(IPOC.GT.4095) IPOC=4095
IF(IPOC.LT.2048) IPOC=2048
CALL ANOUT(7,IPOC)

C ECHO PARAMETERS TO BBC
CALL NUMOUT(PD)
CALL NUMOUT(PD*TOTMCR)
CALL NUMOUT(PON)
CALL NUMOUT(PON*PONMCR)
CALL NUMOUT(POC)
CALL NUMOUT(POC*POC1MCR)
CALL NUMOUT(POC2)
CALL NUMOUT(POC2*POC2MCR)
CALL NUMOUT(POH)
CALL NUMOUT(POH*POHMCR)

C LOOK FOR COMMAND TO START SIMULATION
CALL BYTIN(CTLIN)

```

```

IF(CTLIN.NE.#53H) GOTO 60

C   CALCULATE INITIAL HYDRO FREQUENCY REFERENCE
    FREFI=GFREQI+0.03*POH

C   SET START FLAG FOR DELAY FUNCTIONS ETC
    LSTART=.TRUE.

C   SET FLAG FOR PROCESSOR 2 INITIALISATION
    P2INIT=.TRUE.

C   INITIAL CONDITIONS
    AX=POC
    Y2=POC
    F1=POC
    Q1=POC
    FD=1.0
    AXV=POC
    P2=POC
    PB=1.0
    FREQ=1.0
    MX=Y2
    EM=DELAY(MX,TD,MX)

C   WAIT FOR PROCESSOR 2 TO FINISH INITIALISATION
95  IF(P2INIT) GOTO 95

C   RESET START FLAG
    LSTART=.FALSE.

C   SET UP TIMER 1
    CALL OUTPUT(TIMCTL,#74H)
    CALL OUTPUT(TIMER1,T1LOB)
    CALL OUTPUT(TIMER1,T1HOB)

C   SET UP VECTOR AND UN-MASK FOR TIME INTERRUPTS
    CALL SETINT(#24H,SAMPLE)
    CALL OUTPUT(INTCT2,#0EEH)

C   WAIT FOR INTERRUPTS
30  CONTINUE
    IF(KSIM.NE.1) GOTO 30

C   START PROCESSOR 2
    P2EX=.TRUE.

C   SET PC4
    CALL OUTPUT(PRTCTL,#0BH)

C   CALCULATION AND FILTERING OF GRID FREQUENCY VALUE
    CNTSUM=0
    DO 100 I=1,FSAMPL
        CALL DSABLE
        CNTSUM=CNTSUM+INT4(CNSAMP(I))
        CALL ENABLE
100  CONTINUE
        GFREQ=TIMSCL/FLOAT(CNTSUM)

C   CALCULATE TURBINE OUTPUT POWER
    CALL DSABLE

```

POH=PWSCL*FLOAT(IPOHSM)-POH5V
 IPOHSM=0
 CALL ENABLE

C MASTER PRESSURE CONTROLLER
 PERR=PREF-PB
 DY2=K1*PERR
 MX=Y2+K2*PERR
 MX=LIMIT(MX,0.2,1.2)

C FUEL FEED SYSTEM
 EM=DELAY(MX,TD,MX)
 EM=LIMIT(EM,0.001,1.05)
 DFI=(EM-FI)/TC
 DFD=(FI-QI)/TM
 FD=LIMIT(FD,0.001,1.05)
 QI=MX*FD

C GOVERNOR
 DAX=((FREF-FREQ)/BPC-AX)/TG
 AX=LIMIT(AX,0.001,1.0)

C STEAM VALVE
 IF(AX.GT.AXV) THEN
 TGV=0.7
 ELSE
 TGV=0.1
 ENDIF
 DAXV=(AX-AXV)/TGV

C TURBINE
 P1=AXV*PB
 W1=P1*SQRT(ABS((1-(P2*R/P1)**2.0)*W1ML))
 W2=P2
 DP2=(W1-W2)/TR
 PM1=KH*W1*(1.0-(P2*R/P1)**0.231)*PM1ML
 PM2=KL*W2
 POC=PM1+PM2

C BOILER
 DPB=(QI-W1)/TB

C NUMERICAL INTEGRATION
 AX=AX+H*DAX
 Y2=Y2+H*DY2
 FI=FI+H*DFI
 FD=FD+H*DFD
 AXV=AXV+H*DAXV
 P2=P2+H*DP2
 PB=PB+H*DPB

C WAIT FOR PROCESSOR 2 TO FINISH
 120 IF(P2EX) GOTO 120

C SYSTEM
 PL=PD*FREQ
 DFREQ=((QN*PON+QC1*POC+QC2*POC2-PL)/FREQ+QH*POH/GFREQ)/TA
 FREQ=FREQ+H*DFREQ

C COLLECT DEMAND CONTROL

IPDCTL=IPDSW

```

C   CALCULATE DEMAND VALUE
    IF(LRISEG.AND.IPDCTL.EQ.#00H) THEN
      PDTRIG=PDH
      LRISEG=.FALSE.
      LFALLG=.TRUE.
    ENDIF
    IF(LFALLG.AND.IPDCTL.EQ.#01H) THEN
      PDTRIG=PDL
      LFALLG=.FALSE.
      LRISEG=.TRUE.
    ENDIF
    IF(LAGDEM) THEN
      DPD=(PDTRIG-PD)/TDEM
      PD=PD+H*DPD
    ELSE
      PD=PDTRIG
    ENDIF

C   TEST FREQUENCY INPUT
    FES=1.0-FREQ
    IF(LGFRCR) THEN
      FESCOR=FES+GFREQ-GFREQI
    ELSE
      FESCOR=FES
    ENDIF

    ISPCNT=ISPCNT+1
    IF(ISPCNT.NE.2) GOTO 125
    ISPCNT=0
    FTRACK=SPRS*FLOAT(NPULSE)
    FREFH=FREFI+FTRACK
    FDISC=FESCOR-FTRACK
    IF(LDODGY) THEN
      IF(NPULSE.EQ.0) THEN
        ISPCTL=#03H
        ISPDIP=2048
      ENDIF
      IF(NPULSE.GT.0) THEN
        ISPCTL=#02H
        ISPDIP=1792
        NPULSE=NPULSE-1
      ENDIF
      IF(NPULSE.LT.0) THEN
        ISPCTL=#01H
        ISPDIP=2304
        NPULSE=NPULSE+1
      ENDIF
    ELSE
      IF(FDISC.LT.HFSPRS.AND.FDISC.GT.-HFSPRS) THEN
        ISPCTL=#03H
        ISPDIP=2048
      ENDIF
      IF(FDISC.GT.HFSPRS.AND.FDISC.LT.FDSCLM) THEN
        NPULSE=NPULSE+1
        ISPCTL=#01H
        ISPDIP=2304
      ENDIF
      IF(FDISC.LT.-HFSPRS.AND.FDISC.GT.-FDSCLM) THEN

```

```

NPULSE=NPULSE-1
ISPCTL=#02H
ISPDIP=1792
ENDIF
IF(FDISC.GT.FDSCLM.OR.FDISC.LT.-FDSCLM) THEN
    ISPCTL=#03H
    ISPDIP=2048
    LDODGY=.TRUE.
ENDIF
IF(GFREQ.LT.GFRLML.OR.GFREQ.GT.GFRLMH) THEN
    ISPCTL=#03H
    ISPDIP=2048
    LGFRLM=.TRUE.
    LDODGY=.TRUE.
    NPULSE=0
ENDIF
IF(FREFH.LT.FRFLML.OR.FREFH.GT.FRFLMH) THEN
    ISPCTL=#03H
    ISPDIP=2048
    LSPRLM=.TRUE.
    LDODGY=.TRUE.
ENDIF
ENDIF
IF(FREFH.LT.FRFSNL) THEN
    LLTSNL=.TRUE.
ELSE
    LLTSNL=.FALSE.
ENDIF
125 CONTINUE

C    OUTPUT COAL TYPE 1 POWER OUTPUT
IPOC=2048.0+NINT(POSCL*POC)
IF(IPOC.GT.4095) IPOC=4095
IF(IPOC.LT.2048) IPOC=2048
CALL ANOUT(1,IPOC)

C    OUTPUT HYDRO PLANT POWER OUTPUT
IPOH=2048+NINT(POSCL*POH)
IF(IPOH.GT.4095) IPOH=4095
IF(IPOH.LT.2048) IPOH=2048
CALL ANOUT(2,IPOH)

C    OUTPUT FREQUENCY DISCREPANCY WITH SPEEDER MOTOR INPUT
IFDISC=2048+NINT(FESSCL*FDISC)
IF(IFDISC.GT.4095) IFDISC=4095
IF(IFDISC.LT.0) IFDISC=0
CALL ANOUT(3,IFDISC)

C    OUTPUT COMBINED SPEEDER MOTOR INPUT SIGNAL
CALL ANOUT(4,ISPDIP)

C    OUTPUT COMBINED SPEEDER MOTOR INPUT SIGNAL
IFTRACK=2048+NINT(FESSCL*FTRACK)
IF(IFTRACK.GT.4095) IFTRACK=4095
IF(IFTRACK.LT.0) IFTRACK=0
CALL ANOUT(4,IFTRACK)

C    OUTPUT CORRECTED FREQUENCY DEVIATION IF GRID FREQUENCY OK
C    IF(.NOT.(LGFRLM.AND.LGFRCR)) THEN
C        IFESCR=2048+NINT(FESSCL*FESCOR)

```

```

C      IF(IFESCR.GT.4095) IFESCR=4095
C      IF(IFESCR.LT.0) IFESCR=0
C      CALL ANOUT(4,IFESCR)
C      ENDIF

C      OUTPUT DEMAND VALUE
      IPD=2048+NINT(POSCL*PD)
      IF(IPD.GT.4095) IPD=4095
      IF(IPD.LT.2048) IPD=2048
      CALL ANOUT(5,IPD)

C      OUTPUT GRID FREQUENCY
      IGFREQ=2048+NINT(FGSCS*(GFREQ-1.0))
      IF(IGFREQ.GT.4095) IGFREQ=4095
      IF(IGFREQ.LT.0) IGFREQ=0
      CALL ANOUT(6,IGFREQ)

C      OUTPUT COAL TYPE 2 POWER OUTPUT
      IPOC=2048.0+NINT(POSCL*POC2)
      IF(IPOC.GT.4095) IPOC=4095
      IF(IPOC.LT.2048) IPOC=2048
      CALL ANOUT(7,IPOC)

C      RESET 0.1S FLAG
      KSIM=0

C      RESET PC4
      CALL OUTPUT(PRTCTL,#0AH)

C      LOOK FOR COMMAND TO FINISH SIMULATION
      CALL SCANIN(CTLIN)
      IF(CTLIN.NE.#46H) GOTO 30

C      IF FINISHED DISABLE PROCESSOR INTERRUPTS AND RESTART
      CALL DSABLE
      GOTO 70

      END

```

\$INTERRUPT

```

      SUBROUTINE SAMPLE
      EXTERNAL ANIN
      INTEGER*1 INTCT1,PRTCTL
      INTEGER*1 NSAMPL,NCOUNT,KSIM
      INTEGER*2 IPOH
      INTEGER*4 IPOHSM
      COMMON/SAMPL1/NSAMPL,NCOUNT,KSIM
      COMMON/SAMPL2/IPOHSM
      PARAMETER(INTCT1=#0COH,PRTCTL=#0CEH)

C      RE-ENABLE PROCESSOR INTERRUPTS
      CALL ENABLE

C      SET PC4
      CALL OUTPUT(PRTCTL,#09H)

C      MEASURE TURBINE POWER OUTPUT
      CALL ANIN(1,IPOH)

```

```

IPOHSM=IPOHSM+INT4(IPOH)

C   INTEGRATION CONTROL
    NCOUNT=NCOUNT+1
    IF(NCOUNT.EQ.NSAMPL) THEN
        NCOUNT=0
        KSIM=1
    ENDIF

C   RESET PC4
    CALL OUTPUT(PRTCTL,#08H)

C   SEND EO1 TO PIC
    CALL OUTPUT(INTCT1,#64H)

    RETURN
    END

$INTERRUPT

    SUBROUTINE CYCLE
    EXTERNAL TIMCNT,ANOUT
    INTEGER*1 INTCT1,INTCT2,PRTCTL
    INTEGER*2 TOLAST,ICOUNT
    INTEGER*2 CNSAMP(50)
    INTEGER*1 FSAMPL,I,ICNSMP
    LOGICAL*1 LGFROK
    COMMON/SAMPL3/FSAMPL,ICNSMP,TOLAST,LGFROK,CNSAMP
    PARAMETER(INTCT1=#0C0H,INTCT2=#0C2H,PRTCTL=#0CEH)

C   SET PC5
C   CALL OUTPUT(PRTCTL,#0BH)

C   READ TIMER
    CALL TIMCNT(TOLAST,ICOUNT)
    IF(ICOUNT.GT.24699) ICOUNT=24699
    IF(ICOUNT.LT.24454) ICOUNT=24454

C   SEND COUNT VALUE TO FILTER
    CNSAMP(ICNSMP)=ICOUNT
    ICNSMP=ICNSMP-1
    IF(ICNSMP.EQ.0) THEN
        ICNSMP=FSAMPL
        LGFROK=.TRUE.
    ENDIF

C   RESET PC5
C   CALL OUTPUT(PRTCTL,#0AH)

C   SEND EO1 TO PIC
    CALL OUTPUT(INTCT1,#60H)

    RETURN
    END

REAL*4 FUNCTION DELAY(VAL,TD,STRVAL)
INTEGER*2 I
INTEGER*2 NSTRCL,STPTR1,STPTR2

```

```

REAL*4 VAL,TD,STRVAL
REAL*4 STORE(1200)
REAL*4 H
LOGICAL*1 LSTART
COMMON/SYSTEM/H
COMMON/PRLL4/LSTART
IF(LSTART) THEN
  NSTRCL=NINT(TD/H)
  DO 10 I=1,NSTRCL
    STORE(I)=STRVAL
10  CONTINUE
    STPTR1=0
    STPTR2=1
  ELSE
    STPTR1=STPTR1+1
    IF(STPTR1.GT.NSTRCL) STPTR1=1
    STPTR2=STPTR2+1
    IF(STPTR2.GT.NSTRCL) STPTR2=1
    STORE(STPTR1)=VAL
    DELAY=STORE(STPTR2)
  ENDIF
  RETURN
  END

C  LIMIT FUNCTION
REAL*4 FUNCTION LIMIT(VAL,BTMLIM,TOPLIM)
REAL*4 VAL,BTMLIM,TOPLIM
IF(VAL.LE.BTMLIM) LIMIT=BTMLIM
IF(VAL.GT.BTMLIM) LIMIT=VAL
IF(VAL.GE.TOPLIM) LIMIT=TOPLIM
RETURN
END

```

Slave processor code for hydro-thermal system tests

```

C      MIXED SYSTEM SIMULATOR USING COAL FIRED PLANT MODEL
C      REQUIRES BBC TERMINAL
C      USES EULER
C      INCORPORATES AVERAGING OF TURBINE POWER MEASUREMENT
C      VERSION FOR ELECTRONIC GOVERNOR
C      MULTIPROCESSOR VERSION WITH GRID FREQUENCY ADJUSTMENT
C      CODE FOR PROCESSOR 2
C      CODE FOR ADDITIONAL I/O INCLUDED

EXTERNAL GETSEM,GIVSEM
REAL*4 DELAY,LIMIT
REAL*4 H
REAL*4 POC2,TD2,TR2,BPC2
REAL*4 POC,FREQ
REAL*4 TG,PREF,K1,K2,TC,TR,KH,KB,TB,FREF,TD,TR,BPC
REAL*4 W1ML,PM1ML
REAL*4 AX,Y2,F1,FD,AXV,P2,PB
REAL*4 DAX,DY2,DF1,DFD,DAXV,DP2,DPB
REAL*4 PERR,MX,EM,QI,TGV,P1,W1,W2,PM1,PM2
INTEGER*1 PORTA,PORTB,PORTC,PRTCTL
INTEGER*2 I
INTEGER*1 ISPCTL,IPDSW,IPDCTL
LOGICAL*1 LFLAG2,LFLAG3,LFLAG4,LFLAG5,LFLAG6
LOGICAL*1 SYNC,P2RDY,P2INIT,P2EX,LSTART
COMMON/PRLL1/ISPCTL,IPDSW,LFLAG2,LFLAG3,LFLAG4,LFLAG5,LFLAG6
COMMON/PRLL2/SYNC,P2RDY,P2INIT,P2EX
COMMON/PRLL3/POC2,TD2,TR2,BPC2,FREQ
COMMON/PRLL4/LSTART
COMMON/SYSTEM/H
PARAMETER(PORTA=#0C8H,PORTB=#0CAH,PORTC=#0CCH,PRTCTL=#0CEH)

C      DISABLE PROCESSOR INTERRUPTS
      CALL DSABLE

C      RESET RAISE/LOWER CONTROL BYTE
      ISPCTL=#03H

C      SET UP PARALLEL PORTS
      CALL OUTPUT(PORTA,ISPCTL)
      CALL OUTPUT(PRTCTL,#82H)
      CALL OUTPUT(PORTA,ISPCTL)

C      SYNCHRONISE WITH PROCESSOR 1
10     IF(SYNC) GOTO 10
20     IF(.NOT.SYNC) GOTO 20
      P2RDY=.TRUE.

C      WAIT TO DO INITIALISATION

30     CONTINUE

C      PERFORM I/O FUNCTIONS WHILE WAITING TO DO INITIALISATION

C      OUTPUT RAISE/LOWER CONTROL BYTE
      CALL OUTPUT(PORTA,ISPCTL)

C      READ AND ECHO DEMAND CONTROL SWITCH
      CALL INPUT(PORTB,IPDCTL)
      IPDSW=IPDCTL.AND.#01H
      IF(IPDSW.EQ.#00H) THEN

```

```

        CALL OUTPUT(PRTCTL,#03H)
    ELSE
        CALL OUTPUT(PRTCTL,#02H)
    ENDIF

C    DISPLAY ERROR CONDITIONS
    IF(LFLAG2) THEN
        CALL OUTPUT(PRTCTL,#05H)
    ELSE
        CALL OUTPUT(PRTCTL,#04H)
    ENDIF
    IF(LFLAG3) THEN
        CALL OUTPUT(PRTCTL,#07H)
    ELSE
        CALL OUTPUT(PRTCTL,#06H)
    ENDIF
    IF(LFLAG4) THEN
        CALL OUTPUT(PRTCTL,#09H)
    ELSE
        CALL OUTPUT(PRTCTL,#08H)
    ENDIF
    IF(LFLAG5) THEN
        CALL OUTPUT(PRTCTL,#0BH)
    ELSE
        CALL OUTPUT(PRTCTL,#0AH)
    ENDIF
    IF(LFLAG6) THEN
        CALL OUTPUT(PRTCTL,#0DH)
    ELSE
        CALL OUTPUT(PRTCTL,#0CH)
    ENDIF

    IF(.NOT.P2INIT) GOTO 30

C    COLLECT PARAMETERS
    POC=POC2
    TD=TD2
    TR=TR2
    BPC=BPC2

C    0.05 SECOND INTEGRATION INTERVAL
    H=0.05

C    COAL FIRED MODEL CONSTANTS
    FREF=1.0+BPC*POC
    TG=0.1
    PREF=1.0
    K1=0.015
    K2=5.0
    TC=45.0
    TM=2.0
    R=0.35
    KH=0.2
    KL=0.8
    TB=240.0
    W1ML=1.0/(1.0-R*R)
    PM1ML=1.0/(1.0-R**0.231)

C    INITIAL CONDITIONS
    AX=POC

```

```

Y2=POC
FI=POC
QI=POC
FD=1.0
AXV=POC
P2=POC
PB=1.0
MX=Y2
EM=DELAY(MX,TD,MX)

C   RESET INITIALISATION FLAG
    P2INIT=.FALSE.

C   WAIT FOR NEXT STEP

80  CONTINUE

C   PERFORM I/O FUNCTIONS WHILE WAITING FOR NEXT STEP

C   OUTPUT RAISE/LOWER CONTROL BYTE
    CALL OUTPUT(PORTA,ISPCTL)

C   READ AND ECHO DEMAND CONTROL SWITCH
    CALL INPUT(PORTB,IPDCTL)
    IPDSW=IPDCTL.AND.#01H
    IF(IPDSW.EQ.#00H) THEN
        CALL OUTPUT(PRTCTL,#03H)
    ELSE
        CALL OUTPUT(PRTCTL,#02H)
    ENDIF

C   DISPLAY ERROR CONDITIONS
    IF(LFLAG2) THEN
        CALL OUTPUT(PRTCTL,#05H)
    ELSE
        CALL OUTPUT(PRTCTL,#04H)
    ENDIF
    IF(LFLAG3) THEN
        CALL OUTPUT(PRTCTL,#07H)
    ELSE
        CALL OUTPUT(PRTCTL,#06H)
    ENDIF
    IF(LFLAG4) THEN
        CALL OUTPUT(PRTCTL,#09H)
    ELSE
        CALL OUTPUT(PRTCTL,#08H)
    ENDIF
    IF(LFLAG5) THEN
        CALL OUTPUT(PRTCTL,#0BH)
    ELSE
        CALL OUTPUT(PRTCTL,#0AH)
    ENDIF
    IF(LFLAG6) THEN
        CALL OUTPUT(PRTCTL,#0DH)
    ELSE
        CALL OUTPUT(PRTCTL,#0CH)
    ENDIF

    IF(.NOT.P2EX) GOTO 80

```

```

C      SET PC7
      CALL OUTPUT(PRTCTL,#0FH)

C      MASTER PRESSURE CONTROLLER
      PERR=PREF-PB
      DY2=K1*PERR
      MX=Y2+K2*PERR
      MX=LIMIT(MX,0.2,1.2)

C      FUEL FEED SYSTEM
      EM=DELAY(MX,TD,MX)
      EM=LIMIT(EM,0.001,1.05)
      DFI=(EM-FI)/TC
      DFD=(FI-QI)/TM
      FD=LIMIT(FD,0.001,1.05)
      QI=MX*FD

C      GOVERNOR
      DAX=((PREF-FREQ)/BPC-AX)/TG
      AX=LIMIT(AX,0.001,1.0)

C      STEAM VALVE
      IF(AX.GT.AXV) THEN
        TGV=0.7
      ELSE
        TGV=0.1
      ENDIF
      DAXV=(AX-AXV)/TGV

C      TURBINE
      P1=AXV*PB
      W1=P1*SQRT(ABS((1-(P2*R/P1)**2.0)*W1ML))
      W2=P2
      DP2=(W1-W2)/TR
      PM1=KH*W1*(1.0-(P2*R/P1)**0.231)*PM1ML
      PM2=KL*W2
      POC=PM1+PM2

C      BOILER
      DPB=(QI-W1)/TB

C      NUMERICAL INTEGRATION
      AX=AX+H*DAX
      Y2=Y2+H*DY2
      FI=FI+H*DFI
      FD=FD+H*DFD
      AXV=AXV+H*DAXV
      P2=P2+H*DP2
      PB=PB+H*DPB

C      SEND OUTPUT VALUE
      POC2=POC

C      RESET PC7
      CALL OUTPUT(PRTCTL,#0EH)

C      REPORT FINISHED
      P2EX=.FALSE.

      GOTO 80

```

END

```

REAL*4 FUNCTION DELAY(VAL,TD,STRVAL)
INTEGER*2 I
INTEGER*2 NSTRCL,STPTR1,STPTR2
LOGICAL*1 LSTART
REAL*4 VAL,TD,STRVAL
REAL*4 STORE(1200)
REAL*4 H
COMMON/SYSTEM/H
COMMON/PRLL4/LSTART
IF(LSTART) THEN
  NSTRCL=NINT(TD/H)
  DO 10 I=1,NSTRCL
    STORE(I)=STRVAL
10  CONTINUE
    STPTR1=0
    STPTR2=1
ELSE
  STPTR1=STPTR1+1
  IF(STPTR1.GT.NSTRCL) STPTR1=1
  STPTR2=STPTR2+1
  IF(STPTR2.GT.NSTRCL) STPTR2=1
  STORE(STPTR1)=VAL
  DELAY=STORE(STPTR2)
ENDIF
RETURN
END

C
LIMIT FUNCTION
REAL*4 FUNCTION LIMIT(VAL,BTMLIM,TOPLIM)
REAL*4 VAL,BTMLIM,TOPLIM
IF(VAL.LE.BTMLIM) LIMIT=BTMLIM
IF(VAL.GT.BTMLIM) LIMIT=VAL
IF(VAL.GE.TOPLIM) LIMIT=TOPLIM
RETURN
END

```

Master processor code for wind-diesel system tests

```

C      MIXED SYSTEM SIMULATOR USING WIND TURBINE MODEL
C      REQUIRES BBC TERMINAL
C      USES EULER
C      INCORPORATES AVERAGING OF DIESEL POWER MEASUREMENT
C      VERSION FOR SPEEDER MOTOR INJECTION
C      MULTIPROCESSOR VERSION WITH GRID FREQUENCY ADJUSTMENT
C      CODE FOR PROCESSOR 1

EXTERNAL NUMIN,NUMOUT,BYTIN,BYTOUT,SCANIN,ANINIT,ANIN,ANOUT
EXTERNAL CYCLE,SAMPLE,GETSEM,GIVSEM
REAL*4 LIMIT
REAL*4 H
REAL*4 READMW,TIMSCL,PWSCL,FESSCL,POSCL,POD5V,FGSCL
REAL*4 PD,PL,PON,POD,FG,GFRLML,GFRLMH
REAL*4 QN,QD,TA
REAL*4 FREQ,FES,FESCOR,GFREQ,GFREQI
REAL*4 DFREQ
REAL*4 PODMCR,PONMCR,TOTMCR
REAL*4 SPRS,HFSPRS,FDSCLM,FREFI,FRFLML,FRFLMH,FRFSNL
REAL*4 FDISC,FREFH,FTRACK,TSM,BPD,GC
REAL*4 POW,QW,TOW,TOG,WB,WM,WM1,TE,KC,KCD,TOWN,TEN,WBN,WMN,WOP
REAL*4 WW1,WW2,X1,WPERR,FREFW,POWMCR,PREF,VWSTEP
REAL*4 TOGD,BD,G,VM,VWL,VWH,CP,B,KP,KI,WW5,WW6,KCDIFF,WKC,WKCRNG
REAL*4 DX1,DB,DWB,DWM1,DKC
REAL*4 KCO,KC1,JB,JM1,WTC,TKC,TOFL,WO,BPW,TP
INTEGER*1 INTCT1,INTCT2,PORTA,PORTB,PORTC,PRTCTL
INTEGER*1 TIMER0,TIMER1,TIMCTL,T1LOB,T1HOB
INTEGER*1 CTLIN,CTLOUT,DACSEM(0:7)
INTEGER*1 FSAMPL,ICNSMP,NSAMPL,NCOUNT,KSIM,ISPCTL,IPDCTL,IPDSW
INTEGER*2 I,CNSAMP(50),TOLAST,IPD,IPOD,IFES,IFESCR,IGFREQ
INTEGER*2 IFDISC,ISPDP,NPULSE,IFTRACK,ISPCNT,DACDAT(0:7)
INTEGER*2 IPOW,ITOW,IWB,IWM,IB,IKC
INTEGER*4 CNTSUM,IPODSM
LOGICAL*1 LGFROK,LGFRLM,LRISEG,LRISE,LFALLG,LFALL,LAGDEM
LOGICAL*1 SYNC,P2RDY,LSTART
LOGICAL*1 LLTSNL,LDODGY,LSPRLM
COMMON/SAMPL1/NSAMPL,NCOUNT,KSIM
COMMON/SAMPL2/IPODSM
COMMON/SAMPL3/FSAMPL,ICNSMP,TOLAST,LGFROK,CNSAMP
COMMON/SYSTEM/H
COMMON/PRLL1/ISPCTL,IPDSW,LDODGY,LGFRLM,LSPRLM,LLTSNL
COMMON/PRLL2/SYNC,P2RDY
COMMON/PRLL5/DACSEM,DACDAT
PARAMETER(INTCT1=#0C0H,INTCT2=#0C2H)
PARAMETER(PORTA=#0C8H,PORTB=#0CAH,PORTC=#0CCH,PRTCTL=#0CEH)
PARAMETER(TIMER0=#0D0H,TIMER1=#0D2H,TIMCTL=#0D6H)

C      DISABLE PROCESSOR INTERRUPTS
C      CALL DSABLE

C      CLEAR RAISE/LOWER CONTROL
C      ISPCTL=#03H

C      INITIALISE EXTRA DAC SEMAPHORES
C      DO 2 I=0,7
C      DACSEM(I)=0
2      CONTINUE

C      SYNCHRONISE PROCESSORS
3      CONTINUE

```

```

SYNC=.FALSE.
SYNC=.TRUE.
IF(.NOT.P2RDY) GOTO 3

C 40 SAMPLES PER 0.05 SECOND INTEGRATION INTERVAL
H=0.05
T1LOB=192
T1HOB=0

C SET UP DAC AND INITIALISE CHANNELS TO 0 VOLTS
CALL ANINIT(7)
DO 5 I=0,7
CALL ANOUT(I,2048)
5 CONTINUE

C INITIALISE EXTRA DAC CHANNELS TO 0 VOLTS
DO 7 I=0,7
CALL GETSEM(DACSEM(I))
DACDAT(I)=2048
CALL GIVSEM(DACSEM(I))
7 CONTINUE

C SET UP FREQUENCY MEASUREMENT
LGFROK=.FALSE.
FSAMPL=25
TOLAST=0
ICNSMP=FSAMPL

C SET UP FREQUENCY FILTER
DO 10 I=1,FSAMPL
CNSAMP(I)=1.0
10 CONTINUE

C SET UP FREQUENCY SCALING CONSTANTS
TIMSCL=FLOAT(FSAMPL)*1228800.0/50.0
FGSCL=4096.0/(1.01-0.99)

C SET UP INTERRUPT CONTROLLER
CALL OUTPUT(INTCT1,#13H)
CALL OUTPUT(INTCT2,#20H)
CALL OUTPUT(INTCT2,#0DH)

C SET UP TIMER 0
CALL OUTPUT(TIMCTL,#34H)
CALL OUTPUT(TIMER0,0)
CALL OUTPUT(TIMER0,0)

C SET UP VECTOR AND UN-MASK FOR MAINS CROSS-OVER INTERRUPTS
CALL SETINT(#20H,CYCLE)
CALL OUTPUT(INTCT2,#0FEH)

C RE-ENABLE PROCESSOR INTERRUPTS
CALL ENABLE

C SET UP SBC 86/14 PARALLEL PORTS
CALL OUTPUT(PRTCTL,#0A6H)
CALL OUTPUT(PRTCTL,#0DH)
CALL OUTPUT(PRTCTL,#05H)

C OUTPUT PULSE TO SET UP INPUT PORT

```

```
CALL OUTPUT(PRTCTL,#03H)
CALL OUTPUT(PRTCTL,#02H)

C   ESTABLISH COMMUNICATION WITH BBC
40  CALL BYTIN(CTLIN)
    IF(CTLIN.NE.#10H) GOTO 40
    CTLOUT=#11H
    CALL BYTOUT(CTLOUT)

70  CONTINUE

C   RESET RAISE/LOWER CONTROL
    ISPCNT=1
    ISPCTL=#03H
    NPULSE=0
    FDSCLM=0.01
    LDOOGY=.FALSE.
    LSPRLM=.FALSE.
    LLTSNL=.FALSE.
    FRFLML=0.955
    FRFLMH=1.095
    FRFSNL=1.006

C   SET UP GRID FREQUENCY CORRECTION LIMITS
    LGFRML=.FALSE.
    GFRLML=0.992
    GFRLMH=1.008

C   SET UP AVERAGING OF DIESEL POWER OUTPUT
    NSAMPL=40
    NCOUNT=0
    KSIM=0

C   SEND SWITCH STATUS
    IPDCTL=IPDSW
    CALL BYTOUT(IPDCTL)

C   LOAD PROPORTION OF BASE LOAD PLANT
    CALL NUMIN(QN)

C   LOAD PROPORTION OF DIESEL PLANT
    CALL NUMIN(QD)

C   LOAD PROPORTION OF WIND TURBINE PLANT
    CALL NUMIN(QW)

C   LOAD WIND SPEED
    CALL NUMIN(VW)

C   LOAD WIND TURBINE OPERATING POINT
    CALL NUMIN(WOP)

C   LOAD WIND SPEED STEP SIZE
    CALL NUMIN(VWSTEP)

C   LOAD WIND TURBINE PITCH CONTROL GAINS
    CALL NUMIN(KP)
    CALL NUMIN(KI)

C   LOAD ALTERNATOR TIME CONSTANT
```

```

CALL NUMIN(TA)

C   LOAD GRID FREQUENCY CORRECTION FACTOR
CALL NUMIN(GC)

C   SPEEDER MOTOR CONSTANTS
TSM=10.0
BPD=0.05
SPRS=0.1*BPD/TSM
HFSPRS=SPRS/2.0

C   WIND TURBINE MODEL CONSTANTS
KC0=150.0
KC1=2400.0
JB=3144.0
JM1=25.0
WTC=0.1
TKC=1.0
TOFL=19098.6
WO=157.08
BPW=0.05
TP=0.059
WW1=-0.05*WO
WW2=0.05*WO
WW5=-0.04*WO
WW6=0.04*WO
KCDIFF=KC1-KC0
WKCRNG=WW5-WW1
FREFW=1.0
PREF=WOP
VWL=VW
VWH=VW+VWSTEP

C   SYSTEM CONSTANTS
PON=1.0

C   CALCULATE PLANT MAXIMUM CONTINUOUS RATINGS
PODMCR=4.6
TOTMCR=PODMCR/QD
PONMCR=QN*TOTMCR
POWMCR=QW*TOTMCR

C   SET UP DEMAND STEP CONTROL
LRISEG=.TRUE.
LRISE=.FALSE.
LFALLG=.FALSE.
LFALL=.FALSE.

C   ANALOG OUTPUT SCALING CONSTANTS
FESSCL=4096.0/(1.05-0.95)
POSCL=(4096.0-2048.0)/(1.0-0.0)

C   CALCULATION AND AVERAGING OF GRID FREQUENCY VALUE
75  CONTINUE
    IF(.NOT.LGFROK) GOTO 75
    CNTSUM=0
    DO 77 I=1,FSAMPL
    CALL DSABLE
    CNTSUM=CNTSUM+INT4(CNSAMP(I))
    CALL ENABLE

```

```

77    CONTINUE
      GFREQI=TIMSCL/FLOAT(CNTSUM)

C     OUTPUT INITIAL GRID FREQUENCY
      IGFREQ=2048+NINT(FGSCS*(GFREQI-1.0))
      IF(IGFREQ.GT.4095) IGFREQ=4095
      IF(IGFREQ.LT.0) IGFREQ=0
      CALL ANOUT(6,IGFREQ)

C     SEND INITIAL WIND TURBINE POWER FOR OUTPUT
      IPOW=2048.0+NINT(POSCL*WOP)
      IF(IPOW.GT.4095) IPOW=4095
      IF(IPOW.LT.2048) IPOW=2048
      CALL GETSEM(DACSEM(2))
      DACDAT(2)=IPOW
      CALL GIVSEM(DACSEM(2))

C     SEND INITIAL WIND TURBINE BLADE TORQUE FOR OUTPUT
      ITOW=2048.0+NINT(POSCL*WOP)
      IF(ITOW.GT.4095) ITOW=4095
      IF(ITOW.LT.2048) ITOW=2048
      CALL GETSEM(DACSEM(3))
      DACDAT(3)=ITOW
      CALL GIVSEM(DACSEM(3))

C     WIND TURBINE INITIAL CONDITIONS
      G=VW/1.8378
      CP=WOP/(0.0001372*VW*VW*G)
      B=SQRT((G-5.6-CP/(0.5*EXP(-0.17*G)))/0.022)
      X1=B/KI
      TOW=0.0
      TOG=0.0
      WB=0.0
      WM=0.0
      WM1=0.0
      TOWN=WOP
      POW=WOP
      TEN=WOP
      WBN=1.0
      WMN=0.0
      KC=KCO

C     SEND INITIAL WIND TURBINE BLADE ANGLE FOR OUTPUT
      IB=2048+NINT(2048.0*B/90.0)
      IF(IB.GT.4095) IB=4095
      IF(IB.LT.2048) IB=2048
      CALL GETSEM(DACSEM(6))
      DACDAT(6)=IB
      CALL GIVSEM(DACSEM(6))

C     LOAD MW METER READING
      CALL NUMIN(READMW)

C     CALCULATE DIESEL OPERATING POINT
      POD=READMW/PODMCR

C     MEASURE AVERAGE VALUE OF DIESEL OUTPUT POWER
      IPODSM=0
      DO 20 I=1,NSAMPL
      CALL ANIN(1,IPOD)

```

```

      IPODSM=IPODSM+INT4(IPOD)
20  CONTINUE

      C      ANALOG INPUT SCALING CONSTANTS
      PWSCL=(POD-0.0)/(FLOAT(IPODSM)-2048.0*FLOAT(NSAMPL))
      POD5V=2048.0*PWSCL*FLOAT(NSAMPL)

60  CONTINUE

      C      CALCULATION AND FILTERING OF GRID FREQUENCY VALUE
      CNTSUM=0
      DO 65 I=1,FSAMPL
      CALL DSABLE
      CNTSUM=CNTSUM+INT4(CNSAMP(I))
      CALL ENABLE
65  CONTINUE
      GFREQI=TIMSCL/FLOAT(CNTSUM)

      C      MEASURE AVERAGE VALUE OF DIESEL OUTPUT POWER
      IPODSM=0
      DO 90 I=1,NSAMPL
      CALL ANIN(1,IPOD)
      IPODSM=IPODSM+INT4(IPOD)
90  CONTINUE
      POD=PWSCL*FLOAT(IPODSM)-POD5V
      IPODSM=0

      C      CALCULATE INITIAL DEMAND VALUE
      PD=QN*PON+QD*POD+QW*POW

      C      OUTPUT INITIAL DIESEL POWER OUTPUT
      IPOD=2048.0+NINT(POSCL*POD)
      IF(IPOD.GT.4095) IPOD=4095
      IF(IPOD.LT.2048) IPOD=2048
      CALL ANOUT(2,IPOD)

      C      OUTPUT INITIAL DEMAND VALUE
      IPD=2048+NINT(POSCL*PD)
      IF(IPD.GT.4095) IPD=4095
      IF(IPD.LT.2048) IPD=2048
      CALL ANOUT(5,IPD)

      C      OUTPUT INITIAL GRID FREQUENCY
      IGFREQ=2048+NINT(FGSCLE*(GFREQI-1.0))
      IF(IGFREQ.GT.4095) IGFREQ=4095
      IF(IGFREQ.LT.0) IGFREQ=0
      CALL ANOUT(6,IGFREQ)

      C      ECHO PARAMETERS TO BBC
      CALL NUMOUT(PD)
      CALL NUMOUT(PD*TOTMCR)
      CALL NUMOUT(PON)
      CALL NUMOUT(PON*POMMCR)
      CALL NUMOUT(POD)
      CALL NUMOUT(POD*PODMCR)
      CALL NUMOUT(POW)
      CALL NUMOUT(POW*POWMCR)

      C      LOOK FOR COMMAND TO START SIMULATION
      CALL BYTIN(CTLIN)

```

```

IF(CTLIN.NE.#53H) GOTO 60

C   CALCULATE INITIAL DIESEL FREQUENCY REFERENCE
    PREFI=GFREQI+BPD*POD

C   SET START FLAG FOR DELAY FUNCTIONS ETC
    LSTART=.TRUE.

C   INITIAL CONDITIONS
    FREQ=1.0

C   RESET START FLAG
    LSTART=.FALSE.

C   SET UP TIMER 1
    CALL OUTPUT(TIMCTL,#74H)
    CALL OUTPUT(TIMER1,T1LOB)
    CALL OUTPUT(TIMER1,T1HOB)

C   SET UP VECTOR AND UN-MASK FOR TIME INTERRUPTS
    CALL SETINT(#24H,SAMPLE)
    CALL OUTPUT(INTCT2,#0EEH)

C   WAIT FOR INTERRUPTS
30  CONTINUE
    IF(KSIM.NE.1) GOTO 30

C   SET PC4
    CALL OUTPUT(PRTCTL,#0BH)

C   CALCULATION AND FILTERING OF GRID FREQUENCY VALUE
    CNTSUM=0
    DO 100 I=1,FSAMPL
        CALL DSABLE
        CNTSUM=CNTSUM+INT4(CNSAMP(I))
        CALL ENABLE
100  CONTINUE
    GFREQ=TIMSCL/FLOAT(CNTSUM)

C   CALCULATE DIESEL OUTPUT POWER
    CALL DSABLE
    POD=PWSCL*FLOAT(IPODSM)-POD5V
    IPODSM=0
    CALL ENABLE

C   WIND TURBINE
    WPERR=(FREQ-FREFW)/BPW+POW-PREF
    DX1=WPERR
    BD=KP*WPERR+K1*X1
    B=LIMIT(B,0.0,90.0)
    DB=(BD-B)/TP
    DB=LIMIT(DB,-10.0,10.0)
    G=VW/((1.0+WB/WO)*1.8378)
    CP=0.5*(G-0.022*B*B-5.6)*EXP(-0.17*G)
    TOW=TOFL*(0.0001372*VW*VW*CP*G-WOP)
    DWB=(TOW-TOG)/JB
    WM=WB-(FREQ-1.0)*WO
    DWM1=(WM-WM1)/WTC
    WKC=WM+(TOFL-TE)/KC1
    KCD=KCO

```

```

IF(WKC.LT.WW5) THEN
  IF(WKC.LT.WW1) THEN
    KCD=KC1
  ELSE
    KCD=KCO+(WW5-WKC)*KCDIFF/WKCRNG
  ENDIF
ENDIF
IF(WKC.GT.WW6) THEN
  IF(WKC.GT.WW2) THEN
    KCD=KC1
  ELSE
    KCD=KCO+(WKC-WW6)*KCDIFF/WKCRNG
  ENDIF
ENDIF
DKC=(KCD-KC)/TKC
KC=KC+H*DKC
TOGD=KC*WM
TOGD=LIMIT(TOGD, -TOFL*WOP, TOFL*(1.0-WOP))
TOG=(JM1/WTC)*WM+(KC-JM1/WTC)*WM1
TOG=LIMIT(TOG, -TOFL*WOP, TOFL*(1.0-WOP))
TE=WOP*TOFL+TOG
X1=X1+H*DX1
B=B+H*DB
WB=WB+H*DWB
WM1=WM1+H*DWM1
TOWN=WOP+TOW/TOFL
TEN=WOP+TOG/TOFL
POW=FREQ*TEN
WBN=1.0+WB/WO
WMN=WM/WO

C   SYSTEM
    PL=PD*FREQ
    DFREQ=((QN*PON+QW*POW-PL)/FREQ+QD*POD/GFREQ)/TA
    FREQ=FREQ+H*DFREQ

C   COLLECT DEMAND CONTROL
    IPDCTL=IPDSW

C   CALCULATE WIND SPEED VALUE
    IF(LRISEG.AND.IPDCTL.EQ.#00H) THEN
      VW=VWH
      LRISEG=.FALSE.
      LFALLG=.TRUE.
    ENDIF
    IF(LFALLG.AND.IPDCTL.EQ.#01H) THEN
      VW=VWL
      LFALLG=.FALSE.
      LRISEG=.TRUE.
    ENDIF

C   TEST FREQUENCY INPUT
    FES=1.0-FREQ
    FESCOR=FES+GC*(GFREQ-GFREQI)

C   CALCULATION OF INJECTION SIGNAL
    ISPCNT=ISPCNT+1
    IF(ISPCNT.NE.2) GOTO 125
    ISPCNT=0
    FTRACK=SPRS*FLOAT(NPULSE)

```

```

FREFH=FREFI+FTRACK
FDISC=FESCOR-FTRACK
IF(LDODGY) THEN
  IF(NPULSE.EQ.0) THEN
    ISPCTL=#03H
    ISPDIP=2048
  ENDIF
  IF(NPULSE.GT.0) THEN
    ISPCTL=#02H
    ISPDIP=1792
    NPULSE=NPULSE-1
  ENDIF
  IF(NPULSE.LT.0) THEN
    ISPCTL=#01H
    ISPDIP=2304
    NPULSE=NPULSE+1
  ENDIF
ELSE
  IF(FDISC.LT.HFSPRS.AND.FDISC.GT.-HFSPRS) THEN
    ISPCTL=#03H
    ISPDIP=2048
  ENDIF
  IF(FDISC.GT.HFSPRS.AND.FDISC.LT.FDSCLM) THEN
    NPULSE=NPULSE+1
    ISPCTL=#01H
    ISPDIP=2304
  ENDIF
  IF(FDISC.LT.-HFSPRS.AND.FDISC.GT.-FDSCLM) THEN
    NPULSE=NPULSE-1
    ISPCTL=#02H
    ISPDIP=1792
  ENDIF
  IF(FDISC.GT.FDSCLM.OR.FDISC.LT.-FDSCLM) THEN
    ISPCTL=#03H
    ISPDIP=2048
    LDODGY=.TRUE.
  ENDIF
  IF(GFREQ.LT.GFRLML.OR.GFREQ.GT.GFRLMH) THEN
    ISPCTL=#03H
    ISPDIP=2048
    LGFRML=.TRUE.
    LDODGY=.TRUE.
    NPULSE=0
  ENDIF
  IF(FREFH.LT.FRFLML.OR.FREFH.GT.FRFLMH) THEN
    ISPCTL=#03H
    ISPDIP=2048
    LSPRLM=.TRUE.
    LDODGY=.TRUE.
  ENDIF
ENDIF
ENDIF
IF(FREFH.LT.FRFSNL) THEN
  LLTSNL=.TRUE.
ELSE
  LLTSNL=.FALSE.
ENDIF
CONTINUE

```

125

C OUTPUT FREQUENCY DEVIATION
 IFES=2048+NINT(FESSCL*FES)

```

IF(IFES.GT.4095) IFES=4095
IF(IFES.LT.0) IFES=0
CALL ANOUT(0,IFES)

C   OUTPUT DIESEL POWER OUTPUT
      IPOD=2048+NINT(POSCL*POD)
      IF(IPOD.GT.4095) IPOD=4095
      IF(IPOD.LT.2048) IPOD=2048
      CALL ANOUT(2,IPOD)

C   OUTPUT FREQUENCY DISCREPANCY WITH SPEEDER MOTOR INPUT
      IFDISC=2048+NINT(FESSCL*FDISC)
      IF(IFDISC.GT.4095) IFDISC=4095
      IF(IFDISC.LT.0) IFDISC=0
      CALL ANOUT(3,IFDISC)

C   OUTPUT CORRECTED FREQUENCY DEVIATION IF GRID FREQUENCY OK
      IF(.NOT.LGFRML) THEN
          IFESCR=2048+NINT(FESSCL*FESCOR)
          IF(IFESCR.GT.4095) IFESCR=4095
          IF(IFESCR.LT.0) IFESCR=0
          CALL ANOUT(4,IFESCR)
      ENDIF

C   OUTPUT DEMAND VALUE
      IPD=2048+NINT(POSCL*PD)
      IF(IPD.GT.4095) IPD=4095
      IF(IPD.LT.2048) IPD=2048
      CALL ANOUT(5,IPD)

C   OUTPUT GRID FREQUENCY
      IGFREQ=2048+NINT(FGSCCL*(GFREQ-1.0))
      IF(IGFREQ.GT.4095) IGFREQ=4095
      IF(IGFREQ.LT.0) IGFREQ=0
      CALL ANOUT(6,IGFREQ)

C   SEND COMBINED SPEEDER MOTOR INPUT SIGNAL FOR OUTPUT
      CALL GETSEM(DACSEM(0))
      DACDAT(0)=ISPDIP
      CALL GIVSEM(DACSEM(0))

C   SEND INTEGRATED SPEEDER MOTOR INPUT SIGNAL FOR OUTPUT
      IFTRACK=2048+NINT(FESSCL*FTRACK)
      IF(IFTRACK.GT.4095) IFTRACK=4095
      IF(IFTRACK.LT.0) IFTRACK=0
      CALL GETSEM(DACSEM(1))
      DACDAT(1)=IFTRACK
      CALL GIVSEM(DACSEM(1))

C   SEND WIND TURBINE POWER FOR OUTPUT
      IPOW=2048.0+NINT(POSCL*POW)
      IF(IPOW.GT.4095) IPOW=4095
      IF(IPOW.LT.2048) IPOW=2048
      CALL GETSEM(DACSEM(2))
      DACDAT(2)=IPOW
      CALL GIVSEM(DACSEM(2))

C   SEND WIND TURBINE BLADE TORQUE FOR OUTPUT
      ITOW=2048.0+NINT(POSCL*TOWN)
      IF(ITOW.GT.4095) ITOW=4095

```

```

IF(ITOW.LT.2048) ITOW=2048
CALL GETSEM(DACSEM(3))
DACDAT(3)=IPOW
CALL GIVSEM(DACSEM(3))

C   SEND WIND TURBINE ROTOR SPEED FOR OUTPUT
IWB=2048+NINT(FESSCL*(WBN-1.0))
IF(IWB.GT.4095) IWB=4095
IF(IWB.LT.0) IWB=0
CALL GETSEM(DACSEM(4))
DACDAT(4)=IWB
CALL GIVSEM(DACSEM(4))

C   SEND WIND TURBINE REACTION MACHINE SPEED FOR OUTPUT
IWM=2048+NINT(FESSCL*WMN)
IF(IWM.GT.4095) IWM=4095
IF(IWM.LT.0) IWM=0
CALL GETSEM(DACSEM(5))
DACDAT(5)=IWM
CALL GIVSEM(DACSEM(5))

C   SEND WIND TURBINE BLADE ANGLE FOR OUTPUT
IB=2048+NINT(2048.0*B/90.0)
IF(IB.GT.4095) IB=4095
IF(IB.LT.2048) IB=2048
CALL GETSEM(DACSEM(6))
DACDAT(6)=IB
CALL GIVSEM(DACSEM(6))

C   SEND WIND TURBINE CONTROLLER GAIN FOR OUTPUT
IKC=2048+NINT(2048.0*KC/3000.0)
IF(IKC.GT.4095) IKC=4095
IF(IKC.LT.2048) IKC=2048
CALL GETSEM(DACSEM(7))
DACDAT(7)=IKC
CALL GIVSEM(DACSEM(7))

C   RESET 0.1S FLAG
KSIM=0

C   RESET PC4
CALL OUTPUT(PRTCTL,#0AH)

C   LOOK FOR COMMAND TO FINISH SIMULATION
CALL SCANIN(CTLIN)
IF(CTLIN.NE.#46H) GOTO 30

C   IF FINISHED DISABLE PROCESSOR INTERRUPTS AND RESTART
CALL DSABLE
GOTO 70

END

```

\$INTERRUPT

```

SUBROUTINE SAMPLE
EXTERNAL ANIN
INTEGER*1 INTCT1,PRTCTL
INTEGER*1 NSAMPL,NCOUNT,KSIM

```

```

INTEGER*2 IPOD
INTEGER*4 IPODSM
COMMON/SAMPL1/NSAMPL,NCOUNT,KSIM
COMMON/SAMPL2/IPODSM
PARAMETER(INTCT1=#0COH,PRCTL=#0CEH)

C   RE-ENABLE PROCESSOR INTERRUPTS
CALL ENABLE

C   SET PC4
CALL OUTPUT(PRTCTL,#09H)

C   MEASURE TURBINE POWER OUTPUT
CALL ANIN(1,IPOD)
IPODSM=IPODSM+INT4(IPOD)

C   INTEGRATION CONTROL
NCOUNT=NCOUNT+1
IF(NCOUNT.EQ.NSAMPL) THEN
    NCOUNT=0
    KSIM=1
ENDIF

C   RESET PC4
CALL OUTPUT(PRTCTL,#08H)

C   SEND EOI TO PIC
CALL OUTPUT(INTCT1,#64H)

RETURN
END

$INTERRUPT

SUBROUTINE CYCLE
EXTERNAL TIMCNT,ANOUT
INTEGER*1 INTCT1,INTCT2,PRTCTL
INTEGER*2 TOLAST,ICOUNT
INTEGER*2 CNSAMP(50)
INTEGER*1 FSAMPL,I,ICNSMP
LOGICAL*1 LGFROK
COMMON/SAMPL3/FSAMPL,ICNSMP,TOLAST,LGFROK,CNSAMP
PARAMETER(INTCT1=#0COH,INTCT2=#0C2H,PRTCTL=#0CEH)

C   SET PC5
C   CALL OUTPUT(PRTCTL,#0BH)

C   READ TIMER
CALL TIMCNT(TOLAST,ICOUNT)
IF(ICOUNT.GT.24699) ICOUNT=24699
IF(ICOUNT.LT.24454) ICOUNT=24454

C   SEND COUNT VALUE TO FILTER
CNSAMP(ICNSMP)=ICOUNT
ICNSMP=ICNSMP-1
IF(ICNSMP.EQ.0) THEN
    ICNSMP=FSAMPL
    LGFROK=.TRUE.
ENDIF

```

```
C RESET PC5  
C CALL OUTPUT(PRTCTL,#0AH)
```

```
C SEND EOI TO PIC  
CALL OUTPUT(INTCT1,#60H)
```

```
RETURN  
END
```

```
C LIMIT FUNCTION  
REAL*4 FUNCTION LIMIT(VAL,BTMLIM,TOPLIM)  
REAL*4 VAL,BTMLIM,TOPLIM  
IF(VAL.LE.BTMLIM) LIMIT=BTMLIM  
IF(VAL.GT.BTMLIM) LIMIT=VAL  
IF(VAL.GE.TOPLIM) LIMIT=TOPLIM  
RETURN  
END
```

Slave processor code for wind-diesel system tests

```

C      MIXED SYSTEM SIMULATOR
C      CODE FOR PROCESSOR 2
C      CODE FOR ADDITIONAL I/O

      EXTERNAL ANINIT,ANOUT,GETSEM,GIVSEM
      INTEGER*1 PORTA,PORTB,PORTC,PRTCTL
      INTEGER*2 I,DACDAT(0:7),IDAC
      INTEGER*1 ISPCTL,IPDSW,IPDCTL,DACSEM(0:7)
      LOGICAL*1 LFLAG2,LFLAG3,LFLAG4,LFLAG5,LFLAG6
      LOGICAL*1 SYNC,P2RDY
      COMMON/PRLL1/ISPCTL,IPDSW,LFLAG2,LFLAG3,LFLAG4,LFLAG5,LFLAG6
      COMMON/PRLL2/SYNC,P2RDY
      COMMON/PRLL5/DACSEM,DACDAT
      PARAMETER(PORTA=#0C8H,PORTB=#0CAH,PORTC=#0CCH,PRTCTL=#0CEH)

C      DISABLE PROCESSOR INTERRUPTS
      CALL DSABLE

C      RESET RAISE/LOWER CONTROL BYTE
      ISPCTL=#03H

C      SET UP PARALLEL PORTS
      CALL OUTPUT(PORTA,ISPCTL)
      CALL OUTPUT(PRTCTL,#82H)
      CALL OUTPUT(PORTA,ISPCTL)

C      SET UP DAC
      CALL ANINIT(7)

C      SYNCHRONISE WITH PROCESSOR 1
10     IF(SYNC) GOTO 10
20     IF(.NOT.SYNC) GOTO 20
      P2RDY=.TRUE.

80     CONTINUE

C      PERFORM I/O FUNCTIONS

C      OUTPUT RAISE/LOWER CONTROL BYTE
      CALL OUTPUT(PORTA,ISPCTL)

C      READ AND ECHO DEMAND CONTROL SWITCH
      CALL INPUT(PORTB,IPDCTL)
      IPDSW=IPDCTL.AND.#01H
      IF(IPDSW.EQ.#00H) THEN
          CALL OUTPUT(PRTCTL,#03H)
      ELSE
          CALL OUTPUT(PRTCTL,#02H)
      ENDIF

C      DISPLAY ERROR CONDITIONS
      IF(LFLAG2) THEN
          CALL OUTPUT(PRTCTL,#05H)
      ELSE
          CALL OUTPUT(PRTCTL,#04H)
      ENDIF
      IF(LFLAG3) THEN
          CALL OUTPUT(PRTCTL,#07H)
      ELSE
          CALL OUTPUT(PRTCTL,#06H)

```

```
ENDIF
IF(LFLAG4) THEN
  CALL OUTPUT(PRTCTL,#09H)
ELSE
  CALL OUTPUT(PRTCTL,#08H)
ENDIF
IF(LFLAG5) THEN
  CALL OUTPUT(PRTCTL,#0BH)
ELSE
  CALL OUTPUT(PRTCTL,#0AH)
ENDIF
IF(LFLAG6) THEN
  CALL OUTPUT(PRTCTL,#0DH)
ELSE
  CALL OUTPUT(PRTCTL,#0CH)
ENDIF

C  EXTRA DAC OUTPUTS
DO 90 I=0,7
  CALL GETSEM(DACSEM(I))
  IDAC=DACDAT(I)
  CALL GIVSEM(DACSEM(I))
  CALL ANOUT(I,IDAC)
90  CONTINUE

GOTO 80

END
```

Assembly language subroutines

```

NAMEANALOG
ANALOGSEGMENT 'CODE'
ASSUME CS:ANALOG
PUBLIC ANINIT,ANIN,ANOUT
    
```

```

DACSTS EQU 0A2H
DACDAT EQU 0A0H
DACRST EQU 0A2H
ADCHI EQU 80H
ADCLO EQU 82H
ADCSEL EQU 80H
    
```

```

ANINITPROC FAR;INITIALISES DAC
MOV AL,0;RESET DAC
OUT DACSTS,AL
PUSH BP;GET ADDRESS OF FINISH CHANNEL OFF STACK
MOV BP,SP
PUSH SI
PUSH DS
ADD BP,6
MOV DS,[BP]+2
MOV SI,[BP]
DACINI:IN AL,DACSTS;GET UPI STATUS
AND AL,4;TEST FOR FO
JZ DACINI
MOV AX,[SI];GET FINISH CHANNEL
AND AL,7;MASK OFF IRRELEVANT BITS
OR AL,08;SELECT DAC PROGRAM 2
OUT DACDAT,AL
POP DS
POP SI
POP BP
RET 4
ANINITENDP
    
```

```

ANINPROC FAR;READS VALUE FROM ADC
PUSH BP;GET ADDRESS OF CHANNEL OFF STACK
MOV BP,SP
PUSH SI
PUSH DS
ADD BP,6
MOV DS,[BP]+6
MOV SI,[BP]+4
MOV AX,[SI];GET CHANNEL
OUT ADCSEL,AL
TSTEOC:IN AL,ADCLO;GET ADC STATUS
AND AL,1;TEST FOR EOC
JNZ TSTEOC
IN AL,ADCLO;GET LOB DATA
MOV DL,AL
IN AL,ADCHI;GET HOB DATA
MOV DH,AL
MOV CL,4;RESTORE TO INTEGER FORMAT
SHR DX,CL
MOV DS,[BP]+2;GET ADDRESS OF DATA OFF STACK
MOV SI,[BP]
MOV [SI],DX;STORE DATA
POP DS
POP SI
POP BP
    
```

```

RET 8
ANINENDP

ANOUTPROC FAR;WRITES VALUE TO DAC
PUSH BP;GET ADDRESS OF DATA OFF STACK
MOV BP,SP
PUSH SI
PUSH DS
ADD BP,6
MOV DS,[BP]+2
MOV SI,[BP]
CALL DACWT;CHECK DAC READY
MOV DX,[SI];GET DATA
MOV CL,3;CHANGE FROM INTEGER FORMAT
SHL DX,CL
MOV DS,[BP]+6;GET ADDRESS OF CHANNEL OFF STACK
MOV SI,[BP]+4
ADD DX,[SI];GET CHANNEL, SET UP HOB, LOB DATA
SHL DX,1;FINISH CHANGE FROM INTEGER FORMAT
MOV AL,DL;WRITE LOB DATA
OUT DACDAT,AL
CALL DACWT;CHECK DAC READY
MOV AL,DH;WRITE HOB DATA
OUT DACDAT,AL
POP DS
POP SI
POP BP
RET 8
ANOUTENDP

```

```

DACWTPROC NEAR
DACIBF:IN AL,DACSTS;GET UPI STATUS
AND AL,2;TEST FOR NOT IBF
JNZ DACIBF
RET
DACWTENDP

```

ANALOGENDS

STACKSEGMENT STACK 'STACK'

DW 20 DUP (?);RESERVE STACK SPACE

STACKENDS

END

```
NAME BBCSBC

PORTA EQU 0C8H
PORTB EQU 0CAH
PORTC EQU 0CCH
PRTCTL EQU 0CEH

BBCSBC SEGMENT 'CODE'
PUBLIC NUMIN,NUMOUT,BYTIN,BYTOUT,SCANIN
ASSUME CS:BBCSBC

NUMIN PROC FAR
    PUSH BP
    MOV BP,SP
    PUSH DS
    MOV DS,[BP]+8
    MOV SI,[BP]+6
    MOV CX,4
POLL1: IN AL,PORTC
    TEST AL,01H
    JZ POLL1
    IN AL,PORTB
    MOV [SI],AL
    INC SI
    LOOP POLL1
    POP DS
    POP BP
    RET 4
NUMIN ENDP

NUMOUT PROC FAR
    PUSH BP
    MOV BP,SP
    PUSH DS
    MOV DS,[BP]+8
    MOV SI,[BP]+6
    MOV CX,4
POLL2: IN AL,PORTC
    TEST AL,08H
    JZ POLL2
    MOV AL,[SI]
    OUT PORTA,AL
    INC SI
    LOOP POLL2
    POP DS
    POP BP
    RET 4
NUMOUT ENDP

BYTIN PROC FAR
    PUSH BP
    MOV BP,SP
    PUSH DS
    MOV DS,[BP]+8
    MOV SI,[BP]+6
POLL3: IN AL,PORTC
    TEST AL,01H
    JZ POLL3
    IN AL,PORTB
    MOV [SI],AL
```

```

        POP DS
        POP BP
        RET 4
BYTIN  ENDP

BYTOUT PROC FAR
        PUSH BP
        MOV BP,SP
        PUSH DS
        MOV DS,[BP]+8
        MOV SI,[BP]+6
POLL4: IN AL,PORTC
        TEST AL,08H
        JZ POLL4
        MOV AL,[SI]
        OUT PORTA,AL
        POP DS
        POP BP
        RET 4
BYTOUT ENDP

SCANIN PROC FAR
        PUSH BP
        MOV BP,SP
        PUSH DS
        MOV DS,[BP]+8
        MOV SI,[BP]+6
        IN AL,PORTC
        TEST AL,01H
        MOV AL,0
        JZ NOCHAR
        IN AL,PORTB
NOCHAR: MOV [SI],AL
        POP DS
        POP BP
        RET 4
SCANIN ENDP

BBCSBC ENDS

STACK SEGMENT STACK 'STACK'
        DW 40 DUP(?)
STACK ENDS

        END

```

```
NAME    TIMER

TIMER0  EQU 0D0H
TIMCTL  EQU 0D6H

TIMER   SEGMENT 'CODE'
        ASSUME CS:TIMER
        PUBLIC TIMCNT

TIMCNT  PROC FAR
        PUSH BP
        MOV BP,SP
        PUSH DS
        MOV DS,[BP]+12
        MOV SI,[BP]+10
        MOV AL,0
        OUT TIMCTL,AL
        IN AL,TIMER0
        MOV BL,AL
        IN AL,TIMER0
        MOV BH,AL
        MOV AX,[SI]
        SUB AX,BX
        MOV [SI],BX
        MOV DS,[BP]+8
        MOV SI,[BP]+6
        MOV [SI],AX
        POP DS
        POP BP
        RET 8
TIMCNT  ENDP

TIMER   ENDS

STACK  SEGMENT STACK 'STACK'
        DW 20 DUP (?)
STACK  ENDS

        END
```



```
NAME MPCOMS

MPCOMS SEGMENT 'CODE'
PUBLIC GETSEM,GIVSEM
ASSUME CS:MPCOMS

GETSEM PROC FAR
PUSH BP
MOV BP,SP
PUSH DS
MOV DS,[BP]+8
MOV SI,[BP]+6
RETRY: MOV AL,1
LOCK XCHG AL,[SI]
TEST AL,AL
JNZ RETRY
POP DS
POP BP
RET 4
GETSEM ENDP

GIVSEM PROC FAR
PUSH BP
MOV BP,SP
PUSH DS
MOV DS,[BP]+8
MOV SI,[BP]+6
MOV AL,0
MOV [SI],AL
POP DS
POP BP
RET 4
GIVSEM ENDP

MPCOMS ENDS

STACK SEGMENT STACK 'STACK'
DW 40 DUP(?)
STACK ENDS

END
```

